

# Metasomatic uranium mineralisation of the Mount Isa North Block

**A. Otto, J. Jory, J. Thom, E. Becker**

Paladin Energy Ltd, Perth, Australia

*E-mail address of main author: alexander.otto@paladinenergy.com.au*

**Abstract.** Proterozoic uranium deposits of the Mt Isa North Block are centred 40 km north of Mt Isa, NW Queensland. Regionally, the deposits occur within the Leichhardt River Fault Trough of the Mt Isa Inlier. Uranium mineralisation is likely related to the 1 600-1 500 Ma Isan Orogeny. Structurally-controlled uranium mineralisation is preferentially hosted in greenschist facies basalts and interbedded clastic sediments of the Eastern Creek Volcanics (ECV). Uranium deposits of the Mt Isa North Block are defined by the following general characteristics:

- Pervasive sodium and calcium metasomatism, expressed as red albitite with finely disseminated hematite and calcite, with distal zones of chlorite and magnetite.
- Uraniferous albitite deposits typically comprise en echelon lenses and shoots.
- Mineralisation is developed along N- to NE-striking shear zones with associated brittle deformation of the host lithologies.
- Host rocks are mostly basalt flows with flow-top breccias and interbedded sandstones and siltstones of the ECV; quartzites are also locally mineralised.
- Uranium mineralogy of albitites comprises brannerite, coffinite, uraninite and uraniumiferous zircon.

The Mt Isa North Blocks includes 11 tenements being explored for uranium by Summit Resources. Summit's five uranium resources total 95.7 Mlb U<sub>3</sub>O<sub>8</sub>. Summit is in a 50/50 Joint Venture with Paladin on the Valhalla and Skal deposits. Paladin also has a direct ownership of 81.99% of the issued shares of Summit Resources.

## 1. Introduction

The uranium deposits of the Mount Isa North Block are located north of Mount Isa, Northwest Queensland, Australia (Fig. 1). Historically, uranium mineralisation in the Mount Isa region was considered similar to the Olympic Dam IOCG-type Cu-U-Au deposits and the nearby Ernest Henry Cu-Au deposit. Recent petrographic studies by Paladin have demonstrated that much of the 'red rock' alteration in the Mount Isa uranium deposits is due to albitite and finely disseminated hematite caused by sodium and calcium metasomatism. These uranium metasomatite deposits are analogous to similar deposits which have been mined in Russia, Ukraine, China and Canada (e.g. Beaverlodge and Gunnar). The Valhalla and Skal uranium deposits were discovered by prospectors in 1954 and since then has been explored by MIM, Queensland Mines Ltd and Summit Resources.

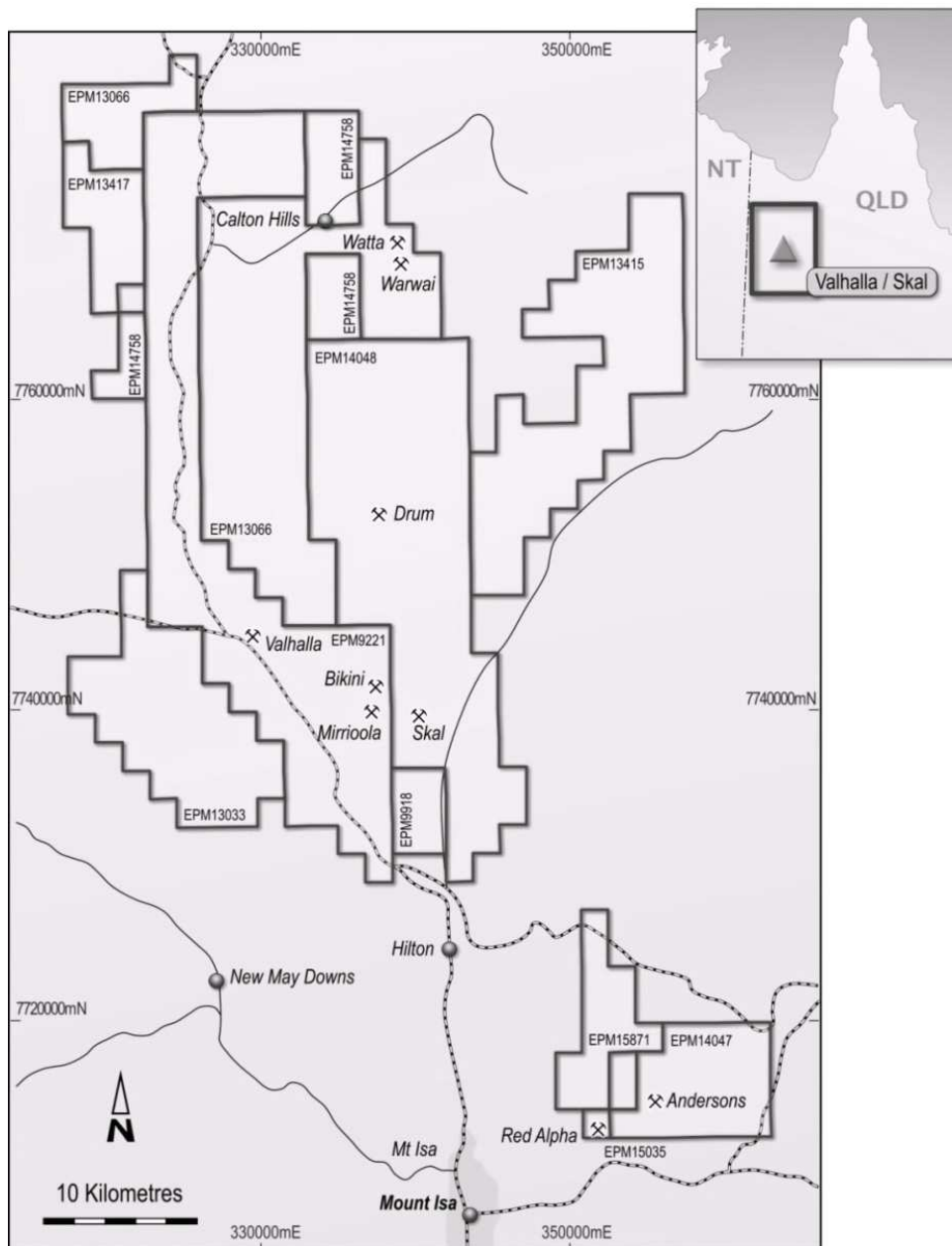


FIG. 1. Location of the exploration tenements of the Mount Isa North Block.

## 2. Regional geology

Two major Proterozoic tectonostratigraphic cycles are recognised in the Mount Isa Inlier [1]. An earlier cycle is represented by basement rocks metamorphosed and deformed during the Barramundi orogeny (1 900-1 870 Ma) (Fig. 2). A later cycle, represented by cover sequences 1-3, was terminated by the Isan Orogeny at 1 620-1 520 Ma [2]. Cover sequence 1 is mainly felsic volcanics, cover sequence 2 includes shallow-water sediments and bimodal volcanics, and cover sequence 3 is mostly fine-grained clastic sediments and carbonates. Large granitic batholiths were emplaced at ~1 860 Ma, 1 800 Ma, 1 740 Ma, 1 670 Ma and 1 500 Ma. Abundant mafic dykes of mostly gabbro and dolerite compositions range from 1 900-1 100 Ma. Extensional deformation during the second cycle was terminated by the compressional Isan orogeny, which consisted of two main phases: 1) early thrusting and folding during north-south compression with localized basin inversion, and 2) upright folding, reverse faulting and dextral wrenching during east-west compression. Subsequent strike-slip faulting divided the area into several tectonostratigraphic belts.

The Mount Isa Inlier is subdivided by north-south-striking faults into three tectonic belts: Western Succession, Kalkadoon-Leichhardt Belt and Eastern Succession [3]. The Western Succession includes the Lawn Hill platform (carbonate rocks), Leichhardt River Fault Trough (mafic volcanic rocks and clastic sediments), and the Myally Shelf (clastic sediments and carbonate rocks).

The Leichhardt River Fault Trough is dominated by mafic volcanic rocks of the Haslingden Group that were deposited in an intercontinental rift setting. The Haslingden Group consists of sandstone and quartzite of the Mount Guide Quartzite unconformably overlain by basalts and interbedded clastic sediments of the Eastern Creek Volcanics [1] dated at 1 807 to 1 710 Ma. A 6km-thick volcanic sequence was regionally metamorphosed to greenschist facies (calcite, chlorite, epidote). These rocks are strongly folded, faulted and foliated, and bedding dips steeply west and north. A total of 107 uranium occurrences have been recorded, including the Valhalla, Bikini and Skal deposits. Most of these occur in the Eastern Creek Volcanics.

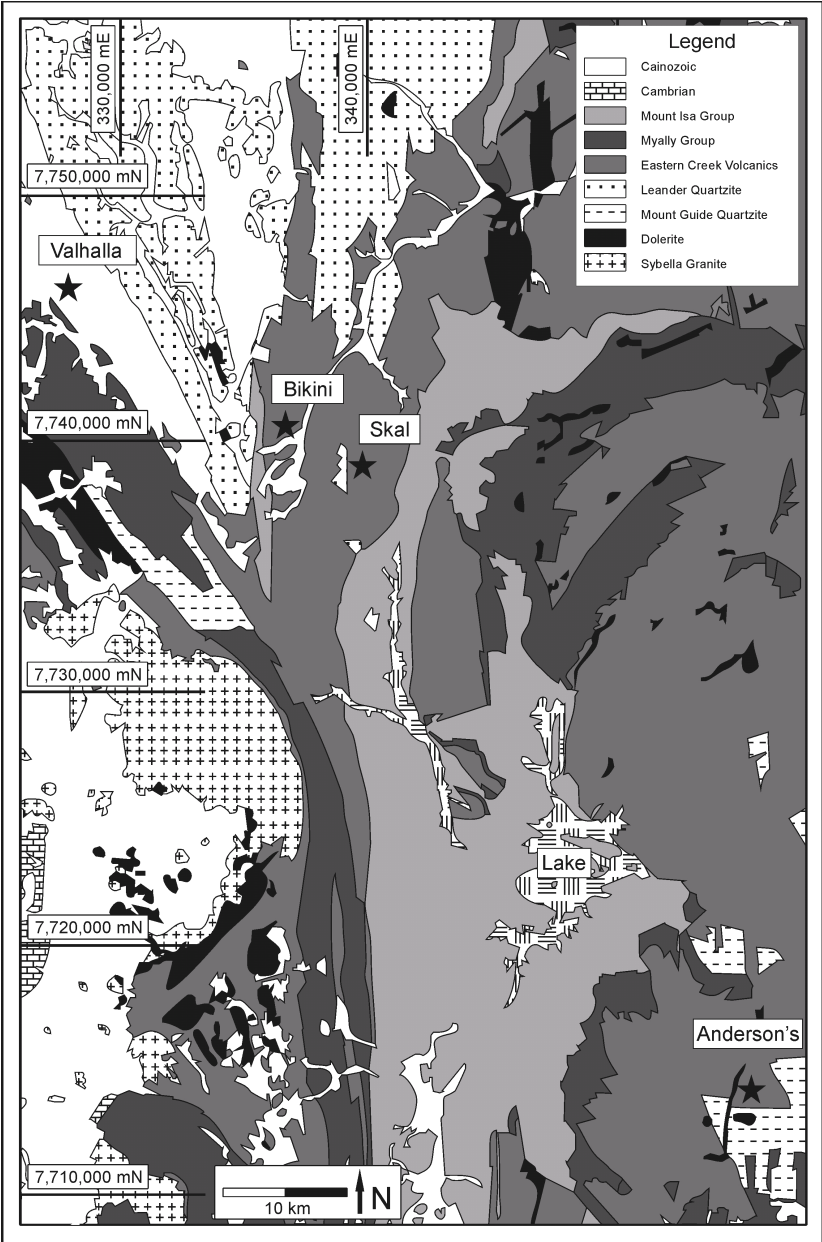


FIG. 2. Regional geology of the Mount Isa North Block [4].

The Haslingden Group rocks were intruded by the Sybella Granite at 1 670 Ma, resulting in extensive contact metamorphism of the Eastern Creek Volcanics. The Mount Isa Group unconformably overlies the Haslingden Group, and consists of carbonaceous and dolomitic siltstones, mudstones and shales. The 1 655 Ma Urquhart Shale of the upper Mount Isa Group hosts the world-class Mount Isa Cu and Pb-Zn-Ag deposits. The Mount Isa region was deformed during the Isan Orogeny from 1 620 to 1 520 Ma, with at least three major deformation events. The D2 event was the most widespread with E-W compression producing N-S-striking upright folds and N-S cleavage. D3 deformation produced NW folds and ductile shears, and reactivation and dilation of older structures.

The Eastern Creek Volcanics are exposed over an area of 150 km N-S by 40 km E-W, with a maximum thickness of 7 km. The sequence is divided into three members: Lower Cromwell Basalt, Lena Quartzite and Upper Pickwick Basalt. Basalt flows have a massive, fine- to medium-grained texture that fines upward into amygdaloidal zones and are locally capped by 2-4 m thick flow-top breccias. Cenozoic alluvial deposits cover 40-60% of the region. The Valhalla deposit is covered by 2-30 meters of laterite and saprolite, whereas Bikini, Skal and Andersons crop out as low ridges and hills.

### 3. Valhalla

Valhalla is classified as sodic and calcic metasomatised, albitite-hosted uranium deposit. Uranium mineralisation is hosted by a 30 to 80 m thick package of albitised basalts and interbedded sediments. Bedding dips to the SW at moderate to steep angles. Regional greenschist facies metamorphism is indicated by the presence of epidote, chlorite and calcite. Sodium and calcium metasomatism are respectively expressed as albite, riebeckite, dolomite and calcite.

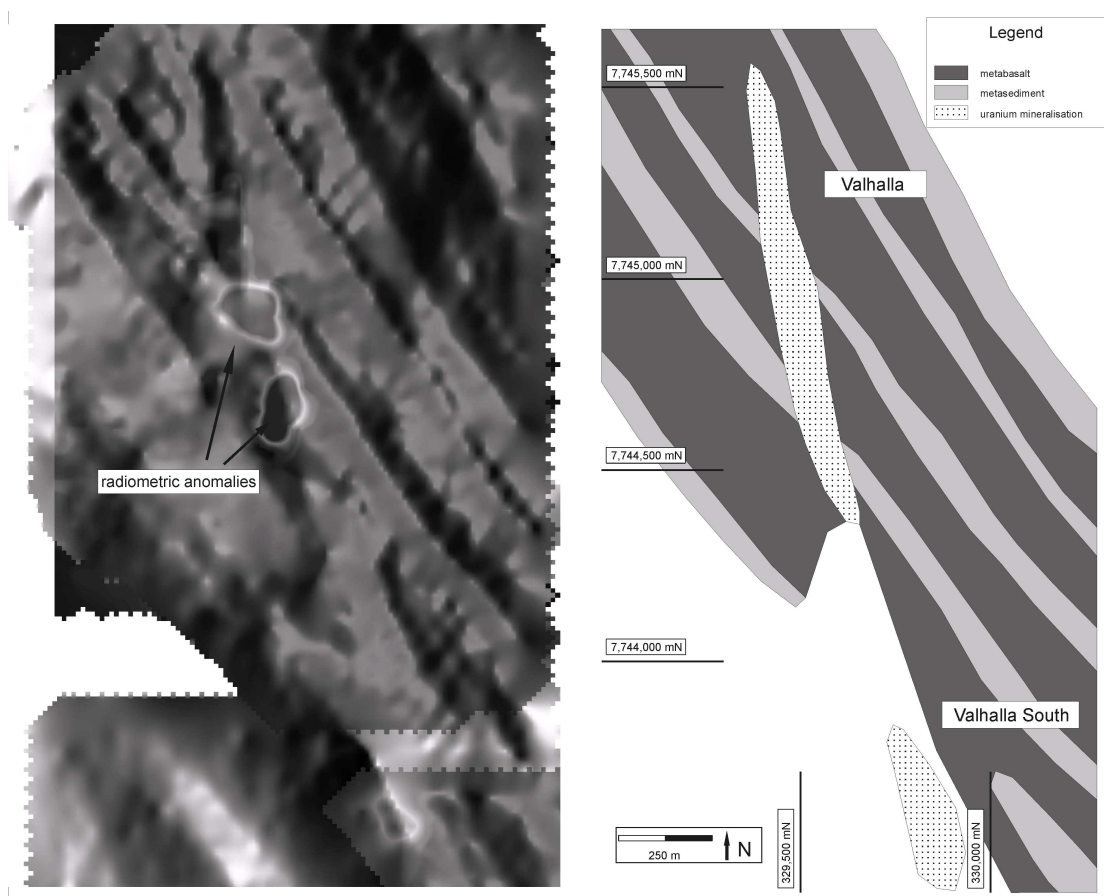
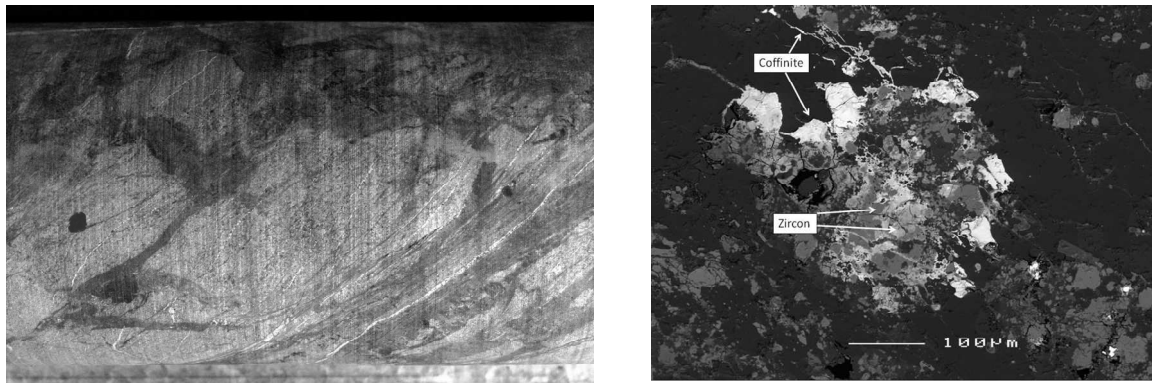


FIG. 3. The picture on the left shows magnetic and radiometrics. The right picture shows the interpreted geology.

The albite is typically accompanied by finely disseminated hematite, producing a characteristic red to pinkish red colour in mineralised zones. Mineralisation occurs along a NNW-striking shear zone. Importantly, the mineralised shear is about 20° oblique to the strike of bedding and is revealed in magnetic maps (Fig. 3). The main mineralised zone is up to 90 m wide, 1 km long and 650 m deep. The deposit geometry is cigar-shaped, which plunges at moderate angles to the SSE. There is a smaller mineralised zone, known as Valhalla South, located 700m SSE of the main body, with dimensions of 400 m long, 30 m thick and 150 m deep.

The albitites are characterised by the assemblage albite – carbonate – hematite. This alteration is marked by grain size reduction and the replacement of quartz, Fe-Mg-silicates and magnetite. The main uranium mineralisation coincides with the brecciation of the albitites (Fig. 4). The clasts are frequently deformed resulting in a rod like shape. The matrix is commonly fine grained but can contain small veins and mineralised voids. The colour is usually dark red relating to hematite but can also be dark green due to epidote and aegirine content. The composition of the matrix is highly variable. It consists mainly of albite, epidote, aegirine, zircon, hematite, carbonate, magnetite and various opaques. The matrix can contain more than 1 wt% uranium and 9 wt% zirconium. The uranium mineralogy is dominated by coffinite, uraninite, brannerite and uraniferous zircon. It appears that zircon is the earliest phase (Fig. 4).



*FIG. 4. The left picture shows a typical ore breccia. The bright clasts are dominated by albite, the dark matrix is highly mineralised. The right picture shows a back scattered electron image of zircon that is partially replaced by coffinite.*

#### 4. Skäl

The Skäl deposits are located 8 km southeast of Valhalla (Fig. 1). The Skäl complex consists of four separate uranium deposits in an area of about 1 km<sup>2</sup>. The uranium mineralisation is associated with intensive albitised quartz-veins, basalts and sediments, which occur in the centre of up to 400 m long and 30 m wide shear zones. The angle between these shear zones and the bedding is up to 45° (Fig. 5). The plunge of the ore shoots are at moderate to steep angles. The quartz veins were formed prior to mineralisation, which were subject to intensive brecciation during metasomatism and mineralisation. The albitisation is characterised by the assemblage albite – carbonate – hematite. This alteration is marked by grain size reduction and the replacement of quartz, Fe-Mg-silicates and magnetite. The uranium mineralisation coincides with the brecciation of the quartz vein (Fig. 6). The matrix represents the pathways for the sodic and uranium rich fluid. The most intensively altered and mineralized zones are at lithological contacts.

The uranium mineralisation is generally very fine-grained and comprises brannerite, uraninite and coffinite. The uranium mineralisation is associated with iron oxide alteration consisting of magnetite, hematite, albite, biotite and stilpnomelane. Traces of pyrite are concentrated in the areas containing uranium mineralisation.

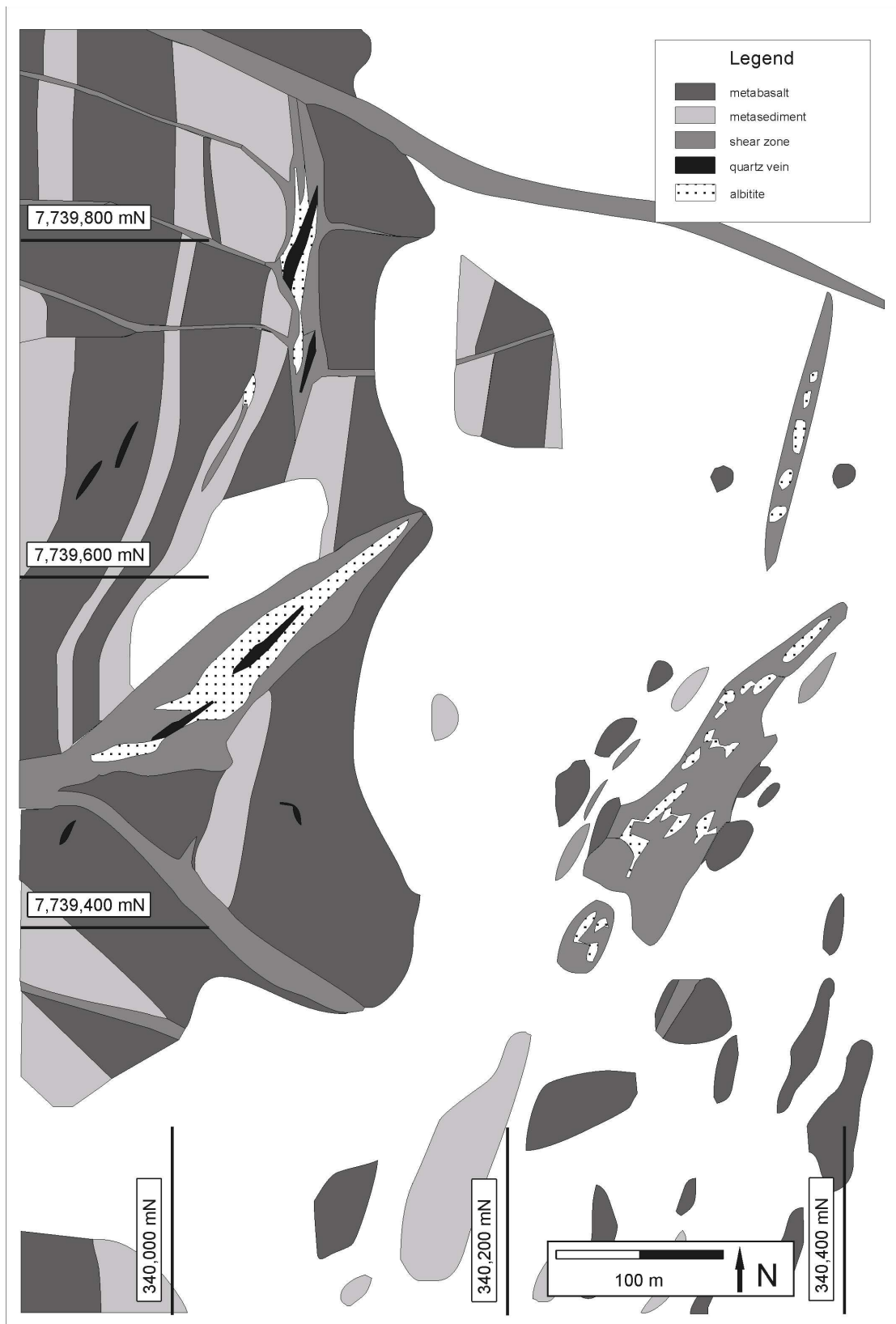


FIG. 5. Simplified geology of the Skal deposit.

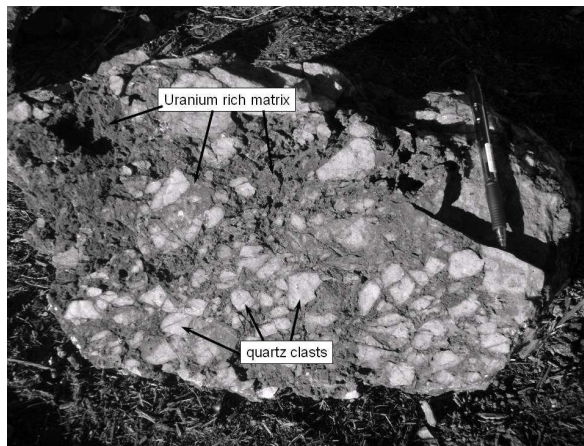


FIG. 6. Typical ore breccia from Skál.

## 5. Anderson's

Numerous north striking, mineralised shears cross cutting the stratigraphy (Fig. 7). The main uranium mineralisation is hosted by metasediments that dip at steep angles to the north. The ore body has a cigar-shaped geometry, which plunges with a steep angle to the east. It is parallel to the intersection lineation of the stratigraphy and the north striking shears. Uranium mineralisation is associated with sodic, calcic and phosphoric metasomatism.

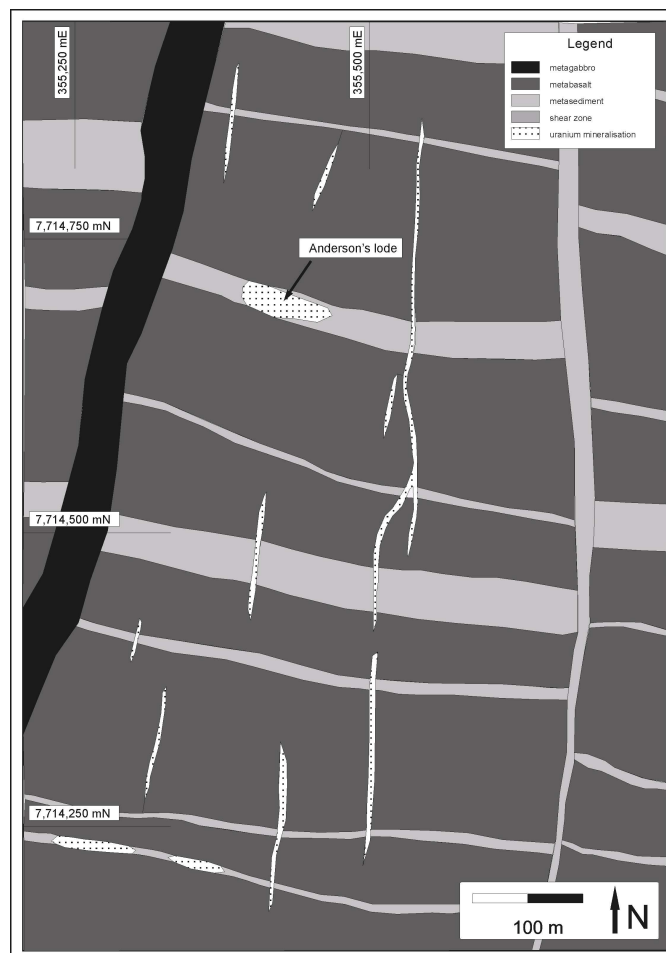


FIG. 7. Simplified geology of the Anderson's lode deposit.

## 6. Conclusions

The main host of uranium mineralisation in the Mount Isa North Block are the Eastern Creek Volcanics. Important factors for mineralisation are the high competency contrast between lithologies and the intersection angle between stratigraphy and mineralising structures. Anderson's lode has the highest grades but forms a steeply plunging and short strike length ore body due to the high intersection angle and thin north striking structures. Whereas Valhalla has a small intersection angle and a large northerly striking structure, which resulted in a moderately plunging and much larger ore body (Table 1.).

Table 1. Resources of the Mount Isa North Block

Deposit		Measured and Indicated Resources			Inferred Resources			Paladin Share
	Cut-off ppm U <sub>3</sub> O <sub>8</sub>	Mt	Grade ppm	t U <sub>3</sub> O <sub>8</sub>	Mt	Grade ppm	t U <sub>3</sub> O <sub>8</sub>	
Valhalla	230	27.80	891	24,765	7.3	799	5,863	91.0%
Skal	250				11.5	483	5,560	91.0%
Bikini	250				10.1	517	5,200	82.0%
Andersons	230				2.0	1,050	2,100	82.0%
Watta	230				4.2	410	1,720	82.0%
Duke Batman	250	0.5	780	388	1.6	630	1,016	100%
Honey Pot	250				2.6	700	1,799	100%
<b>Total</b>		<b>28.30</b>	<b>889</b>	<b>25,153 (55.4Mlb)</b>	<b>39.3</b>	<b>591</b>	<b>23,258 (51.2Mlb)</b>	
<b>Total Resource Attributable to Paladin</b>		<b>25.80</b>	<b>889</b>	<b>22,924 (50.5Mlb)</b>	<b>34.5</b>	<b>597</b>	<b>20,606 (45.4Mlb)</b>	

## REFERENCES

- [1] BLAKE, D.H., STEWART, A.J., "Stratigraphic and tectonic framework, Mount Isa Inlier" (STEWART, A.J., BLAKE, D.H., Eds), Detailed studies of the Mount Isa Inlier, AGSO bulletin 243 (1992) 1-11.
- [2] BETTS, P.G., et al., "Synthesis of the Proterozoic evolution of the Mount Isa Inlier", Australian Journal of Earth Sciences **53** (2006) 187-211.
- [3] BLAKE, D.H., Geology of the Mount Isa Inlier and environs, Queensland and Northern Territory. Bureau of Mineral Resources bulletin 225 (1987),
- [4] BMG, 1978, Kennedy Cap map 1 :10,000

# The main geological types of uranium deposits in Argentina

**L. López**

National Atomic Energy Commission (CNEA), Buenos Aires, Argentina

*E-mail address of main author: [lopez@cnea.gov.ar](mailto:lopez@cnea.gov.ar)*

**Abstract.** Several geological types of uranium deposits have been discovered in Argentina. The current uranium identified resources are 16,060 t U and belong to volcanic and caldera-related and sandstone-hosted models.

## 1. Introduction

The uranium - related activities in Argentina begun in the 1950s and, as a result of the systematic exploration, several types of deposits have been discovered since then: volcanic and caldera-related, sandstone-hosted, vein spatially related to granite (intragranitic and perigranitic) and surficial [1].

This paper briefly describes some examples and their contribution to the uranium resources of the country [2][3][4] (Fig. 1).

## 2. Geological types and resources

The deposits that have been exploited in the past belong to the volcanoclastic type localized in Permian formations associated with synsedimentary acid volcanism in the Sierra Pintada district (Mendoza province) [5][6]. From this deposit 1 800 t U were mined, and the current identified resources are 10 010 t U recoverable at a production cost below US\$130/Kg U [7].

Laguna Colorada deposit in the Chubut province [8] located in the San Jorge basin (Cretaceous) is volcanic and caldera related type, with evaluated resources of 100 t U [7].

Several important uranium occurrences have been identified in Cretaceous fluvial sandstones and conglomerates, among which the most significant is the Cerro Solo deposit (Chubut province) [9][10][11]. In this paleochannel structure, the mineralised lodes are 0.5 - 6 meters wide and 50 - 130 meters deep. The identified resources are 5 950 t U at 0.4 % U, included in the < US\$130/Kg U cost category [7].

Other subtypes of sandstone model have been studied. For instance, the Don Otto deposit (Salta province), located in the Salta Group Basin (Cretaceous - Tertiary), belongs to the tabular U-V subtype [12][13]. This deposit was mined from 1963 to 1980 and produced 270 t of U. The roll front subtype is found in the Los Mogotes Colorados deposit (La Rioja province) which is hosted by Carboniferous continental sandstones [14].

The uranium mineralisation is also found in the veins and disseminated episyenites within peraluminous leucogranites of the Sierras Pampeanas (Cordoba and San Luis provinces). These granites are Devonian - Carboniferous and the related deposits are comparable to those from the Middle European Variscan chain [15][16][17].

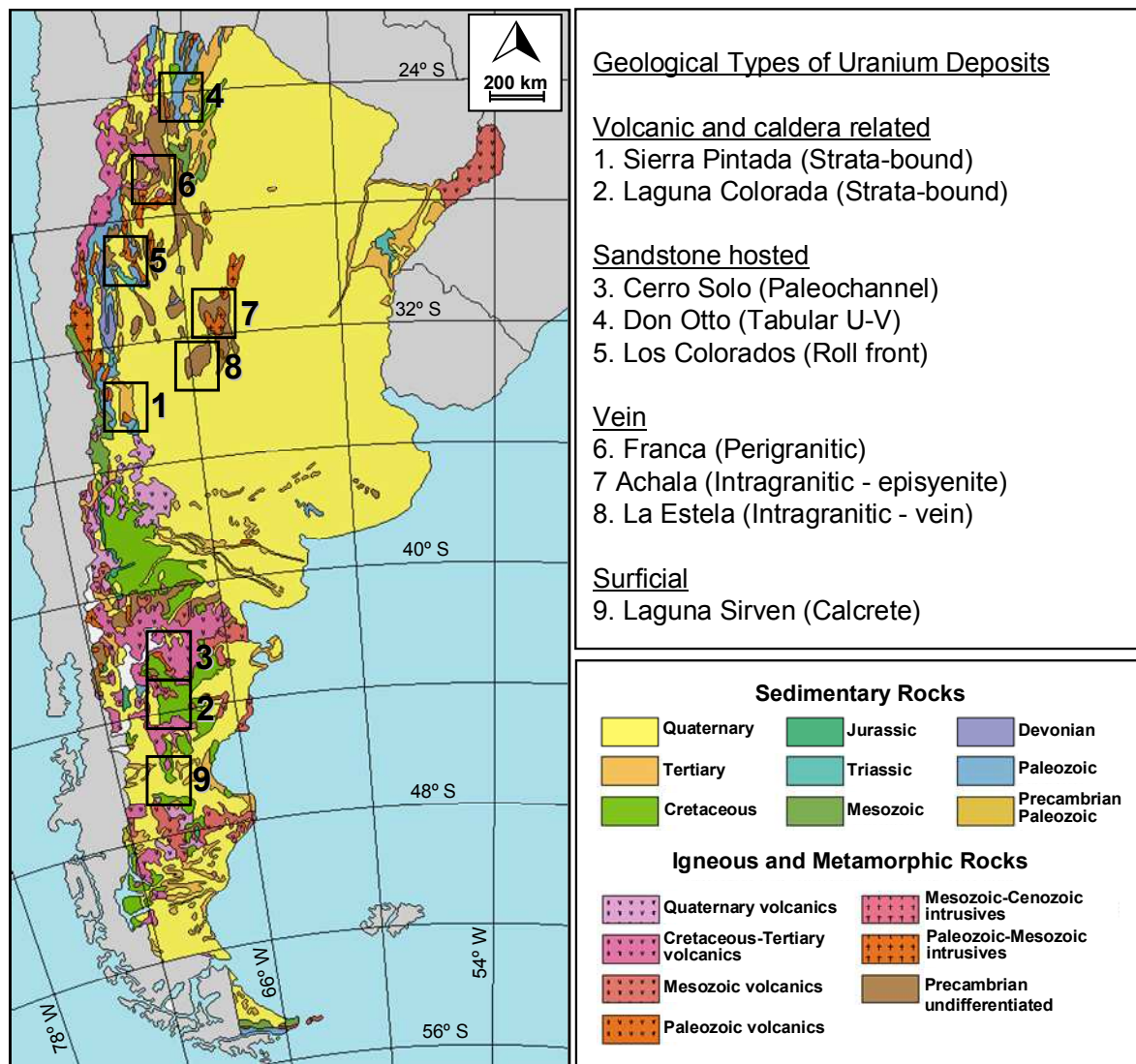


FIG. 1. Location map.

There is also another vein-type uranium deposit located in a metamorphic basement in the periphery of high potassium calcalkaline granites (Franca deposit, Sierras Pampeanas Noroccidentales, Catamarca province) [18][19]. The mineralisation control is mainly structural and the speculative resources have been evaluated with 1 500 t U at a grade of 0.3 % U.

More recently, the pedogenetic calcrete type has been studied in the area of Laguna Sirven (Santa Cruz province) [20][21]. The speculative resources here are about 1 000 – 1 500 t U at 200 ppm U.

### 3. Final considerations

It can be pointed out that the existence of favourable basins and different uranium mineralisation models provide promising conditions to explore new uranium resources. In this context, the uranium mineralisation related to continental sandstones and volcanic and caldera-related appear as the most interesting exploration targets, with current identified resources (16,060 t U) associated to these two models.

### ACKNOWLEDGEMENTS

This contribution attempts to sum up in a few words several studies that were conducted with funding from the National Atomic Energy Commission (Argentina). The author is grateful to his institution for

allowing its presentation. A very special thanks goes out to Kenneth Ford (Geological Survey of Canada) for his constructive suggestions and revising of the manuscript.

## REFERENCES

- [1] DALLKAMP, F., Uranium ore deposits, Springer-Verlag, Berlin (1993).
- [2] LÓPEZ, L., "Uranium favorability and exploration in Argentina", IAEA International Symposium on the "Uranium production and the raw materials for the nuclear fuel cycle – supply and demand, economics, the environment, and the nuclear security. Vienna (Austria), 20-24 June 2005 (CD-ROM) (2005).
- [3] LÓPEZ, L., "La exploración uranífera en Argentina", 16° Congreso Geológico Argentino. La Plata (Argentina), 20-23 September, Proceedings (CD-ROM) (2005).
- [4] LÓPEZ, L., CUNEY, M., "Les principaux types de minéralisations uranifères en Argentine". 22ème Réunion des Sciences de la Terre, Fédération Française de Géologie et de la Société Géologique de France, 21 – 24 avril 2008, Nancy, France. Recueil des Résumés: 577 (2008).
- [5] KLEIMAN, L., "Mineralogía y petrología del volcanismo permo-triásico del Bloque San Rafael en el área de Sierra Pintada, provincia de Mendoza, y su relación con las mineralizaciones de uranio", PhD Thesis, University of Buenos Aires, unpublished (1999).
- [6] SALVARREDI, J., "Yacimiento Doctor Bauliés y otros depósitos del distrito uranífero Sierra Pintada, Mendoza", In: E. Zapettini (Ed.), Recursos Minerales de la República Argentina. Anales N° 35 SEGEMAR (1999) 895-906.
- [7] SARDIN, P., "Tabulación de Recursos Uraníferos en Argentina", Comisión Nacional de Energía Atómica report, unpublished (2009).
- [8] FUENTE, A., GAYONE, M., "Distrito uranífero Laguna Colorada, Chubut". In: E. Zapettini (Ed.), Recursos Minerales de la República Argentina, Anales N° 35 SEGEMAR, p.p. 1253-1254 (1999).
- [9] BENÍTEZ, A., FUENTE, A., MALOBERTI, A., LANDI, V., BIANCHI, R., MARVEGGIO DE BIANCHI, N., GAYONE, M., "Evaluación de la Mina Nuclear Cerro Solo, Prov. del Chubut", XII Congreso Geológico Argentino, Proceedings T. V (1993) 272-278.
- [10] FUENTE, A., GAYONE, M., "Distrito uranífero Pichiñán, yacimientos Los Adobes, Cerro Cóndor y Cerro Solo, Chubut". In: E. Zapettini (Ed.), Recursos Minerales de la República Argentina, Anales N° 35 SEGEMAR (1999) 1255-1259.
- [11] BIANCHI, R., PÁEZ, M., "Tipificación y distribución de depósitos de uranio en la cuenca del Golfo de San Jorge", 16° Congreso Geológico Argentino, La Plata (Argentina), 20-23 September, Proceedings (CD-ROM) (2005).
- [12] GORUSTOVICH, S., "Metalogénesis del uranio en el Noroeste Argentino", PhD Thesis, University of Salta, unpublished (1989).
- [13] ROMANO, H., "Distrito Uranífero Tonco Amblayo, Salta", In: E. Zapettini (Ed.), Recursos Minerales de la República Argentina, Anales N° 35 SEGEMAR (1999) 959-970.
- [14] BELLUCO, A., NORIEGA, C., BRAGANTINI, J., "Yacimiento Los Mogotes Colorados, distrito uranífero Los Colorados, La Rioja", In: E. Zapettini (Ed.), Recursos Minerales de la República Argentina. Anales N° 35 SEGEMAR (1999) 767-772.
- [15] BLASÓN, R., "Yacimiento La Estela, distrito uranífero Comechingones, San Luis", In: E. Zapettini (Ed.), Recursos Minerales de la República Argentina. Anales N° 35 SEGEMAR (1999) 621-624.
- [16] ZARCO, J., "Estudio de los controles estructurales y magmáticos de indicios intragraníticos del batolito de Achala (Córdoba)", Comisión Nacional de Energía Atómica report, unpublished (2005).
- [17] ZARCO, J., ÁLVAREZ, J., "Trabajos de prospección realizados en los indicios intragraníticos del batolito de Achala (Córdoba)", Comisión Nacional de Energía Atómica report, unpublished (2005).
- [18] GUIDI, F., "Geoquímica y ambiente tectónico del granito Los Ratones, Catamarca", 14° Congreso Geológico Argentino, Salta, Proceedings 2 (1999) 163-166.
- [19] FERREIRA, L., ÁLVAREZ, J., GUIDI, F., SOLER, R., "Geología del área del área del depósito de uranio Las Termas, provincia de Catamarca", 16° Congreso Geológico

- Argentino, La Plata (Argentina), 20-23 September, Proceedings CD-ROM) (2005).
- [20] LOPEZ, L., KLEIMAN, L., ANDRADA, P., MALOBERTI, A., "Plan de trabajo para estudios de favorabilidad geológica y exploración uranífera en el ámbito de la provincia de Santa Cruz", Comisión Nacional de Energía Atómica - Fomicruz SE report (2005) (unpublished).
- [21] BENÍTEZ, A., PÁEZ, M. Informes de avance - Depósito Laguna Sirven, provincia de Santa Cruz, (2006 - 2009), Comisión Nacional de Energía Atómica report, unpublished (2005).

# Uranium prospecting in Uruguay

**W. Sierra<sup>a</sup>, A. Reyes<sup>a</sup>, R. Méndez<sup>a</sup>, P. Rossi<sup>b</sup>, S. Cardozo<sup>b</sup>, M. Muro<sup>b</sup>, A. Saizar<sup>c</sup>, A. Inchauspe<sup>d</sup>, J. Alberti<sup>d</sup>, W. Cabral<sup>e</sup>, H. Piano<sup>f</sup>**

<sup>a</sup> Department of Energy and Nuclear Technology - Ministry of Industry Energy and Mining, Montevideo, Uruguay

<sup>b</sup> Department of Geology and Mining - Ministry of Energy and Mining Industry, Montevideo, Uruguay

<sup>c</sup> Department of Environment - Ministry of Housing, Land Management and Environment, Montevideo, Uruguay

<sup>d</sup> Private Sector Department - Ministry of Economy and Finance, Montevideo, Uruguay

<sup>e</sup> Radioprotection National Regulator - Ministry of Industry Energy and Mining, Montevideo, Uruguay

<sup>f</sup> International Cooperation Department - Ministry of Industry Energy and Mining, Montevideo, Uruguay

**Abstract.** Uruguay, the smallest country of South America, without domestic reserves of fossil fuel but uses this source of energy to meet over 50 % of its energy requirements. In order to reduce the country's dependence on imported fuel, the Government of Uruguay gives high priority not only to the use of renewable energy resources, including biomass, wind and small hydropower but also to the exploration of new local energy sources including uranium. In 2007 prospecting for uranium resumed after seventeen years of inactivity. Presently Uruguay is analyzing the legal framework, making adjustments to the Mining Code and determining which entity will be acting as a governmental counter part for this activity. At the same time work is in progress for identifying areas for uranium exploration and establishing terms of references for future contracts with international companies interested in conducting exploration.. In this paper forty years of the uranium exploration history in Uruguay and the future directions are briefly described.

## 1. Introduction

### Background

Uruguay (33° S, 55° W) has a population of 3 241 003 inhabitants and a surface area of 176 220 square kilometers and is the smallest country in South America.

Uruguay has no fossil energy resources, but uses the fossil sources to meet over 50% of its energy requirements. This is supplemented by hydroelectric, biomass and other minor energy sources (Fig. 1) [1].

Uruguay depends on hydropower (installed capacity 1 538 MW) and on thermal power plants (presently about 1 100 MW). On an average, hydroelectricity supplied approx. 80% of the electricity demand. Due to erratic rainfall and droughts, combined with increasing energy demand, hydropower

production is no longer considered sufficient. At present, peak power demand is approx. 1 700 MW, growing 3% annually.

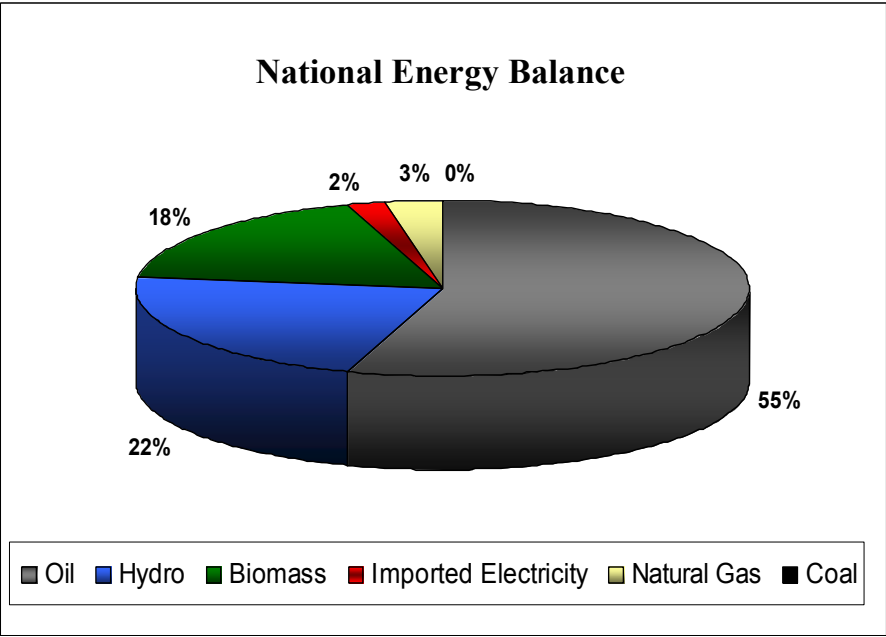


FIG.1. National energy balance 2007.

Since 2000, energy supply from Argentina and Brazil were negotiated as firm power and back-up contracts. However, the transmission capacity from Brazil is small (70 MW), while delivery from Argentina, based on the cheap supply of natural gas, reduced since 2004 due to the energy crisis in that country and the soaring price of natural gas.

In response, Uruguay's national electricity company (UTE), has reformulated the Expansion Plan 2006-2010 to add 500 MW new thermal capacity suitable for fuel-switching (natural gas and fuel oil), in order to match peak electricity demand and as a back-up when hydropower falls short. As part of this plan, the first 300 MW plant at "Punta del Tigre" has been brought online. The projected remaining 200 MW will consist of generators suitable for fuel oil, diesel and natural gas; an LNG regasification project is being considered to improve the reliability of gas supply.

In 2007-2008, UTE has also entered into power purchase agreements (PPAs) to buy electricity from cogeneration units operated by the large paper mills operating in the country. While UTE's average production costs remain fairly low due to the large share of hydro base power, the marginal generating costs are estimated at US\$ 200-280 per MWh, depending on the reference oil price.

In order to reduce the country's dependence on imported fuel, the Government of Uruguay gives high priority not only to the use of domestic energy resources, including biomass, wind and small hydroenergy but also to the exploration of new local energy sources including uranium [2].

The use of domestic energy resources is one of the main pillars of the energy strategy of the Government of Uruguay. The National Electricity Law No. 16.832 provides a framework for an open market, allowing private operators access the grid (1997). It is significant that the Nuclear Power in Uruguay is prohibited by Article 27 of the above mentioned Law [3].

## 2. History of uranium exploration in Uruguay

### 1949 to 1989

Uranium prospecting in Uruguay, began in 1949 as a government investigation. During 40 years were developed in an ongoing activity and it is possible differentiate four distinct phases in terms of:

- i) Systematic of efforts
- ii) Methodology
- iii) Infrastructure and provision of Human Resources
- iv) Source of investment

*Table 2 details the 4 different stages and the characteristics of them.*

Table. 2. Phases of prospective uranium in Uruguay from 1949 to 1989

	Systematic	Methodology	Infrastructure	Investment
1949-1959	Isolated projects	ANCAP-UTE (gov)	ANCAP-UTE(gov)	ANCAP-UTE(gov)
1964-1975	1966/1971-1974	OIEA-CNEA.U	Not specific	Quite low
1976-1983	1976-1979/1981-1983	OIEA-CNEA.A-BRGM	IGU- DINAMIGE	DINAMIGE(gov)
1986-1989	1986-1989	OIEA-DINAMIGE	DINAMIGE(gov)	DINAMIGE(gov)

As a results of activities carried out from 1949 to 1989 was possible acquire the following information:

- i) Systematic geological information base
- ii) Identification of priority areas

Figures 3 and 4 show the main information associated with the development of this first Phase.

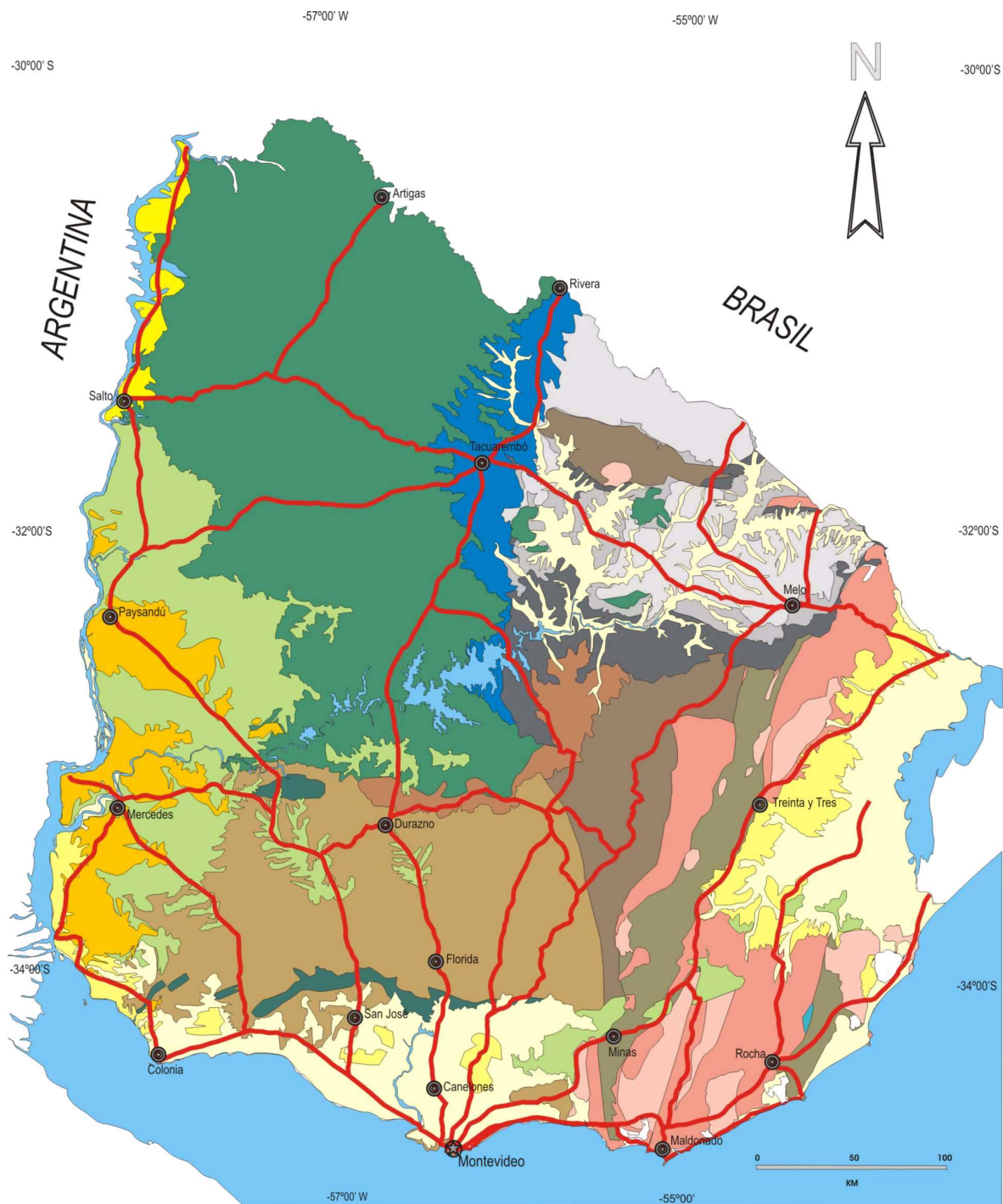
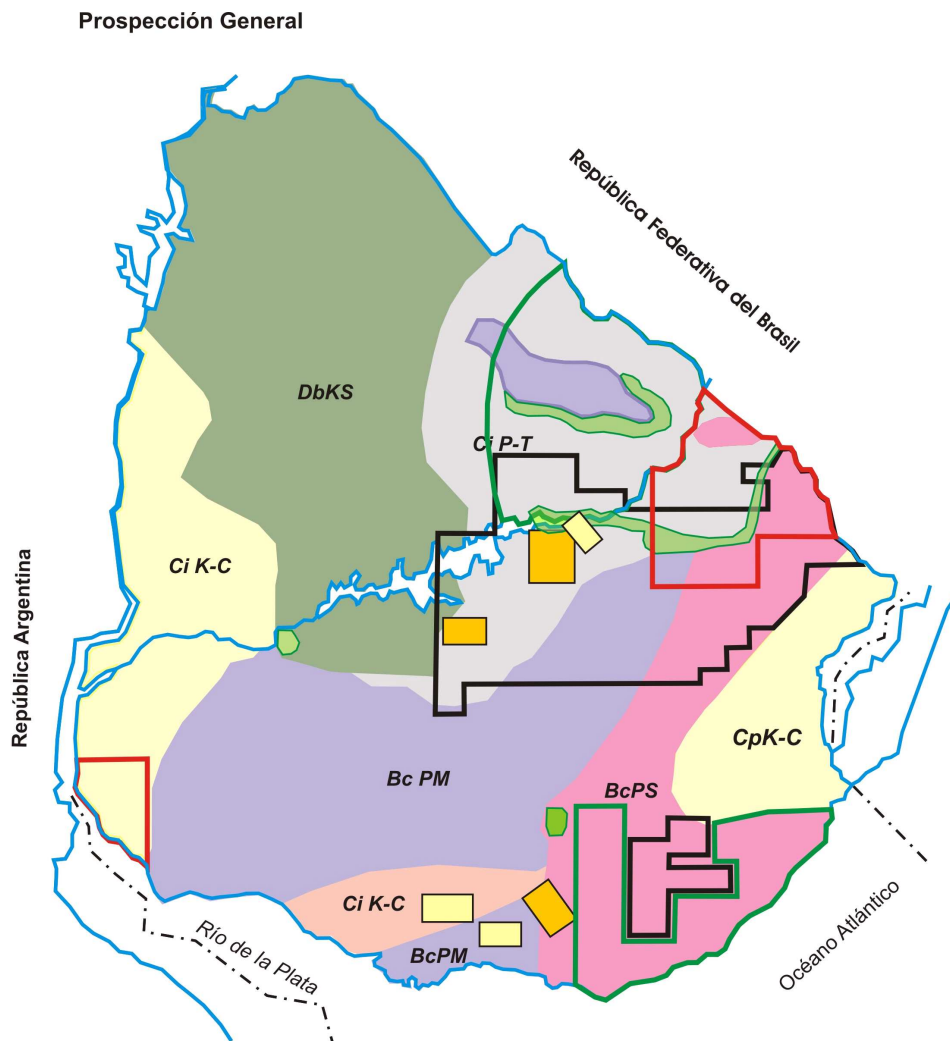


FIG. 3. Geological information – Uruguay.

## 2007 onwards

After seventeen years of inactivity in this field, the decision to resume uranium prospecting activities in Uruguay was taken. By the order of the President of the Republic a "call for expressions of interest in the conclusion of contracts for prospecting, exploration and exploitation of uranium ore in the national territory" was carried out. Several bids were received from leading international companies which were assessed [4].

In the year 2008 an interdisciplinary group composed by the Department of Energy and Nuclear Technology, the Department of Mining and Geology, the National Radiation Regulatory Authority, the Department of Environment and the Ministry of Economy and Finance was established.



### Referencias

CEA 1965 Misión Grimbert (Rct. autoportada, geoquímica)	BRGM 1981-1983. (Rct/e autoportada)
CNEA-U 1966. (Rct autoportada)	BRGM 1981-1983. (Geoq.estratégica-trazas).
CNEA-U 1971 -1974 (Rct autoportada)	
I.G.U - 1976 -1979 (Rct aeroportada)	
CpK-C Cuenca pericratónica Cretácico - Cenozoica	CiK-C Cuenca intracratónicas Cretácico - Cenozoica
Ci P-T Cuenca intracratónica Permo -Triásica	DbKS Derrames basálticos Cretácico Superior
BcPM Terrenos cristalinos Precámbrico Medio	BcPS Terrenos cristalinos Proterozoico Superior

FIG. 4. Overview of uranium exploration in Uruguay.

The main goal of this group is to set up the basis for the bidding activities related to prospecting, exploration and exploitation of uranium in Uruguay [5].

This group has defined two stages in this activity:

- 1) Prospecting
- 2) Exploration and exploitation

Competitive bidding phase for prospecting activities is expected in the second half of 2009.

### **3. Ongoing activities**

Presently the following activities are on track:

- i) Analyzing the adequacy of the legal framework and making adjustments to the Mining Code [6].
- ii) Identifying areas that will be taken up for Prospecting.
- iii) Determining the government entity that will be acting as a counter part of this activity.
- iv) Establishing terms of references for future contracts with companies interested in conducting prospecting, exploration and exploitation of uranium.

### **ACKNOWLEDGEMENTS**

International Atomic Energy Agency (IAEA) - Project RLA/3/006: "Strengthening regional capabilities for uranium mining, milling and regulation of related activities".

### **REFERENCES**

- [1] "National Energy Balance 2007", DNETN-MIEM, Montevideo, Uruguay, (2008).
- [2] "Energy Policy 2005-2030," DNETN-MIEM, Montevideo, Uruguay (2008).
- [3] "National Electricity Law ", Law N° 16.832, June 1997, Montevideo, Uruguay.
- [4] "Call for expressions of interest in the conclusion of contracts for Prospecting, Exploration and Exploitation of Uranium ore in the national territory", Presidential Resolution, May 2007, Montevideo, Uruguay.
- [5] "Creation of the Working Group for drafting bid specifications for the activities of Prospecting, Exploration and Exploitation of Uranium in Uruguay", Presidential Resolution March 2009, Montevideo, Uruguay.
- [6] "Mining Code"- Law N° 15.242, October 1982, Montevideo, Uruguay.

# Uranium and REEs resources in South Eastern desert of Egypt

**M. E-A. Ibrahim**

Nuclear Materials Authority, Egypt

*E-mail address of main author: dr\_mahmadi@yahoo.com*

**Abstract.** Egypt started prospecting and regional exploration for radioactive raw materials since several decades. This resulted in the discovery of some low grade U- occurrences which are related to various geologic formations such as; vein-type (G. El-Missikat), metasomatised granites (G. Um Ara), shear zones in calc-alkaline granite and inter-mountain basin (G. Gattar) and surficial type uranium deposit in sedimentary rocks (Sinai). In 2002, NMA exploration activities in the South Eastern Desert resulted in the discovery of a) hot paragneiss (Abu Rusheid area) cut by discontinuous shear zones and b) metamorphosed sandstone-type uranium deposits (Sikait area). Abu Rusheid- Sikait area (ASA) is located at the South Eastern Desert, 50 km southwest of Marsa Alam from the Red Sea coast. Two nappes are seen; ophiolitic nappe (mafic– ultramafic rocks) and arc assemblages nappe (metapelites, cataclastics, metavolcanics and tonalite rocks) separated by mélange rocks. ASA is traversed by channel-ways represented by strike slip faults (ENE-WSW, NNW-SSE, N-S and NNE-SSW) and post- magmatic activities (lamprophyre -dykes). The cataclastic rocks in Abu Rusheid (3 km<sup>2</sup>) are intruded by hot and depleted granites (highly fractionated calc- alkaline granites and peraluminous granites respectively). The cataclastics are classified into protomylonite, mylonite, ultramylonite and quartzite with gradational contacts. Quartzite are exposed in two locations at Sikait area: the first one elongated NW-SE (1.8 km in length, 100-400 m in width) whereas the second one covers 0.5 km<sup>2</sup>. Hot highly fractionated calc- alkaline granites (U ranges from 20-50 ppm) intrudes and surrounds the quartzite. Two brecciated discontinuous shear zones (NNW-SSE and ENE - WSW) crosscut the cataclastic rocks. Lamprophyre dykes (0.5-1.0 m in width, 0.5-1.0 km in length) with REEs, Zn, U, Cu, Sn, W, Ni & Pb mineralization are emplaced along the shear zones. Uranium contents range from 500-1 500 ppm. Uranium minerals (uranophane and beta-uranophane, kasolite, torbernite, autunite and meta-autunite), sulfides and molybdenite are common in quartzites and lamprophyre dykes, whereas uranophane and uranothorite coating in the foliation planes are common in Abu Rusheid cataclastic rocks. The lamprophyres have abnormal abundance of REEs (up to 1.5%) with average  $\Sigma\text{LREE}/\Sigma\text{HREE}$  ratio equal to (0.14). The HREE enrichment is attributed to heavy minerals (e.g. xenotime, fergusonite, zircon and fluorite). The lamprophyre is characterized by reverse fractionated REE patterns [(La/Yb)<sub>N</sub>= 0.12] and pronounced negative Eu anomalies (Eu/Eu\* = 0.08) with HREE enrichment [(Gd/Lu)<sub>N</sub>= 0.80]. The lamprophyres are mantle derived and enriched in CO<sub>2</sub> and volatiles. Alteration processes in lamprophyres (illite, smectite, hematitization, sulfidization, silicification and flouritization) acted as physical and chemical traps for the mineralization.

## 1. Introduction

The common Egyptian uranium occurrences are mainly: vein-type (G. El-Missikat), metasomatised granites (G. Um Ara), shear zones in calc-alkaline granite and inter-mountain basin (G. Gattar) and surficial type U-deposit in sedimentary rocks (Sinai). In 2002, NMA exploration activities for uranium resources were focusing on the South Eastern Desert of Egypt; these works resulted in the discovery of both; a) hot paragneisse (Abu Rusheid area) cut by discontinuous shear zones and b) metamorphosed sandstone-type uranium deposits (Sikait area).

Abu Rusheid area has been studied by many authors such as [1][2][3][4]. They consider the rocks of Abu Rusheid area are of sedimentary origin (psammitic gneiss). Ibrahim et al. [5] classified these rocks into cataclastic (protomylonites, mylonites, ultramylonites and silicified ultramylonites).

Lamprophyres can be divided into calc-alkaline and alkaline lamprophyres. Calc-alkaline lamprophyres are generally characterized by large absolute contents in REE and other incompatible trace elements as well as strong LREE enrichment suggesting in some cases a genetic link among these types [6]. Lamprophyres are fine-grained hypabyssal rocks, occurring typically in thin dykes or sills. They are strongly porphyritic, with mafic silicates occurring in euhedral crystals of two generations; feldspars are confined to a fine-grained groundmass, but sometimes are found as phenocrysts. Chemically lamprophyres have low SiO<sub>2</sub> (mostly 40 to 47 %), high (MgO + FeO) and (Na<sub>2</sub> + K<sub>2</sub>O) [7].

In 2002, the Nuclear Materials Authority started studying the Abu Rusheid area through project. No previous studies have been carried out on the shear zones hosted lamprophyre bearing-REEs and U in Wadi Abu Rusheid, as well as the new discovery of quartzite rocks at Wadi Sikait, before the project.

## 2. Geologic setting

Abu Rusheid-Sikait granitic pluton elongated in NW-SE (12 km long) and thinning in NE-SW (3 km width) forms a lozenge shape or fish eye-like shape (Fig. 1). The southern part of the pluton is surrounded by layered metagabbros taking the trail of pluton shape. The opposite trend of the granitic pluton (NW) is thinner giving rise to the tip of pluton shape. The metamorphosed sandstones are represented the cap rock for the cataclastic rocks (occupy the core of granitic pluton) and also cover the western part of Sikait upstream (400 m in width, 2 km in length) in the form of boat float on porphyritic granite. The fish eye-like shape is surrounded by mafic ultramafic rocks (meta-peridotites, serpentines, talc carbonate, metapyroxenites and metagabbros) and seem to be a closed basin. The mafic ultramafic rocks are thrust over the ophiolitic mélange. Recumbent folds are common at the contact surface (thrust plane) between the over-thrust rocks and the down thrust ones. Sikait area is traversed by strike slip faults trending NNW-SSE, WNW-ESE and NE-SW.

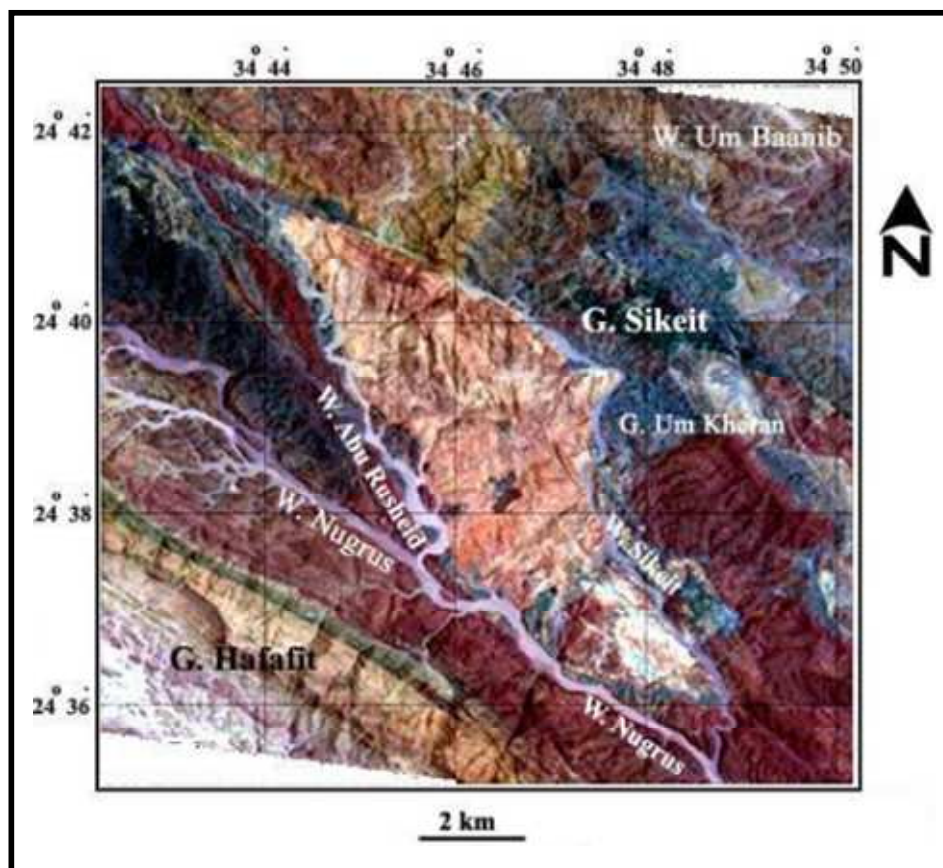


FIG. 1. Landsat image (TM, band 7, 4, 2) for Abu Rusheid – Sikait area, South of Eastern Desert, Egypt.

## A- Abu Rusheid area

The tectonostratigraphic sequence of the Precambrian rock units of Abu Rusheid area (Fig. 2) are arranged as follows: (1) Ophiolitic mélangé, consisting of ultramafic rocks and layered metagabbros set in metasediment matrix; (2) Cataclastic group, consisting of protomylonites, mylonites, ultramylonites and silicified ultramylonites; (3) Mylonitic granites; (4) Post-granite dykes and veins [8].

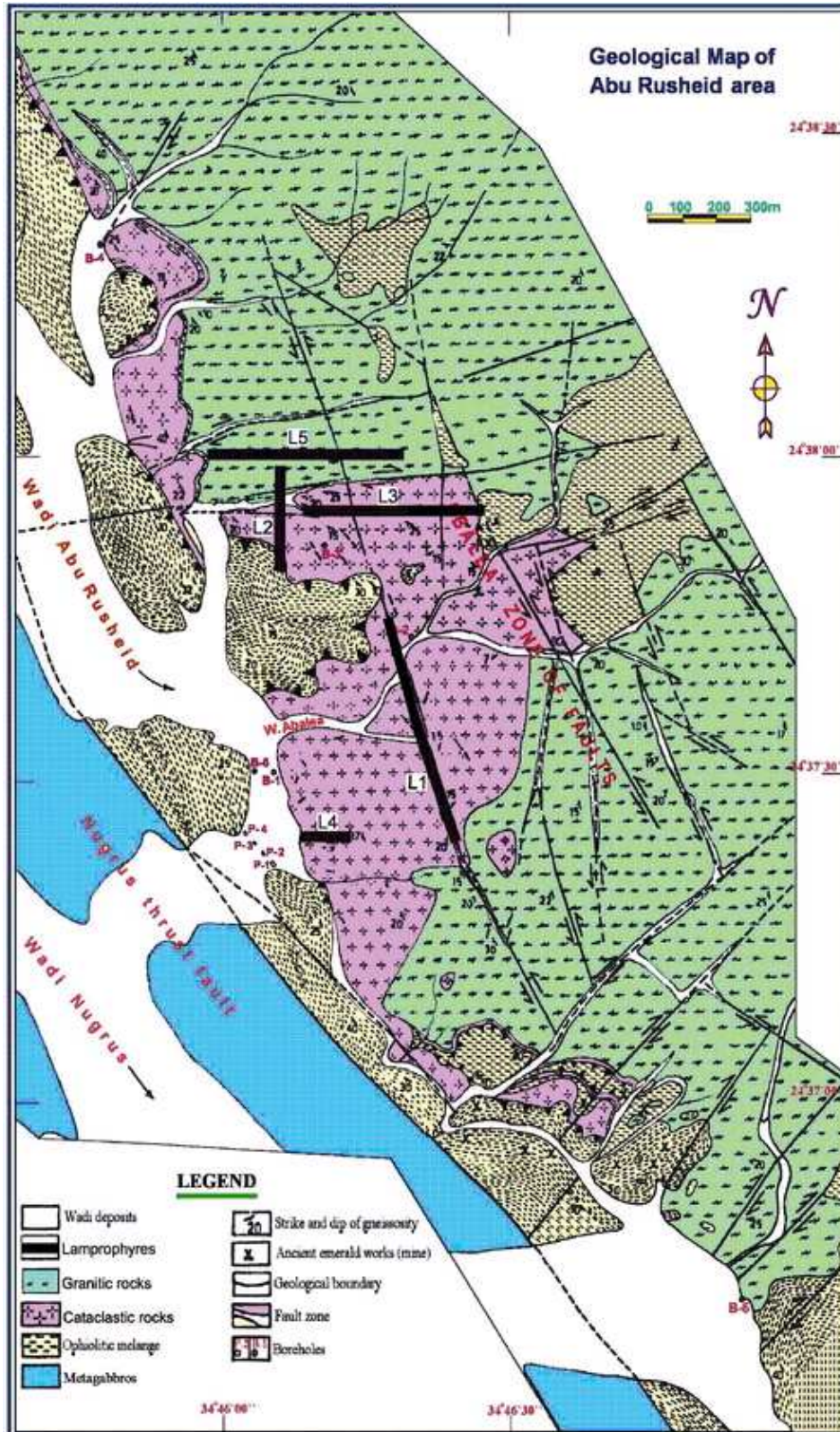


FIG. 2. Geologic map of Abu Rusheid area, South of Eastern Desert, Egypt.

The layered metagabbros are thrust over ophiolitic mélange. Recumbent folds are common at the contact surface (thrust plane) between the over-thrust ophiolitic mélange and the down-thrust cataclastic rocks. Abu Rusheid area is traversed by strike slip faults trending ENE-WSW, NNW-SSE, N-S and NNE-SSW. The main varieties which constitute the cataclastic rocks (3 km<sup>2</sup>) are: a) protomylonite, b) mylonite, c) ultramylonite and d) silicified ultramylonite (quartz >90 in vol. %) with gradational contacts. The cataclastic rocks of Abu Rusheid area are highly sheared, banded, highly gneissose (N-S) and characterized by bedding –parallel digenetic foliations defined by elongate detrital quartz cross-cut by perpendicular shear zones (NNW- SSE and ENE-WSW). The shear zones are discontinuous, brecciated, highly tectonized and dissected by strike–slip faults with a minor displacement (Fig. 3). The lamprophyre dykes vary in their composition and are intruded by pegmatite pockets and quartz vein. Zinc, copper, sulfides, fluorite, smectite-kaolinite, goethite, magnetite, limonite, hematite and manganese dendrites are present as thin films along fractures planes and boxworks in lamprophyre clarify the epithermal events and reducing regime. Many boxworks are formed as a result of leaching processes and are filled by calcite, secondary quartz and base metals (Fig. 4).

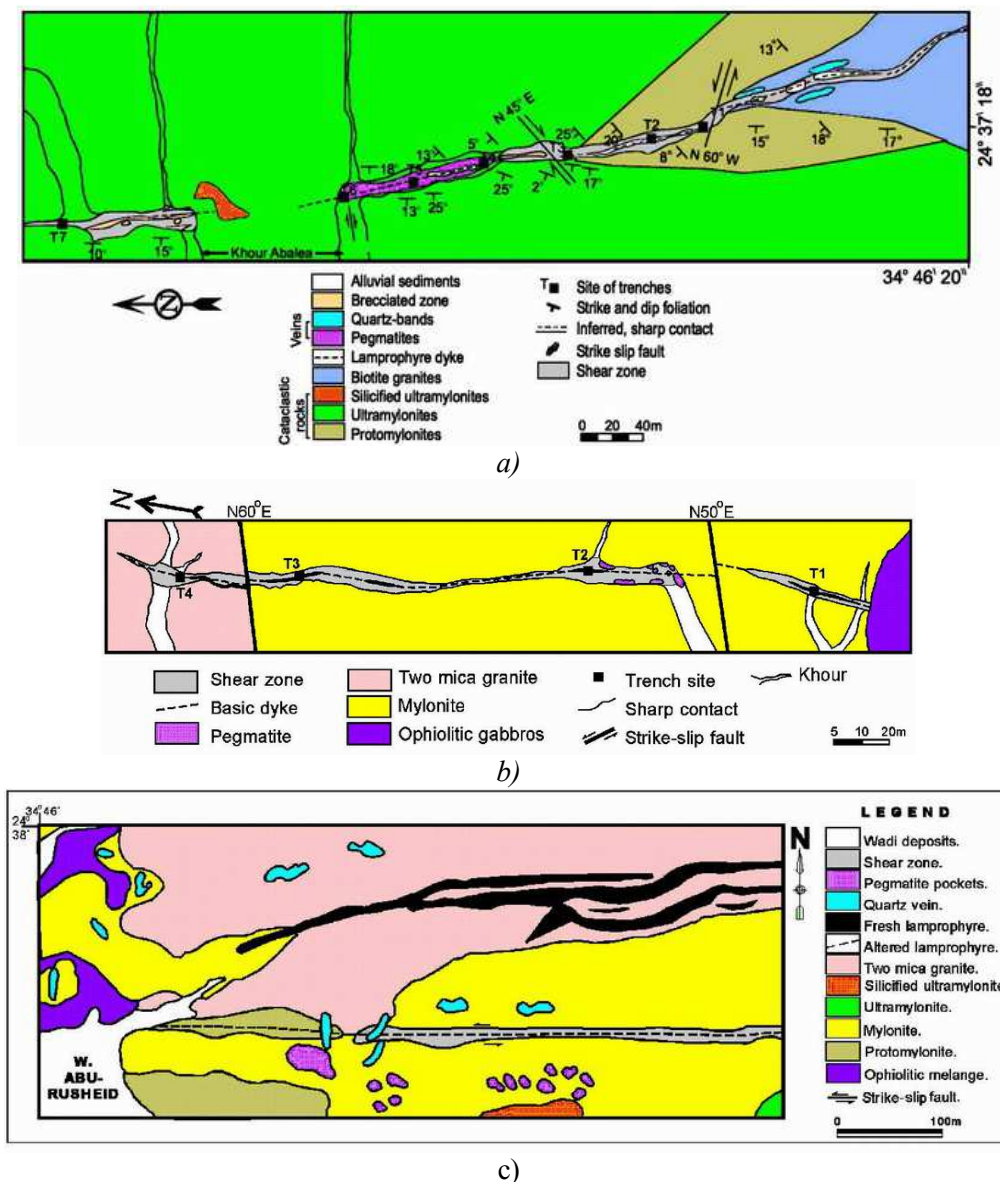
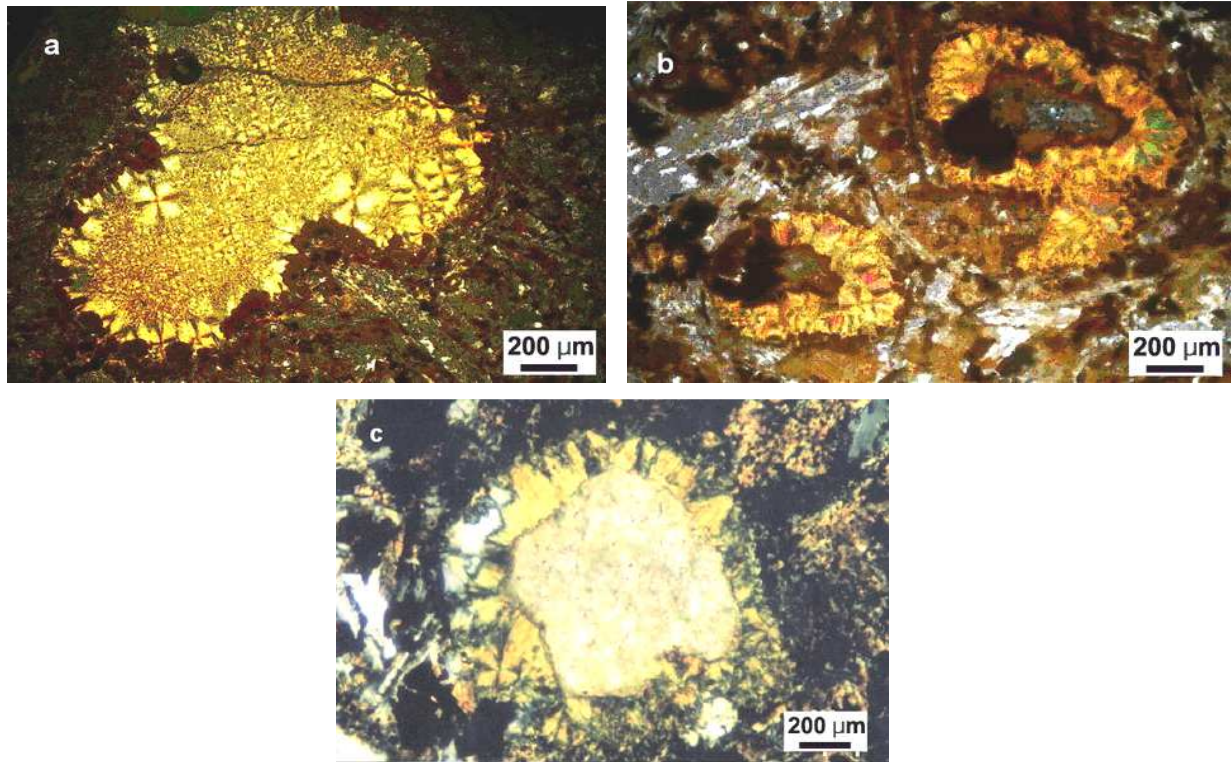


FIG. 3. a) Detailed geologic map of lamprophyre (L1), Abu Rusheid area; b) Detailed geologic map of lamprophyre (L2), Abu Rusheid area; c) Detailed geologic map of L3 (altered) and L5 (fresh) lamprophyre dykes, Abu Rusheid area.



*FIG. 4. View showing boxworks filled with (a) radial secondary U-minerals, (b) corona texture include from inner to outer: calcite, hematite and secondary U-minerals and (c) carbonate surrounded by secondary U-mineral in N-S lamprophyres.*

Table 1 represents paragenetic diagram of primary and secondary minerals in cataclastic rocks and lamprophyres modified after [9].

Microscopically, lamprophyre is mainly composed of plagioclases, amphiboles, phlogopite, relics of pyroxenes and K-feldspar phenocrysts embedded in fine-grained groundmass. Xenotime, fluorite, chlorite and opaques are accessories. Carbonate, quartz, jarosite, pyrite, epidote, sericite and clay are secondary minerals. Pyrite is easily oxidized by ground water in the presence of oxygen to produce either ferric oxide or its hydrate analogy.

### **Uranium Map**

All U-contents more than 200 ppm are excluded. The ophiolitic *mélange* rocks have eU-content less than 1 ppm, whereas Wadi deposits and mylonitic two mica granites ranges from 8-30 ppm eU. The cataclastic rocks are characterized by extremely high eU-contents reaches its maximum values (>210 ppm up to 1 500 ppm) (Fig. 5). The uranium anomalies trends follow the main structural trends within the cataclastic rocks (E-W and N-S fault zones).

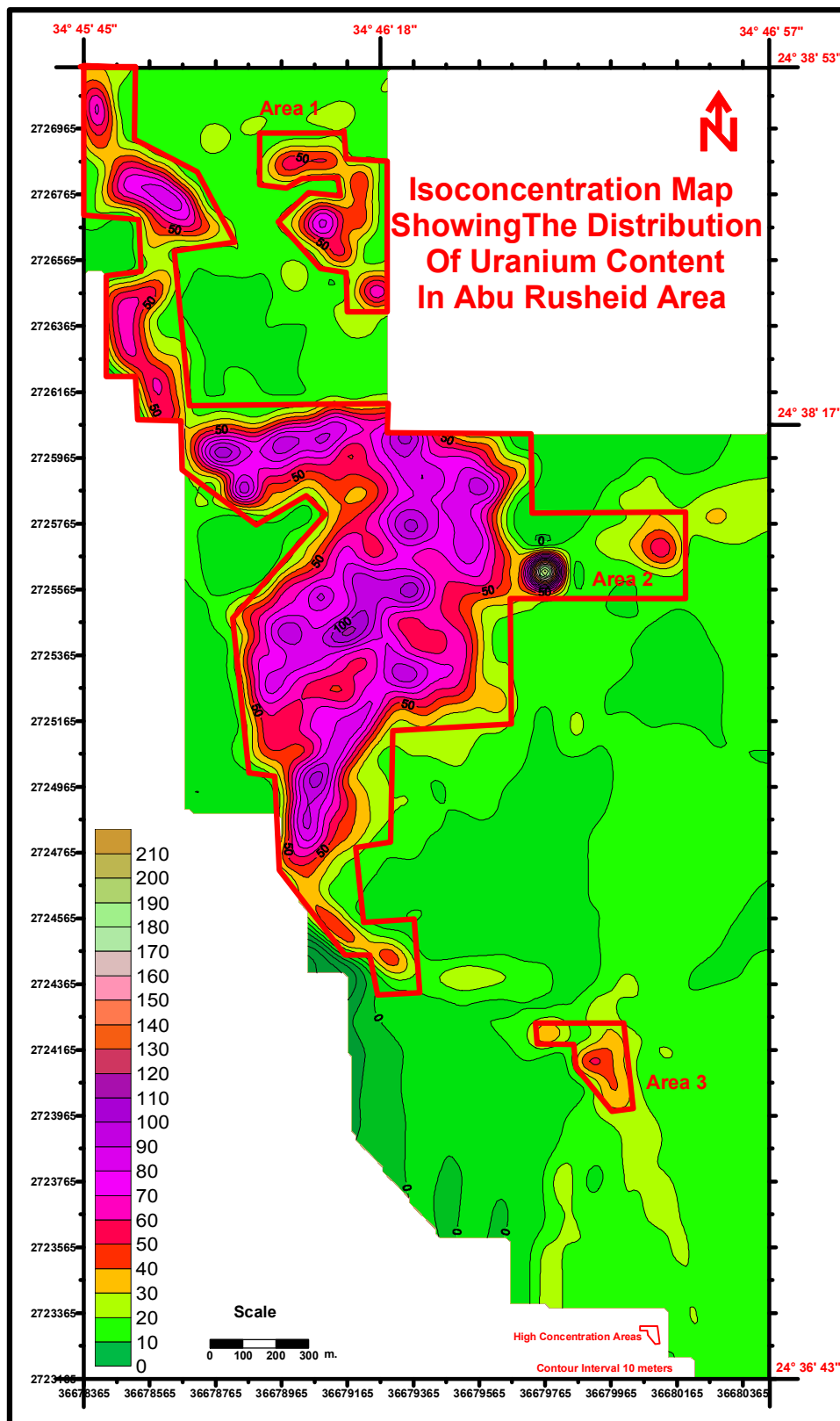


FIG. 5. Isoconcentration map showing the distribution of eU-contents in Abu Rusheid area.

### Thorium Map

All Th-contents more than 700 ppm are excluded. The eTh-contents vary within the cataclastic rocks, where it increases from ultramylonites through mylonites to protomylonites (50 - >650 ppm). The thorium surface distribution map (Fig. 6) was useful in defining thorium enrichment zones. These zones are recommended as follow-up targets for potential heavy rare metals deposits.

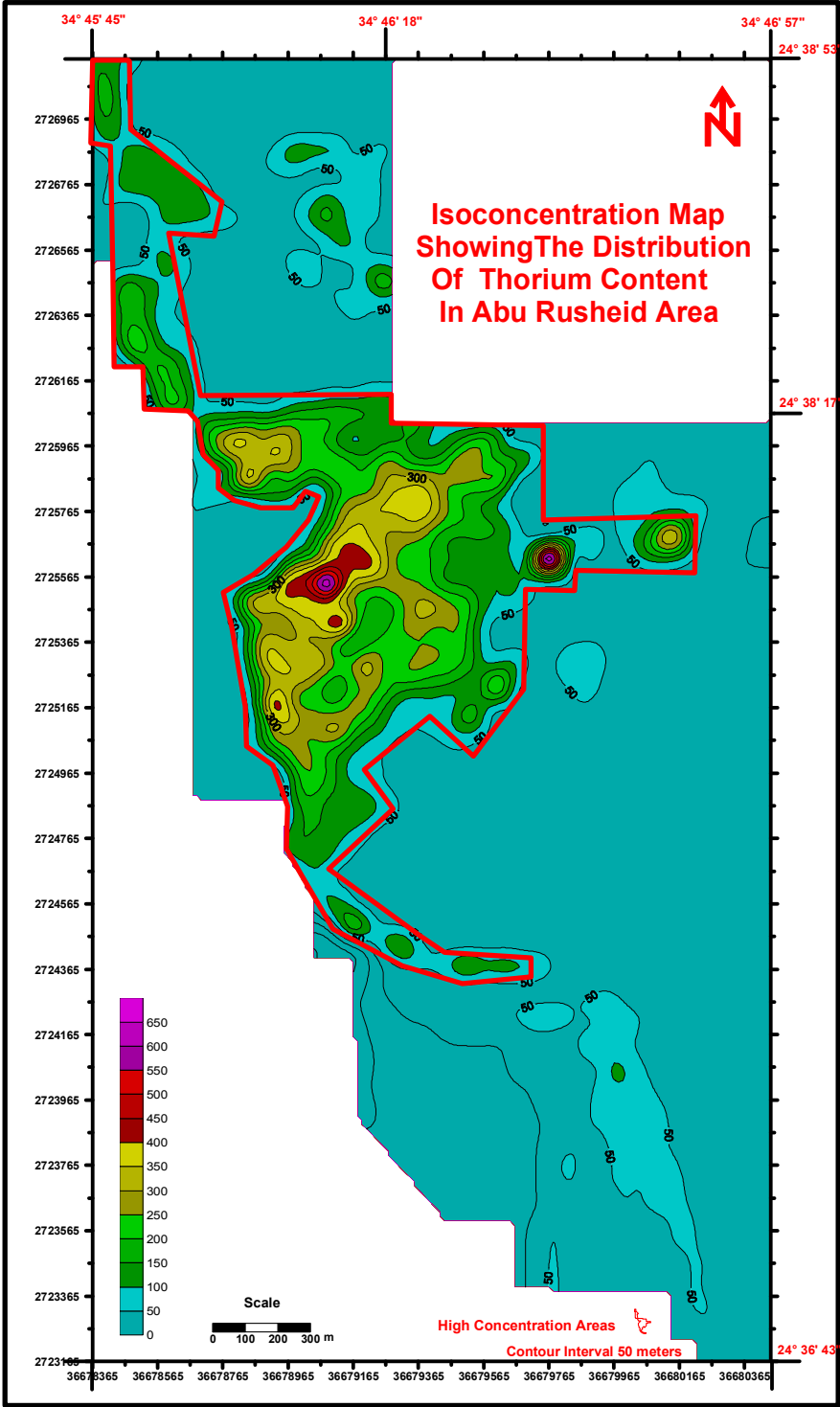


FIG. 6. Isoconcentration map showing the distribution of eTh-contents in Abu Rusheid area.

The cataclastic samples show moderately ( $Eu/Eu^* = 0.11$ ) whereas the lamprophyre samples show low value ( $Eu/Eu^* = 0.08$ ). The  $\Sigma LREE/\Sigma HREE$  (Table 2) is enriched in cataclastic rocks (0.47) compared with lamprophyres (0.14) and wall zone (0.33). The HREE enrichment is attributed to some heavy minerals (e.g. xenotime, astrocyanite, fergusonite, zircon and fluorite), whereas LREE enrichment is related to the presence of allanite and monazite.

Table 1. Paragenetic diagram of primary and secondary minerals in cataclastic rocks and lamprophyres modified after [9][10][11].

Minerals	Stage	Cataclastic rocks	AL			Primary mineralization	Secondary mineralization
			L1+L2	L3+L4	FL (L5)		
Pyrite; (FeS <sub>2</sub> )		√√	√			=====	
Sphalerite; [(Zn,Fe)S]		√√	√			=====	
Chalcopyrite; (CuFeS <sub>2</sub> )		√√	√			=====	
Silver (Ag)			√			=====	
Galena; (PbS)		√√				=====	
Cassiterite; (SnO <sub>2</sub> )		√√					=====
Litharge; (PbO)		√√	√	√	√		=====
Bismuthinite; (Bi <sub>2</sub> S <sub>3</sub> )		√√				=====	
Uranophane; (CaO.2UO <sub>3</sub> .2SiO <sub>2</sub> .6H <sub>2</sub> O)		√√	√				=====
Kasolite; [Pb(UO <sub>2</sub> )(SiO <sub>3</sub> )(OH) <sub>2</sub> ]			√				=====
Autunite; [Ca(UO <sub>2</sub> ) <sub>2</sub> (PO <sub>4</sub> ) <sub>2</sub> .8-H <sub>2</sub> O]			√				=====
Torbernite; [Cu(UO <sub>2</sub> ) <sub>2</sub> (PO <sub>4</sub> ) <sub>2</sub> .8-12H <sub>2</sub> O]			√				=====
Mn-Franklinite; [(Zn,Mn <sup>+2</sup> ,Fe <sup>+2</sup> )(Fe <sup>+3</sup> ,Mn <sup>+3</sup> ) <sub>2</sub> O <sub>4</sub> ]			√	√	√		=====
Woodruffite; [(Zn,Mn <sup>2+</sup> )(Mn <sup>3+</sup> ,O <sub>7</sub> .12H <sub>2</sub> O)]			√	√	√		=====
Columbite; [(Fe,Mn)NbO <sub>6</sub> ]		√√		√			=====
Thorite; (ThSiO <sub>3</sub> )		√√					=====
Uranothorite; [(Th,U)SiO <sub>4</sub> ]		√√		√			=====
Zircon; (ZrSiO <sub>4</sub> )		√√					=====
Xenotime; (YPO <sub>4</sub> )		√√	√				=====
Fluorite; (CaF <sub>2</sub> )		√√	√				=====
Scheelite; (CaWO <sub>4</sub> )			√				=====
Tourmaline				√			=====
Limonite		√√	√				=====
Hematite		√√	√	√			=====
Magnetite		√	√				=====
Goethite		√	√				=====

AL= altered lamprophyre dykes cut cataclastic rocks (L1+L2+L3+L4)

FL= fresh lamprophyre dyke cut monzogranite (L5)

Cataclastic samples exhibit fractionated REE patterns [(La/Yb)<sub>N</sub>=0.27, an average] and display relatively flat LREE [(La/Sm)<sub>N</sub>= 2.2 an average] with relatively enriched HREE [(Gd/Lu)<sub>N</sub>= 1.2 an average] and negative Eu anomalies ( $Eu/Eu^* = 0.11$ ) (Table 3). The lamprophyre samples are characterized by relatively fractionated REE patterns [(La/Yb)<sub>N</sub> = 0.12 an average] and large negative Eu anomalies ( $Eu/Eu^* = 0.08$  an average) with HREE enrichment [(Gd/Lu)<sub>N</sub>= 0.80 an average]. It appears that the hematitization process have caused the enrichment of the REE especially HREE in lamprophyre than cataclastic rocks.

Table 2. Radioelement distribution of eU, eTh and eU/eTh along lamprophyres (L1, L2 and L3).

Shear zone No.	N	eU (ppm)		eTh (ppm)		eU/eTh	
		Range	Av.	Range	Av.	Range	Av.
L1	419	40-1200	360	20-400	270	0.5-4	1.3
L2	114	10-1700	355	40-1600	499	0.2-3	0.75
L3	96	10-1000	200	30-1700	420	0.2-0.9	0.47

N: Numbers of measurements

Table 3. Average of rare earth elements (REE) data of the cataclastic, lamprophyre and wall zones, Abu Rusheid area.

REE	Cataclastic N=11	lamprophyres N=24	Wall zones N=5
La	12	199	15
Ce	29	192	76
Pr	5	110	6
Nd	14	340	20
Sm	3	141	8
Eu	0.13	4	0.7
Gd	5	167	12
Tb	1	71	6
Dy	12	689	52
HO	3	174	15
Er	14	843	39
Tm	3	137	9
Yb	28	1018	60
Lu	5	151	9
Y	61	3770	179
ΣREE	195	8006	506
ΣLREE	62	986	125
ΣHREE	133	7020	381
ΣLREE/ΣHREE	0.47	0.14	0.33
(La/Yb)N	0.7	0.12	0.16
(La/Sm)N	2.2	0.92	1.2
(Gd/Lu)N	1.2	0.80	1.7
Eu/Eu*	0.11	0.08	0.2
Ce/Ce*	1.3	0.4	2.4

N : Number of samples analyzed for REEs (ppm)

### B- Sikait area

Detailed geologic maps for the two metamorphosed sandstone at W. Sikait were constructed (Fig. 7) on the base of a grid pattern 25 x 25 m. The exposed rocks are arranged as follows: 1) ophiolitic mélange (consists of mafic-ultramafic fragments set in metapelites matrix); 2) metamorphosed sandstones; 3) gabbros, 4) granitic rocks (porphyritic biotite granites and mylonitic biotite granites) and 5) post-granite dykes (lamprophyres) and veins (quartz).

The metamorphosed sandstone rocks are fine-grained, white in color, highly sheared, banded, less foliated and cross-cut by lamprophyre dykes (NW-SE, N-S and E-W) and quartz veins (NNW-SSE, NNE-SSW and E-W). The metamorphosed sandstone rocks crop out in W. Sikait at two locations. The first outcrop (major) is located west the upstream of W. Sikait (Fig. 3), whereas the second outcrop (small area) is located at the bending of W. Sikait.

The first metamorphosed sandstone outcrop covers a relatively larger area than the second exposure, with low to medium peaks, highly tectonized, elongated in NW-SE (2 km in length and thinning layering in NE-SW (150-500 m in width) forming float-boat-like shape (Fig. 8) and intruded by fertile porphyritic granite (20 ppm eU) and lamprophyre dykes. The metamorphosed sandstone rocks are traversed by three sets of strike-slip faults trending NW-SE, NNW-SSE and NNE-SSW and one set of dip-slip fault trending ENE-WSW. These faults control the shape and setting of metamorphosed sandstone rocks, where the maximum elongation of metamorphosed sandstone is controlled by NW-SE sinistral strike-slip fault set. The metamorphosed sandstones range in color from pale white to milky white, generally uniform in texture and composed of fused quartz grains.

The rock shows relics of primary bedding, banding and obvious foliation in NW-SE with angle of dip 35°/SW. It has granular appearance on the weathered surface with common vugs (boxworks) filled with secondary mineralization but along a broken surface the quartz grains are usually split. The fractures are usually open spaced, filled with secondary uranium and molybdenite. The common alteration products are represented by hematitization and manganese dendrites. Semi-angular to elongated rock fragments (mainly metagabbros in composition) are enclosed in metamorphosed sandstones, manifesting the greywacke composition. Lamprophyre dykes were emplaced relatively in NW-SE, N-S and E-W trends cutting both metamorphosed sandstones and porphyritic granites. The trend of lamprophyre dykes is concordant with the main structural trends that control setting of the metamorphosed sandstones. These dykes are altered, fine-grained, black grey in color, discontinuous and vary in thickness from 0.5 to 2 m and up to 1.4 km in length.

The second metamorphosed sandstone outcrop, covers a small area (0.5 km), forming low terrain and intruded by the granites. Some scattered goethite and yellow limonite after sulfide crystals are observed on the weathered surface of the rocks. The metamorphosed sandstones are whitish in color, sheared, foliated (NE-SW) and cut by two types of quartz veins. A) barren quartz veins (E-W, N-S and NNE-SSW) dislocated by N-S strike slip faults and cross-cut the foliation planes of metamorphosed sandstones and b) quartz vein (NE-SW)-bearing mineralization (wolframite, cassiterite and xenotime) visible to the naked eye. It varies from 1-2 m in width and extends for 15 m in length parallel to the foliation planes. Microscopically, the metamorphosed sandstone rocks are fine to medium-grained of whitish grey in color and vary from graywacke to arkosic in composition. The characteristic minerals which recorded in metamorphosed sandstone at Sikait are listed in Table 4.

Table 4. Summary of the characteristic minerals recorded in Sikait area.

Minerals	Metamorphosed sandstone	Lamprophyre dykes	Quartz vein
U-minerals	Uranophane, $\beta$ -uranophane, kasolite and autunite.	Uranophane	-
Th-minerals	-	Thorianite	-
U-bearing minerals	Smarskaite	-	-
Base metals	Bunsenite, ilsemanite, galena and nimitite	Bunsenite, pyrite and rosasite	Wolframite and cassiterite
Accessory minerals	Zircon, garnet, fluorite, uraniferous xenotime, and REE-silicate	Ilmenite	Uraniferous xenotime and piedmotite

### Equivalent U-contour map

Matching the equivalent uranium contour map with geologic map reveals two levels of radioactivity. The first level has the lower value ( $\leq 15$  ppm eU) and coincides with porphyritic granites with no specific trend. The second level ranges in intensity from 15 to 85 ppm eU and is associated with metamorphosed sandstones (Fig.8). The abnormal eU contents in metamorphosed sandstones were

relating to high Na- and K-metasomatism. The eU anomalies also reflect visible secondary U-remobilization along the structural trends (NW-SE, N-S and E-W). The tectonic trends act as good traps for U-rich fluids or U-ores.

### Chemical U-contour map

Matching the chemical uranium contour map (Fig. 9) with geologic map reveals two levels of radioactivity. The first level has the lower value ( $\leq 280$  ppm U) and coincides with NE side of metamorphosed sandstones towards W. Sikait. The second level ranges from 280 to 480 ppm U and close contact with fertile porphyritic granites.

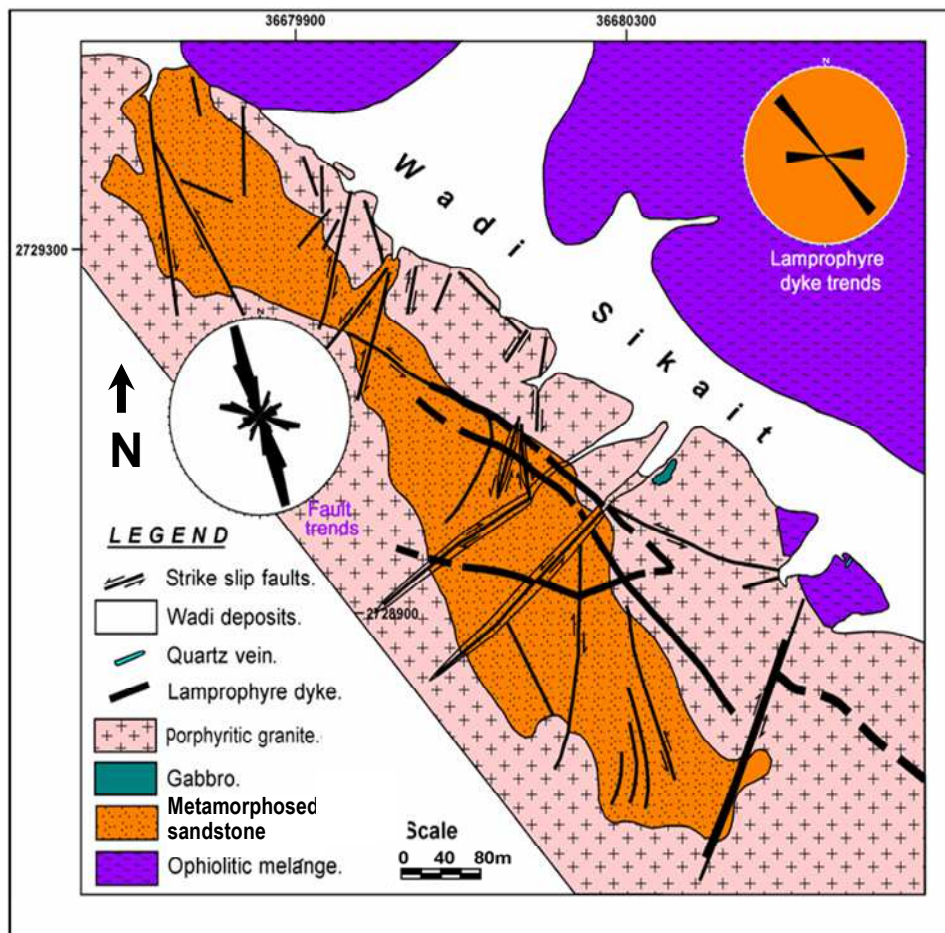


FIG. 7. Detailed geologic maps for the metamorphosed sandstone at W. Sikait.

The abnormal U contents in metamorphosed sandstones were relating to high shearing, tectonic and mobilization. The chemical U content is five times equivalent U content, whereas the chemical U content ranges between 60 to 480 ppm, while the equivalent U ranges between 15 to 85 ppm. This conclusion supports the youngest age (less than million years) for U mineralization.

### Equivalent Th-contour map

Correlation between equivalent Th-contour map (Fig. 10) and geologic map of Sikait indicates two levels of eTh -contents. The first level has the lower value of eTh-content ( $\leq 40$  ppm eTh) and coincides with porphyritic granites, whereas the second level ranges from 40 to 85 ppm eTh and is associated with metamorphosed sandstones.

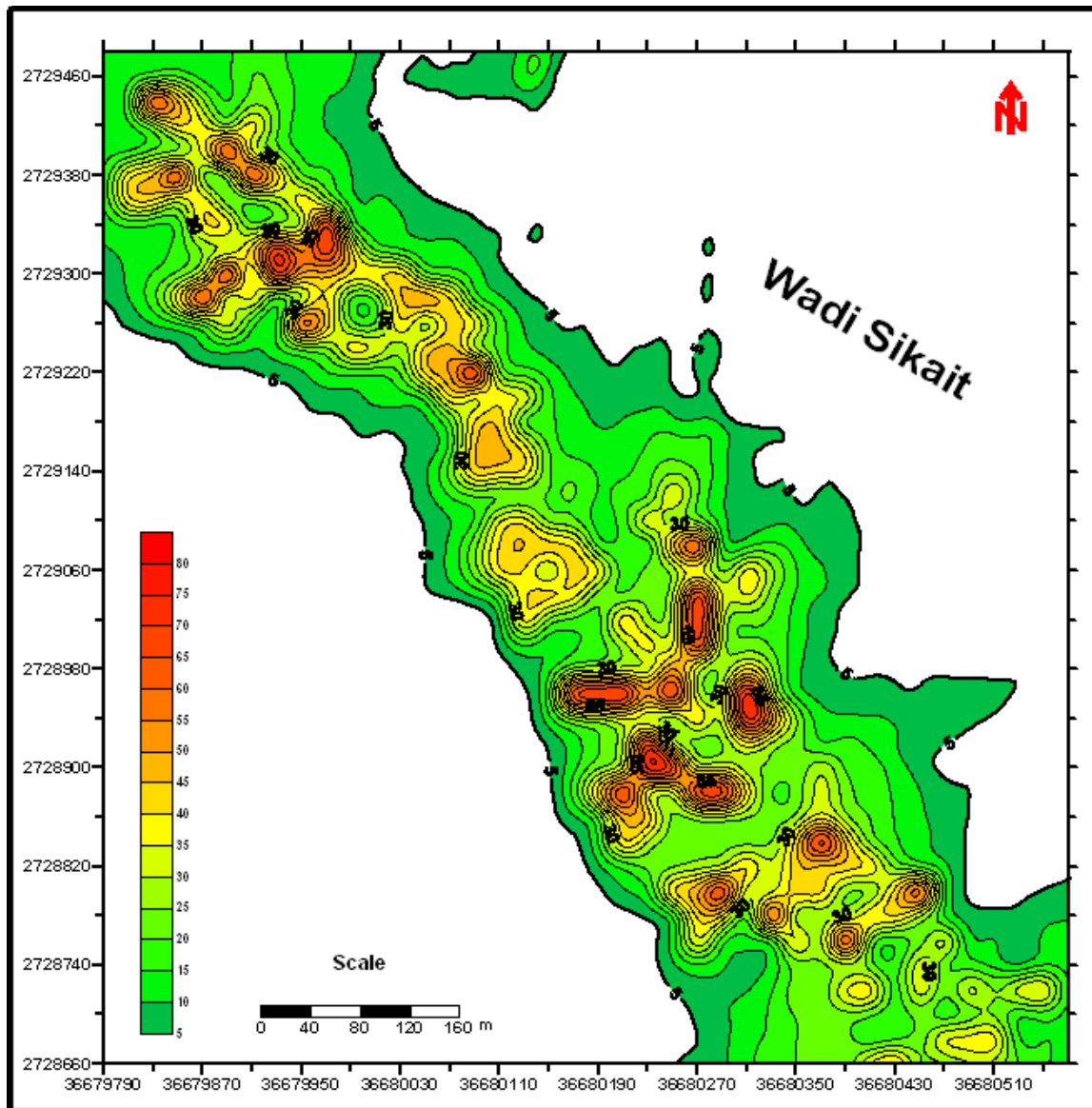


FIG. 8. Equivalent uranium contour map for metamorphosed sandstone Sikait

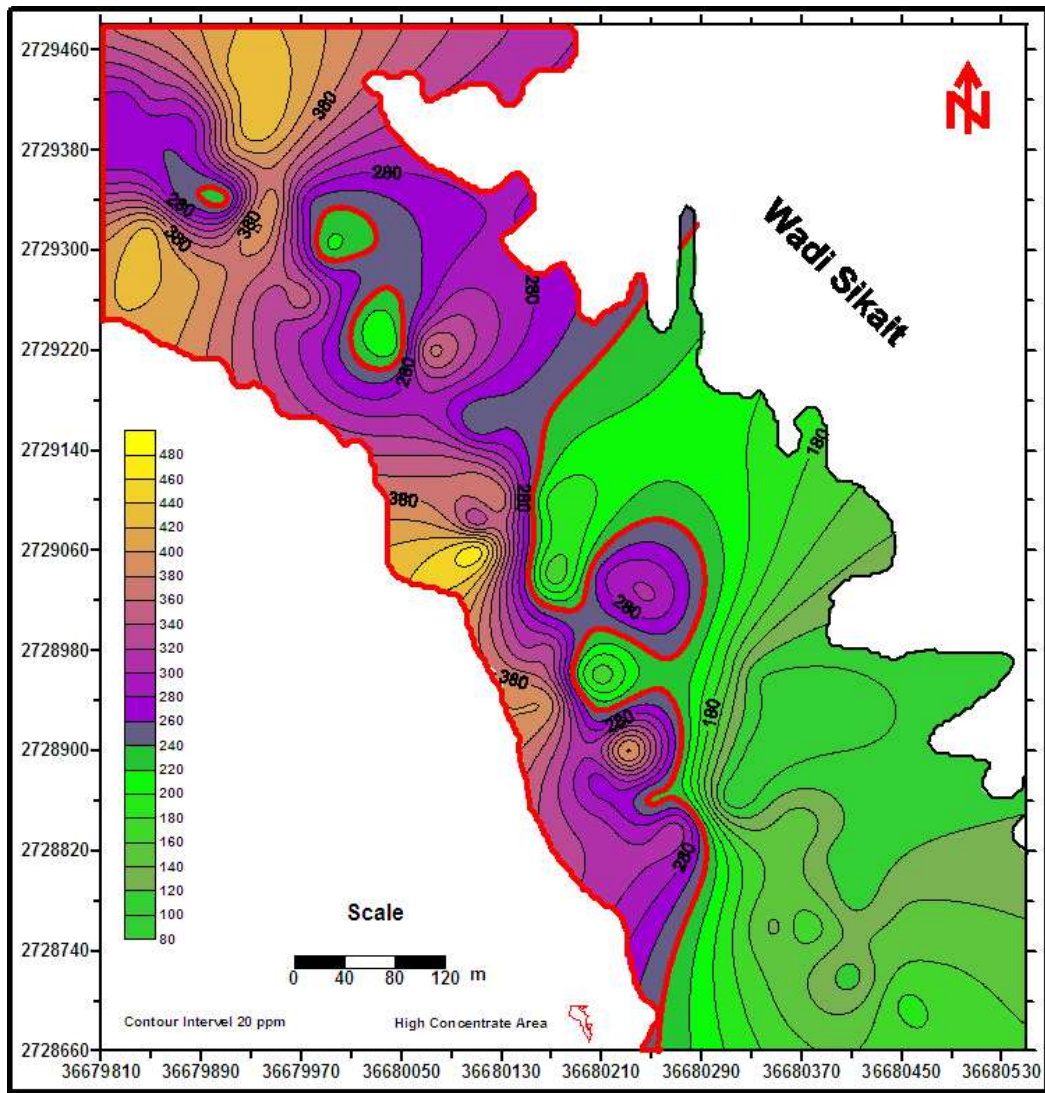


FIG. 9. Chemical uranium contour map for metamorphosed sandstone Sikait.

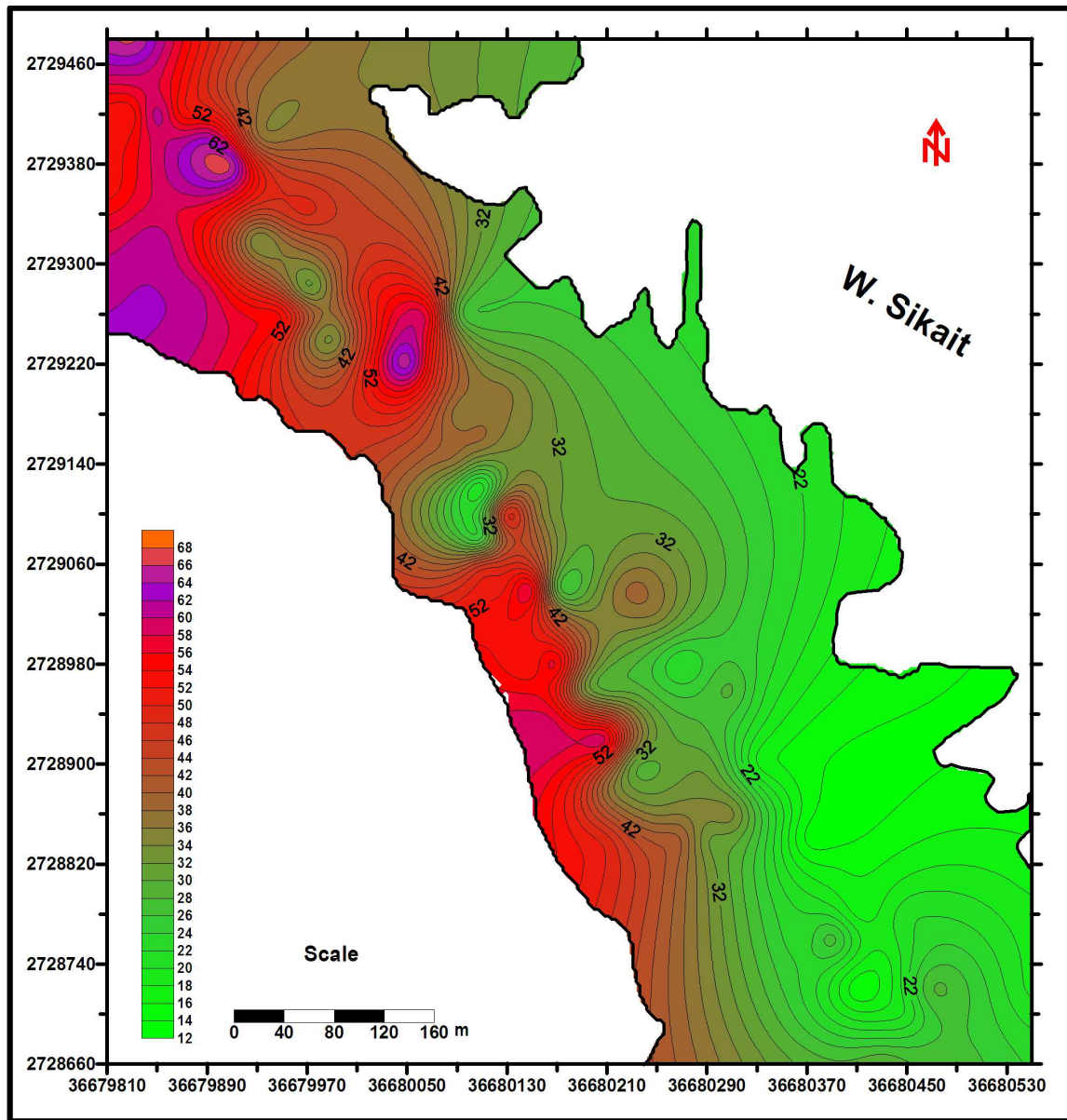


FIG. 10. Thorium radiometric contour map for metamorphosed sandstone at Sikait.

### 3. Conclusions

#### A Abu Rusheid area

- 1- Lamprophyre textures are bladed and banded colloform-crustiform. These textures are common in epithermal base metals, indicative of boiling event and rapid deposition (Hedenquist et al., 1995).
- 2- The REEs minerals are represented by xenotime, astrocyanite, fergusonite, allanite, monazite and zircon.
- 3- The remarkable enrichment in carbonate, sulfide and fluorite in lamprophyre, may propose complexation of REEs with  $\text{HCO}_3^-$ ,  $\text{CO}_3^{2-}$ ,  $\text{SO}_4^{2-}$  and  $\text{F}^-$ . During ascending of hydrothermal solutions in shear zones, the sudden change in the physico-chemical conditions causes the REEs complexes breakdown and the precipitation of the REEs.

- 4- The lamprophyre is mantled-derived with high temperature and volatiles, as well as, CO<sub>2</sub>. The REEs are often transported (either along the foliations and banding of the cataclastic rocks or ascending from hidden peraluminous granites) to the shear zone and precipitated with other rare metals, such as W, Pb, Zn, Ag and Cu on boxworks and clay minerals.
- 5- The hematization process (a good trap for REEs) has caused the enrichment of the HREEs-bearing lamprophyre samples than cataclastic rocks. Precipitation of hematite probably decreased the pH of the solution and rising acidic fluids. The sudden change in the pH and temperature of the fluids will lead to destabilization of rare earth complexes favouring their deposition
- 6- The presence of smectite-illite indicates a rather high temperature epithermal environment, higher than 200° C. The mixing of volatile fluids with meteoric water and fluid-wall rock interaction result in changes in pH and oxygen activity.
- 7- The U-mineralization has been formed as product of the hydrothermal events. It includes secondary U-minerals (uranophane and beta-uranophane, kasolite, torbernite, autunite and meta-autunite) in addition to U-bearing minerals (astrocyanite, betafite and fergusonite).

### **B- Wadi Sikait area**

The metamorphosed sandstone represents the target for uranium and associated minerals. It extends NW-SE for about 2.0 Km in length and ranges from 100-400m in width. The uranium minerals include uranophane, beta-uranophane, kasolite and autunite, and they are affected by some factors:

- 1- The presence of mineralizing source represented in our opinion by both cataclastics (west the mapped area) and hot contact granitic rocks (20 ppm eU).
- 2- The hydrothermal solutions play a major role in dissolution, transportation and deposition of minerals (e.g. wolframite, U-minerals, fluorite, ilsemmite and uraniferous xenotime).
- 3- The good open fracture system which represented by shearing, foliation, and bedding, and acts as good pathways for the solutions.
- 4- The mobilization and migrated uranium from the hot uraniferous porphyritic granite towards metamorphosed sandstone is due to the heat of metamorphism, emplacement of both lamprophyre dykes and granites.
- 5- The effect of post depositional (diagenesis) and alteration processes (sodic, potassic and fluoritization) respectively as well as the reducing condition (sulfides and graphite).

### **REFERENCES**

- [1] SABET, A.H., et al., On the geologic structures, laws of localization and prospects of Abu Rushied rare metals deposit. *Annals. Geol. Surv. Egypt. V. VI* (1976) 181-197.
- [2] EL-GEMMIZI, M.A. On the occurrence and genesis of mud zircon in the radioactive psammitic gneisses of Wadi Nugrus, Eastern Desert, Egypt. *J. Univ. Kawait (Sci.), V. U, No.2* (1984) 285-294.
- [3] EID, A.S. Mineralogy and geochemistry of some mineralized rocks in Wadi El Gemal, Eastern Desert, Egypt. Ph. D. Thesis, Ain Shams Univ. (1986) 165.
- [4] SALEH, G.M., The potentiality of uranium occurrences in Wadi Nugrus area, south Eastern Desert, Egypt, Ph.D. Thesis, El-Mansura Univ. (1997) 171.
- [5] IBRAHIM, M.E., et al., Uranium and associated rare metals potentialities of Abu Rusheid brecciated shear zone I, south Eastern Desert, Egypt (2002) (Internal report).

- [6] STILLE, P. OBERHANSLI, R., WENGER-SCHENK, K., Hf-Nd isotopic and trace element constraints on the genesis of alkaline and calc-alkaline lamprophyres. *Earth and Planetary Science Letters* (1989) 209-219.
- [7] CARMICHAEL, I.S.E., TURNER, F.J., VERHOOGEN, J. *Igneous Petrology*, McGraw-Hill (1974):
- [8] IBRAHIM, M.E., et al., Uranium and associated rare metals potentialities of Abu Rusheid brecciated shear zone II, south Eastern Desert, Egypt (2004) (Internal report).
- [9] IBRAHIM, M.E. et al., Geochemistry of lamprophyres bearing uranium mineralization, Abu Rusheid area, south Eastern Desert, Egypt. The 10<sup>th</sup> Inter. Min., petrol., Metall. Engin, Conf., Assuit Univ., 6-8 March (2007).
- [10] IBRAHIM, M.E., et al., Comparative study between alkaline and calc-alkaline lamprophyre dykes in Abu Rusheid area, south Eastern Desert, Egypt. The 10<sup>th</sup> Inter. Min., petrol., Metall. Engin, Conf., Assuit Univ., 6-8 March (2007).
- [11] IBRAHIM, M.E., et al., Epithermal Base Metal Mineralization in Lamprophyre, South Eastern Desert, Egypt (2006) (In Press).

# Niger's uranium resources and potential

M.O. El Hamet, Z. Idde

Research Centre for Geology and Mining, Niamey, Niger

**Abstract.** The first important uranium shows were discovered in Niger in 1958 by the French BRGM in Azélik; two other French companies specializing in the nuclear fuel cycle, CEA and COGEMA, also carried out exploration activities from 1959 to 1980 in the entire, high potential, Tim Mersoï basin, leading to the discovery of other uranium shows and about twenty world-class deposits. The Aïr basement and two other Palaeozoic basins, Djado and Tafassasset, also have good potential. Niger's uranium provinces comprise 360 000 km<sup>2</sup>. In 1971, SOMAIR began uranium production, followed in 1978 by COMINAK. Both mines are operated by AREVA NC, and they have already produced 110 000 tU in the last forty years, and their current production is 3 200 tU/y. Following a spectacular increase in the price and demand for uranium, exploration activities that were interrupted for more than a decade following the first uranium boom were resumed in 2002; 127 uranium exploration licences have been granted to some fifty foreign mining companies in Niger. All the economic mineralizations are located near the Arlit-In Azaoua fault in detritic sedimentary rocks of the Carboniferous to Cretaceous eras: conglomerates, sandstones and siltites rich in organic material and sulphides. Sedimentological, stratigraphical, redox phenomena and tectonic evolution of the northern Niger region all played an important role in the genesis of Niger uranium deposits. Uranium is mainly found in its primary mineral forms: pitchblende - uraninite group and coffinite. In Imouraren, Imca 25 and Azélik, however, the secondary minerals (gummite, uranotile tyuyamunite, carnotite) predominate. The average grades of the economic deposits vary from: 0.08 to 0.6% U, with a maximum of up to 3% U. Notwithstanding the 110 000 tU already extracted, considerable resources 500 000 tU still remain in Niger (140 000 tU recoverable for less than US \$50/lb). Near the Arlit-In Azaoua fault and its satellite faults, detailed exploration using modern, efficient, methods could lead to the discovery of other deposits. Production in the Imouraren (240 000 tU) and Azélik (14 000 tU) deposits is under way and, with total production expected to reach around 10 000 tU/year, this should bring Niger up into second place amongst worldwide uranium producers.

## 1. Introduction

The first shows of uranium in Niger were discovered in 1958 by the BRGM at Azélik in the Agadez region. Subsequently, the CEA and COGEMA, two French companies specializing in the nuclear fuel cycle, conducted systematic exploration of the entire Tim Mersoï and Djado basins, located in the northern desert of the country (Fig. 1 and 2).

From 1973 to 1980, following the spectacular increase in uranium price and demand, several mining and oil companies (Cogema, Conoco, Pan Ocean, BP, Esso, OURD, IRSA, PNC, etc.) obtained licences for uranium exploration in Niger. These efforts met with great success through the discovery of considerable total resources estimated at more than 500 000 tU and a known potential in the three large sedimentary basins of Tim Mersoï, Djado and Tafassasset, as well as the Aïr basement, which form one of the largest uranium provinces in the world covering a total area of 360 000 km<sup>2</sup>. About twenty world-scale, economic deposits have been discovered there and as a result Niger has been well placed amongst uranium producers for some forty years. The exploitation of two new deposits (Imouraren and Azélik), with production of approximately 10 000 tU/year, will make Niger the world's number two producer in two years' time. Since 2002, 127 exploration licences have been issued to some fifty mining companies [1].

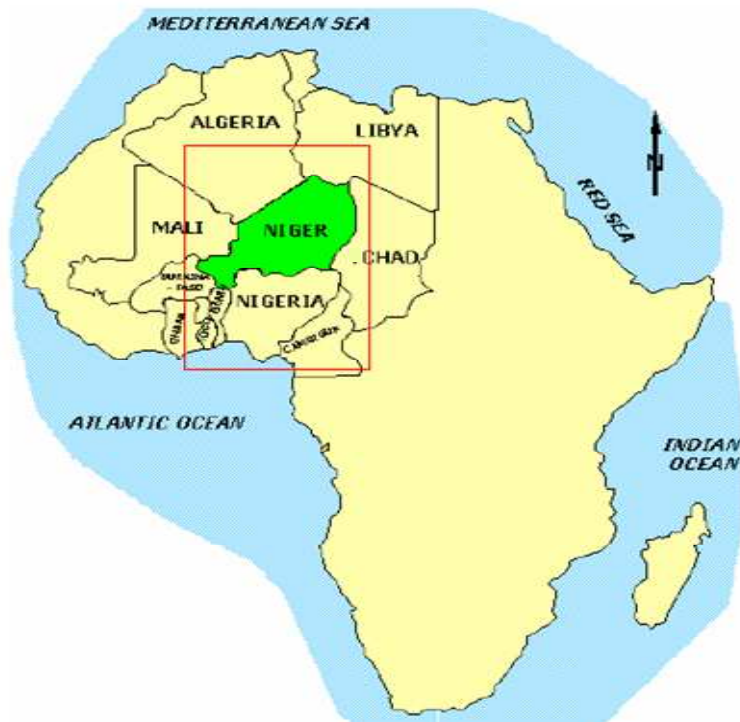


FIG. 1. Location map of Niger.

## 2. Geological framework

Niger is a Sahel country situated in the heart of West Africa sharing common borders with Algeria, Libya, Chad, Nigeria, Benin, Burkina Faso and Mali (Fig. 1). Geologically speaking, five large basins (Tim Mersoï, Chad, Djado, Tafassasset and Iullemeden) overlie the basement in three large regions. The present geology of Niger derives from its belonging to the West African craton and the Central African mobile zone. The major structural regions are:

- Liptako-Gourma basement, which represents the extreme northeast of the Man Ridge and extends from the Burkina Faso border to the Niger river and beyond;
- Aïr, Damagaram-Mounio and South Maradi basement in the central part of the country;
- sedimentary basin of Niger's western basin (Iullemeden Basin);
- sedimentary basin of Niger's eastern basin (Chad Basin); and
- Djado plateau in the far north-east.

### 2.1. *Liptako-Gourma basement*

The Niger Liptako covers 32 000 km<sup>2</sup> and is basically composed of Lower Proterozoic (Birimian) formations arranged in meta volcano-sedimentary belts intersected with granitoids which represent more than 60% of the total area. The green Birimian rocks are mainly those of Gorouol, Téra, Sirba and fragments of meta volcano-sedimentary rocks, the most important of which is the Makalondi slab.

### 2.2. *Pan African basement: Aïr, Tafassasset, Damagaram-Mounio and South Maradi*

These formations belong to the Pan African Upper Proterozoic chain surrounding the West African, Congo and Kalahari cratons. They could be primary sources of uranium since there are several occurrences of this metal in the Algerian Hoggar mountains.

### **2.3. *Aïr***

The Aïr, together with the Hoggar and Adrar des Iforas, forms the Touareg shield. The latter belongs, just like the Benin-Nigerian shield, to the Central African mobile zone affected by Pan African orogeny around 600 Ma. The Aïr crystalline basement outcrops over an area of 62 000 km<sup>2</sup> and comprises a central folded zone that is strongly metamorphized and invaded by Pan African granitoids, and which is separated from the epimetamorphic areas bound by the major thrust faults of Tafadek in the west and Aouzegeur in the east. The epi- to meso-metamorphic supracrustal formations are pre-Pan African, probably Suggarian. The molassic formation of the Proche-Ténéré, attributed to the infracambrian, is very little metamorphized and subhorizontal, and lies in unconformity on the Suggarian basement.

The subvolcanic ring complexes, from the Palaeozoic era, comprising the northern extremity of the “Younger Granites” province, sharply intersect the Suggarian basement. This magmatic activity resulted in the creation of massifs of gabbros, anorthosites, syenites and alkaline and hyperalkaline granites. The Quaternary and Tertiary volcanism is characterized by some thirty trachytic (associated with numerous basalt emissions) and phonolitic structures.

The Aïr structure is an anticlinorium plunging northwards. The kilometre scale, isoclinal and overturned folds to the east are the result of an E-W compression. The Aouzegeur and Tafadek thrust faults with inward dips limit a central overthrust zone from the external zones. These thrusts with an ophiolitic ridge at the base characterize a collision between the West African craton and the Central African mobile zone after Pan African oceanic closure. Also visible in the Aïr is a family of sinistral NW-SE faults as well as a second, more discrete, NE-SW family.

### **2.4. *Damagaram-Mounio and the South Maradi***

The crystalline areas of Damagaram-Mounio (26 000 km<sup>2</sup>) and South Maradi (272 km<sup>2</sup>) are situated in south-central Niger on an 80 km band along the Nigerian border. This constitutes the northern extremity of the Benin-Nigerian shield. It is composed of Precambrian supracrustal formations with Pan African granite intrusions, all intersected with Palaeozoic subvolcanic ring complexes.

### **2.5. *Ténéré basement***

It covers an area of 13 000 km<sup>2</sup> and is a SE extension of the Hoggar outcropping in the form of a narrow NW-SE band bordering the Djado basin to the west. It appears sporadically further south in the Achégour and Fachi regions. Of middle Precambrian age, it is characterized by a folded meta-volcano-sedimentary sequence intersected by granitoids.

### **2.6. *Tim Mersoï basin***

It covers an area of approximately 114 000 km<sup>2</sup> in the north-west part of Niger and forms part of the much larger basin of Iullemeden covering most of western Niger and Mali (Figs 2 and 3). The uranium deposits currently being exploited in Niger are all located in the Tim Mersoï basin. In the east, this basin rests on the Aïr basement and then becomes progressively deeper towards the west and north before starting an uplift on the In Guezzam ridge. Its eastern flank is a gentle slope to the In Azawa lineament. The sedimentation is mainly continental and marginal-littoral after the Lower Devonian. The Irhazer marly clay lacustrine deposits are located in the southern part of the basin. To the north and the west, the basin becomes deeper at the In Azawa lineament intersection; its geological history started as of the Cambrian in the Tin Séririne synclinal structure .

Over the course of the basin's geological history, the sedimentation areas have migrated from north to south. Three large sedimentation areas have been identified as Lower Carboniferous to Lower Cretaceous:

- a Lower Carboniferous basin with successions of fluvio-deltaic floodplain deposits and marine sediments;
- a Permo-Triassic and Jurassic basin, much smaller than the aforementioned one and comprising interlayered volcano-sedimentary flow deposits in fluvial bodies;
- a Lower Cretaceous basin invaded by lacustrine, and subsequently fluvio-deltaic, deposits.

The location of the sedimentation areas is determined by epi-orogenic movements. The basin is made up of a system of narrow, submeridian grabens and horsts, the isostatic readjustments thus leading to sediment movement from the horsts to the grabens. The deposit areas are arranged in submeridian bands alternating with paleo-domes, sometimes covered with condensed series.

The main structural zones of the Tim Mersoï basin are as follows:

- The Tin Séririne synclorium occupying the north of the basin has an internal structure comprising a succession of numerous asymmetric anticlines and synclines;
- The Tim Mersoï graben runs along the In Azawa-Arlit lineament and extends towards the south of the Tin Séririne synclorium;
- The southern part of the basin is made up of alternating narrow ridges and valleys in the NNE-SSW direction;
- The In Azawa-Arlit lineament zone, situated approximately 50 km from the eastern edge of the basin, is made up of a succession of narrow grabens in the north-south direction.

This basin structure is one of the important factors controlling the uranium mineralization as the mineralization is generally up against the flanks of paleo-domes.

## ***2.7. Sedimentary Iullemeden basin***

This basin, with an area of 880 000 km<sup>2</sup> covers virtually all of western Niger and extends into Algeria, Mali, Benin and Nigeria. Over the course of geological time, several individual secondary basins (Tim Mersoï, Tamesna, Kandi, In Gall, etc.) formed within the main basin (Fig 2). The Cambrian to Pleistocene stratigraphic sequence is characterized by alternating deposits of marine influence and continental complexes. Palaeozoic formations outcrop all along the sedimentary margin of the Aïr, in the Tim Mersoï basin. Uraniferous mineralizations are associated with Upper Carboniferous formations, particularly with the sandstones of Guézouman, Tarat and Madaouéla. The Carboniferous also hosts coal deposits in the Anou Araren region.

The Intercalary Continental is a thick sandstone and clay series from the Permian to Lower Cretaceous era. It outcrops mainly in Tamesna, Irhazer and Téguidit. It hosts uranium- and copper-bearing mineralization levels as well as saline horizons which can be mined for salt. The Upper Cretaceous and Lower Tertiary marine formations are characterized by a succession of argillites, marls and fossil-bearing limestones with silty, sandy or gritty horizons. The Hamadian Continental is the equivalent marine Cretaceous continental and covers the Zinder and Maradi regions.

The third continental complex is the Terminal Continental following the Marine Tertiary. This thick detritic series of lignite levels and siderolithic horizons covers western Niger. The Salkadama coal deposit is found in these sequence. The Terminal Continental hosts the main iron shows and deposits known in Niger.

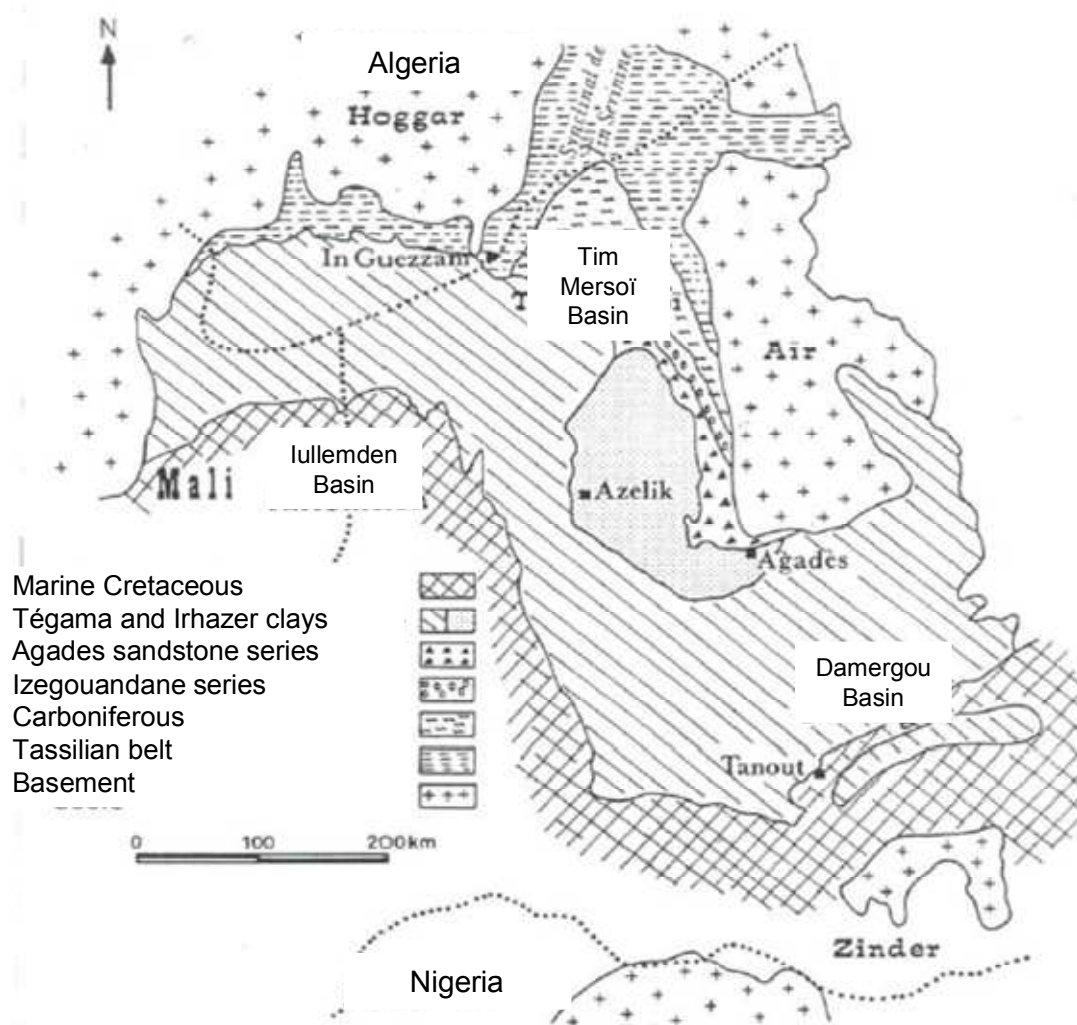


FIG. 2. Simplified geological map of western Niger.

Diagram of the Stratigraphic Series  
of the Eastern Part of the Tim Mersoï Basin  
(adapted from Cazoulat, 1984)

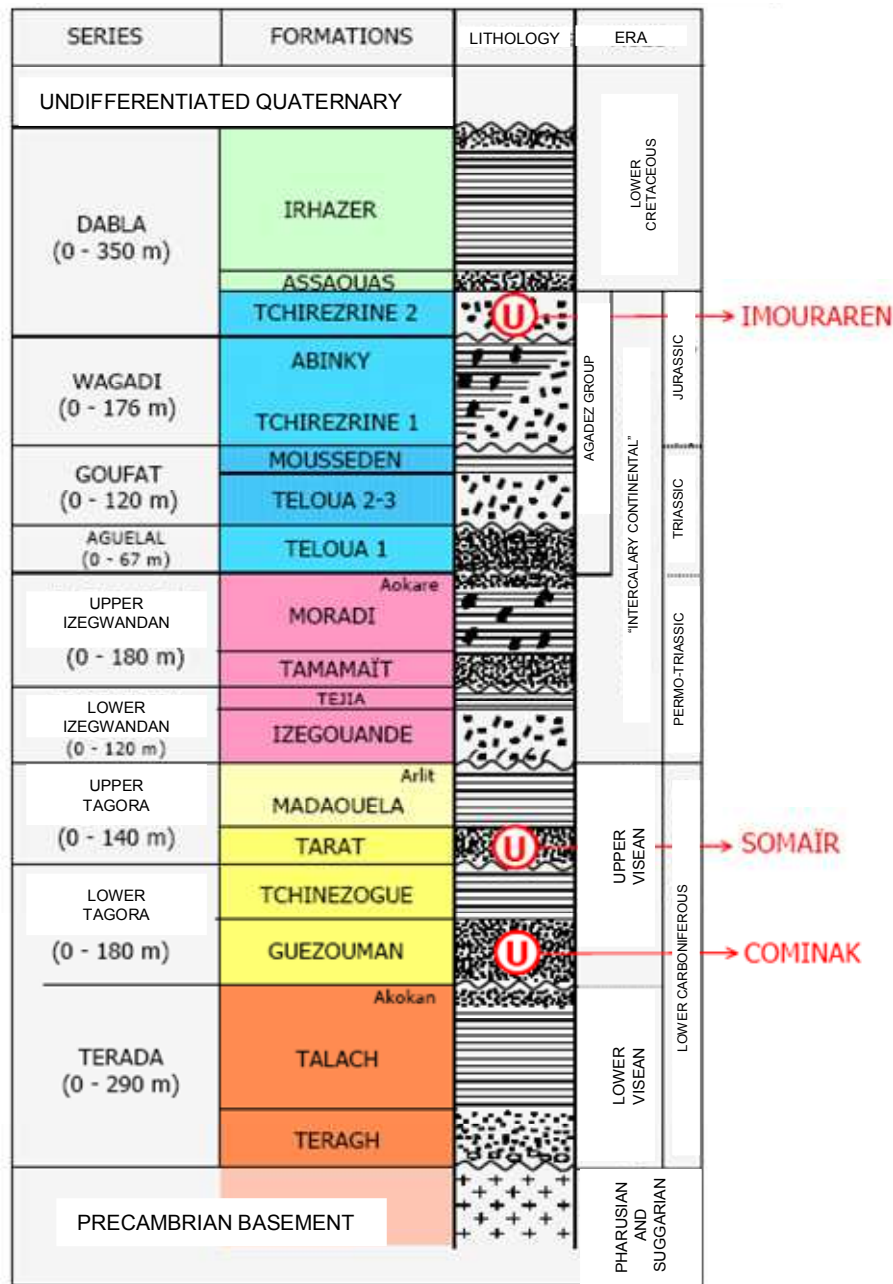


FIG. 3. Lithostratigraphic scale of the south-eastern part of the Im Mersoï basin (adapted).

## 2.8. Djado basin and its western flank

It is characterized by Palaeozoic formations and the presence of Precambrian rocks on its western flank. This basin hosts occurrences of uranium and numerous interesting radiometric anomalies and gypsum, probably the most significant in Niger. The potential for other metals remains entirely unknown. The Carboniferous palaeogeography and lithologies are favourable factors for the stratiform concentration of certain base metals (Cu, Zn and Pb).

## 2.9. Eastern sedimentary basin of Lake Chad

It covers eastern Niger and extends into Libya, Chad and Nigeria. It covers the territory stretching from the Air and Damagaram-Mounio mountain backbone to the eastern border with Chad and the northern border with Libya and Algeria. It hosts Palaeozoic to Quaternary sedimentary formations. The Quaternary deposits cover most of the basin. Oil exploration activity has led to the discovery of a series of relatively deep NW-SE grabens (Kafra, Grein, Agadem, (Ténéré, Temit), West Termit and N'Gel Edji) extending some 1 000 km from the Hoggar in the north to Lake Chad in the south. The thickness of the sediments in these grabens can attain 3 000 to 4 000 m, and even 12 000 m. Significant hydrocarbon reserves have been discovered in the Termit grabens and will be exploited in the near future.

## 3. Production

In 1971, SOMAIR started uranium mining, producing 410 t/year, followed in 1978 by COMINAK. Together, these two mining companies have a production capacity of 4 500 tU/year, but have been producing an average of 3 000 tU per year for almost 40 years. In 2008, they produced 3 200 tU [1]. In 2008 and 2009, two new mining companies (SOMINA and Imouraren Ltd) obtained their licences to exploit the Imouraren and Azélik deposits, with planned production commencing in 2011 and 2012, respectively. This will propel Niger into second place amongst the world's uranium producing countries, producing around 10 000 tU/year (Fig 4). The Madaouela deposits, adjoining those of Arlit, are in the intensive development stage.

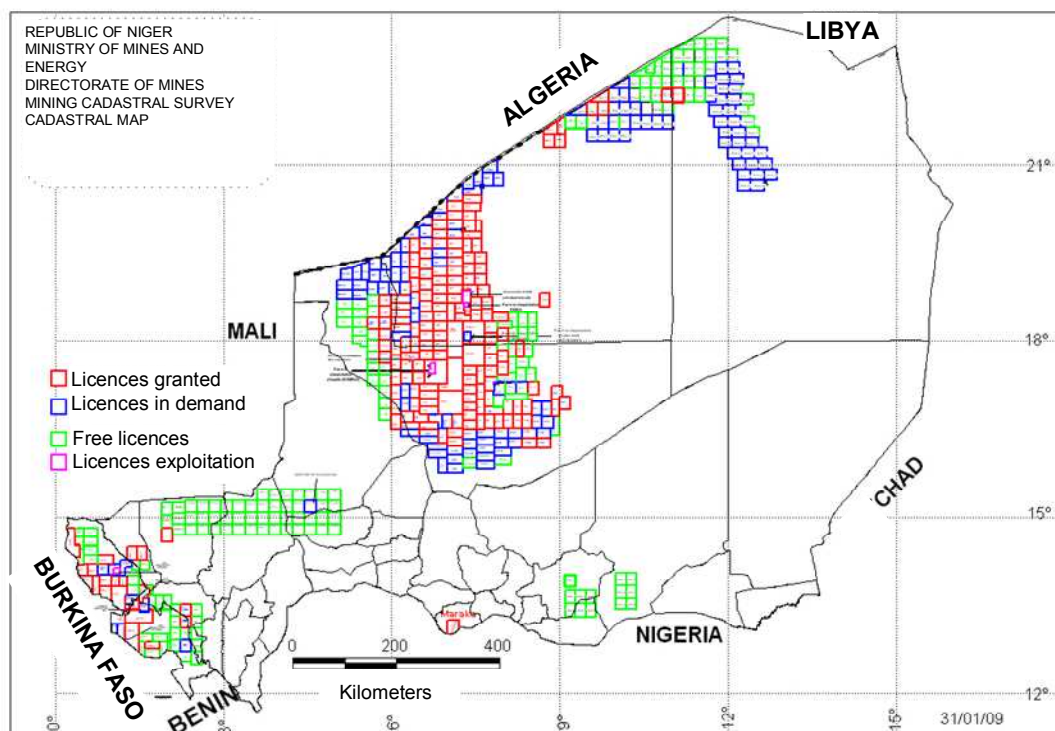


FIG. 4. Mining cadastral survey of Niger.

## 4. Main deposits found in Niger

The extensive survey work carried out mainly by the forerunners of AREVA NC (the French CEA and COGEMA) and Japanese companies (IRSA, OURD, PNC) in the Tim Mersoï intracratonic basin led to the discovery of some twenty economic deposits — Arlette, Ariège, Artois, Ariane, Arthur, Arni, Akouta, Akola, Ebba, Ebene, Ebala, Imouraren, Imaren, Imca 25, Irhawenzegirhan, Azelik, Madaouela, In Gall and Tinégourane. These deposits are situated in the following 5 mining areas for which a brief description is given (Fig 6):

### 4.1. Arlit concession

This concession, covering an area of 360 km<sup>2</sup> was granted to the French CEA, now AREVA NC, in 1968. About fifteen uranium deposits have been found there and four areas, including the main deposits, have been leased to three mining companies: SOMAÏR, COMINAK and SMTT.

#### 4.1.1. SOMAÏR and SMTT lease (55 km<sup>2</sup>)

Established in the period when the uranium price dropped, SMTT was not able to reach the production stage; first it sub-let, then ceded, its area (37 km<sup>2</sup>) to SOMAÏR. In these two areas, the following deposits have been exploited by SOMAÏR: Arlette (10 000 tU), Ariège (15 000 tU), North Taza and South Taza (10 000 tU), Takriza (4 000 tU), Tamou (6 000 tU) and Tamgak (8 000 tU). There are still three deposits that have not yet been exploited: Artois (17 000), Arthur, Ariane, Tabéllé (1 500 tU) [2]; exploitable resources have been discovered in the area in-between these known deposits.

The Arlit uranium deposits are located in the Lower Carboniferous sandstones of Tarat. They comprise: Arlette, which has already been mined, Ariège, being mined, Artois, Ariane, Arthur, Tamgak, Taza, Tamou, Takriza and Tabéllé. The Tarat formation which host mineralization are sandstones with argillaceous-silty intercalations and the continental platform has a fairly uniform relief. Tarat lies in erosional unconformity on the Tchinezogue argillites, covered by alternations of fine sandstone and silty argillite of Madaouela; the fine aolin argillaceous sandstones of the Arlit unit.

The uranium is located in the fine sediments of mudflats and sandstone bodies near river mouth bars. The mineralization is more or less continuously in contact with the sandstone clay alternations. In the sandstone bars it underlines the stratifications and is concentrated in the “bottom set”. The mineralization is generally represented by pitchblende and coffinite. In shallow deposits, like Arlette and Tabéllé, part of the primary minerals have been oxidized and transformed into tyuyamunite, francevillite and carnotite. In clays, part of the uranium is fixed in the form of organometallic complexes that are difficult to process.

Development and exploitation of the various deposits has led to improved knowledge of the total resources in the SOMAÏR mining zone, around 100 000 tU, of which half have already been mined. Exploration is continuing in the area and the experience gained by AREVA NC over 40 years of mining the various deposits will help to increase these resources. The Artois deposit, for which a feasibility study was approved in 2005, hosts approximately 17 000 tU (0.3% U).

Residual resources, estimated at 4000 tU, exist in the area between the various deposits and at the bottom of some quarries where mining has been suspended. Finally, there is 20 000 tU contained in the low grade ore heaps (ore grade > 0.14% U) stored during the years of recession in the uranium market. SOMAÏR resumed heap lixiviation treatment (HL) in 2009 and expects to produce up to 900 tU/year using this process. Thus, SOMAÏR has estimated total resources of 60 000 tU, of which 24 000 tU are classified as reserves that are proven to be economic under current market conditions [3].

#### 4.1.2. *COMINAK lease (Akola and Akouta)*

Two large deposits have been found in this 22.4 km<sup>2</sup> area and are being exploited: Akouta (40 000 tU - 0.6% U) and Akola (20 000 tU - 0.5% U). The uranium deposits in the area leased to COMINAK are located in the Guézouman Carboniferous formation. This is a vast regressive floodplain delta area on a continental platform. The main mineralizations are found on the Akouta channel and its branches.

Structurally speaking, the flexure fault of Arlit-In-Azaoua North-South and in the directions N 40°, N 140° and N 80° are responsible for the isolation of the deposit zone. The uranium is essentially in the form of primary minerals present in the sandstone cement in microscopic black elements (pitchblende and coffinite) and are almost always associated. The associated elements are molybdenum and vanadium. Despite more than 30 years of exploitation, reserves still remain in the Akouta and Akola deposits, proven to be economic under current conditions, estimated at 6 000 tU with an ore grade of 0.4% U. The complementary and supplementary resources are of the order of 35 000 tU.

#### 4.1.3. *The Afasto licence*

The Afasto licence adjoins the southern edge of the Arlit concession, covers an area of 27 325 km<sup>2</sup>, and is currently held by COMINAK, which obtained a mining licence in 2005 for the Ebba deposits. The Afasto licence deposits are in the same geological setup as those of the Arlit concession and are, in particular, an extension of the Akouta deposit. They are linked to the Guezouman Carboniferous formation, which lies generally in erosional unconformity on an essentially clay-silty formation (Talak) and is covered with Tchinezogue argillites. This is a mainly sandstone formation of fluvio-deltaic origin, manifesting marked variations in thickness (40-70 m), arranged in three units:

- Bottom, heterogranular sandstones starting with an erosional conglomerate (Téléfak) with pebbles of clay, rhyolite, quartz and quartzite, embedded in a pyrite or ferruginous sandstone matrix;
- Intermediate deltaic sandstones; and
- Upper alternations of sandstone and fine clay-silty sediments.

Structurally speaking, the Afasto licence deposits are surrounded by the meridian flexure-fault of Arlit-In Azaoua and its satellites in the N 30° direction, and the Madaouela, Izéretagen, Izéguéram Mouron, Autruche and Aguelal-Zéline faults. These events have had a determining influence on uranium entrapment.

Several formations in the Afasto licence are mineralized in uranium: three levels in Guezouman, Tarat and Madaouela and the Permian to Cretaceous formations (Moradi, Teloua, Assaouas). Uranium is manifested as tetravalent (pitchblende, coffinite) and hexavalent forms associated with phosphates in the Agelal sandstones (1% U) from the Triassic era. On the contrary, in the Akouta deposit, uranium is not associated with molybdenum, but rather with vanadium. The mineralization seems to be syndimentary and appears in the cement of sandstones and conglomerates mostly in the first 20 metres at the bottom of Guézouman. The mineralized body is situated at a depth of between 205 and 270 m with mineralized thicknesses ranging from 0.5 to 11 m. It becomes gradually deeper to the south and the west (300 to 400 m).

Mineralization controls are:

- Tectonic: role of the flexure fault of Arlit-In Azaoua and its satellites (Tekaden, Izéguéram, Izéretagen);
- Stratigraphic: link with some particular units at the bottom of Guézouman;

- Lithological: mineralization link with bottom-set sediments of sandstone bars and fine sandstones rich in organic vegetable matter, contact with the Talak; and
- Epigenetic: redox phenomena between the oxidizing waters from the Permian aquifers in contact with the reducing medium of Guézouman.

The total resources of Afasto are currently estimated at 40 000 tU with an average ore grade of 0.37% U, of which 50% (20 000 tU) are classified as economic reserves at the current uranium market price [4]. They have been located in the northern zone of the licence (Ebba deposit). These resources may increase considerably through development of the major shows of Ebala and Ebene situated less than three km further south. Complementary, supplementary and geological resources of the order of 25 000 tU may be attributed to the Ebene and Ebala beds, which are known only from 200 to 1 600 m test boreholes. This also takes into account the fact that certain mineralized impacts are located at depths of more than 300 m.

#### **4.2. Imouraren licence**

It is situated 80 km south of the Arlit concession and covers an area of 313.5 km<sup>2</sup>; in 1963 the CEA discovered the uranium shows of Mont Imouraren in a 40 km<sup>2</sup> area. After granting of the mining licence (128 km<sup>2</sup>) in January 2009 to the Imouraren company, the remainder of the licence was called the Anou Agerouf exploration licence [5].

The Imouraren licence is situated in the eastern part of the Tim Mersoï basin. The geological formations are Carboniferous to Cretaceous continental, terrigenous, detritic formations lying on the Pan African basement dipping gently to the west. The deposit is basically linked to the Jurassic Tchirézrine II formation; this formation is confined at the top and bottom by two formations with very fine grain size distribution and low permeability, Irhazer-Assaouas and Abinky. The mineralization is concentrated in heterogranular sandstone facies of fluvial origin with intercalating levels of analcime. The sandstones of Tchirézrine are generally poorly cemented; the cement is made up of secondary silica, greenish clay, analcime, kaolinite, limonite and haematite. The primary source of uranium seems to be in the Air volcanism, as indicated by analcimolite. In addition to the standard factors (stratigraphic, sedimentological, palaeogeographical and tectonic), mineralization control seems to be the result of two phenomena: dispersion by oxidation of a syngenetic mineralization and reconcentration of an epigenetic mineralization by roll type phenomena.

The Imouraren mineralization is a special case, differing from other known deposits. It is 90% composed of hexavalent secondary uranium minerals (uranotile, meta-tyuyamunite) and 10% of primary minerals (coffinite, pitchblende), appearing in sandstone cement, at the centre of analcime grains and pebbles and in epigenized vegetable debris. Uranotile ( $\text{Ca}(\text{H}_3\text{O})_2(\text{UO}_2)_2(\text{SiO}_4)_2 \cdot 3\text{H}_2\text{O}$ ) is the most abundant mineral and is manifested in small fibroradiated clusters underlining the stratification or filling in the imprints of vegetable debris. These uranium minerals are often associated with copper sulphides and silicates (chalcocite and chrysocolla) and even with native copper; vanadium is present but often linked with chlorites in the form of montroseite.

Unlike the other deposits in the region, the Imouraren uranium mineralization is weakly carbonated (0.2 to 0.5% calcite). Iron minerals (pyrite, haematite, goethite), sulphates (gypsum, barytine) and phosphates (apatite) are not very abundant. Organic matter is rare or absent. The mineralization is spread over three levels in the whole sandstone facies of Tchirézrine II at a cumulative average thickness of 55 m at depths of between 105 and 165 m. Laterally, the mineralization is subdivided into three zones from north to south: Imatra, Imfout and Imola. In the west Arlit-In Azaoua flexure area, two new average size and shallow (25-35 m) deposits, called Imca 25 and Imaren, were found during recent activity.

Development of the Imouraren uranium shows between 1974 and 1977 by the COGEMA-CONOCO-ONAREM association led to the identification of three world-scale deposits (Imfout, Imatra, Imola) in an area of 40 km<sup>2</sup>. The resumption of work in 2006 enabled the discovery of two other shallow

deposits (Imca 25, Imaren), situated 5 km from the previous ones in an area of 1.2 km<sup>2</sup>. The total resources of the Imouraren licence are currently estimated to be 240 000 tU [4] with an average ore grade of 0.08% U of which 70% are classified as measured reserves and are concentrated in the central zone (Imfout) and Imca 25. These reserves are recoverable at an operating cost of less than US \$50/lb.

#### **4.3. Teguida licence**

It is part of the former Abkorun-Azélik exploration licence awarded to the ONAREM-IRSA association in 1974, which discovered several shows and deposits. After the boundaries of this former licence were changed, the central zone where several shows and deposits had been found was named Téguida. It was awarded in 2006 to a group of Chinese companies (SINO-U, ZXJOY INVEST, TRENDFIELD HOLDINGS). The Azélik mining licence (220 km<sup>2</sup>) was granted to SOMINA in 2008 to exploit the Azélik and Irhawenzeghirhan deposits with economic reserves of 14 000 tU having an average ore grade of 0.2% U.

The Azélik and Irhawenzeghirhan uranium deposits appear in the Lower Cretaceous Assaouas formation situated at the base of the Dabla series. Assaouas, a Cretaceous formation forms the base of Irhazer; it is composed of very fine sandstone, grey-brown siltite and brownish silty argillites. The mineralized formation lies in erosional unconformity on the light brown clays at the base of the Permian Izégouandane group or the Jurassic Agadez sandstones. The mineralized body is generally tabular with an average thickness of 2 m.

The Azélik deposit is subdivided into several mineralized bodies which start at the surface and sink gently to a depth of 150 m; the Irhawenzeghirhan deposit, on the other hand, is situated around 10 km further north and is 200-210 m deep. The mineralization is basically composed of secondary uranium minerals (tyuyamunite, carnotite). Primary minerals are virtually non-existent. The uranium minerals appear in the form of yellow products in the sandstone and conglomerate matrix of the lower Irhazer unit. Two deposits with measured reserves (RAR) of 14 000 tU, recoverable at an operating cost of less than US \$35/lb [6] have been discovered:

- Irhawenzeghirhan: 6 000 tU (0.20% U). This deposit is in a tabular layer dipping gently, 0.5 to 3 m thick, in sandstones and polygenetic conglomerates (pebbles of quartz, rhyolite, quartzite, clay);
- Azélik (TGT) 8 000 tU (0.24% U).

In the exploration licence and even inside PEX there are good chances of discovering other resources, especially north of the IR deposit and the Teyndi region: complementary, supplementary and geological resources would be of the order of 15 000 tU, bringing the total resources of the SOMINA mining area to close to 30 000 tU.

#### **4.4. Madaouela licence**

The activities carried out by the CEA in the 1960s led to the discovery of proven reserves of an estimated 6 300 tU (0.36% U) or 9 000 tU [4] with an average ore grade of 0.2% U and an average thickness of 3 m. They are located at a depth of 25 to 70 m at the base of the Guézouman sandstones. While waiting for the results of the exploration activities and confirmation of this high potential licence, the complementary, supplementary and geological resources can be estimated at 21 000 tU, around the numerous mineralized impacts in various sectors.

#### **4.5. Other licences**

Regarding the other licences, security conditions have not allowed much progress as regards exploration activity; the gradual restoration of peace to the northern region of Niger will lead to acceleration of such activity for the following licences: Terzémazour, Toulouk, Tagait, Adrar Imoles,

Agebout, Afouday, Abelajouad, Assamaka which cover an area of 15 000 km<sup>2</sup>, the geological resources can be conservatively estimated at between 60 000 and 150 000 tU, taking into account the geological models of the known deposits and the experience of Areva NC in the region.

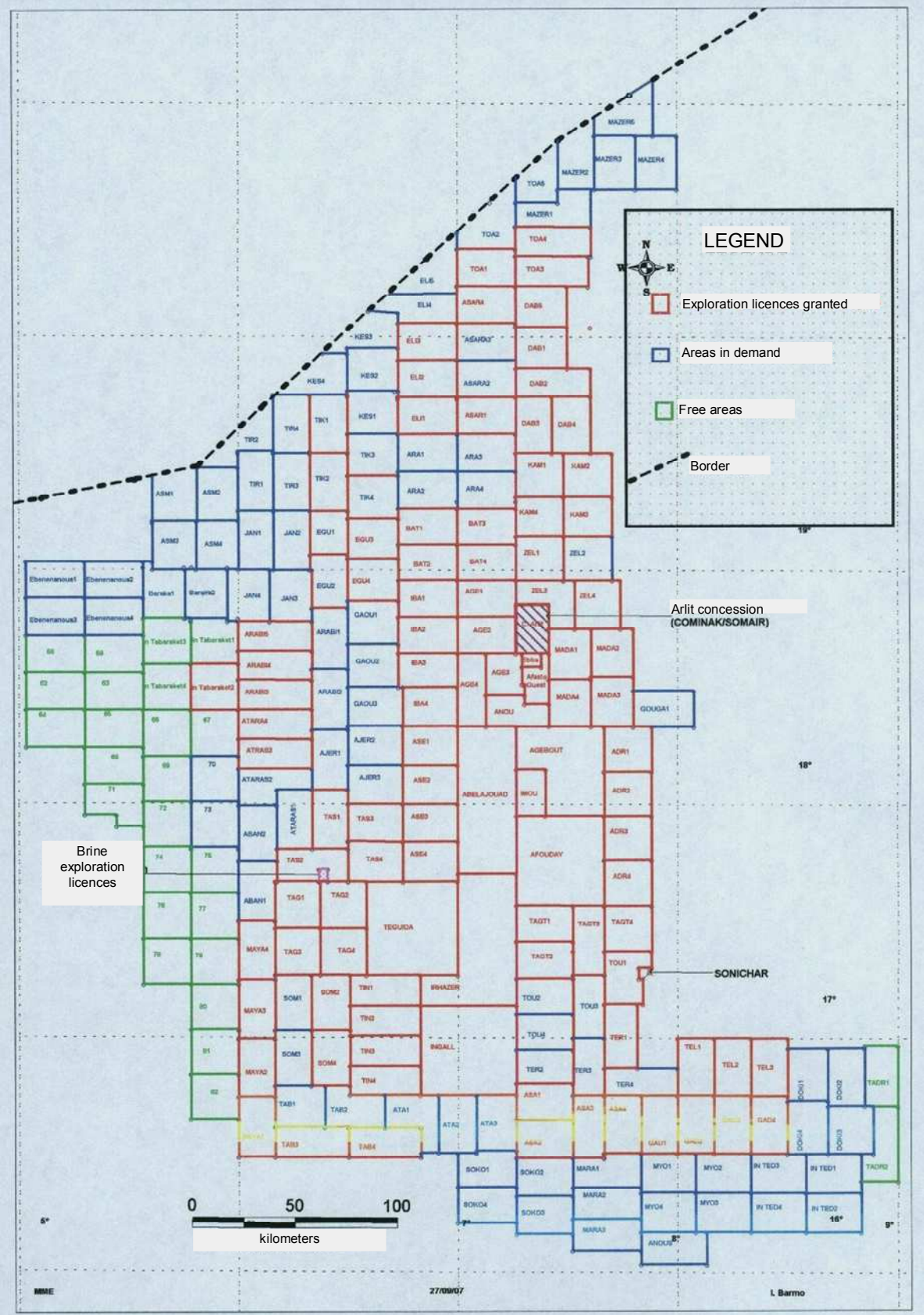


FIG. 6. Mining cadastral survey of the Tim Mersoï Basin uraniferous province.

## 5. Potential

In addition to the deposits that are already being exploited or being prepared for exploitation, there are good chances of discovering others for the following reasons:

- The existence of several surface shows (Takardaît, Tinégourane, Toulouk, Terzemazour, Moradi, central and eastern Djado, etc.);
- General knowledge of known mineralized impacts (200 and 1 600 m) with interesting potential in the main and most favourable geological area, namely the Tim Mersoï basin (straddling zone on the Arlit-In Azaoua flexure fault);
- The numerous uranium anomalies of Aïr, Djado and Tafassasset (Emi Lulu region) where Pan Ocean has identified surface and shallow shows;
- The spectrometric survey of the Aïr basement showing numerous extended zones with pronounced radioactive anomalies which are worth exploring for primary uranium deposits; many primary uranium vein ore deposits have been discovered in the Hoggar basement in Algeria.

In zones near the Arlit lineament and its satellites where there has not been much previous activity, the resumption of exploration as of 2002 using new methods could lead to other uranium deposit discoveries around the many existing mineralized impacts under the following exploration licences: Imouraren, Madaouela, Adrar Imoles, Afasto, Abelajouad, Agelal, Zéline, Tin Négourane, Téguida, Irhazer, Terzémazour, Toulouk, Tagait, Assamaka and In Gall.

Also, on the down dip of the Arlit, Akouta, Madaouela and Ebba deposits there are other shows and deposits at depths of 300 to 1 500 m in the zone to the west and south-west of the Arlit-In Azaoua flexure. The potential of these highly promising zones in the Tim Mersoï basin varies from 14 to 700 tU/km<sup>2</sup>. Recent activity under the following licences has led to significant discoveries that have not yet been made fully public.

### 5.1. *In Gall licence*

Under this licence, located in the southern part of the Tim Bersoï basin to the south-east of the town of In Gall, inferred reserves estimated at 10 000 tU [7], with an average ore grade of 0.02% U, were discovered by Niger Uranium in 2008. The mineralization is of the unconformity type: it is in a continuous 0.5 to 2.5 m level at the base of Tégama in the erosive contact zone with Irhazer. Like the Téguida N'Tessoum deposit, the In Gall deposit is situated in Cretaceous continental formations. The geological environment is marked by a sandstone and clay alternation.

### 5.2. *Agelal licence*

The Agelal licence adjoins the Arlit concession held by AREVA NC and was part of the former Afasto licence operated by Cogema in the framework of an association between OURD and ONAREM at the end of the 1970s. Deep mineralized impacts (500-900 m), with thicknesses of 8 m have been intercepted in the Guézouman sandstones, host to the Akouta, Akola, Afasto and Madaouela deposits. Also, a resumption of exploration by Uranium International Ltd, a Canadian company, has helped to locate shallow resources, suitable for open cast mining, in the Tarat-Madaouela formation (host of the Arlit deposit).

### 5.3. *Adrar Emolès licence*

Deep (300 to 500 m) shows of uraniferous mineralizations have been intercepted by PNC in Guézouman, Tarat, in the Solomi region.

#### **5.4. Air crytalline massif**

Uranium shows and aero-spectrometric anomalies have been identified in the Air massif which, like the Algerian Hoggar, could contain primary mineralisation of uranium.

### **6. Total uranium resources**

At the current state of knowledge, the estimated total uranium resources in Niger, based on data provided by the Ministry for Mines, by the mining companies, and extrapolation of geological models of the known deposits in the Tim Mersoï basin, are 500 000 tU of which 140 000 tU are classified as RAR measured resources recoverable at a total operating cost of between US \$35–50/lb. The breakdown of the various mining areas is as follows:

IMOURAREN SA (Imouraren+ Imca 25):	240 000 tU (RAR : 55 000 tU)
SOMAÏR (Arlit) :	70 000 tU (RAR : 25 000 tU)
COMINAK (Akouta +Akola + Ebba) :	65 000 tU (RAR : 26 000 tU)
SOMINA (Azelik +IR+Teyndi) :	30 000 tU (RAR : 14 000 tU)
MADAOUELA (Mariane +Marylin) :	35 000 tU (RAR : 9 000 tU)
IN GALL :	10 000 tU
Other less known licences:	50 000 tU

To these resources, additional reserves estimated at around 150 000 tU could be added for the licences currently under development: Madaouela, Anou Agerouf, Afasto, Adrar Emoles, Agelal, Agebout and Téguida.

### **7. Conclusion**

Niger has immense uranium resources (500 000 tU, of which 140 000 tU are classified as RAR recoverable at less than US \$50/lb) and offers considerable uranium potential, located mainly in the Tim Mersoï basin. Numerous shows and aero-spectrometry anomalies identified in the Air massif and two other basins (Tafassasset and Djado) leave room to speculate and hope that the resources that remain to be discovered are even larger. To date, less than 10% of the area of these vast metallogenic provinces, covering 360 000 km<sup>2</sup>, have been explored in detail.

This optimistic prognosis is based mainly on:

- The existence of a favourable geological environment for uranium entrapment;
- The existence of source rocks for uranium nearby;
- The existence of numerous surface and underground shows;
- A potential of 14–700 tU per km<sup>2</sup>; and,
- The existence of uranium in solution in aquifers.

### **REFERENCES**

- [1] DIRECTORATE FOR MINES, Personal communication, Directorate of Mines, Niamey, Niger (2009).
- [2] SOULEY, M., Personal Communication (AREVA NC), 2009)..
- [3] SOCIÉTÉ DES MINES DE L'AÏR (SOMAÏR), Reserves Ledger as of 31 December 2008. Company Report, Niamey, Niger,(2009).
- [4] SOCIÉTÉ DES MINES DE L'AÏR (SOMAÏR), Feasibility study for exploitation of the Afasto deposit and reserves ledger for 2008, Niamey, Niger (2009).

- [5] SOCIÉTÉ DES MINES DE L'AÏR (SOMAÏR), Feasibility study for exploitation of the Imouraren deposit. Internal report, Niamey, Niger (2009).
- [6] SOCIÉTÉ DES MINES DE L'AÏR (SOMAÏR), Feasibility study for exploitation of the Azelik deposit. Internal report, Niamey, Niger (2009).
- [7] NIGER URANIUM LIMITED, Internet site, [www.niger-uranium.com/](http://www.niger-uranium.com/).

# Geological setting of the Langer Heinrich uranium deposit, Namibia

**E. Becker, K. Kärner**

Paladin Energy Ltd, Perth, Western Australia

*E-mail address of main author: ed.becker@paladinenergy.com.au*

**Abstract.** The Langer Heinrich Uranium Mine is located in the central Namib Desert, Namibia, some 80km east of the coastal town Swakopmund. Geologically, the Namib Desert lies within the Late Proterozoic Damara orogenic belt consisting of metamorphic sedimentary and volcanic rocks. Different stages of syn- to post-tectonic granites and alaskites have intruded into the Damara rocks, some of them containing naturally high amounts of uranium, e.g. Rössing and Ida Dome alaskites. Rift-related uplift initiated by the break-up of Gondwana in Late Jurassic and related surface denudation of Proterozoic rock units were accompanied by the retreat of the Great Escarpment, which is one of the most prominent morphological features in Namibia and divides e.g. the Namib Desert from the Khomas Hochland plateau. Continuous erosion of the high elevated plateaus and the resulting eastern movement of the Great Escarpment during the Cenozoic led to the deposition of fluvial and alluvial deposits west of the Escarpment. These Cenozoic sediments are host to surficial uranium mineralization throughout the Namib Desert including the Langer Heinrich ore body. The Langer Heinrich ore body occurs over 15 km length and strikes east-west along a palaeo-channel, located between the Langer Heinrich Mountain in the north and the Schieferberge to the south. The host rocks are composed of calcretized conglomerates, grits, and minor sands and silts. The bedding is lenticular with meter-thick fining upward sequences being common. Vertical as well as lateral facies changes are rapid. Carnotite is the only ore mineral and has been precipitated from ground water, with uranium being derived from granites and pegmatites exposed in the vicinity of the Langer Heinrich palaeo-channel. The near-surface mineralisation is between 1m to 30m thick and 50 m to 1 100 m wide depending on the width of the palaeo-valley. At a 250 ppm  $U_3O_8$  cut off grade the current resource comprises 127.1 Mt@0.06%  $U_3O_8$  containing 74 415 t  $U_3O_8$  (164 Mlb  $U_3O_8$ ) including an ore reserve of 50.6 Mt@0.06%  $U_3O_8$  (65.84 Mlb  $U_3O_8$ ). Mining operations started in August 2006. The mine has achieved nameplate production in December 2007 and is now in the process of increasing capacity from the original 2.6 Mlb  $U_3O_8$ /annum (1 000 tU/annum) to 3.7 Mlb  $U_3O_8$ /annum (1 423 tU/annum).

## 1. Introduction

The Langer Heinrich Uranium Mine (LHU) is located in the west of central Namibia, Southern Africa. It lies in the central Namib Desert, some 80km east of the major deepwater port at Walvis Bay and the coastal town of Swakopmund (Fig. 1).

LHU was the first conventional mining and processing operation to be brought into production in over a decade. Paladin was able to deliver the project on schedule and within the original budget of US \$92M despite the significant cost pressures experienced by the mining industry during the twenty month construction term. The mine is currently in full production and in the process of increasing capacity from the original 2.6 Mlb  $U_3O_8$ /annum (1 000 tU/annum) to 3.7 Mlb  $U_3O_8$ /annum (1 423 tU/annum).

Following the discovery of the calcrete hosted uranium mineralisation in the early 1970s, Gencor conducted an extensive project evaluation over an 8-year period up until 1980. The study indicated that the project had good potential for development but it was subsequently placed on care and maintenance due to depressed uranium prices.



FIG. 1. Location map.

In 1998 the project was sold to the Australian listed public company, Acclaim Uranium NL (“Acclaim”) who also completed a highly favourable Pre-Feasibility Study. However, adverse uranium market conditions and low prices in the late 1990s again curtailed development and Acclaim sold its holding in LHU to Paladin in 2002.

Following the acquisition, Paladin initiated a Bankable Feasibility Study (BFS), which was completed in April 2005. This BFS confirmed that the LHU project could generate highly attractive returns using defined reserves only.

Based on a mill throughput design of 1.5Mtpa of ore, the BFS showed 1 180 tpa  $U_3O_8$  can be produced for the first 11 years at a head feed grade of 0.0875%  $U_3O_8$  and 401tpa  $U_3O_8$  over the last 4 years, using the accumulated low grade stockpile grading 0.032%  $U_3O_8$ .

Site works began in September 2005 and the construction and staged commissioning of the Langer Heinrich Uranium Project (LHU) was successfully achieved on 28 December 2006.

The mine was officially opened by the President of Namibia on the 14th March 2007 and the first commercial product shipment occurred in the same month. The operation achieved nameplate production in December 2007. Work is now nearing completion on the Stage II expansion, which will lift production to 3.7 Mlb (1 423 tU).

## **2. Regional geological setting**

The Langer Heinrich Uranium Mine occurs within the Central Zone of the Damara orogenic belt, which is part of the Neoproterozoic system of Pan-African mobile belts. In Namibia, the Damara Orogen has been divided into a N–S trending coastal branch (Kaoko and Gariep belts) and a NE trending inland branch (Damara belt), which has been interpreted as a result of the collision between the Congo, Kalahari and Rio de la Plata cratons [1][2]. The inland branch has been divided into a number of zones [3] based on lithostratigraphical, structural and metamorphic criteria. The Central Zone of the Damara orogenic belt contains a variety of syn- and post tectonic granites, some of them being uraniferous (e.g. [4][5]. The uraniferous granites, e.g. at Rössing, Valencia, Ida Dome, and Goanikontes are also referred to as sheeted leucogranites and alaskites [4].

The Late Proterozoic Pan-African orogeny was followed by a long period of tectonic stability. The break-up of Gondwana and thus the opening of the South Atlantic Ocean from the south started at about 170 Ma [6] to 130 Ma ago with fully marine conditions established about 80 Ma ago [7]. Rift-related uplift and surface denudation of Proterozoic rock units were accompanied by the retreat of the Great Escarpment, which is one of the most prominent morphological features in Namibia and divides e.g. the Namib Desert from the Khomas Hochland plateau (see Figs 2 & 3). Continuous erosion of the high elevated plateaus and the resulting eastern movement of the Great Escarpment during the Cenozoic led to the deposition of fluvial and alluvial deposits in drainage systems west of the Escarpment, namely sediments of the Namib groups [8]. These Cenozoic sediments are host to surficial uranium mineralization throughout the Namib Desert including the Langer Heinrich ore body [9].

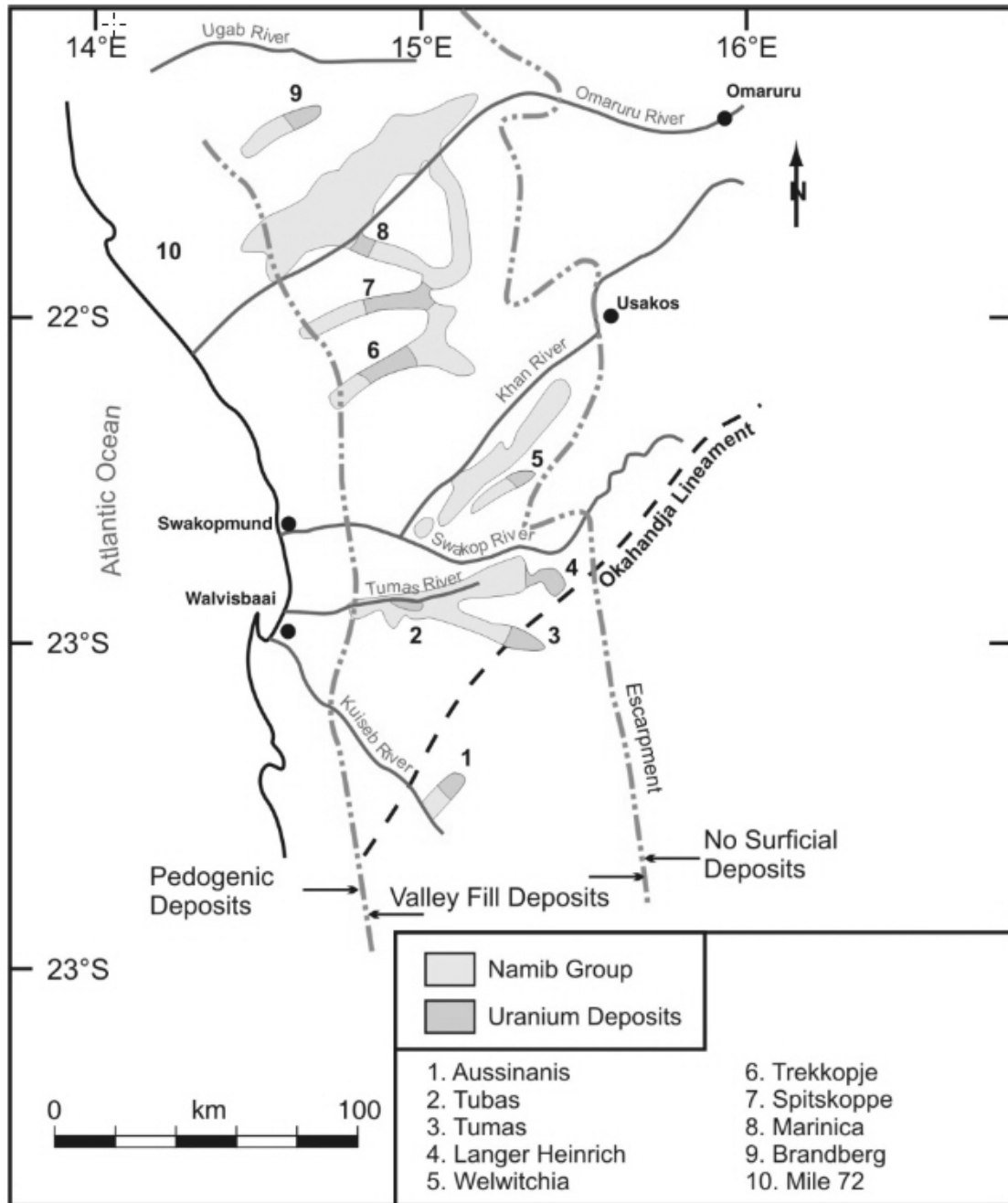


FIG. 2. Generalised map showing the distribution of some major Namib Group deposits and their uranium-bearing zones. Modified after [9].

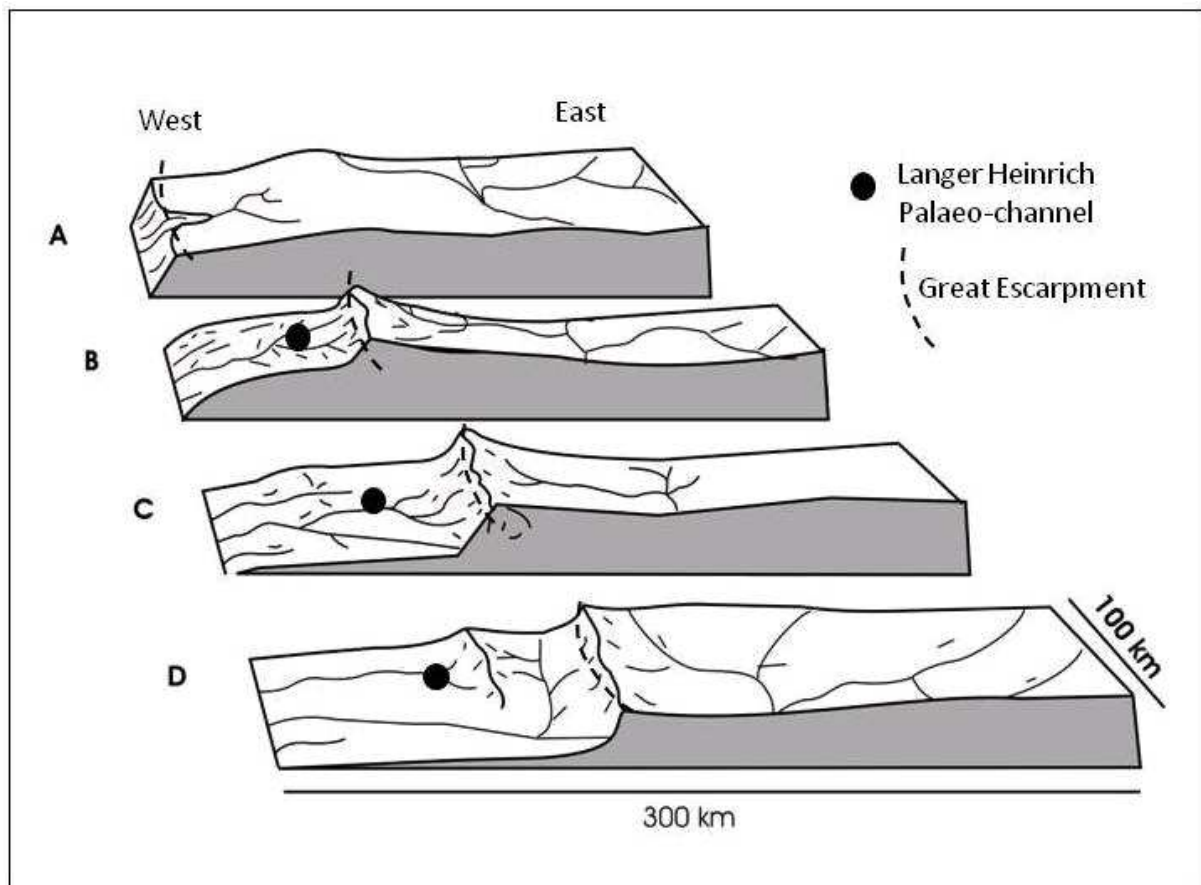


FIG. 3. Morphological evolution of the continental margin of Namibia. A – Late Jurassic/Cretaceous, B – Late Cretaceous/Early Tertiary, C – Tertiary, D – Recent. Modified after [8].

### 3. The Langer Heinrich Palaeo-Channel

#### 3.1. Location and morphology

The east-west trending Langer Heinrich palaeo-channel, which hosts the Langer Heinrich uranium ore body, is located in the central Namib Desert. It has eroded into Proterozoic Damara bedrock and is wedged between the Langer Heinrich Mountain in the north and the Schieferberge immediately to the south [10] (see Fig. 4).

The Langer Heinrich palaeo-valley is 50 to 1 100 m wide. The incision of the palaeo-channel into the underlying Damara bedrock increases in flow direction. Close to the headwaters at the eastern end of the 15 km long Langer Heinrich mining licence, the palaeo-channel eroded not more than 20 m into the bedrock, whereas downstream at the western end of the mining licence the palaeo-channel eroded up to 100 m deep into the Late Proterozoic bedrock.

The base of the paleo-channel (river bed) descends from 710 m above sea-level in the east to 510 m above sea level in the west over a distance of 15 km having a gradient of more than 10 m per kilometer. This steep gradient is typical found in the part of a drainage system, which is close to its headwaters. Indeed, the Langer Heinrich palaeo-channel seems to have its origin at the eastern boundary of the Langer Heinrich mining licence.

The incision of the palaeo-channel was superseded by a depositional cycle during which the palaeo-channel was filled with sediments, which subsequently have been calcretized. These sediments are host to the Langer Heinrich ore body.

The present-day Gawib River (see Fig. 4), which mirrors the course of the underlying palaeo-channel to a large extent, has locally eroded parts of calcretized palaeo-channel sediments. As a result, the Langer Heinrich ore body is exposed at the surface in places.

### 3.2. Local geology

The oldest rocks of the Damara Group comprise quartzites of the Etusis Formation of the Nosib Group, which form the Langer Heinrich Mountain anticlinorium (see Fig. 4). The Schieferberge to the south are composed of a variety of schists and calcsilicates, which are referred to as the Tinkas Formation of the Khomas Subgroup (Swakop Group). Rössing and Khan formations, which are found regionally between the Nosib and Khomas Subgroup are not present in the Langer Heinrich area. Limited outcrop of the diamictites of the Chous Formation occurs west of the Langer Heinrich Mountain (see Fig. 4). Southeast of the Langer Heinrich Mountain, the Bloedkoppie granite, which is a leucocratic late- to post-tectonic Damara granite, has intruded both Nosib and Swakop groups and covers an area of about 25km<sup>2</sup> [10]. Additionally, pegmatites are found throughout the Damara sequence. Some of the pegmatites are interpreted as apophyses of the Bloedkoppie granite; others are syntectonic and follow the regional foliation planes [11]. The thickness of pegmatites is highly variable and lies between some decimeters to more than one hundred meters.

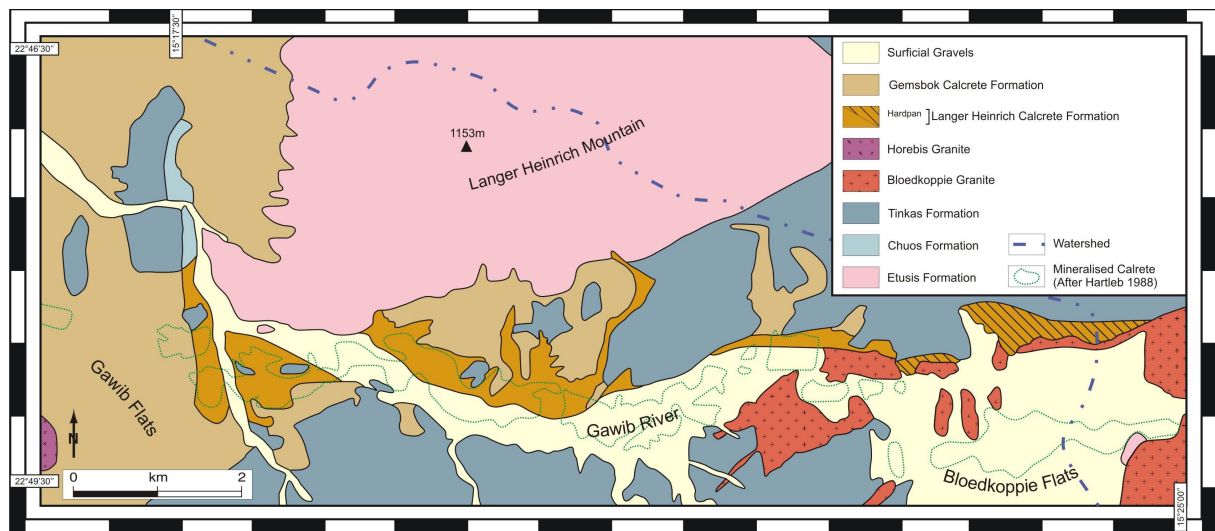


FIG. 4. Map showing the distribution of Proterozoic Damara bedrock as well as Cenozoic cover sediments within the Langer Heinrich area. The Gawib River is a present-day drainage system, which mirrors the course of the underlying Langer Heinrich palaeo-channel to a large extent. From [12].

Within the Langer Heinrich area, the east-west trending palaeo-channel traverses through Damara granites in the east, then it is eroded into schists of the Tinkas Formation before its northern bank is formed by the Tinkas/Etusis formations contact. Further downstream, the palaeo-channel eroded into Tinkas Formation again.

The incision of the palaeo-channel was superseded by a depositional cycle during which the palaeo-channel was filled in with fluvial sediments. These fluvial sediments belong to the Langer Heinrich Formation.

Subsequently, alluvial sediments of the Gemsbok Formation were deposited on top of the Langer Heinrich Formation. The two formations are separated from each other by an erosional discontinuity surface.

Deposits, younger than those of the Gemsbok Formation only occur west of the Langer Heinrich Mountain and are summarized as Gawib Flat deposits by several authors (e.g. [11][9]).

### 3.3. Lithology of Cenozoic host sediments

#### 3.3.1. Langer Heinrich formation

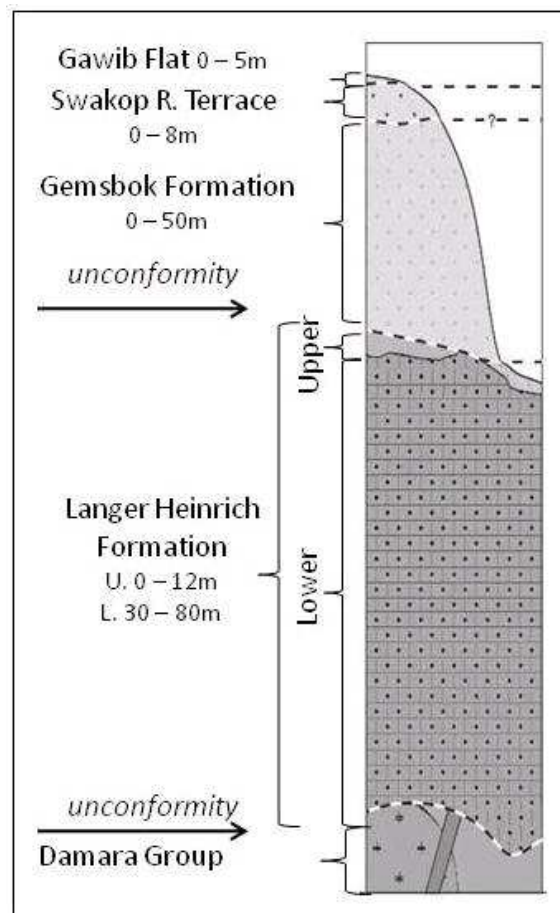


FIG. 5. Idealised composite profile showing the stratigraphy of Cenozoic sediments within the Langer Heinrich area.

The fluvial Langer Heinrich Formation comprises the oldest Cenozoic sediments that have been deposited along the palaeo-channel. Within the Langer Heinrich area they are up to 90 m thick (see Fig. 5) and calcretized to a large extent.

They are mainly composed of unsorted polymictic conglomerates, grits, and minor sands and silts. Vertical as well as lateral facies changes are rapid.

The bedding is lenticular with meter-thick fining upward sequences being common. Additionally, both trough cross bedding and planar bedding occur in places.

The detrital components consist of subrounded quartz and feldspar granules and pebbles as well as subangular lithofragments deriving from the surrounding country rocks, e.g. schists, calcsilicates, quartzites, and minor granites.

The sediments were cemented by calcite (calcretisation) after their deposition under arid to semi-arid climatic conditions. Calcite cement in sediments of the Langer Heinrich Formation generally displays both sparitic and micro-sparitic cement indicating a ground water origin of the calcrete. This formation is host to the Langer Heinrich ore body. Carnotite, which is the only uranium mineral identified at present, has been precipitated from uranium-bearing groundwaters, with uranium being most likely

derived from surrounding Damara granites and pegmatites and vanadium from the schists of the Tinkas Formation.

### *3.3.2. Gemsbok formation*

The Langer Heinrich Formation is unconformably overlain by the Gemsbok Formation (see Fig. 5), which is only exposed in the central and western portion of the Langer Heinrich mining licence, where it reaches a maximum thickness of 50 m.

These sediments are generally coarse-grained. Detrital components are quartz and feldspar as well as a variety of lithoclasts, but mainly schists and calcisilicates of the Tinkas Formation. The main differences between the Langer Heinrich and the Gemsbok formations are a lack of graded bedding and significantly less vertical and lateral facies changes, which give the Gemsbok Formation an alluvial character.

The Gemsbok Formation is partly calcretized displaying macroscopic and microscopic features that are typical for pedogenic calcretes. This formation does not contain economic uranium mineralisation, although stringers and blobs of carnotite have been locally observed within outcrops of pedogenic calcrete.

### *3.4. Ore minerals and textures*

Uranium mineralisation, which is hosted by the Langer Heinrich Formation, occurs as carnotite, an oxidised uranium and vanadium secondary mineral. The uranium deposit occurs along the Langer Heinrich palaeo-channel over 15 km length in seven higher grade pods (*see, Fig. 6*) within a lower grade mineralised envelope.

Mineralisation is near surface, 1 m to 30 m thick and is 50 m to 1 100 m wide depending on the width of the palaeo-valley.

The ore is classified according to its grain size distribution and carbonate content, e.g. calcareous conglomerates and grits, non-calcareous conglomerates and grit. Carnotite occurs as disseminations within the sediment matrix, as veneers lining cavities and fracture planes, but also as coatings on pebbles and boulders.

The distribution of ore within the palaeo-channel shows that the morphology of bedrock and aquifer controlled the precipitation of carnotite to a certain extent. Narrow portions of the palaeo-channel as well as areas close to bedrock highs commonly contain high grade mineralisation and thus most likely represented ponding situations for ground water with high evaporation rates, which resulted in an increased concentration of uranium and vanadium in solution and therefore precipitation of carnotite.

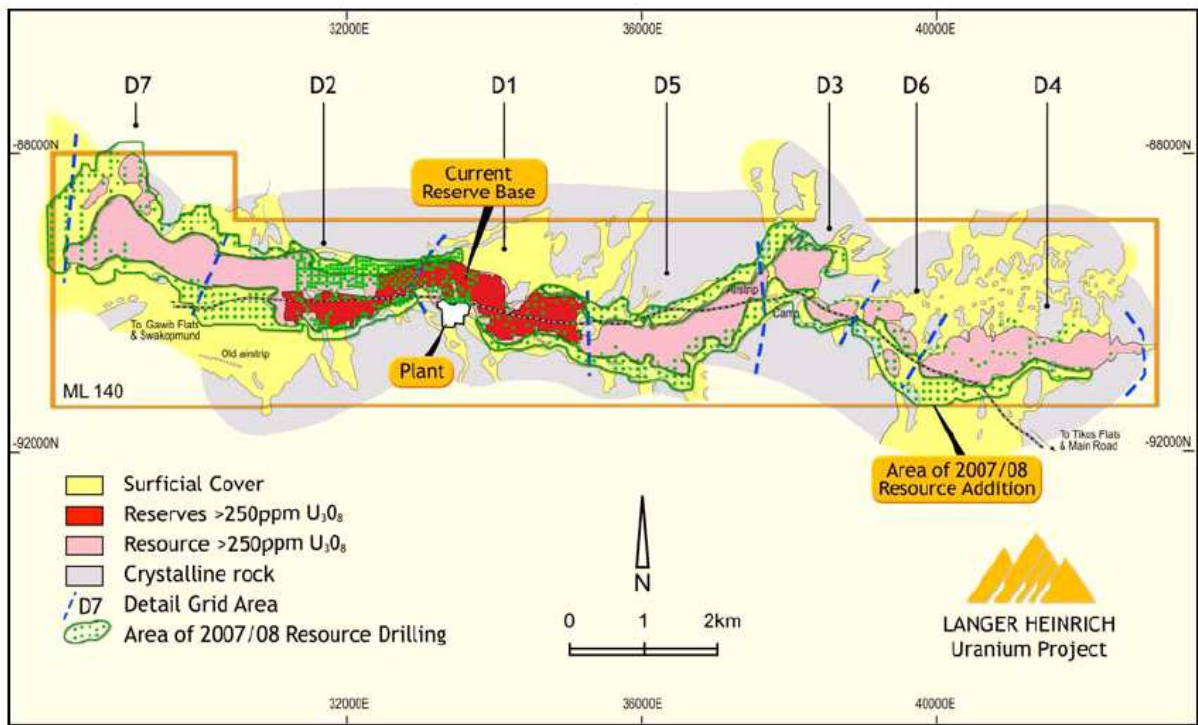


FIG. 6. Mineralisation within the Langer Heinrich palaeo-channel.

### 3.5. Evolution of the ore body

The formation of the Langer Heinrich ore body was strongly controlled by the palaeo-morphological and palaeo-climatic evolution of the Namibian continental during the Cenozoic.

Palaeo-climatic conditions that favour the formation of both calcrete and carnotite were given in Eocene/Oligocene as well as in Lower Miocene. However, erosional unconformities within the Langer Heinrich area, which correlate to major geological tectonic events in central Namibia, indicate that the ore body must have formed pre-Miocene (see Table 1 below).

Table 1. Cenozoic evolution of Namibia's passive continental margin with reference to the Langer Heinrich deposit using [7][13][14][15][8][6][16][17][9][11]

				<b>Major Geological Events</b>	<b>Palaeoclimate</b>	<b>Tectonics</b>	<b>Langer Heinrich</b>				
<b>Quaternary</b>			<i>P.-A. II C.</i>	Formation of main Namib sand sea, Incision of the Swakop River	Arid	Sedimentation	Incision of present-day Gawib River, Erosion of Tertiary sediments				
							Deposition of Swakop R. Terrace and Gawib Flat				
Tertiary	Neogene	<b>Pliocene</b>		<i>Post-African I Cycle</i>	Establishment Benguela current, formation of pedogenic calcrete	Stable land surface	Pedogenic calcrete in Gemsbok Formation				
		Miocene	<b>L.</b>					Semi-arid to arid			
			<b>M.</b>					Semi-humid			
			<b>E.</b>	Semi-humid, (sub)tropical	Sedimentation						
		Palaeogene	<b>Oligocene</b>		<i>African Cycle</i>	Proto-Namib desert phase (eolian Tsondab Formation)	Semi-arid/arid	Uplift/erosion (unconformity)	Ground water calcrete/carnotite in Langer Heinrich Formation		
			<b>Eocene</b>							Stable land surface	Deposition of the Langer Heinrich Formation
	<b>Palaeo-cene</b>		Formation of the 'Namib Unconformity Surface' (NUS)	Humid to semi-arid							
	<b>Cretaceous</b>									Post-Gondwana erosional phase	Humid-subtropical
	<b>Jurassic</b>			Initial break-up of Gondwana							

### 3.6. Resources and reserves

At a 250ppm U<sub>3</sub>O<sub>8</sub> cut off grade the current resource contains 32.8 Mt at 0.06% for 19 582 t U<sub>3</sub>O<sub>8</sub> in the Measured category, 23.6 Mt at 0.06% for 13 276 t U<sub>3</sub>O<sub>8</sub> in the Indicated category and 70.7 Mt at 0.06% for 41 557 t U<sub>3</sub>O<sub>8</sub> in the Inferred category. These resources conform to both the JORC (2004) and NI 43-101 guidelines and are quoted inclusive of any ore reserves.

Ore reserve has been announced and reported conforming to both JORC and NI 43-101 guidelines. Based on the current reserve of 50.6 Mt at 0.06% for 29 874 t U<sub>3</sub>O<sub>8</sub> the project has a life of a minimum of 17 years, based on increased Stage II production rates.

The resource model is currently being up-dated to take into account further resource definition drilling in 2007 and 2008. It is expected that this exercise will result in a significant increase in resources.

## REFERENCES

- [1] PRAVE, A. R. (1996): Tale of three cratons: tectonostratigraphic anatomy of the Damara orogen in northwestern Namibia and the assembly of Gondwanaland. *Geology*, 24, 1115–1118.
- [2] STANISTREET, I. G., KUKLA, P. A. & HENRY, G. (1991): Sedimentary basinal responses to a Late Precambrian Wilson cycle: the Damara orogen and Nama foreland Namibia. *Journal of African Earth Sciences*, 13, 141–156.
- [3] MILLER, R. (1983): The Okahandja Lineament, a fundamental tectonic boundary in the Damara Orogen of South West Africa/Namibia. *Transactions of the Geological Society of South Africa*, 82, 349–361.
- [4] KINNAIRD, J.A. & NEX, P. (2007): A review of geological controls on uranium mineralisation in sheeted leucogranites within the Damara Orogen, Namibia. *Applied Earth Science (Trans. Inst. Min. Metall. B)*, 116, 2, 68 – 85.
- [5] NEX, P., HERD, D. & KINNAIRD, J. (2002): Fluid extraction from quartz in sheeted leucogranites as a monitor to styles of uranium mineralization: an example from the Rössing area, Namibia. *Geochemistry: Exploration, Environment, Analysis*, 2, 83 – 96.
- [6] TINKER, J.H. & DE WITT, M.J. (2004): Balancing erosion and deposition on and around Southern Africa since Gondwana breakup. *Geoscience Africa 2004*, 634 – 635.
- [7] WARD, J.D., SEELY, M.K. & LANCASTER, N. (1983): On the antiquity of the Namib. *South African Journal of Science*. 79, 175 – 183.
- [8] GILCHRIST, A.R., KOOI, H. & BEAUMONT, C. (1994): Post-Gondwana geomorphic evolution of southwestern Africa: Implications for the controls on landscape development from observations and numerical experiments. *Journal of Geophysical Research*, 99, B6, 12211 – 12228.
- [9] HAMBLETON-JONES, B.B. (1984): Surficial Uranium Deposits in Namibia. - In: *Surficial Uranium Deposits: Report of the working group on uranium geology; IAEA-TECDOC- 322; International Atomic Energy Agency; Vienna; pp. 205-216.*
- [10] HARTLEB, J.W.O. (1988): The Langer Heinrich Uranium Deposit: Southwest Africa/Namibia. *Ore Geology Reviews*, 3, 277 – 287.
- [11] HAMBLETON-JONES, B.B. (1976): The geology and geochemistry of some epigenetic uranium deposits near the Swakop River, South-West Africa. - University of Pretoria; Ph.D.Thesis (unpubl.); 306 p.
- [12] TRITTSCHACK, R. (2008): Geological identification and mineralogical characterisation of palaeo-surfaces and channel fills at the Langer Heinrich uranium deposit, Namibia. Unpubl. MSc. Thesis.
- [13] PARTRIDGE, T.C. & MAUD, R.R. (1987): Geomorphic evolution of southern Africa since the Mesozoic. *South African Journal of Geology*, 90, 179 – 208.
- [14] PICKFORD, M. (2000): Neogene and Quaternary vertebrate biochronology of the Sperrgebiet and Otavi Mountainland, Namibia. *Geological Survey of Namibia Communications*, 12, 359 – 365.
- [15] SÉGALEN, L., RENARD, M., LEE-THORP, J.A., SENUT, B. & PICKFORD, M. (2004): Palaeoclimate and palaeoenvironment reconstruction of the Namib Desert during the Neogene. *Geoscience Africa 2004. Abstract Volume 2, University of the Witwatersrand, Johannesburg, South Africa*, 586.
- [16] RAAB, M.J., WEBER, K. & BROWN, R.W. (2002): Quantifying denudation rates with vertical relief fission track profiles in Namibia. *AdG – Forschung und*

Entwicklungszusammenarbeit in Afrika. Göttingen, 28. – 29. Juni.

- [17] WILKINSON, M.J. (1990): Paleoenvironments in the Namib Desert: The Lower Tumas Basin in the Late Cenozoic. - University of Chicago Geography Research Paper No. 231; University of Chicago; 196 p.

# The geology of the Kayelekera uranium mine, Malawi

E. Becker<sup>a</sup>, J. Mwenelupembe<sup>b</sup>, K. Karner<sup>a</sup>, J.C. Corbin<sup>a</sup>

<sup>a</sup>Paladin Energy Ltd, Perth, Western Australia

<sup>b</sup>Paladin (Africa) Ltd, Lilongwe, Malawi

*E-mail address of main author: ed.becker@paladinenergy.com.au*

**Abstract.** The Kayelekera Uranium Deposit is located in the northern part of Malawi, Southern Africa, 40 kilometres west of the township of Karonga. Paladin Energy Limited, an Australian based company holds an 85% interest in the Kayelekera Project through its wholly owned subsidiary Paladin (Africa) Limited. The other 15% is held by the Republic of Malawi. Kayelekera is a sandstone-hosted uranium deposit of the roll front type. At a 300 ppm cut-off the deposit contains a total resource of 19 500 t of  $U_3O_8$  with an average grade of 800 ppm. Reserves include 13 500 tonnes at 1 100 ppm. The deposit is hosted by sediments of the Permian Karoo Sequence in the North Rukuru Basin. Uranium mineralization occurs in four principal lenses developed within arkose units called S and T, the combined mudstone arkose Units U+U+W and arkose unit X. The lenses are superimposed vertically along the axis of a shallow northwest trending syncline. A subparallel fault structure cuts the eastern limb of the mineralised syncline. Uranium mineralisation occurs within reduced and oxidized arkose and is redistributed into mudstones along faults. Coffinite has been identified as the main primary uranium bearing mineral with uraninite being present to a lesser degree. Secondary uranium minerals meta-autunite, boltwoodite and minor uranophane occurs in weathered oxidized rocks near surface and along faults. Paladin completed a Bankable Feasibility Study for the Kayelekera Uranium Project including a comprehensive Environmental Impact Assessment in early 2007 and was granted a Mining Lease in April of that year. Construction started in late 2007 and was completed in March 2009. Ramp up to nameplate production of 3.3 million lbs  $U_3O_8$  (1 269 tU) from 1.5 million tonnes of ore is currently in progress.

## 1. Introduction

The Kayelekera Project is located in northern Malawi, 52 km west of the provincial town of Karonga at the northern end of Lake Malawi, and 575km by road north of the capital city, Lilongwe (see Fig. 1).

Kayelekera is a sandstone-hosted uranium deposit with a resource of 19 900 tonnes of  $U_3O_8$  at a grade of 0.08% using a 0.03% cut-off. The deposit lies within Permian Karoo sandstones in the northern part of the North Rukuru Basin of Malawi.

The Kayelekera uranium deposit was the subject of detailed evaluation in the 1980s by the Central Electricity Generating Board of the United Kingdom (“CEGB”). Their work culminated in the execution of a full feasibility study in 1991, assessing the viability of constructing and operating a conventional open pit mine and supporting infrastructure. Using the engineering and financial parameters adopted by CEGB, the study indicated that the project was uneconomic at that time. CEGB relinquished its tenure in 1992.

Paladin (Africa) Limited, a wholly owned subsidiary of Paladin Energy Ltd, acquired a 90% interest in the Kayelekera Project in early 1998 and increased its equity to 100% in 2005. Shortly after Paladin’s entry into the project the uranium price weakened and remained low until mid 2003, stalling progress towards development. Subsequent to the turnaround in the uranium market Paladin started active work on the project in 2004.

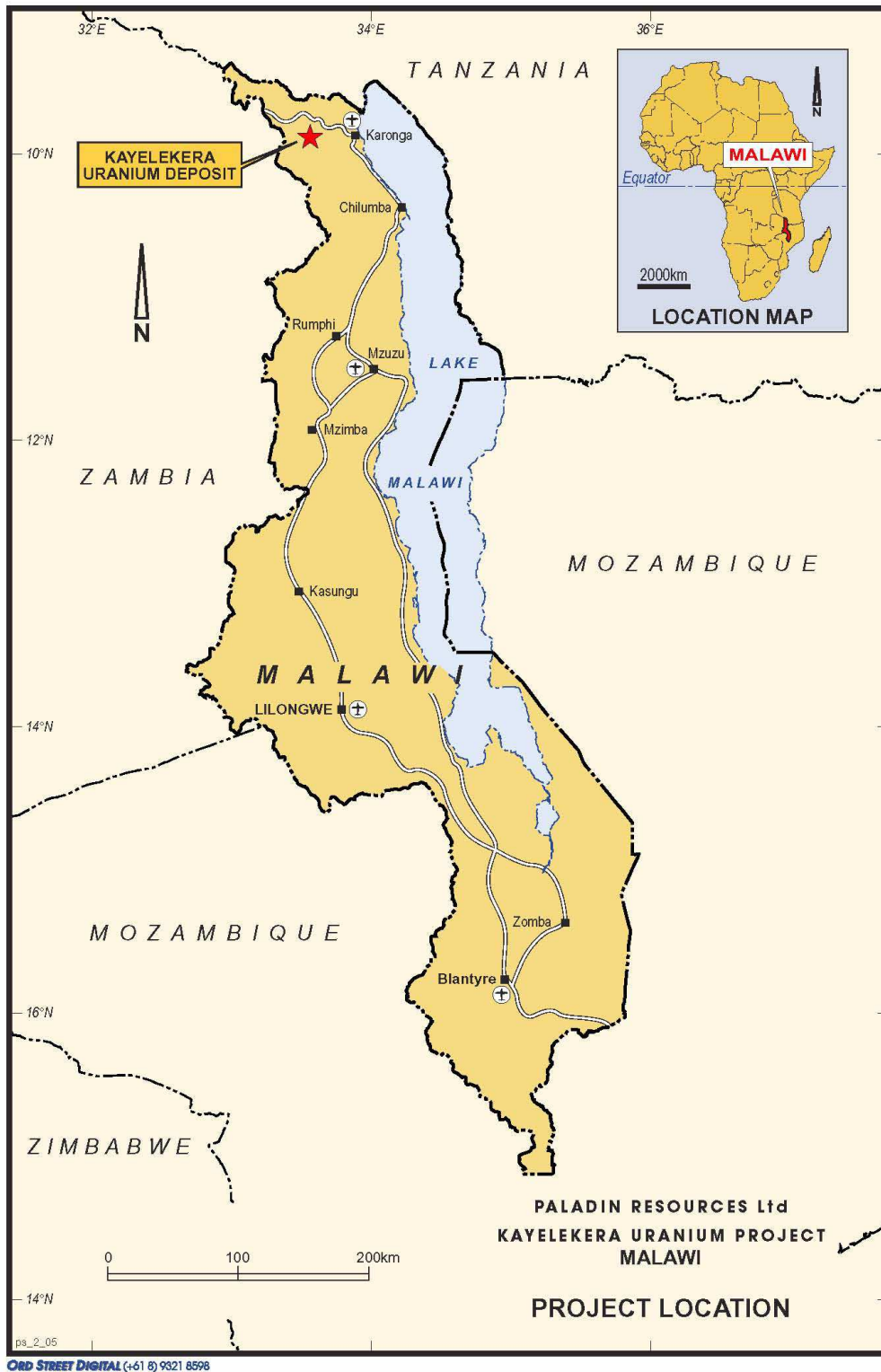


FIG. 1. Location map.

In 2005 Paladin started a Bankable Feasibility Study (BFS) including a detailed resource drilling programme and announced a new resource to JORC standard in 2006. After completing a Development Agreement with the Malawi Government and the BFS together with a full Environmental Impact Assessment in January 2007, the Mining License, ML152, covering 5 550 hectares was granted in April 2007 for a period of fifteen years. Construction started in June 2007 at a budgeted cost of US\$ 200M.

The construction project workforce peaked at around 2 000 persons, with more than 75% of workers being Malawian nationals.

Open pit mining commenced in June 2008 to develop initial stockpiles, with the first blast occurring on 24 July 2008. A grade control drilling programme of approximately 13 000 m was undertaken to define reserves for the first 18 months of mining and results to date show a strong correlation to the updated resource model that was used in the BFS.

Commissioning began in January 2009 with first production achieved mid-April. Production ramp-up is scheduled over the 2009 calendar year, with full design operation targeted for December 2009.

The mine was officially opened on 17 April 2009 by the President of Malawi, Dr. Bingu wa Mutharika.

The project is designed to give an annual production of 3.3 Mlb U<sub>3</sub>O<sub>8</sub> (1269 tU) from the processing of 1.5 million tonnes per annum (Mtpa) of sandstone and associated ores by grinding, acid leaching, resin-in-pulp extraction, precipitation and drying to produce saleable product.

## 2. Access, climate, infrastructure and physiography

The existing access to the Kayelekera project area is via the Karonga - Chitipa road, a journey of about 50 km. The road is un-surfaced for most of its length and allows good access in the dry season but only limited access to vehicles with 4WD and high clearance during the wet season. Construction of an all weather road is currently in progress. Access from the Chitipa road to the project site is via an all weather dirt road constructed by the company in 2008. The nearest airfield is at Karonga. From Karonga, access south is good and the main roads are in excellent condition.

Malawi is a land locked country, and as a consequence all access for imported materials and equipment is either by road through South Africa or via Dar-es-Salaam in Tanzania.

The Kayelekera Project is situated about 10° south of the equator and so has a tropical climate. There are three recognizable seasons during the year established by both rainfall and temperature. A wet season that lasts between mid-November to April, a cool season from May to early August and a hot dry season from August to November (Table 1).

Table 1. Rainfall data for the Karonga District Centres

	Temperature			Rainfall	
	Maximum	Minimum	Mean Annual	Annual	Monthly Max
Chitipa	29°(Oct)	13°(June)	20°	1,039mm	210mm (Jan & Feb)
Karonga	33°(Oct/Nov)	17°(Jul/Aug)	25°	1,165mm	335mm (Mar)

In Kayelekera the annual rainfall is about 1,000mm, with a minimum and maximum of 700 mm and 1 600 mm, respectively. Most rain falls between January and March in a limited number of high intensity tropical storms.

Prevailing winds are generally from the SE and are strongest during March to October.

Local population density is low with only a small number of settlements within the vicinity of the project site.

The project site is located in hilly country at the northern end of Lake Malawi. Topography comprises steep and rolling hills separated by winding river valleys. The ground surface varies between 750 m to 1 200 m in elevation.

The major river in the area is the North Rukuru River, which flows year round from South to North along the eastern side of the property. There are two tributaries of the North Rukuru River, the Sere and the Muswanga Rivers, with permanent flow. Other streams have only seasonal flows.

Regional vegetation consists principally of light deciduous forest with a variety of small shrubs, herbs and grasses (known as Miombo woodland), with some small, seasonally waterlogged, grass covered depressions (known as Dambos). River fringes are more heavily vegetated with woody species, ferns and bamboos.

Areas of cultivation occur principally around the small settlements and along the banks of the Sere River.

The project area supports a moderately diverse fauna typical of less densely populated areas of Northern Malawi. No species recorded appear on lists of threatened or endangered species prepared by the International Union for the Conservation of Nature.

### **3. Regional geology**

The Karonga area is mainly underlain by metamorphic and igneous rocks of the pre-Karoo Malawi Basement Complex (see Fig. 2). These are overlain by several small basins of Karoo sediments and, nearer to Lake Malawi, Cretaceous to Recent lacustrine sediments. The major lithological components of the basement are gneisses and intrusives of the Misuku Belt, the south-eastern extension of the Ubendian Mobile Belt of south-western Tanzania into Malawi.

The whole area was subjected to four episodes of mainly brittle deformation in the late Precambrian and early Palaeozoic (1 200 – 1 100 my; 670, 570, and 450 my).

A long period of erosion of the Misuku Belt was interrupted in early Permian by the deposition of Karoo sediments upon a subdued but irregular topography initially under glacial and periglacial conditions. The Karoo sediments occupied several partially or totally fault bounded basins (half graben structures, but in mid-Karoo times probably covered most of the area. The Karoo sequence mainly comprises gritty arkosic sandstones and shales with thin coal seams near the base of the sequence overlain by calcareous mudstones and limestones. Faulting and subsidence accompanied Karoo sedimentation, which ended with the initiation of the Gondwana erosion cycle in Lower Jurassic.

In Upper Jurassic early rift faulting established a depositional basin in the vicinity of what is now northern Lake Malawi. From the Upper Jurassic to the present day a sequence of uplift, erosion and faulting resulted in periodic lacustrine sedimentation, of which relics are preserved in the Rift Scarp Zone and the Lakeshore Plain. The earliest of these lacustrine sediments are sandstones, shales and marls of the Dinosaur Beds of Upper Jurassic or Lower Cretaceous age. Overlying these and separated by successive unconformities are Tertiary conglomerates and sandstones. These are overlain by limestones, marls, sandstones and conglomerates, pebble beds as well as poorly consolidated sands and muddy sands of Pleistocene age. Early Pleistocene Songwe Tuff beds related to an explosive phase of the Rungwe Volcanic Centre in southwest Tanzania are found in a limited area along the Songwe valley. Recent pebble beds, the Dwangwa Gravels, and lacustrine sands and gravels of the Lakeshore Plain mark the retreat of Lake Malawi to its present position.

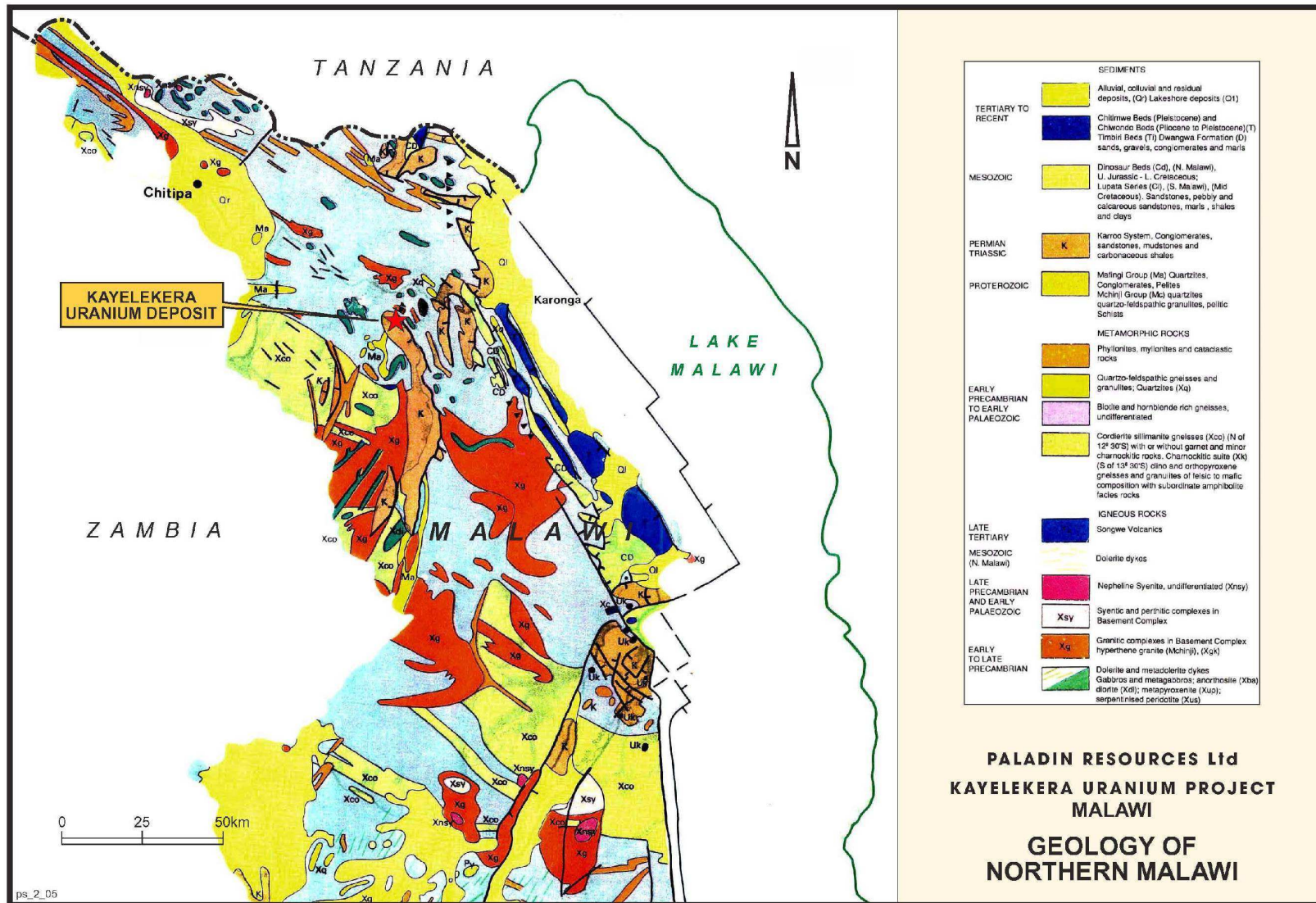


FIG. 2 Geology of Northern Malawi.

### ***3.1. The geology of the North Rukuru Basin***

The Kayelekera uranium mineralization is located close to the north tip of the North Rukuru Basin. The North Rukuru Basin is some 50 km along strike (north - south) and has a maximum width of about 6.5 km. It contains a thick (at least 1 500 m) sequence of Karoo sediments preserved in a half graben about 35 km to the west of and broadly parallel to the Lake Malawi section of the East African Rift System. The faulted eastern margin of the basin probably has been active during sedimentation as some evidence of growth faulting in the Kayelekera open pit shows. To the west, the Karoo sediments rest unconformably on basement gneisses. Figure 3 shows the geology of the northern North Rukuru Basin.

The Karoo sediments at Kayelekera have been divided into three formations, which are from the bottom to the top:

#### **1) Basal Beds (K1)**

The Basal Beds, resting unconformably on metamorphic basement rocks, are glacial, fluvio-glacial and glacio-lacustrine sediments consisting of diamictites, varved shales and calcareous sandstones.

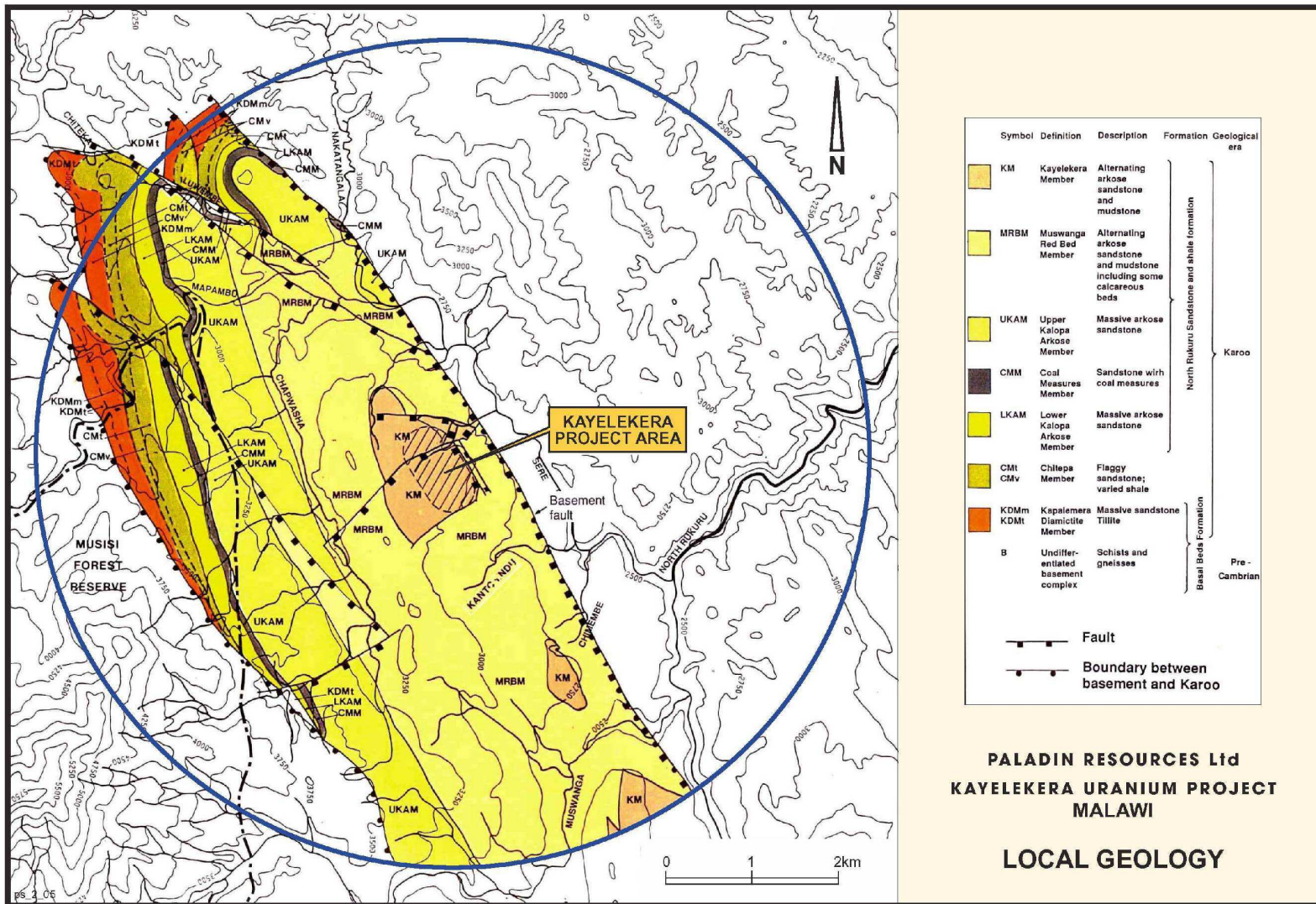
#### **2) Coal Measures (K2)**

Coal measures, sometimes absent, overlie the Basal Beds and consist of discontinuous coal seams, carbonaceous shales and fine grained sandstones.

#### **3) North Rukuru Sandstone and Shale Formation (K3+4)**

The lower part of this formation is a thick arkose unit (Kalopa Member), which is overlain by the Muswanga (Red Bed) Member consisting of fining upward cycles of sheet like coarse grained arkoses, red-brown calcareous mudstones and grey to black carbonaceous silty mudstones. The lower arkose of the Muswanga Member is characterised by a primary oxide (hematitic) matrix, partially altered to goethite/limonite on weathering. This unit is overlain by a distinct fossiliferous bed containing silicified wood, which is thought to be the top of K3.

The overlying Kayelekera Member contains the top 150 metres of the North Rukuru Sandstone and Shale Formation and hosts the uranium mineralization at Kayelekera. The Kayelekera Member is composed of arkoses with a primary reduced (chlorite/pyrite) matrix and abundant carbonaceous debris and is thought to be equivalent of the lower K4.



ORD STREET DIGITAL (+61 8) 9321 8598

FIG. 3. Geology of the northern North Rukuru Basin.

## 4. Local geology

### 4.1. Lithology of the host sediments (Kayelekera Member)

The Kayelekera deposit lies within the uppermost 150 metres of the North Rukuru Sandstone and Shale Formation (Kayelekera Member). Surface mapping and drill hole information indicate a total of eight separate arkose units with intervening silty mudstones and mudstones in an approximate 1:1 ratio. The detailed lithology of the Kayelekera Member is given in Figs 4 and 5 shows the simplified geological features around the Kayelekera deposit.

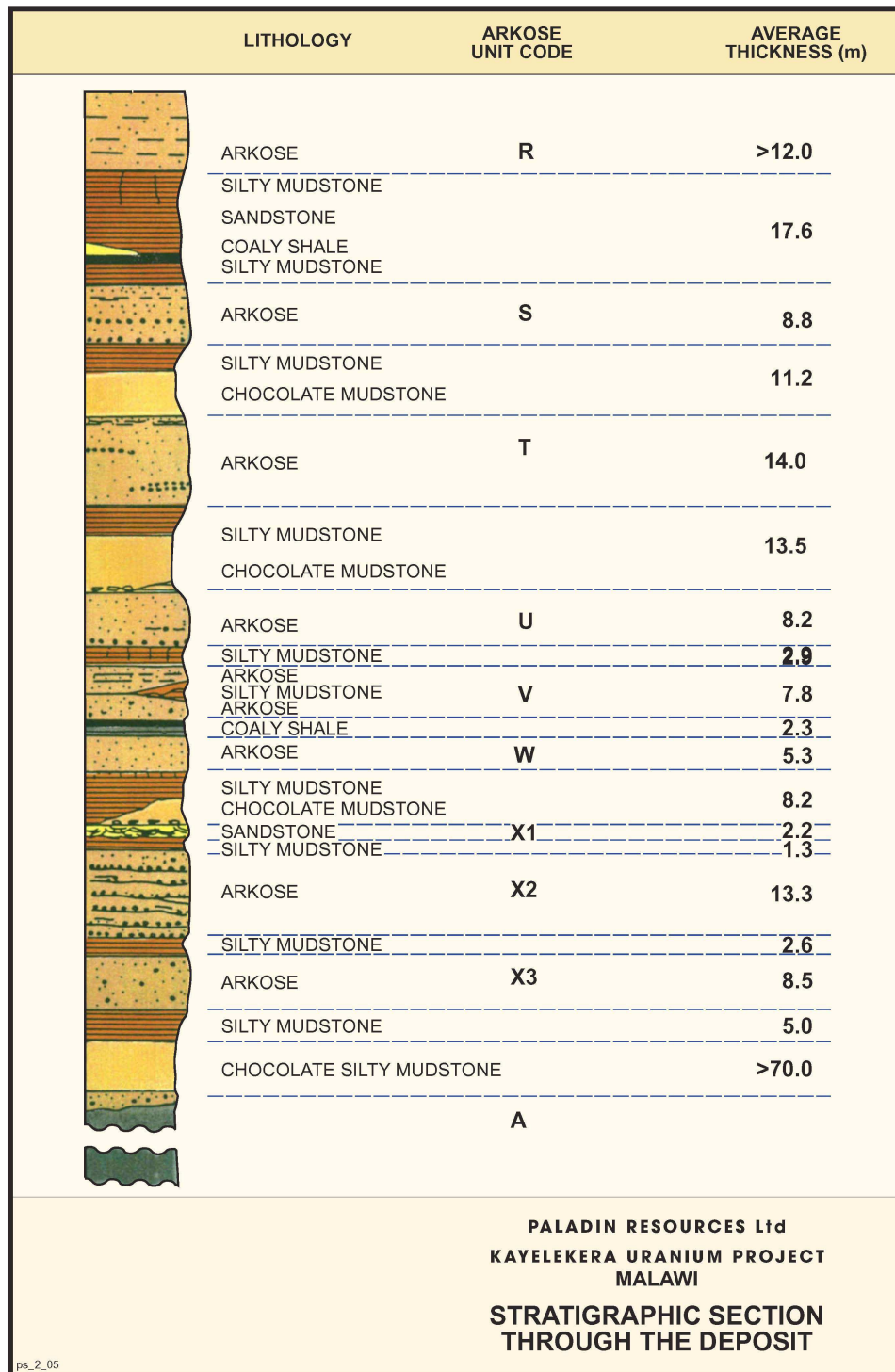


FIG. 4. Stratigraphic section.



FIG. 5. Geological map.

The succession is indicative of cyclic sedimentation within a broad, shallow, intermittently subsiding basin. Each cyclothem generally passes upwards from coarse grained reduced facies arkose through oxide-facies 'red bed' mudstone into reduced facies grey-black carbonaceous silty mudstone. Thin coal rich horizons are present within some cyclothem.

#### *4.1.1. Arkose*

The arkose units, which contain uranium mineralization, are on average about 8 metres thick and are generally coarse grained and poorly sorted with a high percentage of fresh pink feldspar clasts. In reduced intersections, seen in core, pink feldspars contrast strongly with the dark-green pyritic, carbonaceous matrix. Individual units may show several fining upward sequences with quartz and feldspar bearing pebbly conglomerate grading into medium or more rarely, fine grained, micaceous arkosic sandstone. Thin mudstone layers may mark the boundary between fining-up units within the arkoses.

Carbonaceous debris as layers on cross-stratification surfaces, disseminations, and as individual 'woody' fragments of several centimeters in length are commonly present in association with pyrite within reduced facies arkose intersections. Larger fragments of carbonaceous debris are also found within altered oxidized arkose intersections.

The arkose units are of variable thickness, though they generally thicken towards the northwest, whereas mudstones are thinning or cut out altogether in this direction, indicating that a possible channel system was draining towards northwest.

#### *4.1.2. Chocolate-brown 'Red Bed' mudstone*

This lithofacies comprises red to chocolate-brown, homogeneous, fine grained sediments with no discernible bedding. Pale green patchy 'reduction zones' may be present and in the lower units calcareous, concretionary nodules and calcite veining are common.

#### *4.1.3. Grey carbonaceous silty mudstone*

This unit is much more variable than the preceding red beds and comprises a range of lithotypes including:

- a) light to dark grey homogeneous mudstones,
- b) grey silty mudstones containing discrete quartz grains,
- c) silty mudstones containing multi-coloured angular mud clasts;
- d) laminated bedded, carbonaceous, pyritic black shales;
- e) fine grained; current bedded, carbonaceous sandstone and 'coal' shales.

### **4.2. Structure of the ore body**

The Kayelekera Member of the North Rukuru Sandstone and Shale Formation is folded into gentle synclinal structures by drag against the eastern boundary fault (see Figs 3, 5).

The deposit occupies one of the synclinal structures, which is a down-faulted block bounded by normal faults trending NNW. The eastern margin of the deposit is marked by a major fault zone with similar trend and having a throw in excess of 100 metres.

Transverse faults with limited offset cut across the synclinal structure at Kayelekera causing a dip reversal to the north creating a basin structure bounded by faults on three sides.

## 5. Uranium mineralization

Four principal mineralized lenses, developed within arkose units 'S' and 'T', the combined arkose-mudstone units 'U+V+W' and arkose units X<sub>1</sub>-X<sub>3</sub> are present within the deposit to a depth of 100 metres from surface [1-2]. Figure 6 shows a cross section through the deposit.

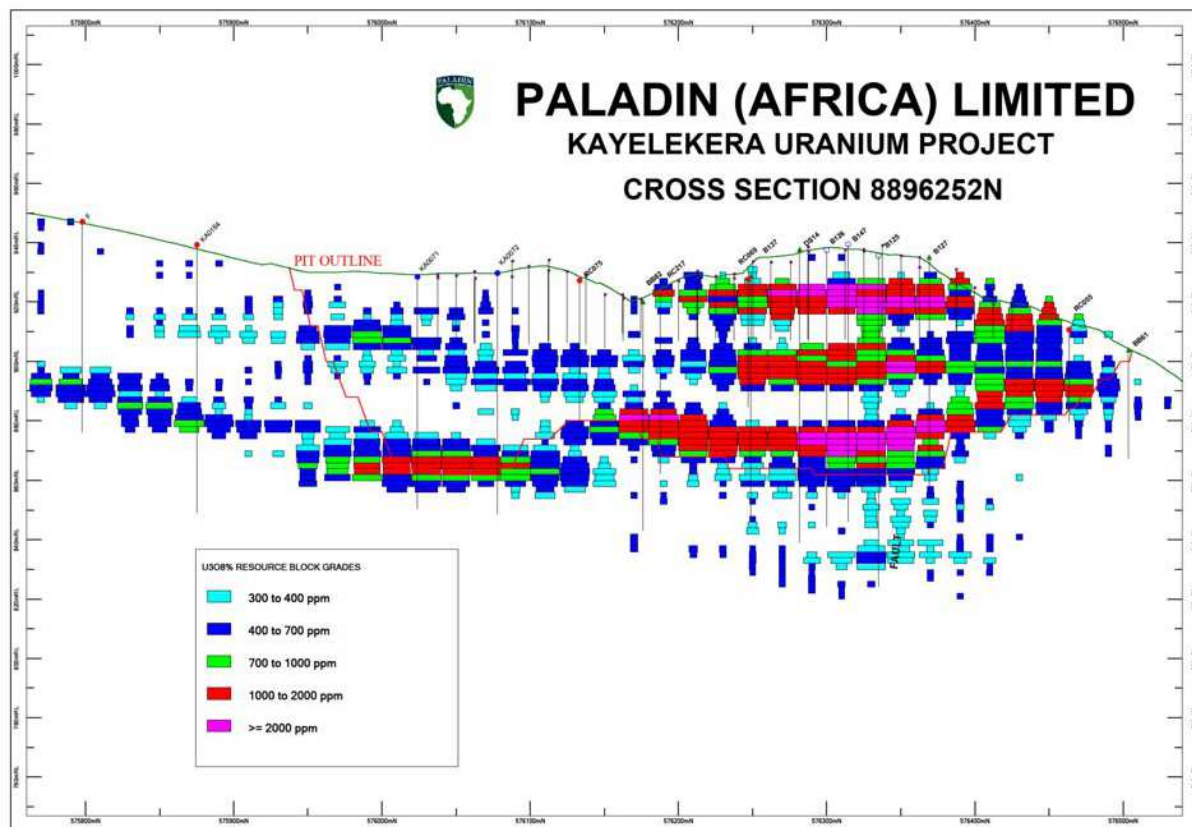


FIG. 6. Cross section 8896252N.

The lenses are superimposed vertically along an axis approximately parallel to the synclinal axis of the fault bounded structure. The mineralization is offset but not confined by the fault structures and potential for extensions of the mineralisation is restricted by outcrop limitations of the hosting lithologies. The mineralization occurs between 0 (outcropping) to 100 metres depth.

Primary mineralization, present within the reduced facies pyritic arkose, is intimately associated with matrix disseminations as well as larger fragments of carbonaceous debris. Coffinite has been positively identified as the principal uranium bearing mineral and occurs together with minor uraninite. An U-Ti mineral, possibly betafite or tanteuxenite, has also been noted.

Near surface weathering of primary (reduced) ore has produced a zone of oxide ore characterised by yellow and green secondary uranium minerals. These have been identified as meta-autunite and boltwoodite. Minor uranophane is also present. Local leaching and redeposition has repeatedly occurred leading to concentration of secondary uranium species in the basal part of the arkoses and in the top of the underlying mudstones.

The mineralizing process appears to be of the geochemical cell type, with cells migrating down dip from the west and southwest. Drill holes in these directions often intersect the 'tails' at the upper and lower surfaces of the oxidised arkose characteristic of the passage of an oxidizing front.

## 6. Ore types

The ore has been classified into four types based on visual identification of the oxidation-reduction state of the hosting lithology [1-2]. These are:

- 1) Reduced arkose ore
- 2) Oxidised arkose ore
- 3) Transitional arkose ore (mixed oxidised – reduced ore)
- 4) Mudstone ore

Approximately 50% of the total ore is hosted by reduced arkoses, 30% by oxidised arkoses, 10% by transitional arkoses and 10% by mudstone.

**Reduced arkose ore** within the arkose units contains fresh feldspars and carbonaceous debris with pyrite and chlorite in the matrix. The principal uranium mineral is coffinite with minor uraninite. An U-Ti mineral, possibly betafite or tanteuxenite, has also been noted. Reduced ore is most prevalent in the lower arkose units of the deposit.

**Oxidised arkose ore** is characterized by feldspar deterioration and the prevalence of iron oxide in the matrix. Near surface weathering of primary (reduced) ore has produced a zone of oxide ore characterized by yellow and green secondary uranium minerals. In general, the oxidized arkoses appear more red or orange-brown than their reduced counterparts and are easily distinguished visually. The uranium mineralization is predominately secondary, with the principal minerals being meta-autunite (bright green) and boltwoodite (yellow). Most of the oxidized ore is found at or near the surface and in zones closer to the periphery of the deposit.

**Transitional arkose ore** is mixed ore that exhibits varying degrees of oxidation.

**Mudstone ore** is a reduced ore and contains mainly coffinite with some uraninite in a matrix of clay minerals. It is concentrated along the arkose/mudstone boundary and close to or within faults zones.

The detrital components are mainly feldspar and quartz. The matrix is composed of iron minerals (hematite, pyrite) with minor amounts of carbonaceous debris and calcite. Mineralogical and textural features noted at Kayelekera are common for sandstone type uranium mineralisation. Uranium could have been derived from either intra- or extra-formational sources. Amongst others it was postulated that uranium was most likely emplaced originally in carbonaceous-rich zones as low grade protore. Then, following rift faulting and associated folding, uranium was mobilized in ground water and re-deposited as ore grade concentrations in trap situations.

## 7. Resources and reserves

Resource definition drilling to accurately define the limits of the ore body and upgrade the resources to indicated and measured categories, comprising 5 433m in 120 holes in 2005 and 9 955m in 132 holes in 2007, resulted in an upgraded resource and reserve estimation. Details are given in Table 2 & 3 below.

Mineral resource estimates conforming to both JORC (2004) and NI 43-101 codes, are as follows:

Table 2. At 300 ppm U<sub>3</sub>O<sub>8</sub> cut-off

	<b>Mt</b>	<b>Grade ppm U<sub>3</sub>O<sub>8</sub></b>	<b>Tonnes U<sub>3</sub>O<sub>8</sub></b>	<b>Mlb U<sub>3</sub>O<sub>8</sub></b>
Measured Resources	3.42	1,211	4,141	9.1
Indicated Resources	18.78	725	13,616	30.0
<b>Total</b>	<b>22.20</b>	<b>800</b>	<b>17,757</b>	<b>39.1</b>
<b>Inferred Resources</b>	<b>3.9</b>	<b>552</b>	<b>2,152</b>	<b>4.7</b>

Table 3. At 600 ppm U<sub>3</sub>O<sub>8</sub> cut-off

	<b>Mt</b>	<b>Grade ppm U<sub>3</sub>O<sub>8</sub></b>	<b>Tonnes U<sub>3</sub>O<sub>8</sub></b>	<b>Mlb U<sub>3</sub>O<sub>8</sub></b>
Measured Resources	2.26	1,612	3,643	8.0
Indicated Resources	8.13	1,121	9,114	20.1
<b>Total</b>	<b>10.39</b>	<b>1,227</b>	<b>12,756</b>	<b>28.1</b>
<b>Inferred Resources</b>	<b>1.0</b>	<b>945</b>	<b>945</b>	<b>2.1</b>

The Ore reserve estimate, conforming to both the JORC (2004) and NI 43-101 codes, is as follows:

Table 4. At 400 ppm U<sub>3</sub>O<sub>8</sub> cut-off

	<b>Mt</b>	<b>Grade ppm U<sub>3</sub>O<sub>8</sub></b>	<b>Tonnes U<sub>3</sub>O<sub>8</sub></b>	<b>Mlb U<sub>3</sub>O<sub>8</sub></b>
Proved Reserve	2.87	1,373	3,943	8.7
Probable Reserve	9.75	959	9,342	20.6
<b>Total</b>	<b>12.62</b>	<b>1,053</b>	<b>13,285</b>	<b>29.3</b>

Economic studies undertaken on the current reserve have indicated a mine life of 9 years and a total project life of between 12 and 13 years, following life of mine scheduling studies and the processing of marginal ores at the end of the mine life.

#### REFERENCES

- [1] RING, U., Tectonic and lithological constraints on the evolution of the Karoo graben of Northern Malawi (East Africa), *Geologische Rundschau* 84 (1995) 607 – 625.
- [2] BOWDEN, R.A., SHAW, R.P., The Kayelekera uranium deposit, Northern Malawi: past exploration activities, economic geology and decay series disequilibrium, *Applied Earth Science, Trans. Inst. Min. Metall. B* 116, 2 (2007) 55 – 67.
- [3] BECKER, E., Project 9151 – Kayelekera Uranium Deposit – Ore Type Classification and Drilling Proposed for Metallurgical Sampling Program (June/July 05) (2005) (unpubl. company report).

# **Spatio-temporal distribution of uranium deposits in Mesozoic – Cenozoic Era in China**

**X. Liu, J. Pan, D. Yu, J. Wu**

East China Institute of Technology, Fuzhou, Jiangxi, China

*E-mail address of main author: liuof99@163.com*

**Abstract.** Over 90 percent of the uranium deposits including the most important granite type deposits, volcanic and caldera-related deposits and sandstone type deposits in China have been discovered in Mesozoic-Cenozoic Era. Spatially, there are five uranium metallogenic provinces dominated by South China uranium metallogenic province in South-East China and Tianshan uranium metallogenic province in North-West China.

The granite type deposits are mainly located in South China uranium province with the mineralization ages of 100 Ma – 165 Ma and 47 Ma – 87 Ma respectively. Current studies indicate that uranium deposits with the mineralization ages of 100 Ma – 165 M are normally characterized by relatively high temperature mineral assemblages such as uraninite associated with scheelite and tourmaline. These have been considered as the early stage uranium mineralization in South China, which is the main exploration target currently in South China. Uranium deposits characterized by quartz-pitchblende veins in host granites with the ages of 47 Ma – 87 Ma are the typical granite type uranium deposits in South China, e.g., Xiazhuang uranium ore field.. The host rocks are previously considered as the intrusive granites of Yanshan epoch. However, new isotopic dating results show that most granite hosting both early or late stage uranium deposits in South China are the intrusive rocks of Indo-Chinese epoch with the age of granites more than 200Ma.

Xiangshan is the biggest uranium ore field dominated by volcanic and caldera-related deposits in South China uranium metallogenic province. Two stages of uranium mineralization have been identified including the early alkaline hydrothermal mineralization of  $115.2 \pm 0.5$  Ma and the late acid hydrothermal mineralization of  $99.0 \pm 6.0$  Ma. The host rocks include rhyodacite and porphyroclastic lava dated of 131 Ma to 158 Ma.

Sandstone type uranium deposits are mainly distributed in Tianshan uranium metallogenic province, such as the deposits in Yili Basin, and in the new exploration areas of Erdos Basin and Er'lian basin. Although there are many publications about the mineralization ages of sandstone type uranium deposits which cover a wide range of ages from 8Ma to 120Ma, it is necessary to understand the main mineralization ages by up-to-date isotopic method.

Since large scale mineralization of nonferrous metal, precious metal and rare metal also took place in Mesozoic-Cenozoic Era, uranium deposits have been regarded as one of the mineral resources of mineralogical series closely related to the tectonic - magmatic evolution in Mesozoic-Cenozoic Era in the mainland of China.

## **1. General spatial distribution of uranium deposits in China**

Over 50 years history of uranium exploration in China have revealed that the spatial distribution of uranium deposits could be limited to three metallogenic domains of Paleo-Asian, Marginal-Pacific and Tethyan, which includes five uranium provinces and eighteen uranium metallogenic regions/belts in the mainland of China [1] (Fig. 1). There are fourteen uranium metallogenic regions/belts located in Marginal-Pacific domain. The uranium deposits in Mesozoic-Cenozoic era, such as the typical granite type, volcanic type and sandstone uranium deposits, are mainly located in Ganhang, Taoshan-Zhuguang and North Tianshan uranium metallogenic regions/belts. With the new discoveries of large

scale sandstone type uranium deposits, North Erdos Basin region is the focus of the current uranium explorations in China.

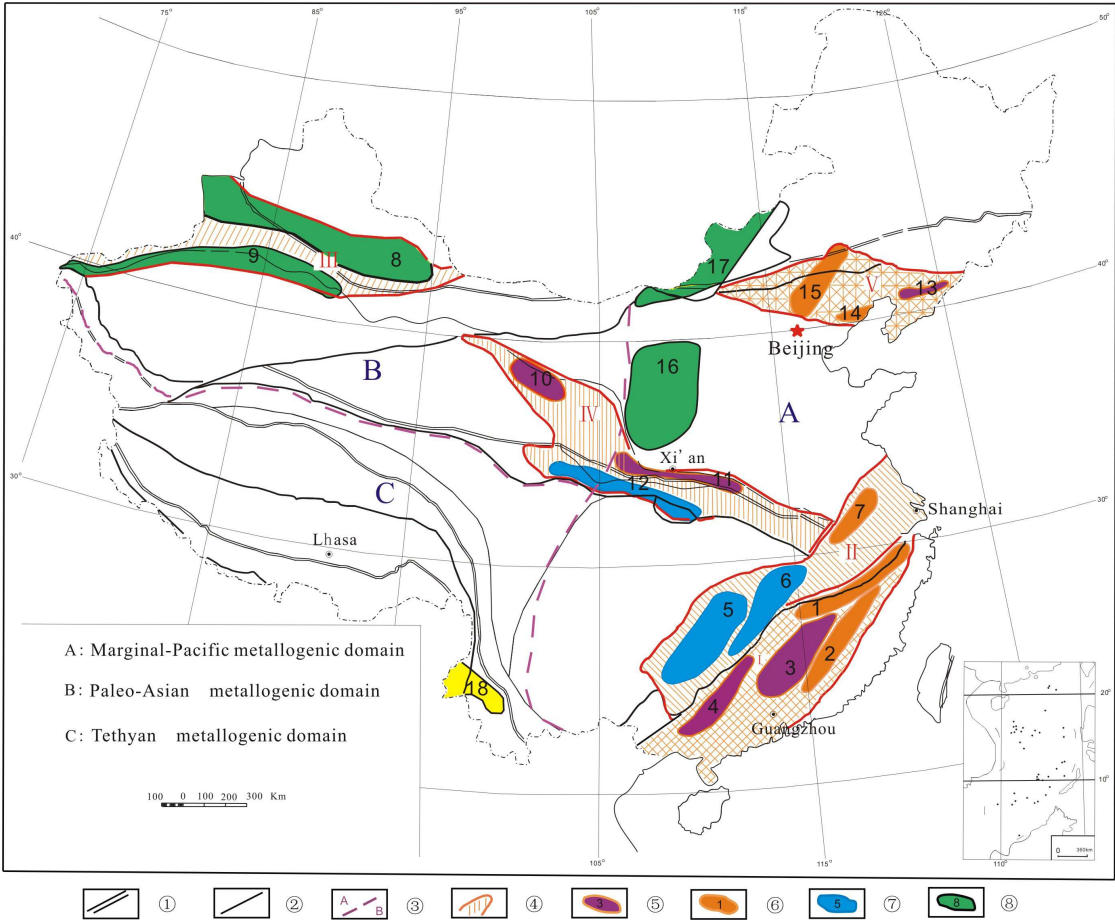


FIG.1. Uranium metallogenic regions/belts in China.

- ① Boundary of First Class Tectonic Domain, ② Boundary of Second Class Tectonic Domain, ③ Boundary of Uranium Metallogenic Domain, ④ Boundary of Uranium Province, ⑤ Granite Type Uranium Deposit Region, ⑥ Volcanic Type Uranium Deposit Region, ⑦ Carbonate-siliceous-pelitic Rock Type Uranium Deposit Region, ⑧ Sandstone Type Uranium Deposit Region I : South China Uranium Province, II : Southeast Yangzi Massif Uranium Province, III : Tianshan Uranium Province, IV : Qilian-Qinling Uranium Province, V : North Margin Uranium Province of North China Massif 1: Ganhang Metallogenic Belt, 2: Wuyishan Metallogenic Belt, 3: Taoshan-Zhuguang Metallogenic Belt, 4: Chenzhou-Qinzhou Metallogenic Belt, 5: Xuefengshan-Jiuwangdashan Metallogenic Belt, 6: Mofushan-Hengshan Metallogenic Belt, 7: Xixiashan-Lucong Metallogenic Belt, 8: North Tianshan Metallogenic Belt, 9: South Tianshan Metallogenic Belt, 10: Qilian-Longshoushan Metallogenic Belt, 11: North Qinling Metallogenic Belt, 12: South Qinling Metallogenic Belt, 13: Gongchangling-Bahechuang Metallogenic Belt, 14: Qinglong-Xincheng Metallogenic Belt, 15: Guyuan-Hongshanzhi Metallogenic Belt, 16: Erdos Basin Metallogenic Region, 17: Er'lian-Celaomiao Metallogenic Region, 18: West Yunnan Sandstone Type Metallogenic Region

(After [1])

**2. Uranium mineralization ages**

Although the oldest uranium mineralization in China could be traced back to over 1 800 Ma, such as the Lianshanguan deposit in Gongchangling-Bahechuang Metallogenic Belt, over 90 percent of the uranium deposits have been discovered in Mesozoic-Cenozoic Era. Figure 2 illustrates that the granite type and volcanic type uranium deposits formed mainly in the age of 40 Ma to 160 Ma, while the sandstone type uranium deposits formed dominantly in Cenozoic era.

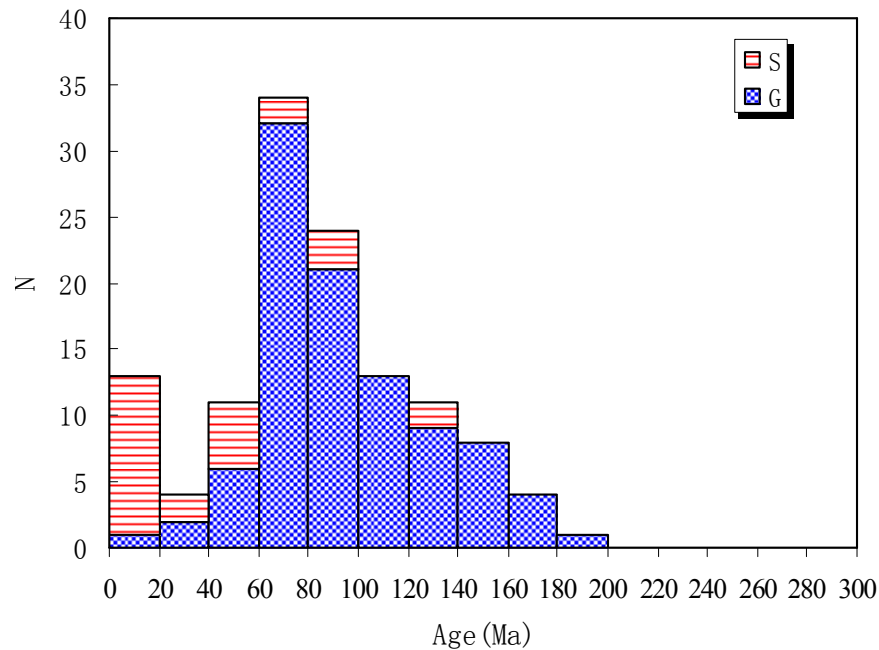


FIG. 2. The age frequency diagram of uranium deposits in Mesozoic-Cenozoic Era.  
G: Granite type and volcanic type uranium deposit; S: Sandstone type uranium deposit.

### Granite Type:

Granite type uranium deposits in Mesozoic-Cenozoic Era dominantly occur in Taoshan-Zhuguang and Chenzhou-Qinzhou metallogenic belts. Typical granite type uranium deposits in South China are characterized by pitchblende veins in host granites and have the mineralization ages of 47 Ma - 87 Ma in the main mineralization stage. The No. 302 uranium deposit, in Taoshan-Zhuguang Metallogenic Belt, is one of the typical granite type deposit with mineralization age of 72 - 95 Ma. The deposit is spatially controlled by faults, having vertical extensions up to 1 000 (Fig.3). Current studies on this deposit indicate that the ore-forming solutions are characterized by high temperature (over 300°C) and salinity of 8 wt% NaCl during the early mineralization stage.

### Volcanic Type:

Volcanic type uranium deposits are mainly located in Ganhang metallogenic belt. The Xiangshan uranium ore field in this belt a typical example. Current exploration have found the new ore bodies hosted in rhyodacite porphyry in Zoujiashan deposit (Fig.4). Two stages of uranium mineralization have been identified, an early alkaline hydrothermal mineralization of about 115 Ma and the late acid hydrothermal mineralization of about 98Ma. Latest single zircon SHRIMP data indicate that the age for porphyroclastic lava in Xiangshan is in the range of 131.2±2.6 Ma to 143.4±0.6 Ma with the average age of 133.2 Ma.

### Sandstone Type:

Sandstone type uranium deposits are mainly found in Tianshan uranium metallogenic province, such as the deposits in Yili Basin. With the discovery of new large scale sandstone type deposits in North Erdos Basin in the last 10 years, the Erdos Basin and Er'lian basin have become the most important uranium metallogenic regions in North China. The reported mineralization ages of sandstone type uranium deposits in China range from 2 Ma to 120 Ma. Because the complexity of metallogenic process for sandstone type uranium deposit, it is difficult to identify the exact mineralization age for an individual deposit. A typical sandstone type deposit represents different mineralization ages in different position. Two examples of sandstone uranium deposits in Erdos basin and in Er'lian basin respectively have been illustrated in this paper (Figs 5, 6). Normally the mineralization age is much older in the tail of the limbs than the age in the roll front (Fig. 5).



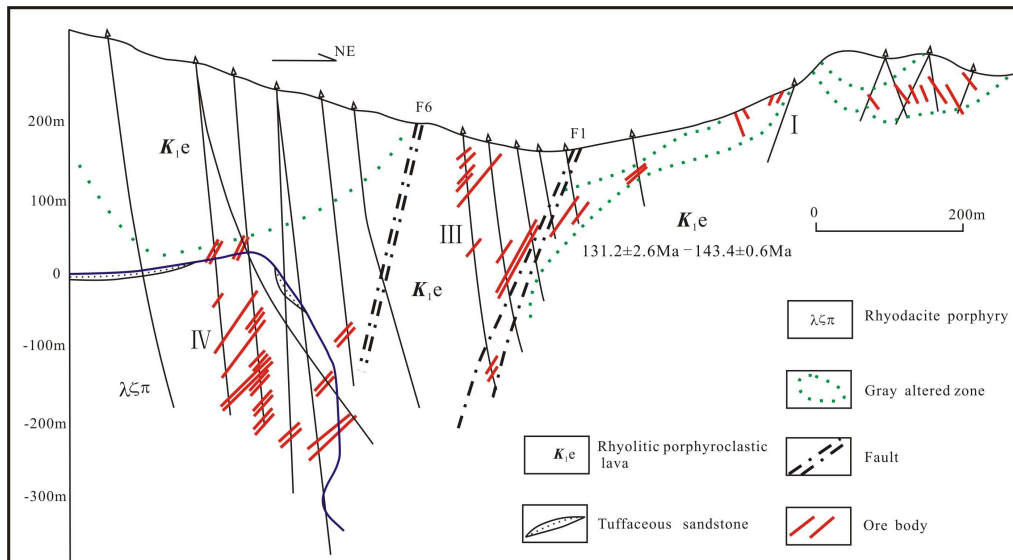


FIG.4. Geological profile of Zoujiashan deposit in Xiangshan uranium ore field.

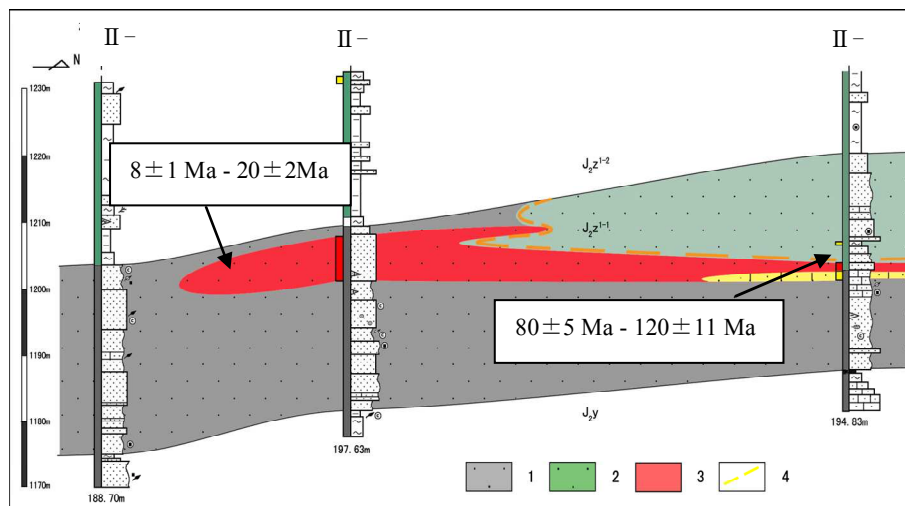


FIG. 5. Geological profile of exploration line No. II in Dongsheng deposit.

1 : Grey Sandstone of Lower Ziluo Formation, 2: Greenish Sandstone of Lower Ziluo Formation, 3: U Ore Body, 4: Heads of Oxidation Zone.

### 3. Discussion

Comparison with the typical epithermal vein type uranium deposits hosted in granites in South China, current studies indicate that uranium mineralization underwent an early stage “hyperthermal uranium mineralization” in Taoshan-Zhuguang metallogenic belt, characterized by:

- \* Controlled by ductile shear zone with the high temperature alkaline alterations
- \* High temperature mineral assemblages such as uraninite associate with scheelite and tourmaline disseminated in granites (Fig. 7)

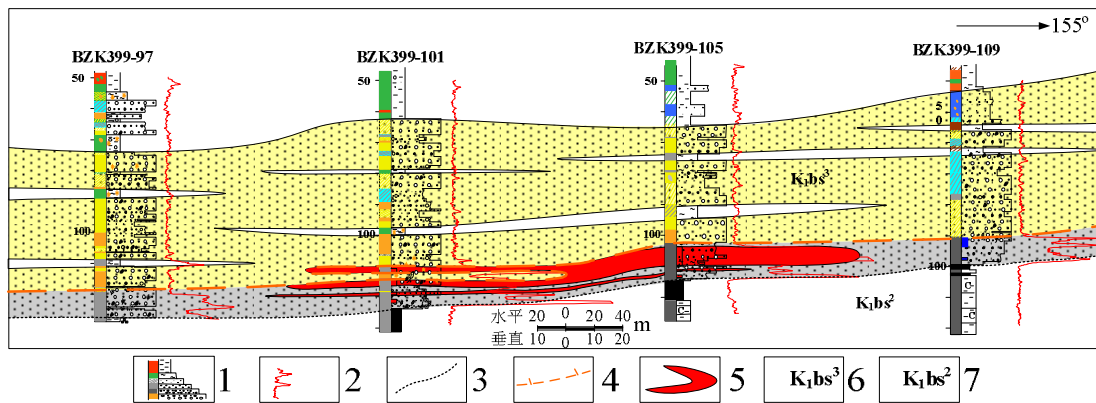


FIG. 6. Geological profile of No. 399 exploration line in Bayingwula sandstone type uranium deposit. 1: Lithology, 2: Geophysical Logging Curve, 3: The Uncomformity Boundary, 4: Heads of Oxidation Zone, 5: Uranium Ore Body, 6: Greenish -grey Sandstone of Upper Hansai Formation, 7: Grey Siltstone, Sand Conglomerate with Mudstone of Lower Hansai Formation. ( The U-Pb isochronic age of the deposit:  $44\pm 5$  Ma)

- \* Uranium mineralization spatially related to the small intrusions such as syntectonic granitoids
- \* The mineralization ages are more than 100 Ma.

Following the studies on this type of mineralization, the “hyperthermia uranium mineralization” is currently considered as the main exploration target with prospect foreground in South China.

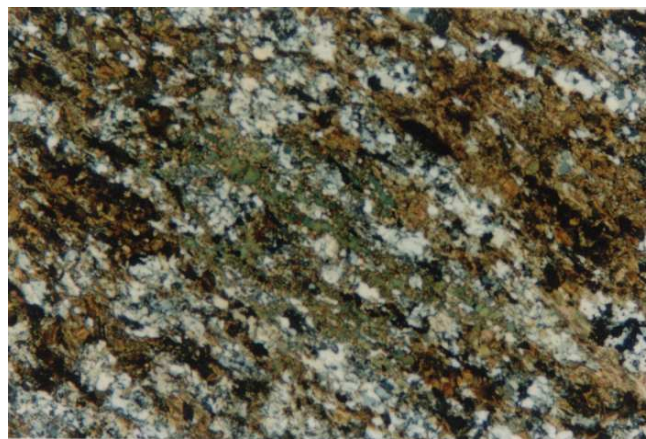


FIG. 7. Uraninite associate with scheelite and tourmaline disseminated in granites, Zhushanxia. deposit in Xiazhuang U ore field

### The Importance of Indo-Chinese Epoch Granite:

With the development of new dating technologies, such as single zircon U-Pb method, the latest results about the ages of granitoids in Xiazhuang, Zhuguang uranium ore field indicate that most granite batholiths are the intrusive rocks of Indo-Chinese epoch, for example, 232-235 Ma single zircon ages for the Baimianshi granite, 223-227 Ma single zircon ages for Caijiang granite,  $236\pm 2$  Ma for Longhuashan granite and  $239\pm 2$  Ma for Jiangnan granite [2]. The Indo-Chinese epoch granite batholiths are considered as the important basis for large scale hydrothermal uranium mineralization in Taoshan-Zhuguang uranium metallogenic belt. Hitherto located granite type uranium deposits have the similar characteristics as that of Yanshan epoch granite, which are superimposed on the Indo-Chinese epoch granites during the mineralization.

## **The Relations of Uranium Mineralization to tectonic – dynamic environments in Mesozoic-Cenozoic Era:**

In addition to uranium, large scale mineralization of nonferrous metal, precious metals and rare metals also took place in Mesozoic- Cenozoic Era in China. Previous studies proved that most of the economic mineral resources discovered in east China (Marginal-Pacific metallogenic domain) are formed during 80 Ma to 180 Ma [3] . The facts imply that these metallogenic systems are closely related to the lithosphere evolution under different tectonic – dynamic environments in Mesozoic-Cenozoic Era in the mainland of China. Therefore, based on the current studies, the relations of uranium mineralization to tectonic-dynamic environment in Mesozoic-Cenozoic era can be briefly described as:

- \* The early uranium mineralization during 135-157 Ma in Taoshan-Zhuguang uranium metallogenic belt coincided with the lithosphere thickening in a compression environment during Upper Jurassic and Lower Cretaceous periods.
- \* Late Lower Cretaceous tectonic-dynamic environment switching from the compression to extension took place after 135 Ma in South China. This led to regional lithosphere thinning and promoted the mantle-crust interactions under tensile tectonics. The extensive volcanism and granitoid intrusions in Ganhang and Taoshan-Zhuguang uranium metallogenic belts also took place under such a tectonic-dynamic environment, for example, the granite porphyry or porphyritic granite in Xiangshan uranium ore field with the ages of 131 Ma to 133 Ma and the trachytic-dacite in North Guangdong province with the age about 135 Ma by single zircon SHRIMP dating [4]. The extensive volcanism and granitoid intrusions in tensile tectonic-dynamic environment and the superimposing of late uranium mineralization of the early stage mineralization are considered as the setting for large scale uranium mineralization in South China.

## **REFERENCES**

- [1] HUANG, J., et al., The uranium metallogenic belts in China. Technical Report, BOG, CNNC (2005).
- [2] CHEN, P., Presentation of BOG seminar in Fuzhou (2009).
- [3] MAO, J., et al., Large scale metallogenesis and large mineralization concentration areas. Geological Publishing House, Beijing (2006).
- [4] CHEN, Z., Technical Report to the Ministry of Land and Resources (2009).

# The latest progress on the study of mineralization genesis in Baimianshi uranium ore field

H.H. Fan<sup>a</sup>, D.B. He<sup>a</sup>, F.G. Wang<sup>a</sup>, D.Z. Gu<sup>b</sup>, J.R. Lin<sup>a</sup>, J.S. Rong<sup>a</sup>

<sup>a</sup>Beijing Research Institute of Uranium Geology, CNNC, Beijing, China

<sup>b</sup>Guiyang Research Institute of Geochemistry, Chinese Academy of Science, Guiyang, China

*E-mail address of main author: fhh270@263.net*

**Abstract.** This paper systematically studies the mineralization related fluid inclusions in fluorite and quartz viz., their shape, composition and homogenisation temperature; contrasts the Sm-Nd, Rb-Sr isotopic characteristics of granite in basement to that of fluorite of ore-forming stage; analysis of the mineralization genesis, typical mineral assemblage and ore-forming age of mineralization in Baimianshi uranium field. The latest research shows that deposits in Baimianshi uranium field are of typical hydrothermal type. The uranium is mainly derived from crustal rocks. A continuous extraction of uranium from the upper crust within granites in the basement by mantle-derived fluids with little of ore-forming elements could have been responsible for the remobilization and transformation of uranium. The mixing of metallogenic elements-rich fluid with groundwater in some draped places overlain by layers of basalt leads to the precipitation of ore-forming materials. Three phases of uranium mineralization exist with ages of 160 Ma, 128 Ma and 103–86 Ma, respectively. The uranium ore deposits in the area formed by a compound metallogeny.

It was formerly believed that deposits in Baimianshi orefield have the same characteristics and genetic types. Syn-sedimentary uranium concentrations and post-diagenetic U-enrichment were responsible for the deposit. The deposit had been considered as sandstone type and volcanic thermal cover subtype on the basis of its genesis. But this paper, taking Huangnihu deposit as an example, points out that Baimianshi orefield is of hydrothermal type. By the study of fluid inclusions, isotopic tracing, mineral assemblages, as well as U-Pb isotopic dating of ores, the metallogenesis has been divided into three stages: the first stage is related to bimodal volcanism; the second stage is related with Yanshanian magmatic activities; and the third stage has a relationship with the diagenesis of sub-volcanic rocks and dikes (quartz porphyry, diabase). The new research results will guide the further prospecting in the deeper parts of this basin.

## 1. Regional geology

Baimianshi uranium orefield is located in the east of Nanling U-polymetallic ore belt, including Baimianshi, Longkong, Shuangkong, Majitang, and Huangnihu deposits, as well as a lot of ore occurrences such as Zhaixia, Xialanfeng, etc. Geotectonically it is located at the Quannan-Xunwu uplift between Cathaysia and South China fold belts[1].

Strata in this region are mainly Pre-Sinian with minor Mesozoics. Magmatic activities are prominent as seen by Baimianshi, Danguanzhang, and Luofu plutons. During the Mesozoic, volcanism has been evidenced by the bottom cover of Baimianshi basin, which is basalt interbedded with mid-Jurassic sandstone, and rhyolite in the upper part. As a result, bimodal volcanic rocks- basalt, rhyolite and rhyolitic porphyry are seen in this area. Besides, in the orefield, dikes with complex lithology such as diabase, lamprophyre, quartz porphyry and rhyolitic porphyry are very common.

Regional structures are mainly faults due to extensional tectonics. Faults closely related to metallogenesis include Quannan-Xunwu E-W fault belt, NNE Yingtan-Anyuan, Shaowu-Heyuan fault belts and N-W basin-controlling fault. The extensional tectonics is controlled by one or more deep faults, mostly as NE or NNE extensional belts. At the junction between basement E-W tectonic belt and NNE extensional tectonics, thermal-uplifting and down-faulting extensional tectonics [2, 3] have taken place along a EW tectonic belt.

## 2. Research progress of Baimianshi orefield

### 2.1. Research on fluid inclusions

Fluid inclusions are the preserved integrated and direct samples of original fluid (or melt) [4, 5]. Study of the composition and mechanism of formation of the fluid inclusions give an understanding of the geologic environment, the genesis and evolution of the deposits.

#### 2.1.1. Types of fluid inclusions

In this paper, fluid inclusions are sampled from the ore-bearing sections of the first layer in Huangnihu uranium deposit, including sandstone, granitic sandstone and basalt. Under microscope, fluid inclusions are primarily epigenetic, mostly located along fissures as linear or group, while a few of them are syngenetic, and occurring like even spots. They are the mainly liquid-gas facies, folowed by liquid facies, and a few are gas facies ones. The ratio of gas to liquid facies is about 20-50. Daughter mineral-bearing tri-facies inclusions are also found, but the daughter minerals are small (<1 $\mu$ m) and seem to be NaCl crystals. Mostly the inclusions are regular round or ellipse, and usually 3-10 $\mu$ m in size. Some of them are larger than 20 $\mu$ m, with irregular branch or knife shapes. Moreover, inclusions <1 $\mu$ m are also frequent. As a whole, in quartz and siliceous veins, the inclusions are small, few and regular, while in fluorite, they are large, many and mostly irregular.

#### 2.1.2. Homogenisation temperature and salinity of fluid inclusions

Table 1 shows the homogenisation temperature and salinity analysis result of fluid inclusions in Huangnihu deposit. Histogram Fig.1 gives the statistical homogenisation temperature with 10 $^{\circ}$ C as a unit. Histogram Fig. 2 is the statistical salinity taking 0.5 wt%NaCl as a unit. From the histograms we can see that , in Huangnihu deposit, the homogenisation temperature has a large range (70-438 $^{\circ}$ C), with two peaks: low temperature (T1) of 100-170 $^{\circ}$ C and mid-high temperature (T2) of 270-350 $^{\circ}$ C. On another side, the salinity variation includes three ranges: low salinity (S1) of 0.5-1.5 wt%NaCl, middle salinity (S2) of 6-10.5 wt%NaCl and high salinity (S3) of 15.5-16.5 wt%NaCl. It is believed that in most cases the temperature has decreased with geologic age, that is to say, multi-staged fluid activities are indicated by the existence of fluid inclusions with different homogenisation temperatures and salinities [5]. According to the relationship between temperature and salinity (shown in Table 1), fluids in this district can be divided into: low-temperature and low-salinity fluid, mid-low-temperature and low salinity fluid, mid-low-temperature and middle salinity fluid, mid-low-temperature and high salinity fluid, mid-high-temperature and middle salinity fluid, high-temperature and volatile-rich fluid (Figs 1-6).

Table 1. Homogenisation temperatures and salinity of fluid inclusions of Huangnihu Uranium ore-field\*

Sn	Mineral	Size ( $\mu$ m)	V/L (%)	Inclusions of the same stage and the same type	
				Homogenisation Temperature ( $^{\circ}$ C)	Salinity(wt%NaCl)
HN-3	Q	3~8	5~30	70, 73, 77, 83(2), 86(4), 88(2), 90(3),	2.57( 2) , 2.90(2), 2.07(2)
				92, 107, 110(3), 113(4), 117, 121(3), 127, 130(3), 137, 140(5), 147, 151(3), 153, 169, 171, 177, 187	

Sn	Mineral	Size ( $\mu\text{m}$ )	V/L (%)	Inclusions of the same stage and the same type	
				Homogenisation Temperature ( $^{\circ}\text{C}$ )	Salinity(wt%NaCl)
HN-15	Q	3~6	10~30	143, 147, 167, 178(2), 183, 185, 197, 240, 242, 249, 256	7.17(2), 7.45(2), 8.28 (2)
	Fl	6~20	5~10	123, 126(2), 127(7), 128(4), 129(5), 130(5), 133(2), 136(3), 137(2), 139(4), 140(6), 141(2), 144	8.82, 8.98, 9.13, 9.29(2), 9.59(2), 9.74(2), 9.89(3), 10.19, 10.33, 10.48(2), 10.62(3), 10.77( 2) , 10.91, 11.19, 15.98(2), 16.05(2)
	Fl	15~20	10~20	134, 136(2), 138(3), 141	10.19, 10.48, 10.62(2), 10.91(2), 11.19
	Fl	4~20	5~20	130(2), 131(3), 132(2), 133(2), 134(3), 135(3), 136(3), 138(3),140	8.66, 9.13, 9.44, 9.89(2) , 10.48(2), 10.62, 10.91, 14.18(2), 14.29, 15.75(3)
HN-1	Fl	10~30	0~10	96(2), 100(3), 103(2), 105, 107(2), 110(2), 128, 130, 137, 146, 149	16.40(2), 16.55(2), 16.98(2), 17.12(2)
	Fl	4~6	10~20	123, 127(2), 129, 137, 139, 140(2), 141	16.85(2), 16.79(2), 16.55(3), 16.40(2)
	Fl	10~20	10~20	120, 123, 130, 133, 136, 142(2), 144(3), 146(2), 149(3), 157(2), 160, 169, 174(2)	16.55, 16.40, 16.30(2), 14.64(2), 12.16, 12.02
	Fl	4~20	5~20	115(2), 116(2), 119(2), 120(2), 123, 127(3), 129(4), 130(3), 133(4), 136(2), 138(4), 140(2), 147(2), 149(4), 152(2)	
Continuous					
HN-2	Q Vein	6~12	0~20	106, 124, 146, 149(2), 166, 170, 179(2)	7.17(2), 8.59(3), 9.08, 9.21(2)
	Q Vein	3~10	10~20	156, 160(2), 162, 166(2), 169, 200(2), 220, 230, 234(2), 253, 260, 270(2), 277	4.96(2), 5.26(2), 5.86(2), 6.45, 6.88(2), 6.74, 7.73
	Q Vein	6~10	30~50	319, 322, 327, 339(2), 342(2), 348(3), 379(3), 383(2)	6.45(2), 6.59(2)
	Q Vein	3~10	30~50	250, 253(2), 255, 260, 266(2), 279(2), 290, 293(2), 300(2), 330, 332, 337, 340(3), 343(2), 345(2), 353(4), 355, 357, 360(3)	9.34(2), 8.55(3)
	Q Vein	3~8	20~30	220, 227, 229(2), 322, 327, 330(2), 351, 353(2), 357	
HN-4	Q	8~20	0~5	80(2), 83(2), 87(2), 89(2), 109, 113, 120	1.23(2), 1.74(2)
	Q	5~20	5~10	150, 153(2), 158(2), 160, 167, 169, 173	7.73(2), 7.86, 8.95
	Q	5~20	10~30	178(3), 181, 183(2), 190(2), 196, 273, 277, 279, 290, 293(2), 265, 278, 290, 300(3), 311(3), 318(2), 322, 331 277, 279(2), 283, 287, 290(3),	0.53, 0.71(2), 0.88, 1.23(3), 1.57(2), 6.45, 6.88(2), 7.31, 7.59, 8.55, 8.68, 7.73, 7.45
	Q	5~20	30~60	293(4), 297, 310(2), 307, 350, 353, 357	
	Q	5~20	70~80	370, 373, 377, 380, 385	
HN-1 3	Q	2~20	5~10	151, 153(2), 155, 163, 166, 169(2), 208(2), 210(2)	5.86, 6.16, 7.45(2), 7.73(2)
	Q	2~20	10~20	187, 189(2), 190, 193, 204, 206(2)	1.40(3), 1.74(2)
	Q	2~20	20~30	276, 280, 300, 306, 331, 350	
	Q	4~10	30~50	358, 360, 390, 420	
HN-1 3-1	Q Vein	3~10	5~10	120, 124(2), 126(3), 130(5), 133, 137(2), 141(2), 147(2), 150(2), 153, 163, 166	4.65, 4.80, 4.96(2), 5.11(2)
	Q Vein	3~6	10~30	170, 177, 179(2), 207, 257, 259, 287, 293(2), 302, 312, 355(2)	
Continuous					

Sn	Mineral	Size (μm)	V/L (%)	Inclusions of the same stage and the same type	
				Homogenisation Temperature (°C)	Salinity(wt%NaCl)
HN-13-1	fL	4~10	5~20	117, 122(3), 134, 136, 141, 147, 150	5.86, 6.16, 7.45(2), 7.73(2)
	Q Vein	3~15	5~20	97, 104, 114(3), 123, 129, 131, 137, 140, 144, 176, 179(2), 191, 207, 211, 229, 233, 235, 238	

\* Analysed by F.I. Laboratory, BRIUG with LINKHAM THMS600 based on EJT 1105-1999; number in brackets means the times of the same datum.

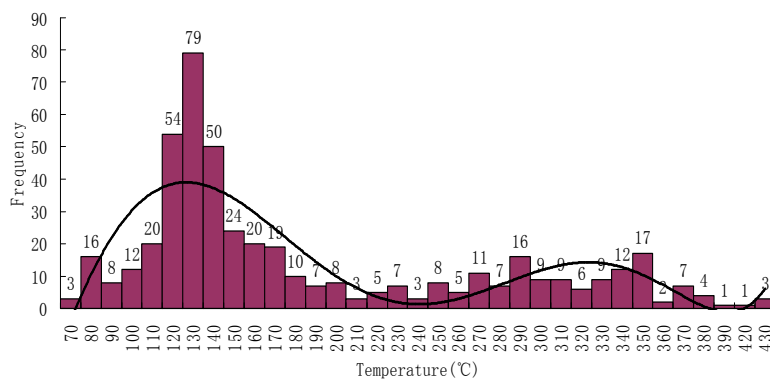


FIG.1. Histograms showing homogenisation temperatures of fluid inclusions in Huangnihu uranium ore-field.

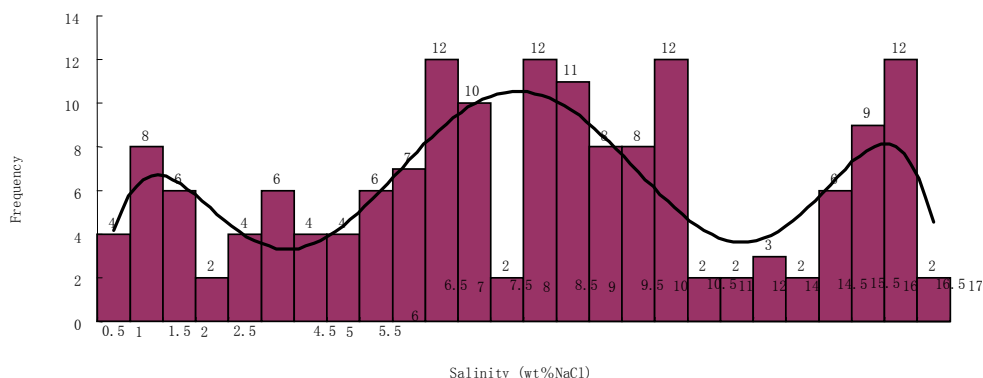
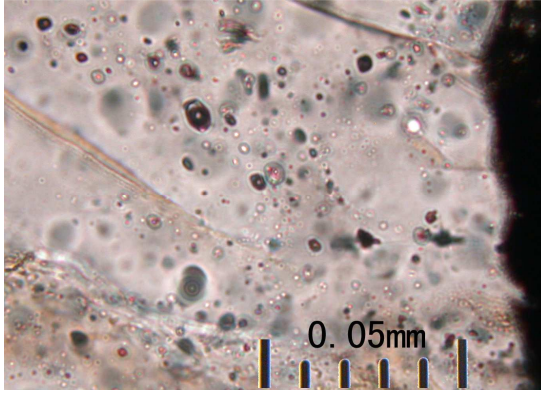
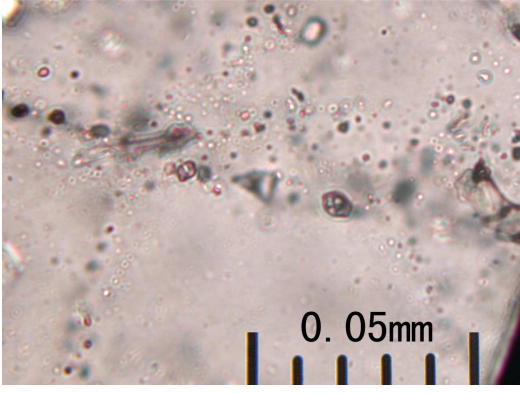
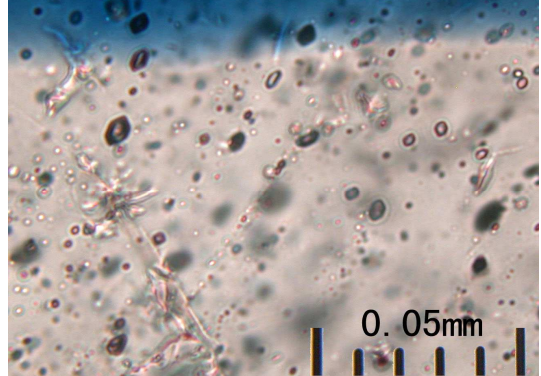
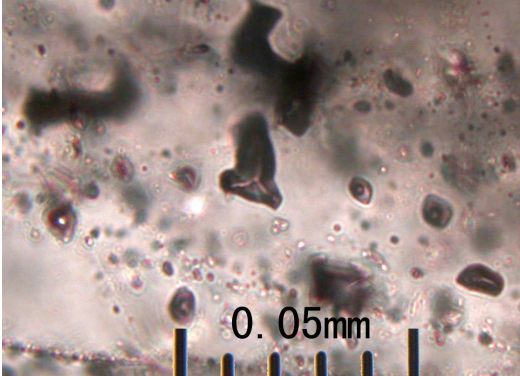
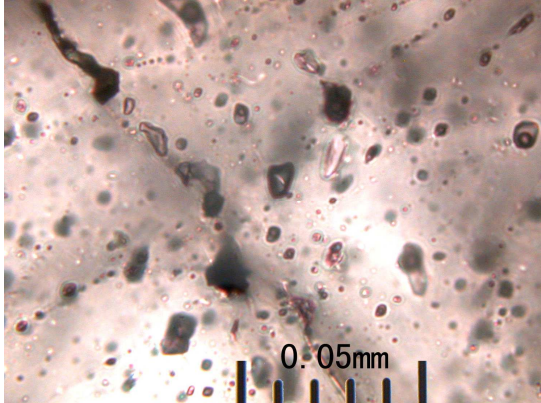
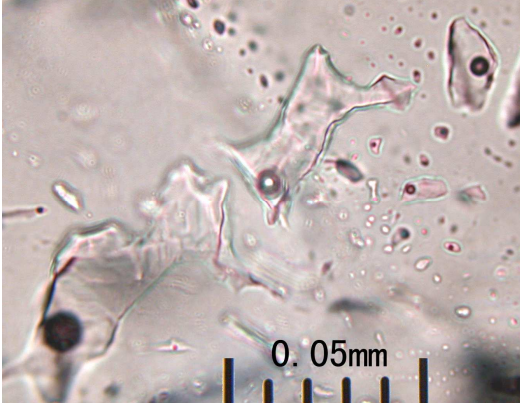


FIG.2. Histograms showing salinities of fluid inclusions in Huangnihu uranium ore-field.

### 2.1.3. Composition of fluid inclusions

Because Raman spectra is activated only by covalent bond but not, electrovalent bond [6], the Raman analysis did not give the salinity composition of fluid inclusions. The Laser Raman analytical result of fluid inclusions in Huangnihu deposit (Table 2) shows that the gas-facies of inclusions are composed of H<sub>2</sub>, CO<sub>2</sub>, CH<sub>4</sub> and H<sub>2</sub>O. Besides, liquid-facies of inclusions in siliceous veins in HN-3 basalt contain liquid-facies CO<sub>2</sub>, and a weak peak of NO<sub>3</sub><sup>-</sup> is also found in liquid-facies of inclusions in quartz veins associated with HN-13 pitchblende.

In sandstone, gas-facies of fluid inclusions in fluorite veins are primarily H<sub>2</sub>, which is relatively high in some inclusions. In basalt, gas-facies of inclusions in siliceous vein are mainly CO<sub>2</sub> with a little CH<sub>4</sub>. In granitic sandstone, gas-facies of inclusions in siliceous veins are mostly CO<sub>2</sub> with traces of

 <p>0.05mm</p>	 <p>0.05mm</p>
<p><i>Fig.2 Syngenetic gas inclusions in quartz associated with pitchblende, sample No.HN-13 (under plane polarized light microscope)</i></p>	<p><i>Fig.3 Daughter mineral-bearing inclusions in quartz associated with pitchblende, sample No.HN-13 (under plane polarized light microscope)</i></p>
 <p>0.05mm</p>	 <p>0.05mm</p>
<p><i>Fig.4 Epigenetic gas inclusions in quartz associated with pitchblende, sample No.HN-13 (under plane polarized light microscope)</i></p>	<p><i>Fig.5 Gas inclusions in quartz vein in granitic sandstone, sample No.HN-4 (under plane polarized light microscope)</i></p>
 <p>0.05mm</p>	 <p>0.05mm</p>
<p><i>Fig.6 Gas inclusions located along fissures in quartz vein in basalt, sample No.HN-2 (under plane polarized light microscope)</i></p>	<p><i>Fig.7 Irregular inclusions in fluorite vein associated with pitchblende, sample No.HN-13-1 (under plane polarized light microscope)</i></p>

CH<sub>4</sub>. Gas-facies of inclusions in quartz veins associated with pitchblende are CO<sub>2</sub>, while those in fluorite veins are primarily H<sub>2</sub> with a little CH<sub>4</sub>.

The compositions of mantle fluid are known to be mainly CO<sub>2</sub> and H<sub>2</sub>O, minor CO, CH<sub>4</sub>, H<sub>2</sub>, N, S, alkali metals and rare gas such as He, Ar, etc. [7][8][9]. However, the fluid from lower mantle or mantle-core boundary, as well as hydrogen circle of outer core contains higher H<sub>2</sub>, and about 97.8% [10~11] of them are CH<sub>4</sub> and H<sub>2</sub>. Gas-facies of fluid inclusions in this area are rich in CO<sub>2</sub>, H<sub>2</sub> and CH<sub>4</sub>, indicating part of the fluid is from mantle.

#### 2.1.4. *Fluid stages*

In most cases, the homogenisation temperatures of fluid inclusions decreases with geologic age [5], so fluids in this district evolved from high temperature to low. According to their shapes, homogenisation temperature, salinity, composition of gas-facies, and corresponding relationship (Tables 1, 2) of the inclusions, fluid in this district is divided into 4 categories (6 sub-categories):

I. High temperature volatile-rich fluid: the homogenisation temperature is higher than 360°C and up to 438°C; the inclusion-hosting mineral is quartz; inclusions are located as spots or groups, with regular round or ellipse shapes; liquid-facies fluid inclusions with high gas-liquid ratio or gas-facies inclusions are mostly syngenetic inclusions in quartz, of which the gas-facies are mainly CO<sub>2</sub>, with a little CH<sub>4</sub>, but without H<sub>2</sub>.

II. Mid-high temperature and middle-salinity fluid: the homogenisation temperature is 270-350°C; the salinity is intermediate (about 6~9wt%NaCl); the inclusion-hosting mineral is quartz; inclusions are located as group or band, with regular ellipse shapes; gas-liquid ratio is mainly 30-50%; the gas-facies are mainly CO<sub>2</sub> and CH<sub>4</sub>, and traces of NO<sub>3</sub><sup>-</sup> in liquid-facies.

Table 2. Chemical compositions of Gas in the fluid inclusions in Huangnihu uranium ore-field\*

Sn	Mineral	Facies	Raman Peak ( $\text{cm}^{-1}$ )	Raman Intensity	Composition	Characteristic Peaks ( $\text{cm}^{-1}$ )
HN-1c	Fl	L	3418.76	9241.41	H <sub>2</sub> O	3310~3610
		G	4156.73	14338.9	H <sub>2</sub>	4154~4165
HN-1e	Fl	G	4158.12	9431.29	H <sub>2</sub>	4154~4165
		L	3457.68	10857.1	H <sub>2</sub> O	3310~3610
HN-2b	Q	G	1388.47	7287.05	CO <sub>2</sub>	1386~1390
		G	1388.47	7501.63	CO <sub>2</sub>	1386~1390
		L	3409.09	2974.97	H <sub>2</sub> O	3310~3610
HN-2e	Q	G	1387.03	6210.11	CO <sub>2</sub>	1386~1390
		G	2917.63	461.683	CH <sub>4</sub>	2913~2919
		G	2915.58	708	CH <sub>4</sub> Validated	
HN-3a	Q	G	1388.47	5235.86	CO <sub>2</sub>	1386~1390
		G	2916.19	2187.39	CH <sub>4</sub>	2913~2919
		L	1384.15	1971.85	CO <sub>2</sub>	1382~1386
HN-4a	Q	G	3433.59	3493.47	H <sub>2</sub> O	3310~3610
		G	1386.92	7956.77	CO <sub>2</sub>	1386~1390
		G	2917.06	973.179	CH <sub>4</sub>	2913~2919
HN-4e	Q	G	1387.03	3524.06	CO <sub>2</sub>	1386~1390
		G	2916.19	669.518	CH <sub>4</sub>	2913~2919
		G	2915.58	961	CH <sub>4</sub> Validated	
HN-13a	Q	G	1386.92	6907.7	CO <sub>2</sub>	1386~1390
HN-13c	Q	G	1387.03	6550.49	CO <sub>2</sub>	1386~1390
		G	2915.58	1387	CH <sub>4</sub>	2913~2919
		L	1046.9	3701.64	NO <sub>3</sub> <sup>-</sup>	1040~1060
HN-13-1c	Q	G	1387.03	2722.21	CO <sub>2</sub>	1386~1390
HN-13-1g	Fl	G	2918.45	4045.15	CH <sub>4</sub>	2913~2919
		G	4158.12	12432.3	H <sub>2</sub>	4154~4165

\*Analysed by the Institute of Physics, CAS with LABHR-VIS LabRAM HR

III. Mid-low temperature fluid: the homogenisation temperature is 120-180°C; the inclusion-hosting minerals are quartz and fluorite; inclusions are located as group or band, with regular shapes; gas-liquid ratio is mainly 5~30%; the gas-facies are mainly CO<sub>2</sub>, CH<sub>4</sub> and H<sub>2</sub>; 3 sub-categories can be recognized based on salinity:

III-1. Mid-low temperature and low salinity fluid, of which the salinity is 0.53-1.74wt% NaCl and the hosting mineral is mainly quartz;

III-2. Mid-low temperature and middle salinity fluid, of which the salinity is between III-1 and III-3 (2.07-14.64wt% NaCl) and the hosting minerals are fluorite and quartz;

III-3. Mid-low temperature and high salinity fluid, of which the salinity is 16.30-17.12wt% NaCl and the hosting mineral is mainly fluorite, characterized by the occurrence of H<sub>2</sub> in gas-facies.

IV. IV. Low-temperature and low-salinity fluid: the homogenisation temperature is 80~90°C; the salinity is 1.23-1.74wt% NaCl; the inclusion-hosting mineral is quartz; inclusions are located as band, with irregular shapes; gas-liquid ratio is lower than 10%; the gas-facies are mainly H<sub>2</sub> and CH<sub>4</sub>.

On the whole, fluid salinity in this district varies from low to high; low because the fluid is mixed with other low-salinity fluid, the salinity variation is irregular as fluid is primarily of low-salinity. Genetically, fluid with such an irregularly varying salinity is the result of deep-derived high-temperature high-salinity fluid mixing in different proportion with supergene low-temperature low-salinity fluids.

## 2.2. Research on isotopes

Rb-Sr isotopes data (Table 3) of metallogenetic purple fluorite in Huangnihu deposit shows that in fluorite the  $(^{87}\text{Rb}/^{86}\text{Sr})_i=0.721895-0.722994$ , which is characteristic of crust; however, it is lower than  $(^{87}\text{Rb}/^{86}\text{Sr})_i$  in Baimianshi basement granite as 0.72462 [1, 2].  $\epsilon_{\text{Sr}}$  value is 250-265, which is also lower than that of granite (292-296). The Sm-Nd isotopes of fluorite (Table 4) are lower compared with basement granite, while the ratio of Sm/Nd is obviously higher. In fluorite,  $\epsilon_{\text{Nd}}(t) = -12.5856$  to  $-13.7974$ , and in basement two-mica granite,  $\epsilon_{\text{Nd}}(t) = -10.4741$  to  $-12.3052$ .  $\epsilon_{\text{Sr}}$  and  $\epsilon_{\text{Nd}}$  indicate the metallogenetic fluid is partly composed of paleo-crust, as it is derived from CHUR source area with low Sm/Nd which represents paleo-crust or the addition of paleo-crust. For fluorite,  $t_{\text{DM}}=1\ 971\sim 2\ 069$  Ma, and for granite,  $t_{\text{DM}}=1\ 873\sim 2\ 021$  Ma. Both don't differ very much with each other, and are the result of crust-mantle differentiation of the same stage. Comparison between the fluorite and basement granite shows that the fluid which produced the fluorite was derived from deep granitic magma with source differentiation or directly from CHUR with contamination of many paleo-crust materials on its way up.

Table 3. Rb-Sr isotopic data of fluorite in Huangnihu uranium ore-field\*

Sn	color	Rb( $10^{-6}$ )	Sr( $10^{-6}$ )	$^{87}\text{Rb}/^{86}\text{Sr}$	$^{87}\text{Sr}/^{86}\text{Sr}$	t (Ma)	$(^{87}\text{Rb}/^{86}\text{Sr})_i$	$\epsilon_{\text{Sr}}$
HN-14-1	Colorless	0.4	47.1	0.0245	0.721951	160	0.721895	249.62
HN-14-2	Purple	0.13	37.5	0.0104	0.723018	160	0.722994	265.22
HN-12	Purple	0.51	28.2	0.0523	0.722975	160	0.722856	263.26
HN-1	Purple	1.31	29.1	0.1299	0.723037	160	0.722742	261.63

\* Analysed by Isotopic Laboratory, BRIUG, based on EJ/T 692-92 with ISOPROBE-T No.7734.

Table 4. Sm-Nd isotopic data of fluorite and basement-granite of in Huangnihu uranium ore-field\*

Sn	color	Sm ( $10^{-6}$ )	Nd ( $10^{-6}$ )	$^{147}\text{Sm}/^{144}\text{Nd}$	$^{143}\text{Nd}/^{144}\text{Nd}$	Sm/Nd	T	$\epsilon_{\text{Nd}}(t)$	$t_{\text{DM}}$ (Ma)
HN-14-1	Colorless	2.58	4.7	0.3314	0.512072	0.57	160	-13.7974	2069
HN-14-2	Purple	1.39	3.84	0.2193	0.511991	0.37	160	-13.0878	2012
HN-12	Purple	0.95	2.74	0.2103	0.511952	0.36	160	-13.665	2058
HN-1	Purple	1.2	3.32	0.2186	0.512016	0.37	160	-12.5856	1971
B2-1	Basement Granite	7.43	52.38	0.0858	0.51192	0.15	249.9	-10.4741	1873
B3-11		7.31	48.13	0.0918	0.511836	0.16	249.9	-12.3052	2021
HN-9		6.43	37.7	0.1031	0.511873	0.18	249.9	-11.9438	1992

\* Analysed by Isotopic Laboratory, BRIUG based on EJ/T 546-91 with ISOPROBE-T No.7734

### **2.3. Indicator minerals**

Five ore mineral groups can be recognized in Baimianshi orefield: U-hematite, U-chlorite, U-sulfide, U-fluorite and U-carbonate types. The primary uranium minerals are uraninite, brannerite, coffinite, etc., and occur as bands, breccia, zoned, vein, disseminated, and concretions. The gangue minerals are galena, hematite, marcasite, sphalerite, etc., occurring in irregular shapes or as veins.

Track etching, radioactive photography and electron microscopy, show that besides brannerite and pitchblende, uranium also occurs in mineral fissures and margins in organic material or in clay cement as discrete particles or as disseminations. (Figs 8 - 13).

Electron microscopic analysis for uranium minerals reveals that brannerite has molar ratio of Ti/U in the range 0.84-2.18, and considering isomorphous Th, Pb, Ca, Mg, Fe and Mn in the calculation, the molar ratio is 0.76-1.85. Therefore, uranium minerals are indicated not to be uniform, and primarily uraninite, brannerite, but also their mixture. These brannerite are not inherited from the diagenesis of basement granite, but from hydrothermal Ti. As the fluids are not mixed homogeneously, the content of Ti varies largely, with TiO<sub>2</sub> up to 34.71%.

### **2.4. Metallogenic ages**

U-Pb isotopic dating of pitchblende in ores of the area gives two ages: the early one is 160.4±0.5 Ma, while the late one is 128±0.8 Ma. Previous studies had indicated one more younger age. The first stage of uranium metallogenesis is 160.4±0.5Ma, related to bimodal volcanism (diagenetic age of basalt is 172.8±7.7 Ma, and rhyolite is 164.8±0.57 Ma); the second age is 128±0.8 Ma, related to Yanshanian magmatism (in north of the basin, Danguanzhang rock body and multi-stages of complements); and the third one is 103~86 Ma, related to sub-volcanic rocks and dikes, namely quartz porphyry (99 Ma) and diabase (105 Ma). Furthermore torbernite, autunite, etc., indicate secondary alteration after hydrothermal mineralization.

## **3. Conclusions and discussion**

(1) Baimianshi uranium orefield is hydrothermal type. The source of metals is from crust, and the fluid could be partly from mantle. As the fluid migrated up, it extracted metals from crust and basement granite, then deposited them in favorable area in the upper levels.

(2) In Baimianshi orefield, main metallogenesis include three stages: the first stage is related to bimodal volcanism; the second one is related to Yanshanian magmatism; and the third is related to sub-volcanic rocks, and dikes (quartz porphyry and diabase).

(3) As per homogenisation temperature, salinity and composition, the fluids can be divided into four categories (6 sub-categories). Fluid contributing to metallogenesis are mainly mid-low temperature (270-350°C, 100-170°C), in which the salinity varies largely, indicating the mixture of high-salinity (15.5-16.5 wt%NaCl) and low-salinity fluids (0.5-1.5 wt%NaCl).

(4) On the whole, the metallogenesis of Baimianshi orefield appears to be effected by different ages of volcanic eruption, magmatic intrusions, and cross-cutting dikes, and the orebody is characterized by composite genesis.

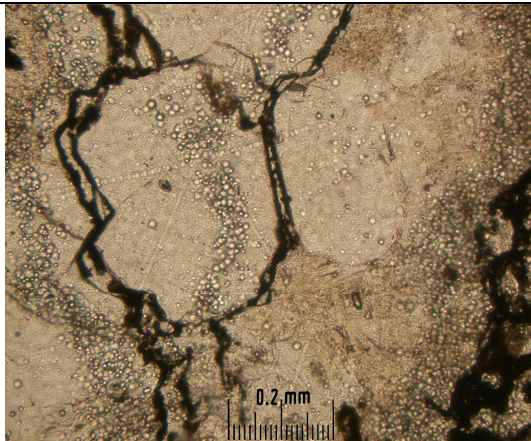


Fig.8 Uraninite distributed between intergranule of quartz grains.

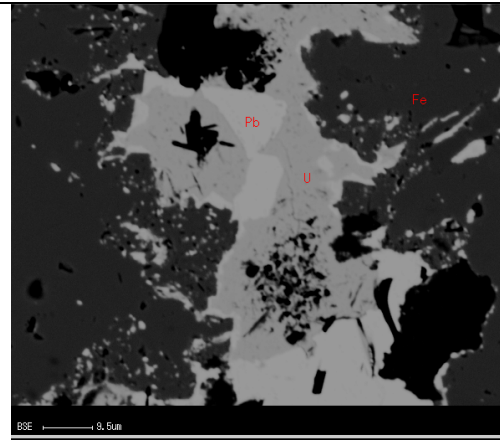


Fig.9 The coexist of uraninite, pyrite and galenite .

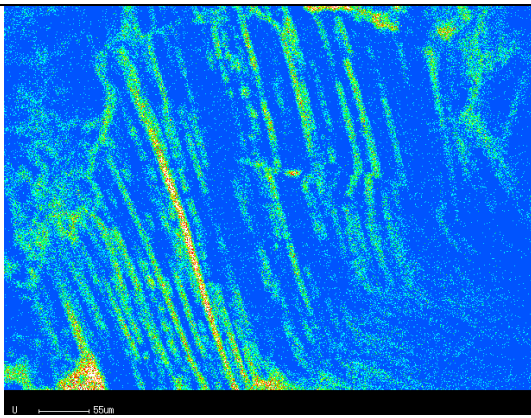


Fig.10 Uranium distributed in the cleavage of muscovite.

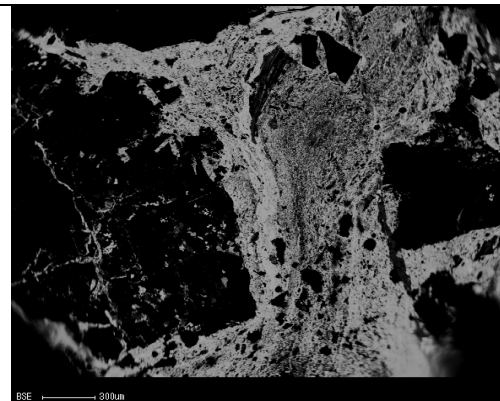


Fig.11 Micro quartz containing pitchblende vein distributed between the intergranule and fracture of quartz grains.

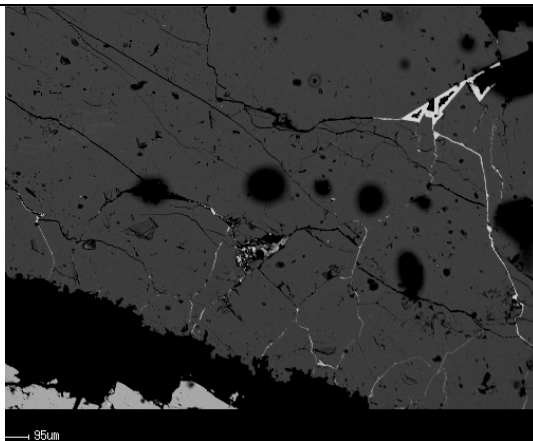


Fig.12 Uranium (white) distributed in the fracture of fluorite vein (black).

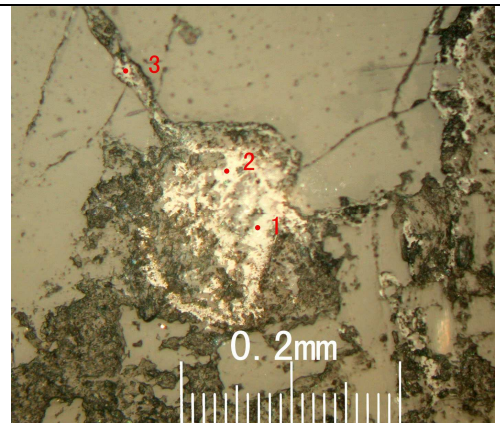


Fig.13 Brannerite (light) located in the node of quartz (gray), and the black part of surface is chlorite.

## REFERENCES

- [1] HUANG, J-B., et al., Generality of Uranium Metallogenetic Belt in China (2005).
- [2] CHEN, Y-H., LI, J-H., Two important types of extensional tectonics controlling uranium deposits in South China, *Mineral Deposits* 13(supplement) (1994) 50-52.
- [3] ZHANG, W-L., et al., Basic Geological Features and Future of Uranium Ore in the Anyuan Hot Dome in Jiangxi, *Mineral Resources and Geology* 19(2) (2005) 122-126.
- [4] LU, H-Z., et al., *Geochemistry of Fluid Inclusion*, Geology Publishing Company, Beijing (1990).
- [5] LU, H-Z., et al., *Fluid Inclusion*, Science Publishing Company, Beijing (2004).
- [6] XU, P-C., et al., *Raman Spectrum in Geologic Science*, Science and Technology Publishing Company, Shanxi, Xi'an (1996).
- [7] DU, L-T., "Natural elements and reducing gas in pyrolite", *Geochemistry on mantle fluid and asthenosphere*, Geology Publishing Company, Beijing (1996).
- [8] BERGMAN, S.C, DUBESSY, J., CO<sub>2</sub>-CO fluid inclusions in a composite peridotite xenoliths: implications for upper mantle oxygen fugacity, *Contrib Mineral Petrol.* 85 (1984) 1-13.
- [9] TOLSTIKHIN, I.N, et al. Low mantle plume component in 370 Ma old Kola ultrabasic-alkaline-carbonatite complexes: evidence from rare gas isotopes and related trace elements, *Russian J Earth Sci.* 1(2) (1999) 125-143.
- [10] LIU, C-Q., et al., *Mantle fluid and its metallogenesis: taking Mianning REE deposit, Sichuan Province as an example*, Geology Publishing Company, Beijing (2004).
- [11] LIU, J-M., et al., Ore Forming Fluid Systems in Crust, *Advance in Earth Sciences* 13(4) (1998) 161-165.

# A special kind of sandstone type uranium deposit in Northeastern Ordos Basin, China<sup>\*</sup>

Z.Y. Li<sup>a</sup>, X.H. Fang<sup>a</sup>, Y. Sun<sup>a</sup>, A.P. Chen<sup>b</sup>, Y.Q. Jiao<sup>c</sup>, Y.L. Xia<sup>a</sup>, K. Zhang<sup>d</sup>

<sup>a</sup> Beijing Research Institute of Uranium Geology, Beijing, China

<sup>b</sup> Geological Exploration Team 208, Inner Mongolia, China

<sup>c</sup> China Geological University, Wuhan, China

<sup>d</sup> Zhongshan University, Guangzhou, China

*E-mail address of main author: zyli9818@126.com*

**Abstract.** The large Dongsheng sandstone type uranium deposit was discovered recently in northeastern Ordos Basin, China. It is a unique kind of deposit, different from other known sandstone type deposits because of its distinctive signatures. It is generally controlled by a transitional zone between greenish and greyish sandstones, both indicating presently reduced geochemical environments. The greenish colour of the paleo-oxidized sandstones is mainly due to chloritization and epidotization related to oil and gas secondary reduction processes. The deposit, which is of more complex origin, has undergone not only paleo-oxidation mineralization process, but also oil-gas fluid and hydrothermal reworking processes and therefore is genetically different from other known sandstone uranium deposits. The metallogenic model for this uranium deposit is put forward, and exploration outcomes summarized in this paper.

## 1. Introduction

Dongsheng sandstone-type uranium deposit is a large deposit, recently discovered in the Jurassic Zhiluo Formation of northeastern Ordos Basin. The uranium mineralization occurs in the transitional zones between grey-green and grey sandstones of the Zhiluo Formation [1]. The discovery of this uranium deposit, a very important energy mineral resource after oil-gas and coal deposits found in the basin, mark it as an “energy resources basin” [1] [2]. The sandstones both in oxidized and reduced ore zones show reduced colour of grey-green. That unique feature of this deposit is different from that of ordinary sandstone type uranium mineralization which occurs between oxidized yellow and reduced grey colour zones [1][3][4]. Formation of Dongsheng sandstone-type uranium deposit and its unique metallogenic phenomena are closely related to the geological, structural and sedimentary evolution of the basin, as well as the geochemical conditions. Besides uranium deposits, there are large coal deposits found in Lower-Middle Jurassic Yan’an Formation and a number of oil and gas indications and occurrences in the study area [5][6][7][8]. Therefore, to study the origin and establish metallogenic model is of not only important practical significance for further exploration, but also has theoretical significance for understanding the metallogenic processes and relationships with other energy mineral resources such as oil, gas and coal.

---

<sup>\*</sup> Funded by both key national research and development plan project (code : 2003CB2146) and BOG uranium geological research project (code : HDKY20020501)

## 2. Geologic setting

The study area is located at the southern margin of Yimeng uplift block in northeast Ordos Basin, adjacent to Hetao graben at the northern margin. Mesozoic sedimentary strata are mainly exposed in the study area (Fig. 1)[9]. The Upper-Triassic Yanchang Formation is mainly composed of gravel-bearing sandstone interbedded with siltstone and mudstones, bearing oil- and coal-deposits, The Lower-Middle Jurassic Yanan Formation is mainly composed of coal producing arkose, mudstone and siltstone. The Middle Jurassic Zhiluo Formation is the uranium-bearing host, composed of grey, grey-green sandstone and mottled siltstone and mudstone, which is parallel or locally angular to the unconformably underlying Yanan Formation. The Anding Formation is composed of grey-green argillaceous sandstone, purple-red fine-grained sandstone, mudstone interbedded with white fine-grained calcareous sandstone, which is parallel to unconformably underlain by the Zhiluo Formation. The Upper Jurassic Fenfanghe Formation is poorly developed in the study area. The Lower Cretaceous strata are mainly composed of purple, grey-green sandy conglomerate, sandstone and purple-red, brown-red silt mudstone interbedded with thin beds of sandstone and conglomerate, which has angular unconformities with overlying and underlying formations [10][11]. The Tertiary strata are absent, the Quaternary sands and soils range from several to tens of meters in thickness. Sedimentary strata show that the study area underwent multiple tectonic events [6], and are closely related to uranium mineralization. Uranium mineralization occurs in the transitional zones between grey-green and grey sandstones of the Zhiluo Formation.

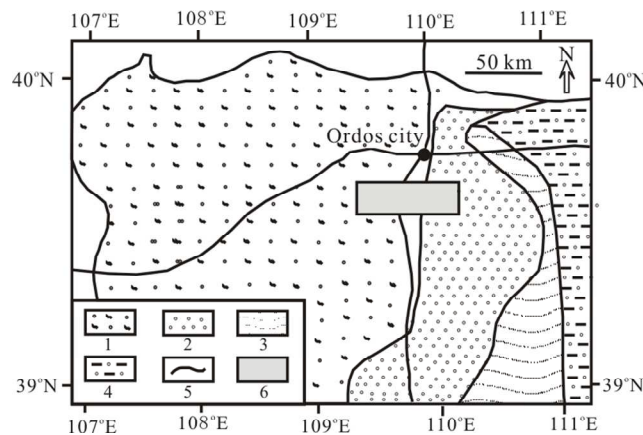


FIG. 1. Simplified geological map of Dongsheng area in Ordos Basin.

1—Lower Cretaceous series, 2—Jurassic system, 3—Triassic system, 4—Paleozoic erathem, 5—Road, 6—Study area [12]

## 3. Petrology of ore bed sandstone

The host rock is a graded horizon with rhythmical change in grain size and cross-stratification. The grains are loosely cemented; the clastic grains are both poorly rounded and sorted, being mostly sub-angular to sub-rounded in shape. It is mainly composed of gravel-bearing grit, medium-coarse grained sandstone, coarse-grained sand bearing medium-grained sandstone, medium- and fine-grained sandstone. The mineral compositions are mainly quartz, feldspar, debris and mica.

The matrix in the sandstones are usually less than 10%, and carbonates less than 0.5%. Contact cementation dominates followed by the porous cementation in the matrix. Some sandstones are strongly altered by carbonatization, the contents of the carbonates range from 10% to 20%, in cases of basal cementation, the carbonate even up to more than 50%, forming “psammitic limestone”. Almost all of the carbonates exist as calcite. The calcite usually shows form of large bright crystal grains, in some cases micro-crystal aggregates ranging from 0.002 mm to 0.005 mm in diameters, and sometimes also spherulites, which should form later.

The host sandstones are quite complicated in mineralogical compositions, which are dominated by quartz, also containing a lot of feldspar, debris, mica and some heavy accessory minerals.

The host sandstones of the lower member of Zhiluo Formation are debris-bearing arkose with abundant feldspar clastics and debris in the study area, indicating fast deposition, in environments close to the provenance area. Major rocks of provenance areas are inferred to be granitic and metamorphic rocks, a few volcanic rocks according to the debris compositions.

#### 4. Features of grey-green sandstone

Grey-green sandstone is located in north and northeast parts of the study area, surrounding grey sandstone as semi-circular and incising grey sandstone as a tongue in north-south section, which shows typical spatial distribution features of interlayered oxidation zone.

Hand specimen of grey-green sandstone looks compact and greenish in colour with different tones. Pyrite and carboniferous debris (or organic veinlets) could not be observed by naked eyes or even with hand lens. Further, a quite thin oxidized circle around the muddy gravel can be identified. Sometimes grey-green sandstone is interbedded by grey-purple calcareous sandstone with high content of carbonate, in which strongly oxidized carbonaceous plant clastics could be observed. These features confirm that grey-green sandstones underwent strong oxidation process prior to attaining the present grey-green colour [12]. The oxidized residues, which have not completely become greenish, are due to enclosing effect of strong carbonation.

Petrologic studies show that grey-green sandstone does not greatly differ from grey sandstone in mineral composition, only small difference in content of chlorite. Grey-green sandstone contains more chlorite than grey sandstone. Chlorite have been identified to be pennine and thuringite, their contents are usually less than 1%. The pennine can be considered to be alteration product of biotite, but thuringite is produced by alteration of plagioclase. However, most biotite are not altered, only some of them have been altered to be greenish biotite. In addition, some epidote and greenish illite in the matrix of sandstone can be identified. The greenish sandstones usually contain few pyrite grains. Some grey-green sandstones are strongly carbonatized, and biotite underwent locally strong oxidation and is replaced partially by carbonate. In addition, few ilmenite remains in the grey-green sandstone, being almost replaced by crystal druse of anatase.

The clay data indicate that grey-green sandstone has undergone stronger alteration than grey sandstone. The difference in clay composition between both kinds of sandstones is marked by content of kaolinite and chlorite. Kaolinite is richer in grey sandstone with average value of 45.0% than that in grey green sandstone with average value of 26%. However, the chlorite is just opposite, with average value of 3% and 20.75% respectively (Table 1). The scanning electron microscope (SEM) study shows that thin acicular-leaf and spheroidal chlorites cover the surface of grains in grey-green debris-bearing arkose (Fig. 2). So, it can be concluded that high content of chlorite is reason for greenish colour in those grey green sandstones.

Table 1. X-ray diffraction quantitative analysis of clay minerals \*

Sample number	Lithology	Relative content of clay minerals (%)				
		S	I/S	I	K	C
Ave.(2)	Light grey medium-grained debris-bearing arkose	49.5		2.5	45	3
Ave.(4)	Grey-green medium-grained debris-bearing arkose	50.5	/	2.75	26	20.75

\* analyzed in Experiment and Research Center of Petroleum Geology, Research Institute of Petroleum Exploration and Development, PetroChina. S: Smectite, I: Illite, K: Kaolinite, C: Chlorite

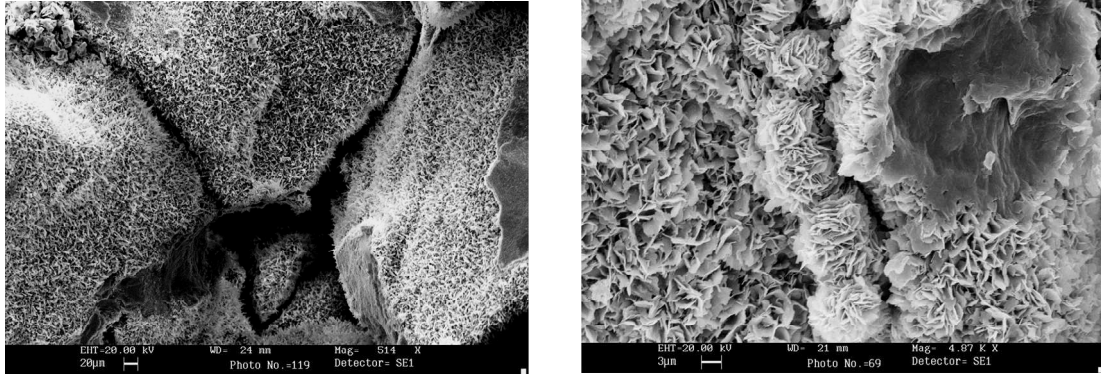


FIG. 2. Micro-features of ore bed sandstones.

Left: Thin acicular-leaf chlorite covering the surface of grains in grey-green debris-bearing arkose (SEM photo); Right: Acicular-leaf and spheroidal chlorites covering the surface of grains in grey-green debris-bearing arkose (SEM photo).

## 5. Origin of grey-green sandstone

The petrological, mineralogical and geochemical studies show that grey-green sandstones had undergone initial oxidation process and later second reduction process during geotectonic evolution [12].

Evidences of grey-green sandstones undergoing oxidation process in the initial stage are listed as follows:

- (1) They are located in north and northeast part of the study area, as semi-circular exposures surrounding grey sandstone and incising grey sandstone as a tongue shape in north-south section, which is typically the spatial distribution feature of an interlayered oxidation zone.
- (2) A thin oxidation layer around muddy gravel in grey-green sandstone can be observed, furthermore, the oxidized minerals and plant debris can be found in the impermeable matrix of calcareous sandstone interbeds because of carbonate alteration.
- (3) Compared with grey sandstone, the grey-green sandstone contains less pyrite and organic material, but higher content of clay minerals, and ilmenite is almost completely oxidized as well.
- (4) Geochemically, grey green sandstones contain lower sulfur and organic carbon, but higher  $\text{Fe}_2\text{O}_3/\text{FeO}$  ratio, which are in concordance with their mineralogical data. In addition, the ore element U and associated elements Mo, V etc. obviously move out.

Second reduction processes took place after the formation of uranium deposit in the Zhiluo Formation. These processes transformed the sandstones in the paleo-oxidation zone to green or grey-green colour, indicating geochemical reduction environments. The greenish colour mainly results from chloritization and epidotization. The ore bodies are clearly located in the transitional zone between grey and green coloured sandstones. This is a special feature of Dongsheng deposit, different from other sandstone type uranium deposits. As pointed out before, the greenish colour of grey-green sandstones is due to very thin layers of acicular-leaf chlorite around clastic grains. The second reduction process with alteration of chlorite is closely related to natural oil and gas. A lot of oil and gas inclusions have been found not only in the paleo-oxidation zone, but also in the ore body zone, which show multiple oil and gas inclusions and reworking processes [13][12].

## 6. Uranium mineralization

When uranium bearing fluids flow to the places where physical and chemical conditions change, stable and complex compounds become unstable, and gets precipitated. The importance in changing conditions of the uranium bearing fluids are the organic matter, which plays the reduction and absorption role.

In reducing conditions, adsorption by organic matter is related with humic and fulvic acids. The absorption of  $UO_2^{2+}$  is determined by both enrichment of  $UO_2^{2+}$  ion and the agglomeration degree of uranium organic complex compounds. In the acidic condition of pH=3.4, the adsorption of uranium is at the highest.

Nearly all solid bitumen and many kinds of coal (with humic acid) have ability to reduce uranium [14]. The materials which can reduce uranium are plant debris formed during sedimentation process, and bitumen and oil migrating into ore beds after diagenesis. The rate of reduction depends on the organic matter character and reaction temperature.

The study area has undergone a tecto-thermal event after uranium mineralization. Because of high temperature, the thermal fluids have strong migration ability and are rich in U, Mo, Re, V, Se, Si, Ti, P, REE etc. These fluids are usually alkaline. Under condition of strong oil reduction, fluid feature changes from alkaline to acidic and uranium precipitates from the fluids.

Dongsheng deposit occurs in the redox zone, i.e. transitional zone between oxidation and reduced zones. The redox transitional zone was formed by both paleo-phreatic and interlayer oxidation processes. So, it has both vertical and horizontal zonations [15], which are also under pinned by geochemical and mineralogical zonations. Analytical data for U, Se, Mo, V, Re and S show systematic increase from oxidation to original zones in both vertical and horizontal sections. Goethite, kaolinite, and hematite are typical in the oxidation zone, in contrast with pyrite in the original zone. The ore bodies show roll-front shape with long tails.

## 7. Metallogenic model

The formational conditions, controls and mineralization mechanism of the sandstone type uranium deposit in the northeastern Ordos Basin, are very complicated [16]. It underwent multiple mineralization processes, such as tectonic multi-periodic “dynamic-static” coupling movements, superposition of paleo phreatic oxidation and interlayered oxidation and composite transformation by oil-gas and thermal fluids[17][18]. Therefore, a metallogenic superposition model has been put forward for the deposit in the northeastern Ordos Basin (Fig. 3).

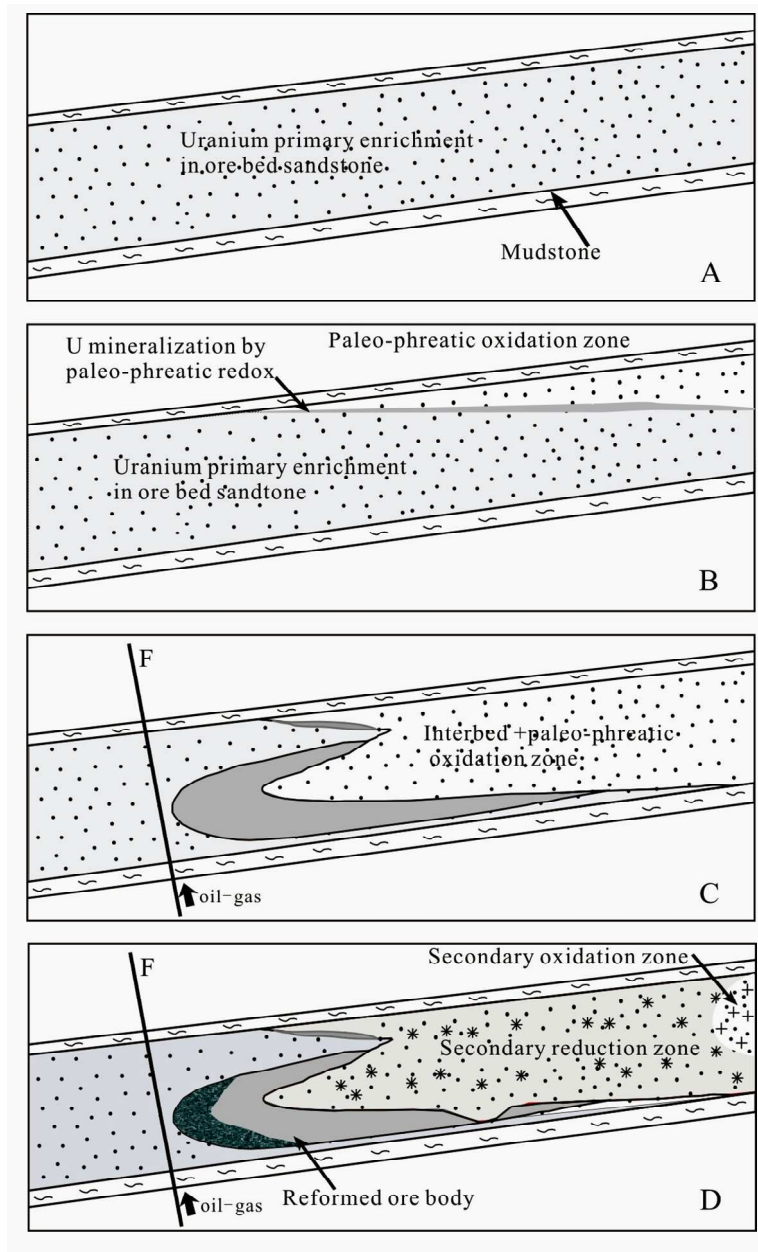


FIG. 3. Metallogenic model of Dongsheng sandstone type uranium deposit in northeastern Ordos Basin.

A: Preliminary enrichment stage; B: Paleo-phreatic oxidation stage; C: Paleo-phreatic+ Paleo-interlayer oxidation stages; D: Oil-gas reduction+ Thermal modification stages.

The grey sandstones of braided river facies in Zhiluo Formation is the host for uranium mineralization. They were deposited in humid condition favorable for development of reducing materials and initial uranium enrichment. The initial uranium enrichment of ore beds is one of important sources for uranium mineralization.

Paleo-phreatic oxidation process took place in middle and late Jurassic after the deposition Zhiluo Formation. This was due to up-lift of the basin and inclined movement coupled with paleoclimate change from humid to dry and semi dry, which is favorable for surface and vertical oxidization processes to develop, and uranium enrichment and mineralization began in the ore bed.

Paleo-interlayer oxidation process occurred in the late Jurassic to early Cretaceous. Uplift of the study area exposed to surface most part Zhiluo Formation, promoting weathering and oxidizing processes. When the paleoclimate was dry, oxygen- and uranium-bearing fluids moved into the ore beds and interlayered oxidation process led to development of uranium mineralization.

The multi-stage oil-gas reduction in the mineralized zones have been inferred from the many oil-gas inclusions, indicating its role in the uranium mineralization. Post mineralization tectonic movements, uplift and decompression lead to multiple oil-gas diffusions, which in turn promoted second reduction of ore beds, and transformed earlier oxidation zone to grey-green.

Analytical data show that thermal modification of the deposit happened Ca. 20-8 Ma after the deposit formed. It is probably due to this modification that coffinite (Fig. 4), selenium, sulfide minerals formed under relatively high temperature, leading to the superimposed enrichments of elements like P, Se, Si, Ti and REE over uranium. The complex uranium mineralization and modification processes make this deposit unique, different from other sandstone type uranium deposits. The presence of coffinite indicates that uranium mineralization formed at relatively higher temperature and more reducing environment than those of the other deposit. The higher temperatures are also evidenced from inclusion studies on vein carbonates ranging from 70°C to 170°C, and the salinity from 8% to 20%, which also indicate that Dongsheng area has been imprinted with hydrothermal events.

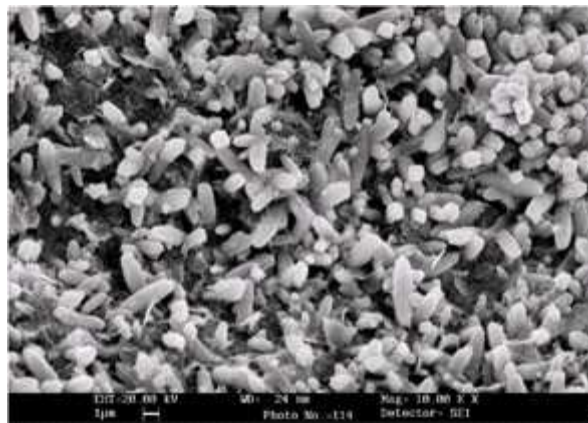


*FIG. 4. Coffinite crystal found in uranium ore sample.*

## **8. Exploration criteria**

As discussed above, Dongsheng deposit is characterized by its unique features, which are related to its complicated origin. The deposit was formed not only under redox processes, but also underwent oil-gas and hydrothermal reworking. Therefore understanding of the genesis is of practical significance to exploration. Major criteria for exploration are:

- (1) Tectonic slope: The slope must have a favorable dipping angle not more than 10 degrees and should have undergone subsidence and uplift to maintain acceptable depth of target horizons and erosion period for uranium mineralization.
- (2) Connected sandstone bodies and lithologically transitional zone: Sandstone bodies should be well connected as stable horizons. Uranium mineralization often occurs in the transitional zones associated with lithologic, grain-size, facies or colour changes.
- (3) Paleo-oxidation zones: Greenish or green sandstones are special features, which reflect secondary reduction processes. They are actually secondary-reduced paleo-

oxidation zones. Uranium mineralization is controlled by transitional zones between grey (original rock) and green (paleo-oxidized) sandstones.

## REFERENCES

- [1] LI, Z.Y., et al., “Metallogenetic conditions and Exploration Criteria of Dongsheng Sandstone type uranium deposit in Inner Mongolia, China”, *Mineral Deposit Research* (MAO, J.W., BIERLEIN, F.B., Eds), Springer (2005) 291-294.
- [2] LI, S., *Depositional systems in energy- resources bearing basins- case studies of the continental and paralic depositional systems in China*, Wuhan, China University of Geosciences Press (1996) 32-45.
- [3] ADAMS, S.S., SMITH, R.B., *Geology and Recognition Criteria for Sandstone Uranium Deposits in Mixed Fluvial-shallow Marine Sedimentary Sequences, South Texas*. U.S. Department of Energy, Grand Junction Office, Colorado (1981).
- [4] HUANG, S.J., Formation conditions and prospecting criteria for interlayered oxidation sandstone type uranium deposits, *Uranium Geology* 10 (1) (1994), 6—13 (in Chinese with English abstract).
- [5] HE, Z.X., *Evolution of Ordos Basin and oil-gas*, Beijing Oil Industry Press (2003) (in Chinese with English abstract).
- [6] ZHANG, K., *Tectonics and resources of Ordos facult block, Xi’an*, The Science and Technology Press of Shannxi (1989).
- [7] WANG, S.M. et al., *Coal accumulative pattern and resource evaluation of Ordos Basinm*, Coal Industry Press, Beijing (1996).
- [8] WANG, F.G., *Geochemical characteristics and prospective evaluation of oil and gas potentials in Hangjinqi area, Ordos Basin*, *Geophysical and Geochemical Exploration* 27(2) (2003) 104-114 (in Chinese with English abstract).
- [9] Bureau of Geology and Mineral Resources of Inner Mongolian Autonomous Region, *Regional Geology of Inner Mongolian Autonomous Region*, Beijing, Geological Publishing House (1991) (in Chinese).
- [10] JIAO, Y.Q., et al., Sand body heterogeneity: one of the key factors of uranium metallogenesis in Ordos basin, *Uranium Geology* 21 (1) (2005) 8—16 (in Chinese with English abstract).
- [11] LI, S.T., et al., *Sequence stratigraphy and depositional system in northeastern Ordos basin* Beijing, Geological Publishing House(1992) (in Chinese).
- [12] LI, Z.Y., et al., Origin of grey-green sandstone in ore bed of sandstone type uranium deposit in North Ordos Basin, *Science in China, Series D, Vol.50*, Science in China Press, Beijing (2007) 165-173.
- [13] LU, H.Z., FAN, H.R., NI, P., *Fluids inclusions*, Beijing, Science Press (2004) (in Chinese).
- [14] SUN, Y., LI, Z. Y., XIAO, X.J., Relationship between oil-gas traps and uranium metallogenesis in Northern Ordos Basin, *Uranium Geology* 20 (6) (2004) 337-343 (in Chinese with English abstract).
- [15] XIAO, X. J., et al., Preliminary study on features of mineralogical zoning of epigenetic alteration of Dongsheng sandstone-type uranium deposit in Ordos Basin, *Uranium Geology* 20 (3) (2004) 136-140 (in Chinese with English abstract).
- [16] LI, Z.Y., et al., Origin and Superposition Metallogenic Model of the Sandstone Type Uranium Deposit in the Northeastern Ordos Basin, *Mineral Deposit* 25 (2006) 245-248.
- [17] OU, G.X., et al., Leakage of oil-gas and its relationship with sandstone uranium ore-formation in North China, *Proceedings of the 20th Chinese Geophysics Annual Meeting, Xi’an Xi’an Alta Press*(2004).21—26 (in Chinese).
- [18] SUN, Y., LI, Z.Y., Study on the relationship between coal-derived hydrocarbon and formation of sandstone-type uranium deposits in the basins of North China, *Mineral Deposit Research* (Mao, J. W., Bierlein, F.B., Eds), Berlin: Springer(2005) 315-316.

# Latest progress of seismic survey method in hydrothermal uranium deposits exploration in China

G. Xu<sup>a</sup>, H. Liu<sup>a</sup>, D. Zhao<sup>a</sup>, B. Zhu<sup>b</sup>

<sup>a</sup>Beijing Research Institute of Uranium Geology,  
Beijing, China

<sup>b</sup>No. 290 Geological Brigade of Nuclear Industry,  
Shaoguan, China

*E-mail address of main author: guilaixu@163.com*

**Abstract.** Since 1950s, many non-seismic geophysical survey techniques, such as radioactive geophysical survey method, induced polarization (IP), high resolution magnetic survey method, AMT and CSAMT have been applied and have played a very important role in exploration for hydrothermal uranium deposits in China. However, up to the early part of 21<sup>st</sup> century, seismic survey method has been hardly utilized in hydrothermal uranium deposits exploration. It is mainly due to the more complicated geological settings where hydrothermal uranium deposits occur compared to oil, gas or coal fields. These complicated geological settings include, for example, complicated ore shapes, small dimensions and as various lithologies are involved, wave impedance difference between the medium on each side of the interface is small. If the ground surface conditions are rough, there will be a lot of high-energy interference waves. Since 2007, based on studies of hydrothermal uranium ore formation mechanism and ground surface characteristics in uranium ore field, seismic work group of BRIUG has carried out a lot of systemic tentative work on excitation type of seismic source, layout of geophones, data analysis and processing techniques, and has obtained obvious success in detection of ore-control factors, such as basement or faults with high angle of inclination. We are sure that seismic survey method developed by BRIUG will become one of the most important technique for hydrothermal uranium deposits exploration in future.

## 1. Introduction

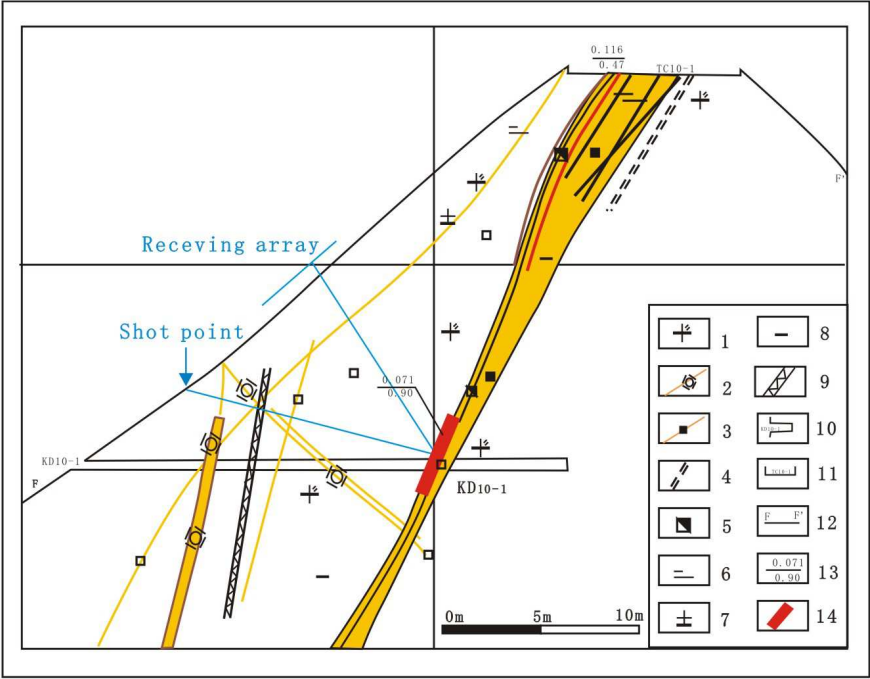
Due to poor surface conditions, large dip angle and small scale of the fault, as well as the marker horizon being not evident, for more than 50 years, seismic survey method has been hardly utilized in hydrothermal uranium deposits exploration in China. With the rapid development of nuclear industry in China, the demand for uranium resources has increased dramatically, and new geophysical methods and techniques should be developed to improve the efficiency of uranium exploration. Since 2007, based on studies on hydrothermal uranium ore formation mechanism and ground surface characteristics in uranium ore field, seismic work group of BRIUG has carried out a lot of systemic tentative work on excitation type of seismic source, layout of geophones, data analysis and processing techniques, and has obtained obvious success in detection of ore-control factors, such as basement or faults with high angle of inclination.

## 2. Methodology and advantages

### 2.1. Methodology

In general, the geologic environment of hydrothermal ore field are much more complex involving different approach than the conventional seismic survey used in oil and coal prospecting field. The surface conditions are complicated, dip angle of detecting target is large and the marker bed is not

evident, and all of those have brought great difficulties to the application of reflection seismic survey in hydrothermal uranium exploration. However, as the angle between ground surface and the fault is usually small, reflected wave of the fault could be directly received in a specific direction. The geological model for detection is shown in Fig. 1. Owing to the limitation of hillslope length, practical working modes adopted are: 1) Receiving terminal: geophones are of concentrated spread (Fig. 2), so that signal to noise ratio is higher; 2) Measurement mode: point measurement along the measuring line is adopted instead of CDP profile survey. By special processing of the acquired data extensions of the faults could be inferred.



1-middle coarse grained porphyritic two-mica granite 2-silicified zone 3-chalcedony vein  
 4-fissure zone 5-hematitization 6-sericitization 7-kaolinization 8-chloritization  
 9-fractured zone 10-gallery and its number 11-trench and its number 12-number of  
 profile 13-grade of ore body (or mineralized)(%)/thickness(m) 14-orebody (or mineralized)  
 and its number

FIG. 1. Geological model of unconventional seismic survey method.



FIG. 2. Concentrated spread of geophones.

## **2.2. Advantages**

Advantages of this method are:

### **(1) Strong adaptability**

Application preconditions for seismic survey are lowered, and application range of seismic survey is expanded. Fault detection could be performed in the area where the environment could hardly meet the demands of application preconditions for conventional seismic survey.

### **(2) Strong pertinence**

Usually, field construction of seismic survey method aimed at detecting faults is carried out according to common depth point stack (CDP) technique along the measuring line. After corresponding data processing, it can tell whether or not there is a fault through events comparison.

### **(3) High efficiency**

In this method, point-by-point moving technique of CDP method is not used and point measurement is adopted instead of profile survey, which could reduce workload and improve detection efficiency.

### **(4) High signal-to-noise ratio**

Twenty four or more times stacking could be realized by making the geophones in form of concentrated spread, which is hard to be achieved through CDP method in a small site.

## **3. Field methodology and results**

### **3.1. Field methodology**

An experimental case study has been carried out on the known fault No.7 in a hydrothermal uranium ore field in south China (Fig. 3). Eight measuring points are located between P1 and P2. Space between two points is 10 meters and explosive mass is 1 050 grams each time. Other acquisition parameters are listed as follows:

- Receiving channel: 24
- Offset: 20m
- Sampling interval: 0.5ms
- Record length: 1s

### **3.2. Results**

As shown in the upside of Fig.3., time section could be plotted after format conversion, filtering and stacking processing. Obvious reflection events appear between 213 ms and 238 ms, and depths calculated are 502 meters (distance from P2 to the reflection surface) and 560 meters (distance from P1 to the reflection surface) respectively. Actual distances (which are calculated based on the geological profile provided by No. 261 Geological Brigade of Nuclear Industry) are as follows: about 556 meters from P2 to the reflection surface and its detecting error is 10.8%; about 634 meters from P1 to the reflection surface and its detecting error is 13.3%.

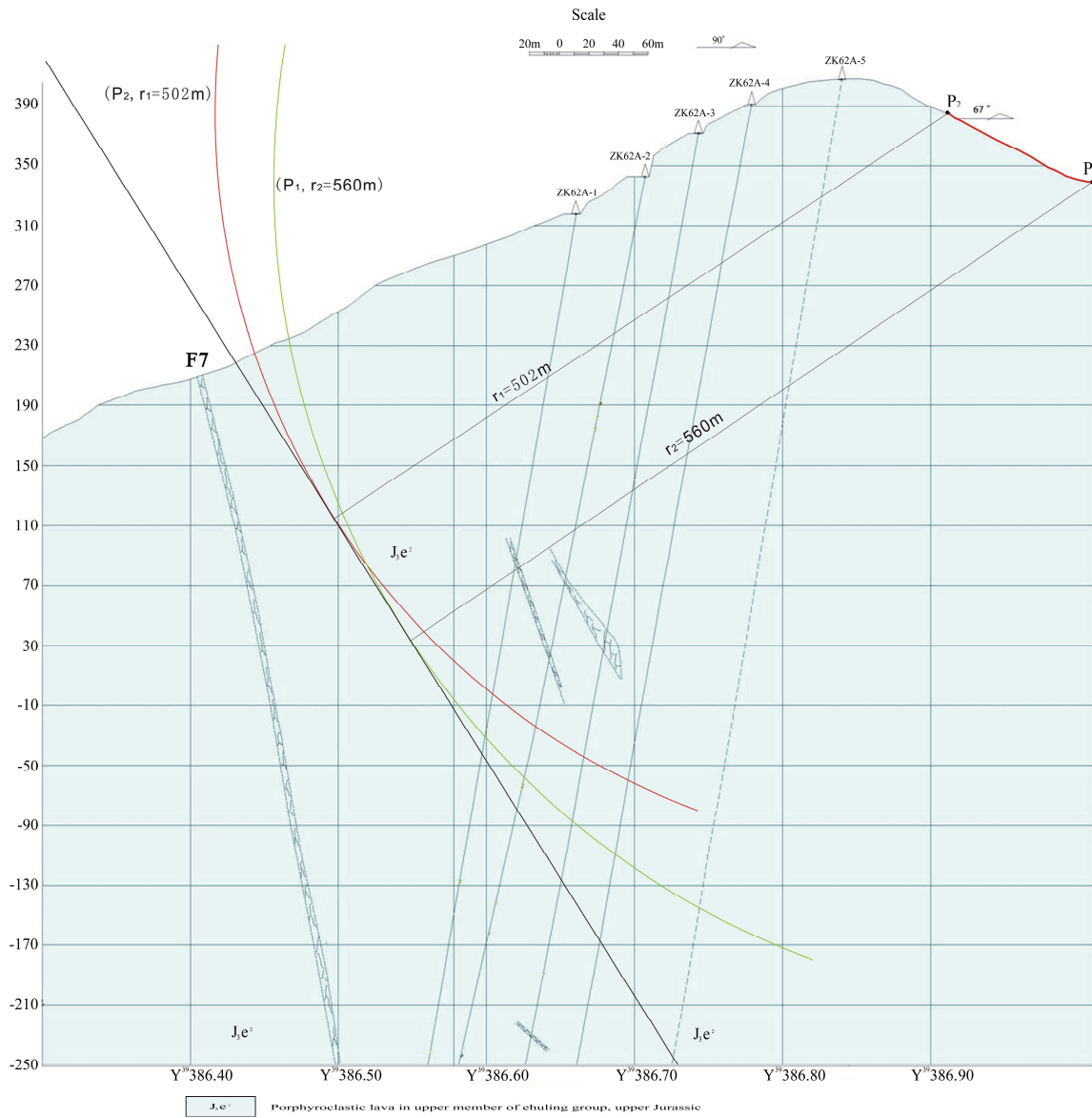
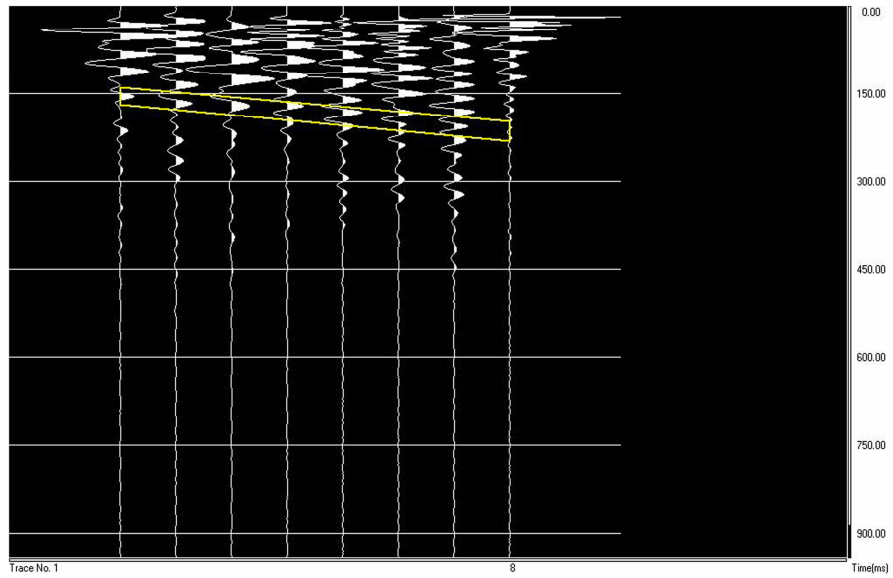


FIG. 3. Experimental result of unconventional seismic survey.

#### **4. Conclusions**

Based on the research result, it is thought that the newly developed seismic survey technique could be applied to detect faults in mountain areas. This technique can provide important evidences for uranium resources evaluation in hydrothermal uranium ore field by further improving the methodology. The details are:

- (1) The detection result of a known fault by seismic survey technique indicates that not only reflected wave of the fault surface could be received, but also the error of vertical depth detected is less than 15%, and that will provide important information for geological evaluation of the work area.
- (2) Concentrated spread of geophones makes it possible to realize multiple stacking in the work area of smaller range, and the signal-to-noise ratio is increased effectively, so detectability of this technique is improved.
- (3) Valuable results could be obtained by improving data acquisition, data analysis and geological interpretation abilities of this technique.

# **Application of multi-source remote sensing information in uranium exploration**

**Y. Zhao, D. Liu, D. Lu**

Beijing Research Institute of Uranium Geology, Beijing, China

**Abstract.** Uranium exploration needs new technology. Remote sensing technology are now being developed rapidly, including multi-spectral imaging, hyper-spectral imaging, radar etc., and as more and more information can be extracted from the images, they provide important means for uranium exploration. In this study, a new technology, optical-energy integration was developed, and the advantages of optical satellite remote sensing information and radioactivity energy spectrum are utilized. Characteristics of lithology can be classified very well with the above technique

## **1. Introduction**

Commercial satellite technical capabilities presently include better spatial resolution, spectrum resolution and time resolution which are important in various applications. Currently, these capabilities are being developed very quickly in terms of higher spatial resolution, narrower spectrum bandwidth and shorter periods. In uranium exploration, the nature of spatial and spectrum resolution are more important, because it gives information of lithology, structure and alterations [1][2].

As the information received by the satellite sensors is surficial, water and vegetation can be recognized easily. Structures and terrains can also be identified. In many areas, because of the influence of vegetation, no distinct differences in the colour and texture of various rocks are visible. Therefore it is difficult to identify the lithology, though many processing routines for vegetation removal have been adopted. It is well known that the energy spectrum data can reflect the energy spectrum information of the rocks covered by vegetation, based on the content of U, Th and K in the rocks. So it is feasible to identify the lithology by using the energy spectrum. Good results have been achieved in the Lucong basin, Erdos basin and Lingquan basin in identification of different types of rocks by the colour on the composite images of U, Th, and K and the cluster images, but it was difficult to determine the contact between different formations.

## **2. Geological setting**

The Lucong basin of Anhui Province is located in the fault depression zone in the middle and lower reaches of the Yangtze River and is covered by thick vegetation, where the main strata are the Jurassic and the Cretaceous. The Middle Jurassic consists of sandstone of the Luoling Formation, which is distributed around the rim of the basin. The Upper Jurassic and the Lower Cretaceous are composed of volcanic rocks and intrusive rocks, and can be divided into four cycles, Longmenyuan, Zhuanqiao, Shuangmiao and Fushan, which consist of a suite of the mugearite system [3][4][5][6].

The Lingquan basin in Manzhouli, another study area, is located southeast of Manzhouli from Jalai Nur to Taodaojing. Volcanic rocks of the Jurassic and the Cretaceous are the main rock types in the basin. The Jurassic consists of lava and pyroclastic rocks, and can be divided into the Tamulangou and Shangkuli formations. The Cretaceous is composed of the Damoguaihe Formation, which is formed by conglomerate and sandstone. The basin is covered by thick vegetation.

### 3. Lithologic identification by the visible light-energy spectrum fusion technique

Visible light and energy spectrum are both characteristic information of the rocks, so there must be some intrinsic relation between them. This paper first discusses the relation between the light spectrum and the energy spectrum. The relations between the light and the energy spectrum data can be clearly seen from the tables, which indicates that they are indeed correlative. Factor analysis was used to reduce the number of variables to a few significant non-correlated factors, which can explain the total variation in the observation set. A new image, the light-energy image, was generated after the light spectrum and energy spectrum data were processed by the factor analysis, and histogram equalization applied on the composite image with three principal factors. This new image contains not only the light spectrum information but also the energy spectrum information. Different formations are shown in different colours and textures, so that the boundary lines between various formations can be interpreted. Besides, in the Lucong basin, the boundary between the Huangmeijian quartz syenite rock body and the volcanic rock can be clearly defined and the structures can be interpreted. In the Lingquan basin, with the same technique, different types of rocks were also identified. At the same time, Jurassic lava was found on the Yujishan beschtuite rock body, which was not marked in the original geological map. Field investigation has proven the results of interpretation by using the light-energy spectrum fusion technique are accurate. The fusion technique contains both the light and the energy spectrum information, and it is proven by its applications in the Lucong and Lingquan basins that different types of rocks can be identified, and therefore is a good method in uranium investigations.

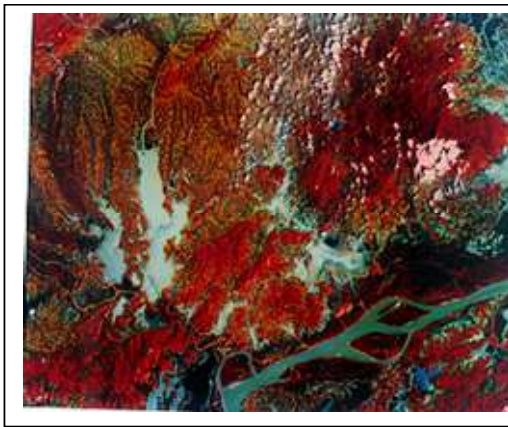


FIG. 1. Landsat TM image of Lucong region (R: band5; G:band3; B:band1).

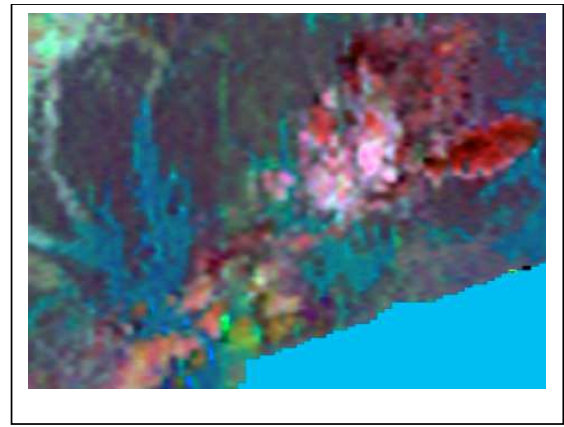


FIG. 2. Airborne radioactivity image of Lucong region (R: K; G: K/U; B: K/Th).

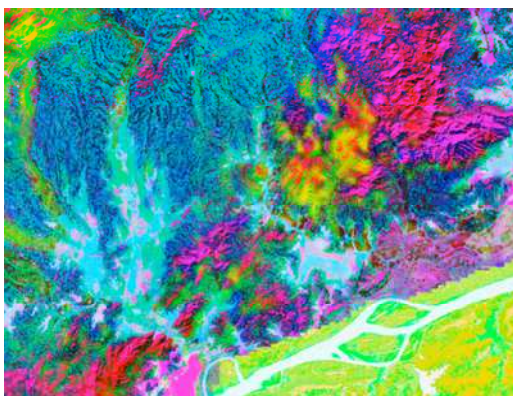


FIG. 3. Light-energy fusion image of Lucong region.



FIG. 4. Light-energy fusion image of Lingquan region.

#### 4. Techniques in multi-source remote sensing in uranium exploration

Multi-spectral data are collected in several bands with low spatial resolution and large coverage, eg., Landsat, SPOT, ASTER. Multi-spectral data can be used to interpret structure [7].

Hyper-spectral remote sensing represent the important future trend. It can analyze components of surficial matter and classify it in detail. Hyperspectral imaging can be used in mineral mapping based on characteristic spectrum of rock or strata. Examples of commercial hyper-spectral sensors are MODIS and Hyperion. It is believed that hyper-spectral remote sensing will play a very important role in uranium exploration.

Compared with optical remote sensing, SAR can collect data in all-weather and day and night. But, SAR image is more difficult to process and visually interpret because of noise. Radar signals can penetrate through top layers in arid areas, and hidden fault can be revealed. In Zhungeer basin of Xinjiang, TM image and JERS radar image are fused using HIS transform, and the hidden fault identified (Fig. 5).

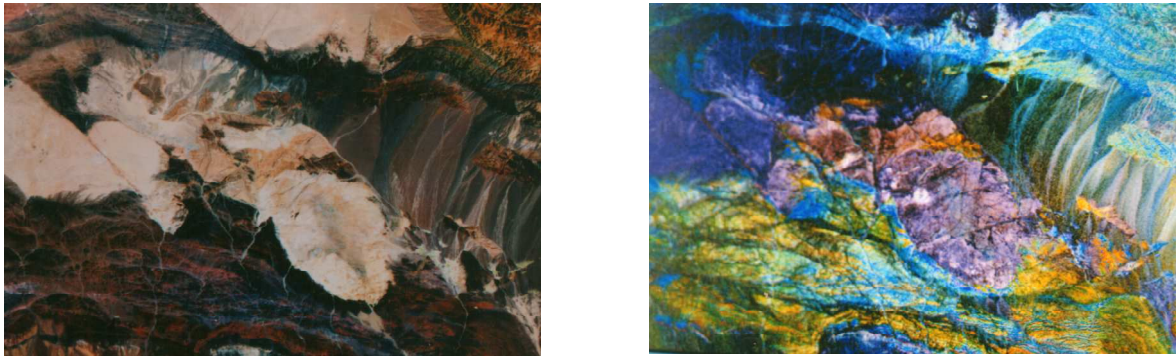


*FIG. 5. Landsat TM image of Zhungeer in Xinjiang (Left).  
Fusion image of TM and JERS radar image (Right).*

The application of remote sensing in uranium exploration must also be combined other geo-data, such as geo-map, DEM, airborne magnetic data and these data or information can be managed by GIS tools (Fig. 6).

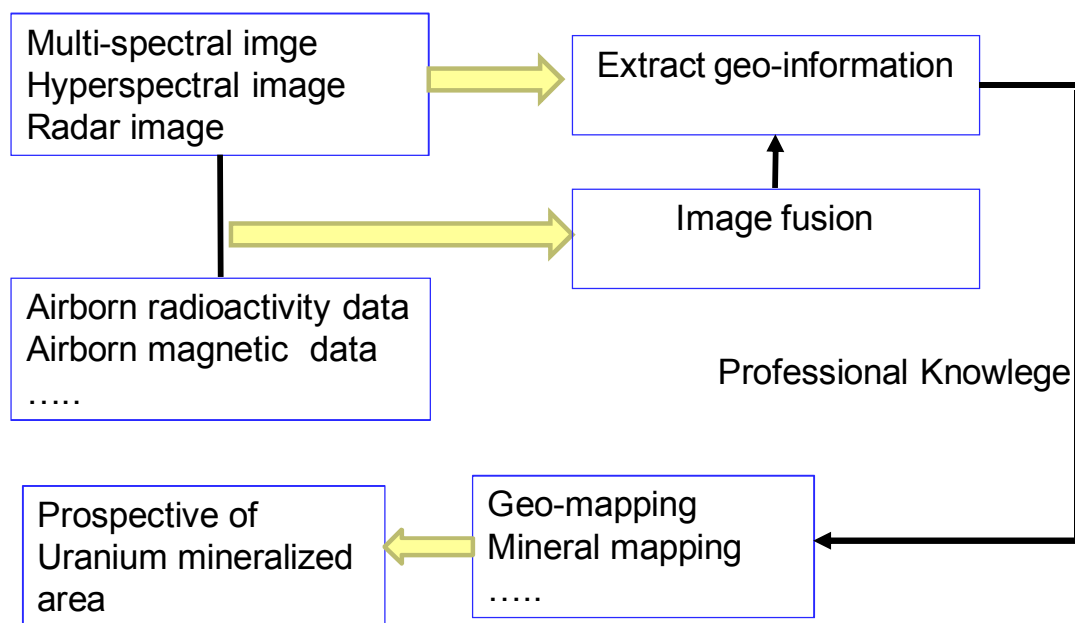


FIG. 6. Technique of multi-source remote sensing image in uranium exploration.

## 5. Conclusion

The paper discussed techniques to recognize lithology through multi-source remote sensing data, such as multi-spectral image and airborne radioactivity data. A new image is generated by fusion of two kinds of data and good results are obtained.

The advantages of three kinds of remote sensing image are also summarized. The techniques of using multi-source remote sensing image in uranium exploration is put forward.

## REFERENCES

- [1] FENG, M., et al., The application of light-energy spectrum fusion technique in charting geological map of Lingquan basin. Beijing: Research Institute of Uranium Geology (1997) 88.
- [2] LIU, D., et al., Integration Technique of Multi-source Information Dominated by Aerial Radiometric Measurement and Its Application. Science in China (series B) (3) (1994) 659-664.
- [3] REN, Q., et al., The formation and evolution of the Lujiang-Zongyang volcanic-structural depression in Anhui and its relation to mineralization. Acta Geologica Sinica (Eng. ed.), 6(4) (1993) 411-428.
- [4] YANG, R., REN, Q., XU, Z., XU, L., The Bajiatan volcanic dome in the Mesozoic volcanic terrain of the Lujiang-Zhongyang area, Anhui Province. Geological Review 42(2) (1996) 136-143 (in Chinese with English abstract).
- [5] ZHAI, J., XU, G., ZHANG, B., HU, K., Comagmatic Characteristics of the Luzhong Volcanic Rocks and Subalkaline Quartz Syenite Rock-Belt and Their Genesis. Geological Review 45 (Sup.) (1999) 707-711 (in Chinese with English abstract).
- [6] ZHAO, D., XIAO, Z., WANG, Y., Petrological Characteristics and Genesis of the Cenozoic Volcanic Rocks in Tancheng-Lujiang Fault Belt and the Adjacent Areas. Acta Geologica Sinica, 57(2) (1983) 128-141 (in Chinese with English abstract).
- [7] ZHAO, Y., The application of multi-source information fusion technique in the analysis and forecast of minerogenetic environment. Master's thesis at the Beijing Research Institute of Uranium Geology (1995) 44.

# Uranium mineralization in late Cretaceous sandstones in parts of Meghalaya, India

P.S. Parihar<sup>a</sup>, R. Mohanty<sup>b</sup>, A. Majumdar<sup>c</sup>

<sup>a</sup> Atomic Minerals Directorate for Exploration and Research, Hyderabad, India

<sup>b</sup> Atomic Minerals Directorate for Exploration and Research, Shillong, India

<sup>c</sup> Atomic Minerals Directorate for Exploration and Research, Nagpur, India

E-mail address of main author: addldir-op2.amd@gov.in

**Abstract.** Late Cretaceous Lower Mahadek sandstone of Meghalaya has been established as the potential host rock for sandstone type of uranium mineralisation in India. To date, nearly 16 000 tonnes of U<sub>3</sub>O<sub>8</sub> reserves have been estimated in four locations viz., Domiasiat, Wahkyn, Tyrnai and Lostoin, in the southern part of Meghalaya plateau. The uranium investigations are primarily confined to the areas where the Lower Mahadek sandstones are exposed either on the surface or along deep river cuttings, otherwise concealed by thick cover of Tertiary sediments. The area poses major logistical challenges due to thick forest and remoteness. Out of nearly 1 800 km<sup>2</sup> of extent of the Mahadek Basin, only 28% of the area exposes Lower Mahadek sediments. The discovery of uranium mineralization so far achieved, is confined to the exposed area. Survey in recent years has also established a few more occurrences at Umthongkut, Wahkut and Rongcheng Plateau in Balphakram area. These occurrences exhibit very strong uranium mineralization on the surface and are technically ripe for exploratory drilling. Large scale exploratory drilling is planned in these areas, which may substantially add to the uranium resources of the region. Systematic study of available surface and subsurface data has revealed that mineralization is controlled by palaeo channel configuration of Mahadek sediments and also the typical geochemical interface. Regional and local tectonics also have played an important role in distribution and concentration of uranium mineralisation in the area. It is observed that the deposits and the very promising occurrences described above fall strikingly along an E-W lineament. Litho-structural studies indicate that the southern block appears to have gone upwards relative to the northern block in contrast to other such signatures in the area. This might have influenced ground hydrodynamic flow pattern and helped in concentration of uranium. The Lower Mahadek sandstones, host rock of these deposits are mostly sub-arkosic to arkosic, grading sometimes to felspathic arenite. The main uranium minerals are pitchblende, coffinite and organo-uranyl complex. Uranium mineralization is associated with bituminous organic matter occurring as dense inclusions, isolated clusters and lumps of various sizes and as clayey – dusty organic matter associated with cementing material. The work so far has been confined to the shallower part of the basin (28% of the total area). There is no reason not to believe that many more concealed deposits in the remaining 72% of unexposed Lower Mahadek sediments may be present. Multidisciplinary investigations have been initiated to locate such concealed occurrences. Geophysical investigations, mainly magnetic survey is in progress in some identified blocks in the area between Wahkyn and Umthongkut which are otherwise covered by 300-400 m thick Tertiary sediments. Such surveys would help in delineating magnetic lows which indirectly points to the presence of buried palaeochannel. Integrated Remote Sensing studies using high resolution satellite data of IRS LISS-III and LISS-IV are being undertaken to delineate broad lithological and structural patterns between Umthongkut and Wahkyn. The role of neo-tectonics in disposition of Lower Mahadek sandstone is being evaluated prior to taking up deeper subsurface exploration. Thus, the Lower Mahadek sandstones covered by thick Tertiary sediments in the larger part of the Mahadek basin are being probed by indirect techniques in order to discover more sandstone type of uranium deposits in Meghalaya.

# 1. Introduction

Mahadek basin of Meghalaya plateau in northeastern India is identified as a ‘Uranium Province’ [1] wherein, two sizeable deposits of economic grade (Domiasiat and Wahkyn) and four satellite deposits (Gomaghat, Tyrnai and Philandiloin and Lostoin) have already been established. The Mahadek sediments are exposed along the southern fringe of Meghalaya Plateau over a 180 km length stretch from Lumshong of Jaintia Hills in the east to Balphakram of South Garo Hills in the west with an average width of 10 km (see Fig. 1). The Mahadek Basin covers about 1 800 sq km (8%) area of Meghalaya state and out of this, about 500 sq km (28%) area exposes Mahadek sediments, which have been largely explored. Uranium bearing Lower Mahadek sediments are considered to be predominantly fluvial, whereas the Upper Mahadek sediments are deposited under fluvial to marginal marine environment. Over the last four decades, nearly 250 uranium occurrences of varying dimension and grade hosted by the Lower Mahadek sandstone have been discovered (see Fig. 1).

Systematic multidisciplinary studies [2][3][4] have defined many fundamental aspects on geology, sedimentology and uranium exploration in the Mahadek formation such as (i) recognition of fluvial component of the Mahadeks, (ii) its division into two members Lower and Upper Mahadeks (reduced and oxidized facies respectively) and (iii) characterization of ore grade mineralization and its geomorphic expression, (iv) fertile nature of the provenance and (v) role of organic matter.

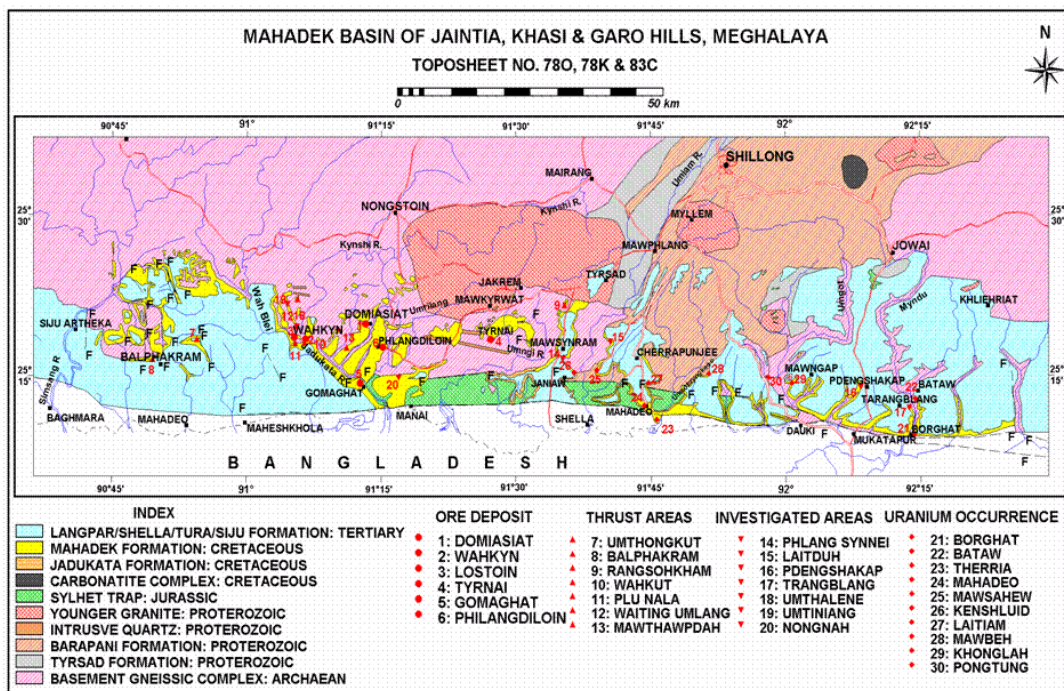


FIG. 1. Regional geology of Meghalaya.

This paper describe the potential of uranium mineralisation in the Mahadek Formation of Meghalaya and the multidisciplinary exploration strategy to identify exploration targets in the areas covered by thick Tertiary sediments in the light of the experience gained over the past four decades.

# 2. Geology

Meghalaya Plateau is considered to be an uplifted horst-like feature bounded by major tectonic features like Brahmaputra lineament in the north, Dauki fault in south, Haflong Fault in the east and Rajmahal-Garo gap in the west. The plateau is considered to be the northeasterly extension of the Indian Peninsula and comprise Archaean gneisses/schist and Palaeo- to Meso-Proterozoic Shillong Group of rocks with intrusive Neo-Proterozoic granite plutons [5]. Prominant granitic plutons are

South Khasi Batholith (690±19 Ma), Myllem (607±13 Ma), Nongpoh (550±15 Ma) and Kyrдем (479±26 Ma) granites [6]. Uplift of the Meghalaya Plateau commenced in Late Jurassic period, associated with extrusive Sylhet traps which culminated during the Cretaceous period. Granite and granite gneisses are the dominant rock types in the basement with high intrinsic uranium content of 8 to 59 ppm and form the fertile provenance for Mahadek sediments.

A generalized stratigraphic succession modified after Geological Survey of India 1974 [5] is given in Table 1.

Table 1. General stratigraphic succession

Era/Period	Group	Formation	Member/Beds
Miocene	Garo	Chengapara 700m	Sandstone, siltstone, clay and marl
Oligocene		Baghmara 530m	Feldspathic sandstone, conglomerate and clay
Eocene	Jaintia	Kopili-Rewak 500m	Shale, sandstone and marl
Palaeocene		Shella 600m	Alternations of sandstone and limestone
		Langpar 50-100m	Calcareous shale, sandstone and impure limestone
Cretaceous	Khasi	Mahadek 215m	Upper: purple, coarse to fine arkosic purple sandstone and shale (Ca. 190m) Lower: grey, coarse to medium grained feldspathic sandstone, arkose (25 - 60m)
		Jadukata 235m	Sandstone - conglomerate alternations
~~~~~Unconformity~~~~~			
Jurassic	Sylhet	Sylhet Trap	Basalt, alkali-basalt and acid tuff, alkaline rocks and carbonatite complexes
~~~~~Unconformity~~~~~			
Neoproterozoic	Intrusive Granites	Kyrдем Granite	Coarse porphyritic granite, pegmatite, aplite and quartz vein. Epidiorite and dolerite.
		Nongpoh Granite	
		Myllem Granite	
Palaeo-Mesoproterozoic	Shillong	South Khasi Batholith	Quartz arenite, arenite and quartzite
		Barapani (Arenaceous)	
		~~~~~Sheared/Stretched Conglomerate~~~~~	
		Tyrsad (Argillaceous)	Phyllite, quartzite, mica schist
~~~~~Unconformity~~~~~			
Archaean	Granite gneiss, migmatite, mica schist, sillimanite quartz schist and granulite		

### 3. Uranium mineralization

The Mahadek Formation is divided into two members. The Lower Mahadek member consisting of medium to coarse grained, grayish-green to dark gray, immature feldspathic sandstone with abundant carbonaceous matter and pyrite and tuffaceous matter [7] having average thickness of 20 to 60m. The lithologic units are deposited in a fluvial environment and occur as channel fill, cross-bedded, unsorted grayish feldspathic arenite to quartz arenites, predominantly composed of clast and a little matrix (<10%) with cement and clays in varying proportion. Quartz is predominant component followed by minor feldspar, rock fragments, garnet and accessories like zircon, monazite, rutile, sphene and opaques (oxides and sulphides). It also contains varying proportion of organic matter. Pyrite is of both biogenic framboidal and melnicovite type. The main uranium mineral is pitchblende and minor phases include coffinite, uraninite, brannerite, U-Si-C, which occur as clusters, blebs and botryoidal forms intimately associated with migratory coaly matter (0.5 to 5%) and biogenic pyrite (0.5 to 1%). Repeated remobilization and deposition processes resulted in the formation of rich grade uranium deposit at Domiasiat [8]. The carbon isotopic values ( $\delta^{13}\text{C}$ ) falling between -17.1 to -23.4 ‰ (relative to PDB standard) indicate abundance of algal plant material [9]. Host rock and mineralization characteristics of the six uranium deposits established so far in this province are listed in Table 2.

Table 2. Characteristics of U deposits in Mahadek basin, Meghalaya

Parameters	Domiasiat	Wahkyn	Gomaghat	Tyrnai	Phlangdiloin	Lostoin
Host Rock	Feldspathic quartz arenites & Arkosic sediments	Arkosic to subarkosic Sandstone	Feldspathic wacke	Medium to coarse grained sandstone	Feldspathic sandstone	Arkosic to subarkosic Sandstone
Nature of orebody (see Fig.2)	Tabular/Pene- concordant	Tabular/Pene- concordant	Tabular/Pene- concordant	Tabular/Pene- concordant	Tabular/Pene- concordant	Tabular/Pene- concordant
Dimension (m)	1700 x 200	1300 x 1000	1300 x 900	1000 x 500	2000 x 500	1200 x 400
Mineralogy	Pitchblende, Coffinite	Pitchblende, Uraninite, coffinite, U+Ti+Si Complex	Uraninite, Coffinite, Autunite, Torbernite, Pyrochlore	Pitchblende, Zircon, Sphene, Limonite, Monazite	Pitchblende, coffinite, organo-uranium compound, zircon and monazite	Pitchblende, coffinite, U+Ti+Si Complex
Associated elements	V, As, Co, Mo, Se(Tr.)	V, Co, As, Se, Mo	V, Cu, Pb, Se, Mo		Cu, V, Mo, Cr, Ga, Ti, Zr, Th	V, Co, As, Se, Mo
Grade %eU <sub>3</sub> O <sub>8</sub>	0.104	0.101	0.048–0.036	0.102	0.101	0.064
Thickness (m)	4.07	3.41	1.41 – 2.03	1.53	1.8	1.5
Uranium Reserves	Medium tonnage	Medium tonnage	Low tonnage	Low tonnage	Low tonnage	Low tonnage
Disequili-brium	15% towards U	32-44 % towards U	20% towards U	--	--	--
Leachability	92-96%	80 – 87 %	N.D	N.D	N.D	N.D.
Organic matter	0.5-<1%	<1 to 5%	N.D	N.D	N.D	N.D.

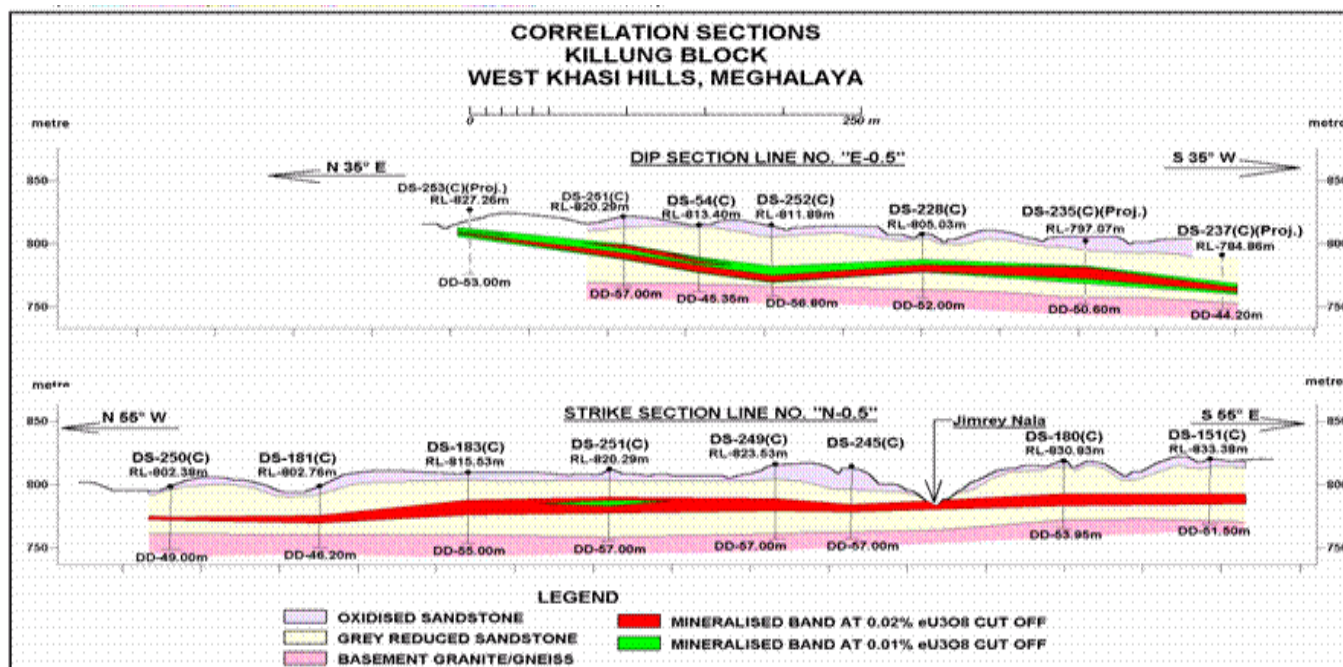


FIG.2. Correlation sections, Killung Block.

#### 4. Umthongkut – Balphakram – The emerging prospect

The recent discovery of uranium mineralisation in the Lower Mahadek member at Umthongkut in the West Khasi Hills district and Balphakram in the South Garo Hills district [10][11] (see Fig. 3) has opened up vast areas for uranium exploration in the western part of the Mahadek Basin. Significant uranium mineralisation was recorded in Umthongkut sector over a dimension of 1 500 x 300 m x 1-15 m [11]. Sixteen radioactive occurrences were found exposed along the escarpment/nala sections to the west of Umthongkut village. Pitchblende and coffinite were identified as major radioactive minerals.

The potential area between Wahkyn South and Umthongkut has been taken up for multidisciplinary and subsurface exploration. Recently, integrated geophysical investigations and remote sensing studies were initiated on a wider scale between Wahkyn and Umthongkut area which are otherwise covered by 300-400 m thick Tertiary sediments. The studies have indicated the significant role that tectonics have played in uplift/downthrow of lithological units and redistribution of associated uranium mineralization. These areas are under active exploration to augment the uranium resources of the Mahadek Basin.

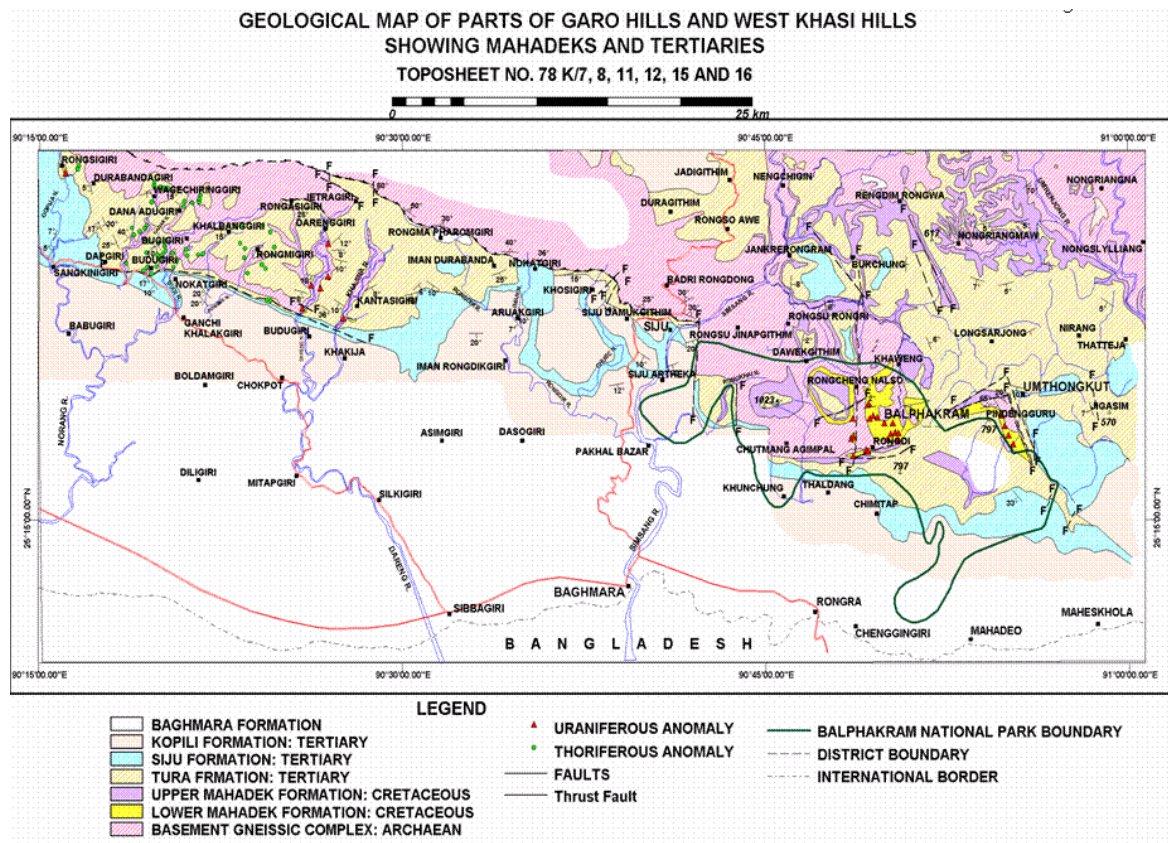


FIG. 2. Geological map Umthongkut and Balphakram areas.

#### 5. Ore geometry and genesis

The general geometry of ore bodies in the Mahadek Basin is tabular/peneconcordant. The depth to the ore bodies varies generally between 30 to 50 m, occasionally up to 212 m. Medium to large lenticular bodies, disposed in en-echelon pattern are normally intercepted but at some places ore bands are persistent over 500 to 1 000 m. The ore zone thickness varies from 1.50 to 5m. Lower Mahadek member hosts most of the uranium deposits/occurrences, where uranium mineralisation is intimately associated with reductants, such as organic matter and pyrite. However, at Gomaghat redox interface

has played an important role in concentration of uranium in fluvial to marginal marine sediments of distal facies.

Bulk of uranium is introduced into the basin from extrinsic sources. South Khasi Batholith, Myllem granite and migmatite containing anomalous uranium content of 7–110 ppm are noted in the provenance which supplied uranium rich detritus to the Mahadek Basin. Continued subsidence of the basin pari-passu with sedimentation ensured speedy burial of the sediments which arrested the oxidative decomposition of the organic matter and facilitated conversion of the vegetal matter into coaly/carbonaceous substances and formation of diagenetic pyrite thus creating reducing environment for later uranium precipitation from solutions. It is also believed that oxygenated acidic ground water leached labile uranium from the overlying sediments that percolated down along hydraulic gradient encountering reducing environments. Continued upliftment of Meghalaya plateau may also have provided oxygenated ground water causing further remobilization and precipitation as per the multiple migration accretion hypothesis of Gruner. Uranium ore genesis in Mahadek Basin can be summarized as i) uranium is derived from the fertile basement provenance mostly from granitic and migmatitic terrain with minor basic components; ii) uranium is transported from the source to the depositional locales by circulating mildly acidic ground water through permeable horizons of Lower Mahadek sediments; iii) uranium in the mineralised solution is reduced by the organic matter or by adsorption mechanism; iv) high concentration of uranium up to the ore grade levels is formed due to multiple migration and accretion and deposited in suitable locales along paleochannels having favourable conditions, as discussed above.

## **6. Geophysical studies**

Ground geophysical surveys, mainly magnetic and resistivity soundings were initiated over an area of about 20 km length between Wahkyn and Umthongkut. The area was taken up on the basis of the results of the drilling data at Wahkyn uranium deposit in the east and discovery of significant uranium occurrences at Umthongkut in the west. In the Wahkyn area it has also been established that the palaeo-channels trending NW-SE and NE-SW controlled the uranium mineralisation. The faults/fractures in the basement granite-gneisses might have also been transformed into channels in which greater thickness of Lower Mahadek sediments is expected and greater porosity and permeability along these palaeo-channels may act as loci for mineralizing solutions. Hence locating major structural features within the basement and depth of the basement are the targets for geophysical surveys in the area [12].

The magnetic anomaly map of a part of the area indicated the well developed E-W trending low with associated high which is interpreted as a signature of the Chira fault, a major lineament along which lie most of the significant uranium occurrences in the Mahadek Basin. The change in the trend of the contour pattern within this magnetic low (NE of Pormawdher) might be due to the combined effect of the E-W trending Chira fault and NW-SE trending Porjri lineament. A magnetic low in NE of Kulang corresponding to another magnetic high at Pakut (Nongjri) is also established.

## **7. Exploration strategy and challenges**

In the western part of the Mahadek basin the Lower Mahadek member, the host for uranium mineralization, is by and large concealed below the Tertiary sediments of 300-400 m thickness and poses challenges for the survey and exploratory drilling programme in the basin.

The paleo-channels and the basement lows which have been established as the receptacles of better grade mineralization are also difficult to locate under the thick Tertiary cover sediments. Therefore, integrated ground geophysical and remote sensing studies are being used to identify targets for exploration in these areas. Vast inputs of heliborne geophysical surveys, including Time Domain Electro Magnetic, Gamma Ray Spectrometric and Magnetic methods are to be deployed in this basin. Airborne and ground based geophysical surveys are expected to generate huge volume of data for delineation of favourable areas for mineralization. Poor communication and infrastructure facilities coupled with adverse public opinion with respect to uranium exploration are other challenges. The

host Mahadek Formation exposes only along the steep escarpments and stream sections. The sedimentological studies such as, lithofacies mapping, size analysis and heavy minerals studies can only be practiced in a limited area for identification of the target areas.

## 8. Conclusions

Uranium exploration in Mahadek basin of Meghalaya Plateau has continued over the last four decades. Sustained efforts have resulted in identifying favourable target horizons hosting sandstone type uranium mineralisation. The discovery of uranium deposits at Domiasiat and Wahkyn, besides four smaller satellite deposits have established Mahadek Basin as a Uranium Province for sandstone type deposits in India. The deposits are well understood and controls have been well defined. The uranium mineralisation in Mahadek sediments is controlled by several factors like fluvial character and proximal facies of sediments, mode of occurrence of organic matter, nature of source rocks and basement topography and these parameters have greatly helped in mobilization and fixation of uranium. The favourability factors present in Lower Mahadek Formations point towards the likely addition of more medium size and medium-grade sandstone type deposits in these sediments. There are prime target areas at Umthongkut, Balphakram and between Wahkyn and Umthongkut where large scale drilling is contemplated to prove additional uranium resources. Multidisciplinary integrated studies are being utilised in this geologically favourable terrain, covered by Tertiary sediments, to demarcate sites for subsurface exploration.

## ACKNOWLEDGEMENTS

The authors are highly indebted to Dr. Anjan Chaki, Director, AMD for permission to publish this paper.

## REFERENCES

- [1] SINGH, RAJENDRA., Status Report on uranium exploration in Mahadek Formation of Meghalaya for field workshop. Unpublished Report of NER, AMD, Hyderabad, India (1986).
- [2] KAK, S.N., SUBRAMANIAM, A.V., "Depositional Environment and Age of Mahadek Formation of Wahblei River Section, West Khasi Hills, Meghalaya", Jour. Geol. Soc. India 60 (2002) 151-162.
- [3] D'CRUZ, E., et al., "Depositional system and their bearing on the ore-grade uranium mineralization in the Cretaceous Domiasiat uranium deposit, West Khasi Hills district, Meghalaya", Geol. Soc. India. Memoir 37 (1996) 387-403.
- [4] MAMALLAN, R., et al., "Effective utilization of geomorphology in uranium exploration : A success story from Meghalaya, Northeast India", Curr. Sci.68, No.11, (1995) 137-1140.
- [5] GEOLOGICAL SURVEY OF INDIA "Geology and Mineral Resources of India", Miscillaneous Publication of Geological Survey of India 30 (1974) 77.
- [6] GHOSH, S., et al., "Geochronology and geochemistry of granite plutons from East Khasi Hills, Meghalaya", Jour. Geol. Soc. India 37 (1991) 331-342.
- [7] SUBRAMANIAM, A.V., et al., "Volcanic tuff in Lower Mahadek Formation of Meghalaya Plateau. Implications on uranium source", Journal of Atomic Mineral Science 5 (1997) 73-79.
- [8] SENGUPTA, B., et al., "Discovery of a sandstone type uranium deposit at Domiasiat, West Khasi Hills district, Meghalaya, India", Current Science 61 (1991) 46-47.
- [9] HAMILTON, S., et al., "Stable carbon isotope evidence for two sources of organic matter and its significance in uranium mineralisation at Domiasiat, West Khasi Hills district, Meghalaya", Int. Conf. on Isotopes in the Solar System, PRL, Ahmedabad (1997) 66-67.
- [10] YADAV, G.S., et al., Unpublished Report of AMD, NER, Shillong (2001).
- [11] SRIVASTAVA, S.K., et al., Unpublished Report of AMD, NER, Shillong (2006).
- [12] MOHANTY, R., Unpublished Report of AMD, NER, Shillong (2008).

# **Proterozoic unconformity related uranium mineralization in the Srisailam and Palnad Sub-Basins of Cuddapah Basin, Andhra Pradesh, India**

**U. Konka, K.K. Achar, P.B. Maithani**

Atomic Minerals Directorate for Exploration and Research / Department of Atomic Energy, Hyderabad, India

*Email-address of main author: kumamaheswar.amd@gov.in*

**Abstract.** The intracratonic, Mesoproterozoic Cuddapah basin has been identified as one of the promising targets for locating unconformity related uranium mineralization in India. Two sub-basins, namely, Srisailam and Palnad lie in the northern part of the basin, with arenaceous, argillaceous and calcareous sediments resting on basement granitoids of Archaean to Paleoproterozoic age, basic dykes of Paleoproterozoic age and greenstone belts of Archaean age. Exploration in northern parts of Srisailam sub-basin has established three small tonnage, medium grade uranium deposits at Lambapur, Peddagattu and Chitrial, Nalgonda district, Andhra Pradesh. Exploration efforts in the northwestern margin of Palnad sub-basin has resulted in locating a low-grade small tonnage uranium deposit at Koppunuru, Guntur district, Andhra Pradesh. Uranium mineralization in the Srisailam sub-basin is mainly confined to the fractured basement granites close to unconformity, with shallow depth persistence. These deposits occur as elongated pods proximal to the unconformity, with richer pockets at the intersection of N-S, NNE-SSW and NW-SE trending fractures. Pitchblende is the main uranium mineral identified which is closely associated with drusy quartz, galena, chalcopyrite and pyrite. Illitization and chloritization are the common alteration features observed. In the Koppunuru uranium deposit of Palnad sub-basin three distinct uranium mineralized bands, hosted by quartzite/shale, gritty- quartzite and altered basement granites have been delineated. Pitchblende and coffinite are the primary uranium phases associated with pyrite and carbonaceous matter. Mineralization occurs in the form of fine veins, fractures, cavities and grain boundary fillings. The southward continuity of the litho-structural setup associated with uranium deposits in both sub-basins along with favorable factors, such as the Paleoproterozoic fertile, fractured granitoid basement, Meso-Neoproterozoic cover rocks and repeated phases of tectonic activity, indicate the potentiality of both these sub-basins to host more such deposits. Airborne, ground geophysical and geochemical surveys are planned to locate concealed unconformity type of uranium deposits in the deeper parts of these sub-basins.

## **1. Introduction**

Unconformity related uranium deposits constitute the most promising large tonnage, high grade uranium resources of the world. These deposits typically occur as fracture/breccia fillings in Paleoproterozoic metapelites and arenaceous Mesoproterozoic cover sediments close to the unconformity [1][2][3]. Search for such deposits was initiated in several Proterozoic basins of India since 1990. Consequently, the Meso-Neoproterozoic Cuddapah basin in the eastern Dharwar Craton of peninsular India was identified as one of the promising targets for locating such deposits. Srisailam and Palnad sub-basins lie in the northern margin of Cuddapah basin, exposing the sediments of Meso-Neoproterozoic Cuddapah Supergroup and Neoproterozoic Kurnool Group respectively. Intensive uranium exploration in these sub-basins has resulted in identifying substantial uranium reserves in four deposits namely Lambapur, Peddagattu, Chitrial in Nalgonda district and Koppunuru in Guntur district. Subsurface exploration is still being carried out to establish additional uranium resources in the adjoining areas of these deposits and in the deeper parts of these sub-basins.

## 2. Geology and structure

### 2.1. Regional geological setting

The crescent shaped Cuddapah basin (Fig. 1), having an extent of 44 000 sq km, contains over 12 km thick sequence of sedimentary and volcanic rocks belonging to the Meso-Neoproterozoic Cuddapah Supergroup and Kurnool Group. The western margin of the basin is marked by a nonconformity, with the formations resting on Archean gneisses, narrow linear greenstone belts and granites of Paleoproterozoic age. The eastern margin of the basin is marked by a thrust contact, where the older Achaean gneisses / Dharwar metasedimentary rocks are thrust over rocks of the Cuddapah basin [4]. The Cuddapah Supergroup is predominantly arenaceous to argillaceous, with subordinate calcareous to dolomitic units; developed in Papaghnai, Nallamalai and Srisailam sub-basins, whereas, carbonate facies sediments are developed in Kurnool and Palnad sub-basins.

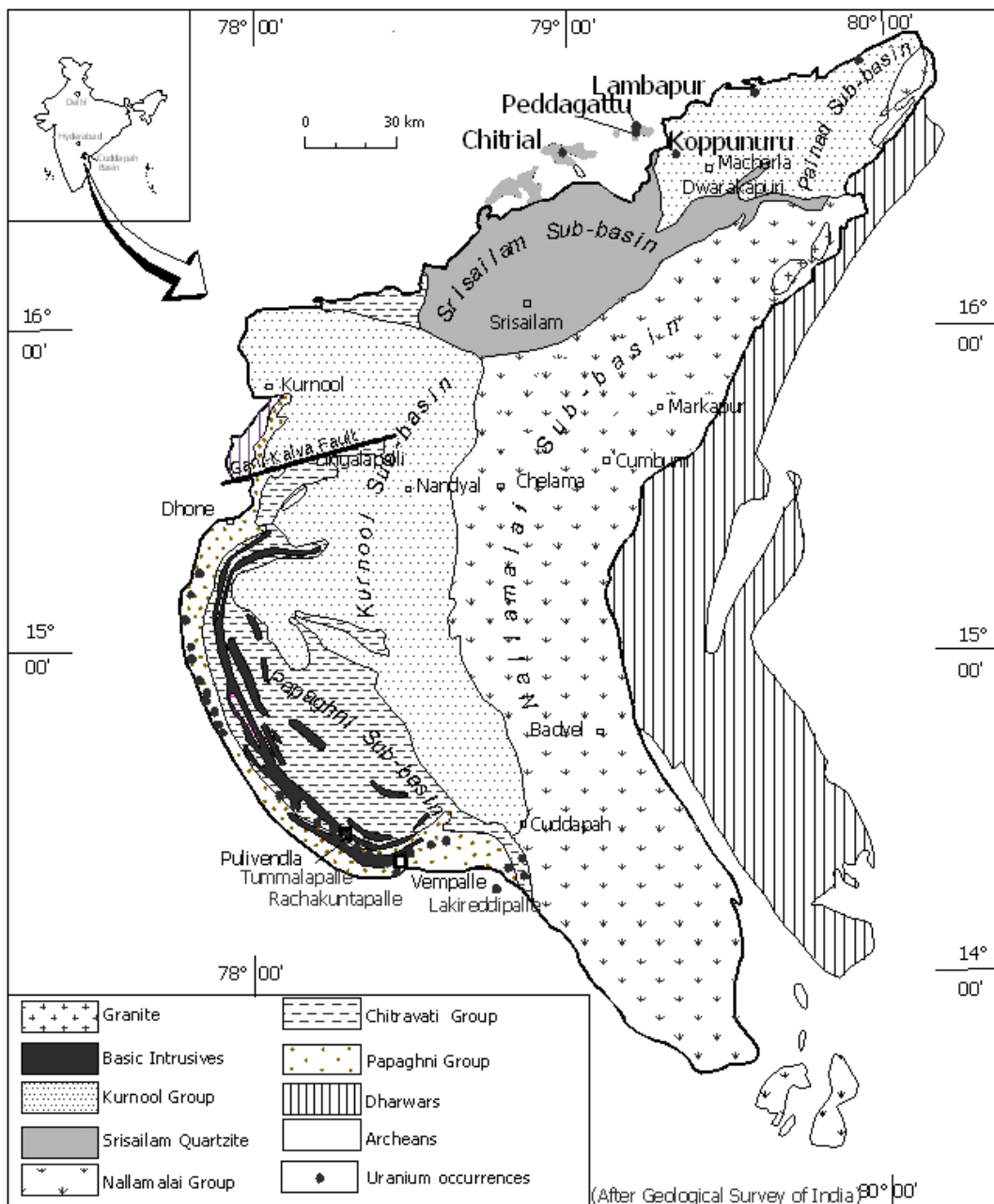


FIG. 1. Geological map of Cuddapah Basin, Andhra Pradesh.

In the northern margins of Cuddapah basin, the basement comprises Archean schist (Peddavoora Schist belt) and gneisses, Paleoproterozoic granite, basic dykes, pegmatites and quartz veins. Three generations of basic dykes are observed in the basement mostly trending N-S/NE-SSW, E-W/ ENE-WSW and NE-SW; which are also the trend of major fractures/faults. Major faults affecting the basement, as well as, overlying sediments generally trend NNE- SSW and ENE-WSW.

## 2.2. Srisailam sub-basin

Neoproterozoic Srisailam Formation, the youngest unit of Cuddapah Supergroup, developed in the Srisailam sub-basin forms a prominent plateau with an extent of around 3 000 sq km in the northern part of Cuddapah basin. It is mainly an arenaceous unit with subordinate shale intercalations. The sediments display sub-horizontal dips due southeast, and attains a maximum thickness of 300 m [4].

Along the northern margins, the sediments of Srisailam Formation directly overlie the basement rocks consisting of Archean gneisses and granites of Paleoproterozoic ( $2\,268\pm 32$  Ma to  $2\,482\pm 70$  Ma) age [5]. In the southeastern margin, the Srisailam Formation is underlain by Nallamalai Group metasediments with an angular unconformity (Fig. 2). In its northern fringes the Srisailam sub-basin has a highly dissected topography with several flat topped outliers occurring within the basement and rising 100 to 150 m above ground level. The Lambapur, Peddagattu and Chitrial uranium deposits are located in three such separate outliers detached from the main Srisailam sub-basin.

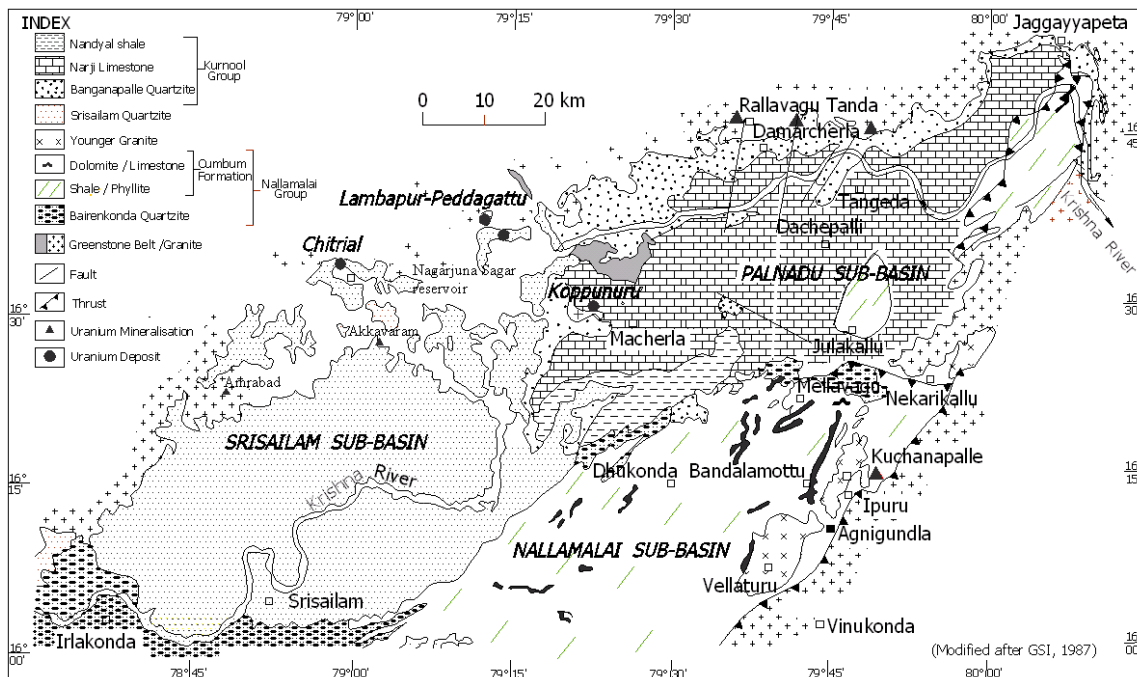


FIG. 2. Geological map of northern part of Cuddapah Basin.

## 2.3. Palnad sub-basin

The Neoproterozoic Palnad sub-basin (Fig. 2) extends over 3 400 sq km and comprises arenaceous, argillaceous and calcareous sediments (equivalent to Kurnool Group in main Kurnool sub-basin) unconformably overlying basement granite/gneisses. The sediments comprise Banganapalle quartzite/shale, Narji limestone/calcareous shale, Owk shale and Paniam quartzite. The thickness of the sediments varies from 10 m to 450 m, with gentle south easterly dip. The basement granite/gneisses are essentially composed of quartz, plagioclase and alkali feldspars along with biotite, apatite monazite and allanite as accessories. Basic dykes (<1m to 60m width) trending N-S, E-W & NW-SE and quartz veins trending N-S, traverse the basement rocks.

### 3. Uranium mineralization

Uranium anomalies located by ground radiometric surveys, along the unconformity between basement granite and overlying Srisailam sediments in the Lambapur outlier, in the northern fringes of the Srisailam sub-basin, [6] led to the first major breakthrough in the search for unconformity related uranium deposits in the Cuddapah basin. Detailed exploration at Lambapur and in adjacent outliers resulted in establishing three uranium deposits at Lambapur, Peddagattu and Chitrial. Continuity of litho-structural set up and proximity of the major uranium deposits in the Srisailam sub-basin to the adjacent Palnad sub-basin, led to extension of uranium investigations into the Palnad sub-basin as well. This eventually resulted in establishing the Koppunuru uranium deposit; close to the unconformity between the basement granite and sediments of Kurnool Group [7]. Salient features of the deposits in both sub-basins are discussed below.

#### 3.1. *Lambapur - Peddagattu-Chitrial uranium deposits in Srisailam Sub-basin*

Lambapur, Peddagattu and Chitrial uranium deposits have similar lithostructural setup and nature of uranium mineralization with comparable geological and geochemical controls. The basement granite has been characterized as biotite-granite, essentially containing quartz, orthoclase, microcline, perthite, biotite and plagioclase. Apatite, zircon and allanite are the other accessory minerals present, whereas, chlorite, sericite, calcite and epidote are the secondary minerals formed due to alteration. Pyrite, chalcopyrite, galena, ilmenite, anatase and hydrated iron oxides are the opaque minerals observed. The uranium content of the granites varies from 10 to 116 ppm with U/Th ratios ranging from 0.34 to 2.32. Geochemical studies of the granites of these areas indicate that they are potassic ( $K_2O/Na_2O > 1$ ), peraluminous (A/CNK: 1.05-2.18) and low Ca-granite, without showing significant differentiated character and probably formed by partial melting of silicic crustal material [8].

The basement granites/gneisses are intruded by three prominent sets of basic dykes trending NNW-SSE, NW-SE and N-S, which are older to the Srisailam Formation [9]. The Srisailam Formation generally starts with a pebbly gritty arenite horizon, overlain by shale and shale/quartzite intercalations, followed by massive quartzite. The thickness of the Srisailam Formation varies from 5-70 m with gentle dips of  $3^\circ$  to  $5^\circ$  towards southeast.

In all the deposits, uranium mineralization occurs close to the unconformity, both in the basement granites and the overlying Srisailam pebbly arenite, with most part (>85%) in the former unit (Fig. 3). Basic dykes and vein quartz within the basement, close to the unconformity, are also mineralized at places. Lead and copper mineralization is also associated with vein quartz. Features of hydrothermal activity, both in the basement and overlying sediments, is evidenced by high amounts of sulphides. Fluid inclusion studies of quartz occurring in mineralized granite indicate that highly saline solutions of 100-200°C temperature are responsible for deposition of uranium. Sm-Nd isochron dating of uraninite from Lambapur area indicates an age of  $1327 \pm 170$  Ma, whereas, U-Pb data yield radiogenic Pb ages of about 480-500 Ma [10].

Exploration by core and non-core drilling at regular grid of 400 m x 400 m, 200 m x 200 m and 100 m x 100 m over the entire Lambapur, Peddagattu and a part of Chitrial outliers has indicated that the ore shoots are confined to NNE-SSW, N-S and NW-SE trends. Owing to the pronounced control of both the unconformity plane and the fractures in the basement, the ore body is in the form of lenses and elongated pods, with rich ore shoots at fracture intersections [11]. The intensity of fracturing apparently controls the loci of mineralization and the grade. The mineralization is attributed to presence of botryoidal and massive pitchblende in fractures / segregated masses in feldspars and along weak planes. Coffinite is found marginally replacing massive pitchblende at places.

Nearly 14 000 t of  $U_3O_8$  has been estimated in the three deposits of Srisailam sub-basin. Of the three, the Lambapur uranium deposit has been studied in detail and exploration of the deposit is complete, whereas it is on-going in the other two outliers. Systematic and integrated exploration is in progress in contiguous areas as well, to establish additional uranium resources.

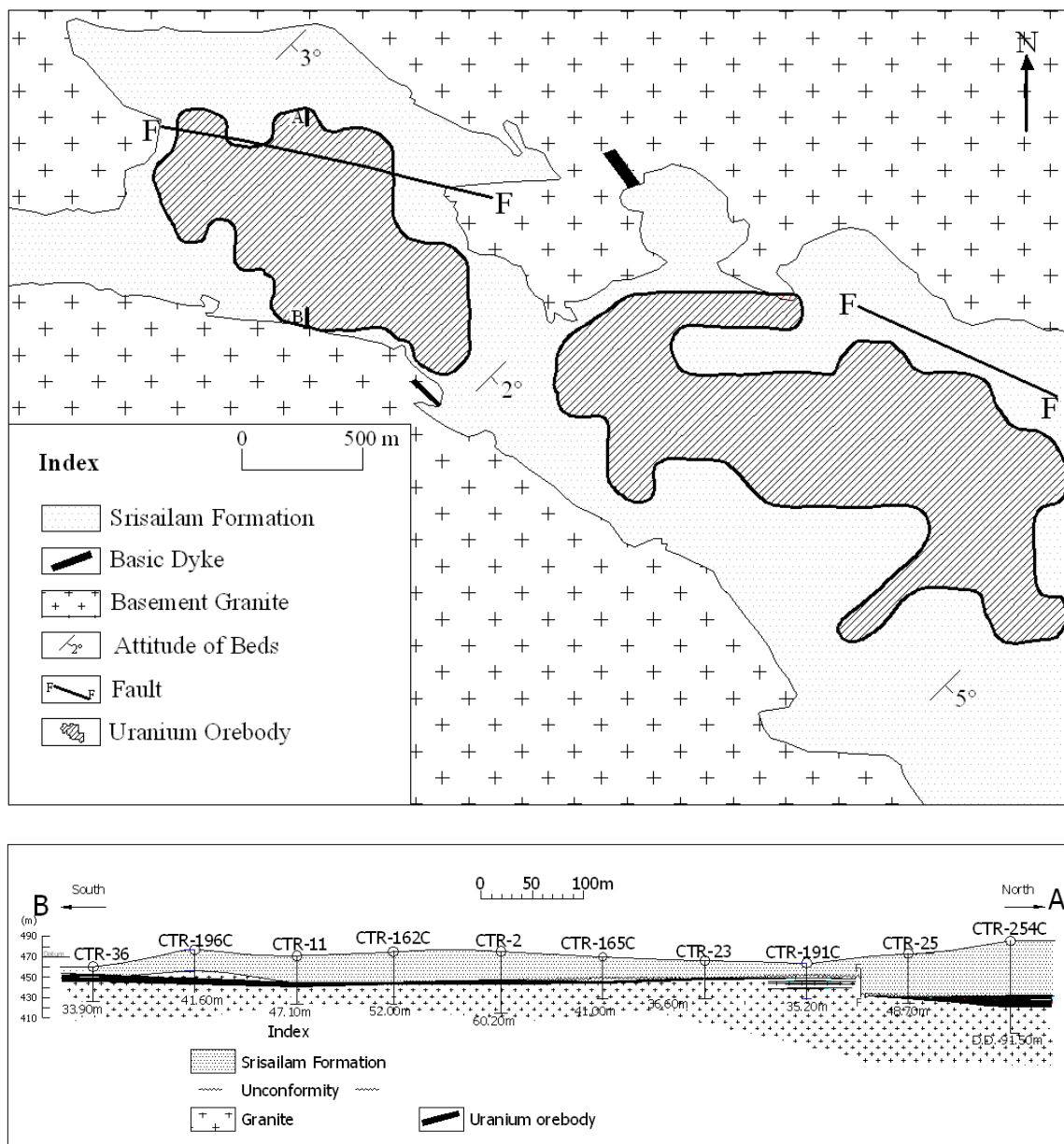


FIG. 3. Ore body outline at Chitrial, Nalgonda District, Andhra Pradesh and section along A-B.

### 3.2. Koppunuru uranium deposit in Palnad Sub-basin

The Koppunuru-Dwarakapuri uranium deposit falls in the western part of the Palnad sub-basin which comprises Neoproterozoic Kurnool Group of sediments [12]. The Archaean Gneisses and Paleoproterozoic basement granites are nonconformably overlain by the sub-horizontal Kurnool Group of sediments. Basement granite is also exposed as an inlier, extending over an area of 6 km x 2.5 km, to the east of Koppunuru and along the up thrown block of the regional WNW- ESE trending Kandlagunta fault. This fault is in turn offset by younger north-south trending minor faults (Fig. 4). The basement rocks and the overlying Banganapalle Formation are fractured and traversed by quartz veins trending N-S, NNE- SSW and WNW- ESE. The Banganapalle quartzites are grey coloured, well sorted and sacchroidal in nature with high degree of mineralogical maturity and are composed of sub-rounded clasts dominantly constituted by quartz (97%) and feldspar (3%) [13]. Basement granites plot mainly in the 'granite' field and subordinately in 'quartz-monzonite, granodiorite and tonalite' fields in Ab-An-Or space [14]. In Rb-Ba-Sr space [15] most of the samples plot in 'normal' to 'anomalous' granite fields with a few in strongly differentiated granite field. The basement granite, is characterized

by higher intrinsic uranium (Ave. 32 ppm; n=16) and with high U/Th ratios (Ave. 4.41; n=16) as compared to the average uranium and U/Th ratio of normal granite (U/Th =0.25).

Subsurface exploration by drilling in Koppunuru area reveals fracture controlled correlatable uranium mineralization hosted by Banganapalle Formation, as well as, the basement granites. Three sub-horizontal ore lodes have been established; two of which are in the arenite facies and the third one in the basal polymictic grit/conglomerate of Banganapalle Formation, at places transgressing along the fractures into the underlying basement granites. About 2 300 t of  $U_3O_8$  has been estimated in Koppunuru block.

Primary uranium minerals identified in Koppunuru are pitchblende and coffinite occurring as stringers and veins. Pitchblende occurs as colloform aggregates and veinlets often showing coffinitization; secondary uranyl minerals occur along margins of detrital clasts. Traces of carbonaceous matter are associated with uranium mineralization along with sulphide minerals.

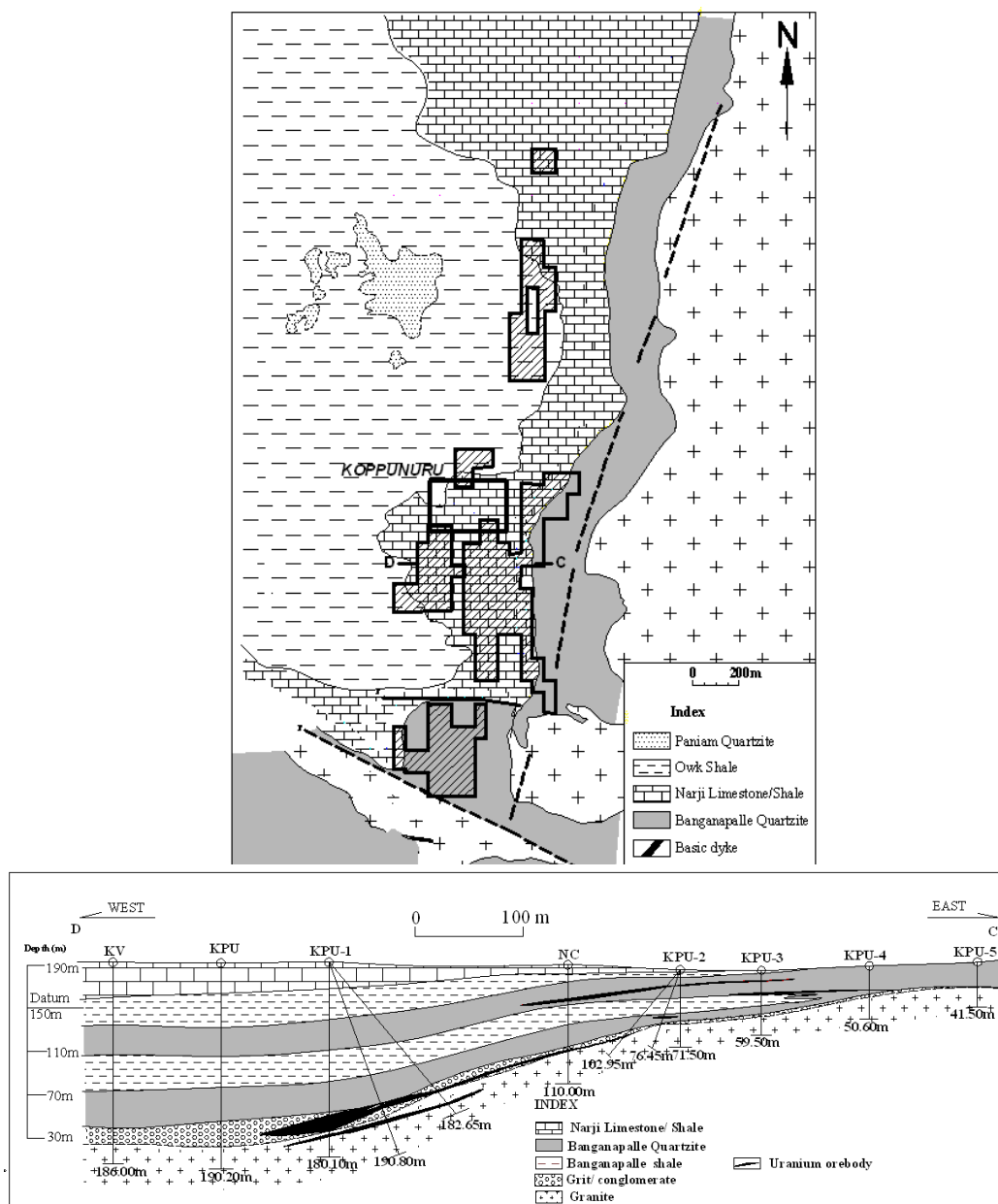


FIG. 4. Geological map showing distribution of ore bodies in Koppunuru area, Guntur district, Andhra Pradesh and section along C-D.

Uranium metallogeny at Koppunuru is attributed to the remobilization of uranium from the fertile basement granite, as a consequence of episodic reactivation of pre-existing faults in post- Kurnool times. Major among these are the WNW-ESE trending Kandlagunta fault and the N-S to NNE-SSW trending fault east of Koppunuru (Fig. 4.). The basal polymictic conglomerate, deposited as a channel lag deposit and porous sacchroidal quartz arenites, with grey carbonaceous shale intercalations, with associated sulphide minerals, were favourable hosts for the uranium mineralization. Fractures, fine veins, cavities and grain boundaries in the basement/sediments, proximal to the unconformity plane, trapped the labile uranium resulting in its precipitation. Hence mineralization at Koppunuru area is characterized as low temperature-epigenetic type of uranium mineralization.

#### **4. Discussion**

The Cuddapah basin in the eastern Dharwar craton of peninsular India holds high potential to host unconformity related uranium deposits, although some of the salient geological features (such as the different nature of the basement) of the classical unconformity type of deposits are absent in the Cuddapah basin. However, the northern margin of the Cuddapah basin hosts unique uranium deposits in Lambapur, Chitrial and Peddagattu in Srisailam sub-basin and Koppunuru in Palnad sub-basin.

With a view to locate additional such deposits, ground radiometric surveys were carried out in the remaining outliers and along the margins of main Srisailam sub-basin. This resulted in locating a number of uranium anomalies; significant among them being the Amrabad and Akkavaram anomalies (Fig. 2). Similarly, ground radiometric surveys along the northwestern margin of Palnad sub-basin revealed presence of a number of uranium anomalies; in the basement granites proximal to the unconformity. Significant among them is the Musi river anomaly, Damaracherla sector. Intensive sub surface exploration is envisaged in these areas.

#### **5. Conclusion**

The uranium deposits at Lambapur, Peddagattu and Chitrial in Srisailam sub-basin and Koppunuru in Palnad sub-basin are mainly confined to the unconformity plane between the Paleoproterozoic fertile, fractured granite and Meso-Neoproterozoic arenaceous facies cover rocks. The mineralization is associated with the basement fractures, basic dykes, carbonaceous matter and extensive alteration. The main ore minerals are uraninite, pitchblende and coffinite, which are generally associated with sulphides like pyrite, pyrrhotite, galena, chalcopyrite and pentlandite. The mineralization is low temperature hydrothermal in nature.

The southward continuity of the lithostructural setup of known uranium deposits in both sub-basins such as the Paleoproterozoic basement, Meso-Neoproterozoic cover rocks, increase in thickness of cover sediments (>300m) and repeated tectonic activity indicate the potentiality of these subbasins to host more uranium deposits. In this light, air borne, ground geophysical and geochemical surveys are planned to obtain signatures for possible concealed uranium deposits, at greater depths in both Srisailam and Palnad sub-basins of Cuddapah basin.

#### **ACKNOWLEDGEMENTS**

The Authors thank Dr.Anjan Chaki, Director, AMD for encouragement. They express their sincere thanks for the help rendered by various scientists working in the field areas and laboratories for enabling in preparation of this paper.

#### **REFERENCES**

- [1] JEFFERSON, C.W., et al., Unconformity-associated uranium deposits of the Athabasca Basin, Saskatchewan and Alberta (GOODFELLOW, W.D. Ed.), Mineral Deposits of Canada, A synthesis of Major Deposit-Types, District Metallogeny, the Evolution of Geological Provinces, and Exploration Methods, Geological Association of Canada, Mineral Deposits Division, Special Publication No.5 (2007) 273-305.

- [2] NEEDHAM, R.S., ROARTHY, M.J., "An overview of metallic mineralization in the Pine Creek Geosyncline" (FERGUSON, J., GOLEBY, A.B., Eds), Uranium in Pine Creek Geosyncline, IAEA, Vienna (1980) 157-173.
- [3] SIBBALD, T.I.I., "Geology and genesis of Athabasca basin uranium deposits. In: recognition of Uranium provinces", IAEA, Vienna (1988) 61-105.
- [4] NAGARAJA RAO, B., RAJURKAR, S., RAMILIGASWAMY, G., RAVINDRA BABU, "Stratigraphy, structure and evolution of the Cuddapah basin. In: Purana basins of Peninsular India", Geol. Soc. Ind. Mem. 6 (1987) 33-86.
- [5] PANDEY, B.K., et al., "Rb-Sr whole rock ages for the granites from parts of Andhra Pradesh and Karnataka", Fourth national symposium on mass spectrometry, Indian Institute of Science, Bangalore, India. (1988) EPS-3/1.
- [6] SINHA, R.M., PARTHASARATHY, T.N., DWIVEDI, K.K., "On the possibility of identifying low cost, medium grade uranium deposits close to the Proterozoic unconformity in the Cuddapah basin, Andhra Pradesh, India", IAEA-TECDOC-868, IAEA, Vienna (1996) 35-55.
- [7] NAGESWARA RAO, P., et al., "Proterozoic unconformity related uranium occurrence around Rallavagu Tanda, Palnadu Sub-basin, Andhra Pradesh", J. Geol. Soc. Ind. 66 (2001) 11-14.
- [8] SHRIVASTAVA, V.K., PARTHASARATHY, T.N., SINHA, K.K., "Geochemical study of the uraniferous granites from Lambapur area, Nalgonda district, Andhra Pradesh, India", Exploration and Research for Atomic Minerals, 5 (1992) 41-52.
- [9] VERMA, M.B., et al., "Geochemistry of host granitoids of uranium deposit at Chitrial area, Srisailam subbasin, Nalgonda District, Andhra Pradesh", Geol. Soc. Ind. Mem., 73 (2008) 37-54.
- [10] PANDEY, B.K., "Geochronology of the rocks and radioactive minerals in the parts of Andhra Pradesh and Karnataka with special reference to episodes of uranium mineralization during the Proterozoic", AMD special report, December (2004).
- [11] SINHA, R.M., SHRIVASTAVA, V.K., SARMA, G.V.G., PARTHASARATHY, T.N., "Geological favorability for unconformity related uranium deposits in northern parts of the Cuddapah basin: evidences from Lambapur uranium occurrence, Andhra Pradesh, India", Exploration and Research for Atomic Minerals, 8 (1995) 111-120.
- [12] JEYAGOPAL, A.V., PRAKHAR KUMAR, SINHA, R.M., "Uranium mineralization in the Palnad Sub-basin, Cuddapah basin, Andhra Pradesh, India", Current science, 71 12 (1996) 957-959.
- [13] LATHA, A., UMAMAHESWAR, K., VERMA, M.B., MAITHANI, P.B., "Petrological characterization of uranium bearing host rocks at Koppunuru, Guntur District, Andhra Pradesh", The Indian Mineralogist, 42 (2008) 81-88.
- [14] O'CONNOR, J.T., "A classification of quartz-rich igneous rocks based on feldspar ratios", US Geol. Surv. Proj. Paper 525-B (1965) 79-84.
- [15] EL BOUSEILY, A.M., EL SOKKARY, A.A., "The relation between Rb, Ba and Sr in granitic rocks", Chem. Geol. 16 (1975) 207-220.

# Prospects and potentialities for uranium in North Delhi Fold Belt: A case study from Rohil, Rajasthan, India

L. K. Nanda<sup>a</sup>, V. J. Katti<sup>a</sup>, P. B. Maithani<sup>b</sup>

<sup>a</sup> Atomic Minerals Directorate for Exploration and Research, Jaipur, India

<sup>b</sup> Atomic Minerals Directorate for Exploration and Research, Hyderabad, India

**Abstract.** North Delhi Fold Belt (NDFB) of Western Indian Craton consists of Palaeo–Meso Proterozoic volcano–sedimentary rocks of Delhi Supergroup deposited in a half graben. These rocks have undergone polyphase deformation, metamorphism and intrusion by late granites. Younger pegmatite, aplite and albitite occur along major structural breaks. The three sub–basins of NDFB comprise Khetri, Alwar and Lalsot–Bayana. The Khetri sub–basin forms an important metallogenic province and hosts important uranium and base metal resources. A NE–SW trending prominent crustal scale fracture system, known as Kaliguman lineament, tectonically separates Delhi Supergroup metasediments from basement rocks. Widespread zone of albitization along this lineament, with 170 km strike extent, is popularly known as “albitite line”. Since 1950, more than a hundred U and Th anomalies, associated with structurally weak zones in metasediments have been reported in NDFB. One such zone at Rohil hosts a low tonnage, low grade uranium deposit. This deposit comprises five sub–vertical, en–echelon ore lodes occurring over 340–686 m strike with average thickness of 4.27 m. Major uranium mineral is uraninite with minor brannerite, coffinite with common association of chalcopyrite, pyrrhotite, molybdenite and pyrite. The mineralized rocks exhibit strong hydrothermal alterations like chloritization, silicification, ferruginization and albitization. The uraniferous samples contain significant levels of Cu, Mo, Ni, Co and Pb. Preliminary Pb isotopic ratios indicate age of uraninite as 839±19 Ma. At Rohil, uranium ore lodes extend below surface to 600 m depth. Coincidence of strong EM conductivity, high chargeability and low magnetic intensity with uranium lodes have successfully guided application of ground geophysical exploration programme in contiguous alluvium–covered blocks. Further, for quicker delineation of favourable targets in the Khetri sub–basin, multi–parameter high–resolution heliborne geophysical surveys have been completed over 105 km × 15 km and anomalous zones identified. Mathematical modeling of exploration data may be applicable in effective exploration planning.

## 1. Introduction

In the Western Indian Shield of Rajasthan important uranium occurrences are associated with metasediments of Palaeo–Meso Proterozoic Delhi Supergroup in North Delhi Fold Belt (NDFB) [1][2][3]. Exploration activities in NDFB by the Atomic Minerals Directorate for Exploration and Research (AMD) dates back to 1950s [4]. These resulted in identification of numerous uranium occurrences at Rohil, Ghateshwar, Diara, Saladipura, Kerpura, Hurra ki Dhani, Maonda, Pachlangi, Khetri, Kolihan, Sior, Siswali, Antri–Biharipur, Mewara–Gujarwas, Ladi Ka Bas, Kalatopri, Kho–Dariba, Dhani Basri, Bairat and other areas (Fig. 1). The Khetri sub–basin of NDFB, which is well known for base–metal mineralization, also hosts innumerable uranium occurrences in shear zones forming prominent lineaments. The mineralized shear/fracture zones follow NNE–SSW trend, within the zone of albitization better known as ‘albitite line’ of Rajasthan [5][6]. The albitite line follows Khetri lineament in northeast and Kaliguman lineament in southwest (Fig 2). Several post–Delhi granitic bodies are emplaced along this lineament.

Integrated exploration over the years has brought to light one ore block of 700 m (length) × 200 m (width) × 600 m (depth) dimension, containing low tonnage, low grade uranium deposit at Rohil, in the southwestern part of Khetri sub basin (KSB). This paper deals with the polymetallic mineralization at Rohil with association of U, Mo, Cu, Ni, Co, Pb, and Zn. The success of delineating uranium

deposit at Rohil is based on integrated geological and geophysical exploration and drilling. The heliborne geophysical data generated over the NDFB resulted in identification of several areas suitable for detailed investigations.

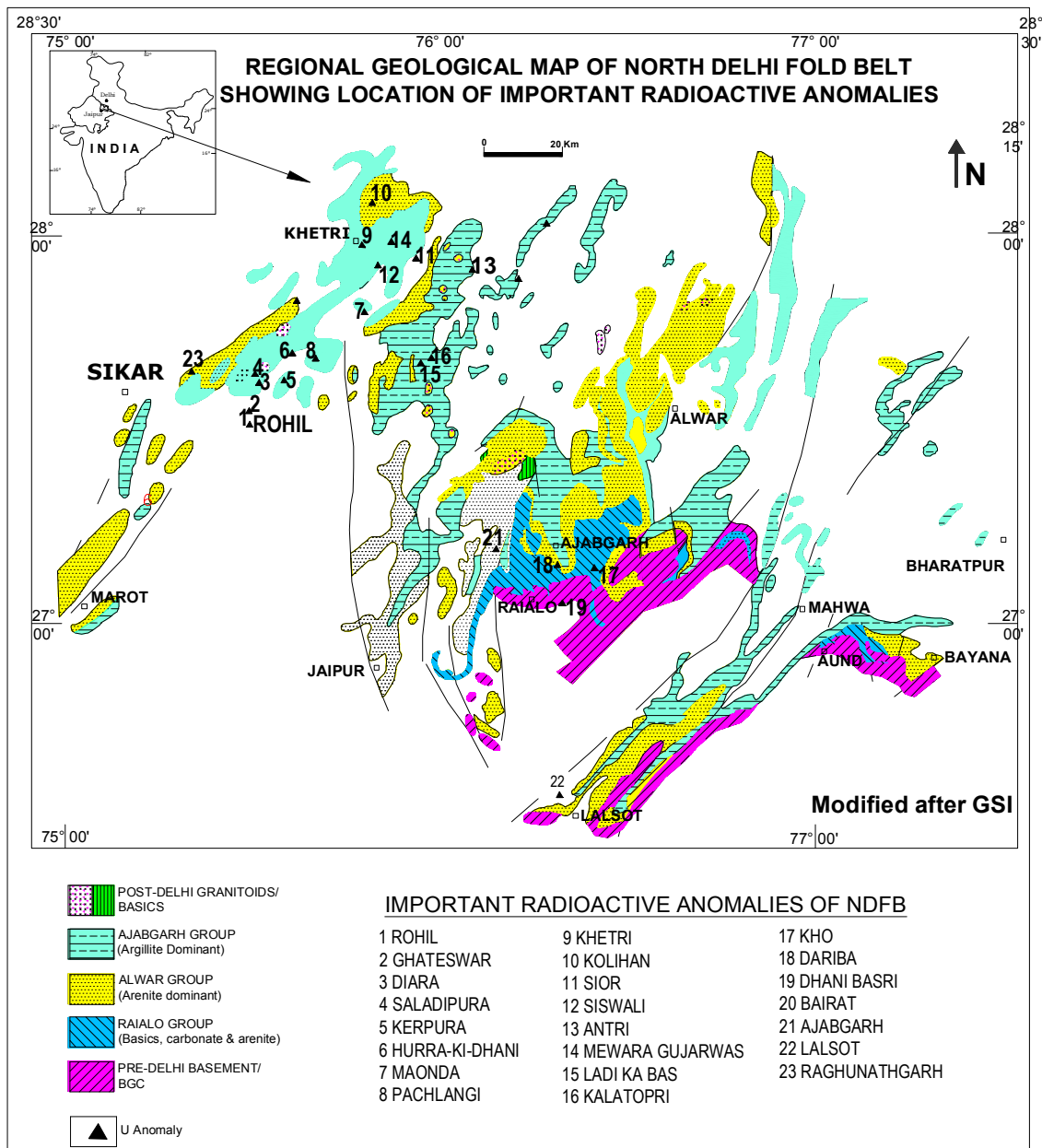


FIG. 1. Regional geological map of NDFB showing location of important radioactive anomalies.

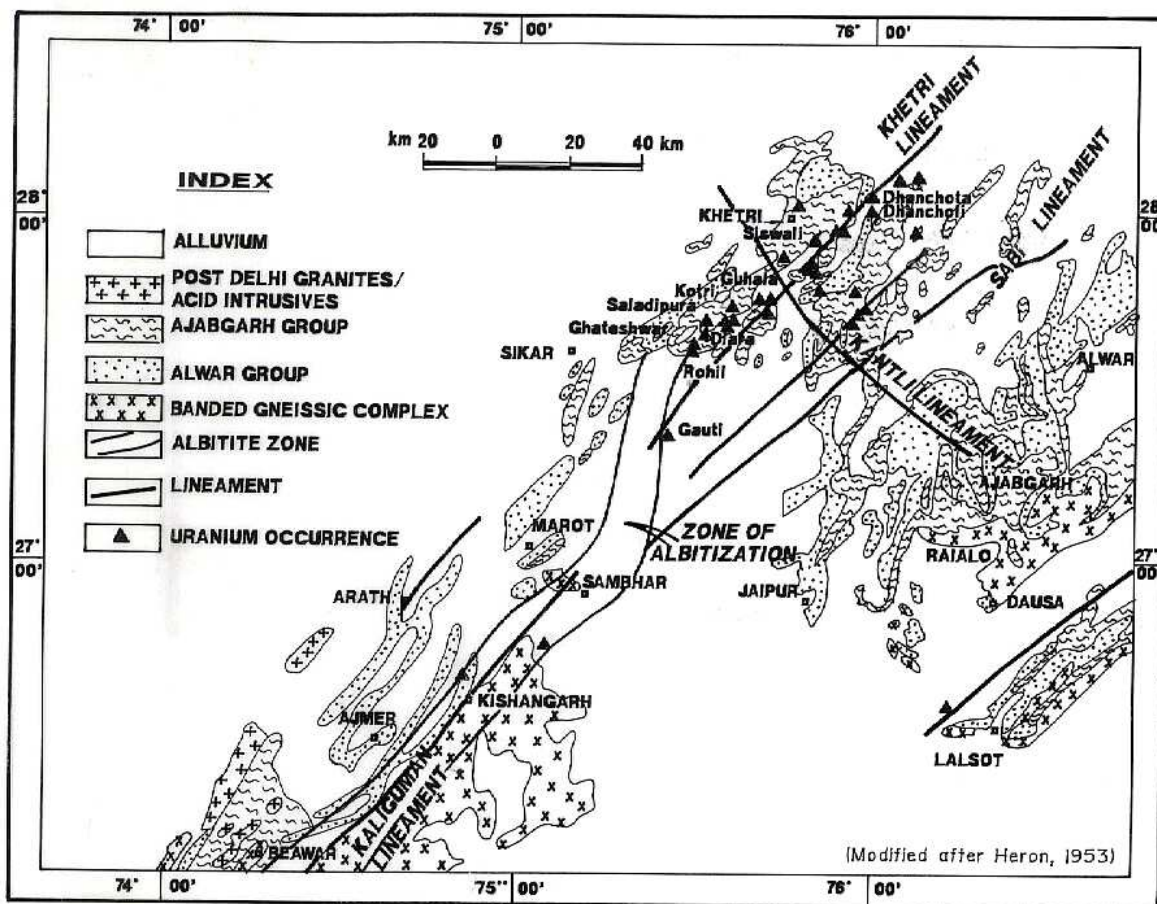


FIG. 2. Albitite zone of NDFB showing uranium occurrences.

## 2. Geological setting

The rocks of Palaeo–Meso Proterozoic Delhi Supergroup form a narrow belt extending from Haryana in the north to Gujarat in the south [7]. This belt has been divided into North Delhi Fold Belt (NDFB) and South Delhi Fold Belt (SDFB), separated by a migmatitic gneiss track around Ajmer [8][9]. The NDFB consists of three sub-basins designated as Khetri, Alwar and Lalsot–Bayana from west to east, respectively. The generalized stratigraphy of the NDFB is presented in Table 1.

The Archaean Banded Gneissic Complex (BGC≡Mangalwar Group) comprising high-grade metamorphic and migmatized rocks form the basement. It is unconformably overlain by dominantly calcareous metasediments of Raialo Group. The Raialo Group in turn is unconformably overlain by arenaceous metasediments of Alwar Group. The metapelites of Ajabgarh Group show gradational contact with the Alwar Group. The rocks of Delhi Supergroup are metamorphosed up to amphibolite facies.

The rocks record imprints of three phases of deformation of Delhi orogenic cycle. The folds of earlier generations ( $F_1$  and  $F_2$ ) are coaxial with broad NNE–SSW axial trends, forming prominent lineaments. The first generation ( $F_1$ ) folds are isoclinal and second generation ( $F_2$ ) folds are normal, upright to inclined with shallow to moderate plunge due NNE/SSW. The third phase of deformation has resulted in folds ( $F_3$ ) with WNW–ESE trending axial planes and has caused broad swing in trends from NNE–SSW to NNW–SSE. Cross folding has resulted in development of doubly plunging synforms and antiforms [10].

The NDFB has witnessed post–Delhi acidic and basic magmatic activities. Rb–Sr studies on granites of KSB yield an age of  $1463 \pm 71$  Ma with initial  $^{87}\text{Sr}/^{86}\text{Sr}$  ratio of  $0.7313 \pm 0.0024$  (MSWD=24). Sm–

Nd model age on these granites vary from 2 204 to 2 335 Ma. Two major phases of acid intrusives are 1 480±40 Ma for Saladipura granite equivalent [11] and ~ 700 Ma for younger Malani igneous suite. The older granites are peraluminous with distinct S-type characteristics [12]. Biotites of older granites recorded thermal activity around 700 Ma [4], corresponding to Pan African event.

Albitite intrusives are widespread along NNE–SSW trending zone over an extent of 170 km with maximum width of 10 km. This zone, defined as the albitite line, follows Khetri and Kaliguman lineaments. In the Rb–Sr plot, albitites of KSB align along 1 400 Ma line. The albite and microcline from albitised pegmatite indicate Rb–Sr model ages of 464 to 671 Ma, respectively [13]. The albitised pegmatites are dated as 550±26 Ma and 477±9 Ma by Rb–Sr method, with initial  $^{87}\text{Sr}/^{86}\text{Sr}$  ratio of 0.74134±0.00060 (MSWD=6.26) and 0.73644±0.00049 (MSWD=3.82), respectively [14]. Opinions vary for origin of albitites, one school of thought emphasizing magmatic origin [5] and others advocating metasomatic concept [15][16][17].

Table 1. Generalised stratigraphy of North Delhi Fold Be

	Post-Delhi Intrusives	Amphibolite Granite, aplite, pegmatite
Delhi Supergroup (Palaeo–Meso Proterozoic)	Ajabgarh Group	Carbonaceous phyllite and minor quartzite Phyllite interbanded with quartzite Schist and marble Carbon phyllite Ferruginous spongy quartzite Impure banded siliceous marble
	Alwar Group	Massive quartzite Schist, phyllite, flaggy quartzite Pebbly arkosic grit with iron bands — Unconformity —
	Raialo Group	Quartzite, conglomerate Schist Basic flows (amphibolite) Quartzite with thin conglomerate bands Dolomitic marble Quartzite and conglomerate — Unconformity —
	Archaean	Banded Gneissic Complex (Mangalwar Group)

### 3. Uranium exploration history in the KSB

The uranium exploration history in the KSB dates back to 1950s and has been carried out in three discrete phases. The first uranium anomaly associated with the flesh coloured quartzo–felspathic rock occurring at the contact of epidiorites and carbonaceous phyllite was located in 1950–51 at Kolihan mines. Several other occurrences were located in the KSB, including Rohil–Ghateshwar anomaly in 1953–54. In 1955, shallow boreholes drilled at Ghateshwar intercepted lean grade uranium mineralization. During 1956–1962, in Kolihan area, lean uranium mineralization associated with quartzo–felspathic body was intercepted. Identification of brannerite, limited strike length, lensoidal nature of the ore body and poor grades resulted in closing of this phase of exploration.

In the second phase during 1972–73, underground drilling work was taken up in the Kolihan mines. Significant widths of radioactive horizon i.e. upto 15m in boreholes from 424 m level were intercepted. Surface drilling revealed a radioactive band with 200 m strike length, 140 m slope width and 2.50 m average thickness. A total reserve of 140 tonnes of  $\text{U}_3\text{O}_8$  was estimated under inferred category. Reconnoitry drilling in Siswali and Sior intercepted lean mineralization in most of the boreholes. In the year 1973, while prospecting for molybdenum in Ghateshwar area, the Geological Survey of India (GSI) drilled many boreholes. Gamma–ray logging of these boreholes by AMD

revealed encouraging results and uraninite was identified. During 1973–76, boreholes drilled in Ghateshwar by AMD intercepted lean mineralization which resulted in closure of phase II.

In Phase III, during 1994–95, radiometric ground checking of 500 sq km of the NDFB was carried out. Discovery of uraniferous chlorite schist, confirmation of uraninite as the principal radioactive phase in Kerpura, Hurra-ki-Dhani and Maonda areas and location of new anomalies associated with albitites gave boost to the exploration programme. A 50 km long and 6 km wide belt was defined as a potential target for detailed uranium exploration [16]. In the period 1994–96, subsurface investigations were carried out at Diara and Kerpura–Narsinghpur–Tiwari ka bas. Lean mineralization was intercepted in some boreholes. One of the anomalies at Rohil was taken up for detailed exploration and evaluation work in the last decade. Besides, exploratory/reconnoitry drilling has been carried out in contiguous areas at Kerpura, Raghunathgarh and Ladi-ka-bas areas.

### ***3.1. Uranium mineralization in KSB***

In the KSB more than 250 radioactive occurrences have been located by ground radiometric surveys. The radioactivity is largely due to uranium mineralization with rare instances of small contribution due to thorium. The mineralization, hosted by a wide spectrum of lithologies encompassing quartz-biotite schist, quartzite, calc-silicate, quartz albitites/albitites, phyllites ( $\pm$  carbonaceous), granites, mafic rocks and quartzo-feldspathic injections, is associated with polymetallic sulphides in sheared and altered zones.

Extensive exploration efforts have been made by integrated geological and geophysical investigations and drilling at Rohil, resulted in establishing a sizeable uranium deposit. The characteristics of Rohil uranium deposit are therefore, discussed in detail in a separate section.

## **4. Alwar sub-basin**

In the Alwar sub-basin, large number of radioactive occurrences are associated with granitic and pegmatitic intrusives and hydrothermal veins in granites and metasediments. Uranium investigations were mainly confined to shear zones cutting across basement rocks as well as the Delhi cover sediments. Shear zones traversing basement rocks in Dhani Basri area host uranium and copper mineralization. Investigations along Dariba shear zone of Kho-Dariba area resulted in identification of significant uranium anomalous zones. In Bairath granite, a number of radioactive zones have been located; most of them associated with ferruginous cherty/quartz breccia and sheared granite, nearer to the contact with quartzite.

## **5. Bayana–Lalsot sub-basin**

In this sub-basin, limited radiometric surveys have been undertaken. The area remains unexplored and possibility of locating uranium mineralization is high along the unconformity between basement and rocks of Delhi Supergroup as well as along fractures within the metasediments.

## **6. Rohil uranium deposit**

### ***6.1. Location***

Rohil is situated in Sri Madhopur Tehsil of Sikar district in Rajasthan. The district is well connected by national and state highways. Rohil village around which the exploration blocks lie, is approximately 120 km from Jaipur.

### ***6.2. Geology of Rohil***

The area around Rohil is mainly covered by 40 – 50 m thick soil/alluvium with a N–S trending sub vertical sheared quartz ridge of 500 m  $\times$  200 m. The sheared eastern and western contacts of the quartzite with quartz-biotite schist show hydrothermal alterations viz. albitization, chloritization and

silicification. The lithounits comprise quartzite/amphibole quartzite, quartz–biotite  $\pm$  amphibole  $\pm$  chlorite  $\pm$  garnet  $\pm$  graphite schist, carbonaceous/ graphitic phyllite, calc–silicates/impure marble. These are traversed by quartz reef/vein, calcite, pegmatite, aplite, albitite, amphibolite and hornblendite. Rohil uranium anomaly is of limited extent and is confined to the eastern sheared contact. The geological succession of the area based on subsurface data is presented in Table 2.

Table 2. Geological succession at Rohil

Age	Supergroup	Group	Lithology
Recent			Alluvium
Upper Proterozoic		Post–Delhi intrusives	Quartz/calcite carbonate veins Granite/pegmatite/aplite/albitite Metabasites/amphibolite (hornblendites)
Palaeo–Meso Proterozoic	Delhi Supergroup	Ajabgarh Group	Quartzite Quartz–biotite–schist $\pm$ carbonaceous / graphite schist with intercalatory bands of quartzite, and calc–silicate
Unconformity			
Archaean / Lower Proterozoic (?)			Basement not exposed

### 6.3. Uranium mineralization

Uranium mineralization at Rohil is structurally–controlled, hydrothermal vein–type and occurs in the form of lodes, veins and lenses, confined to shear/fracture zones in quartz–biotite schist  $\pm$  graphite, quartzite, carbonaceous phyllite and calc–silicates. Hydrothermal alterations are manifested as chloritization, albitization, feldspathization and silicification. Five sub–parallel, sub–vertical uranium lodes occur in an en–echelon pattern along N–S to NNE–SSW trending Rohil shear zone defined by brecciated and silicified quartzite ridge, having sheared contact with schistose rocks on two sides (Fig 3).

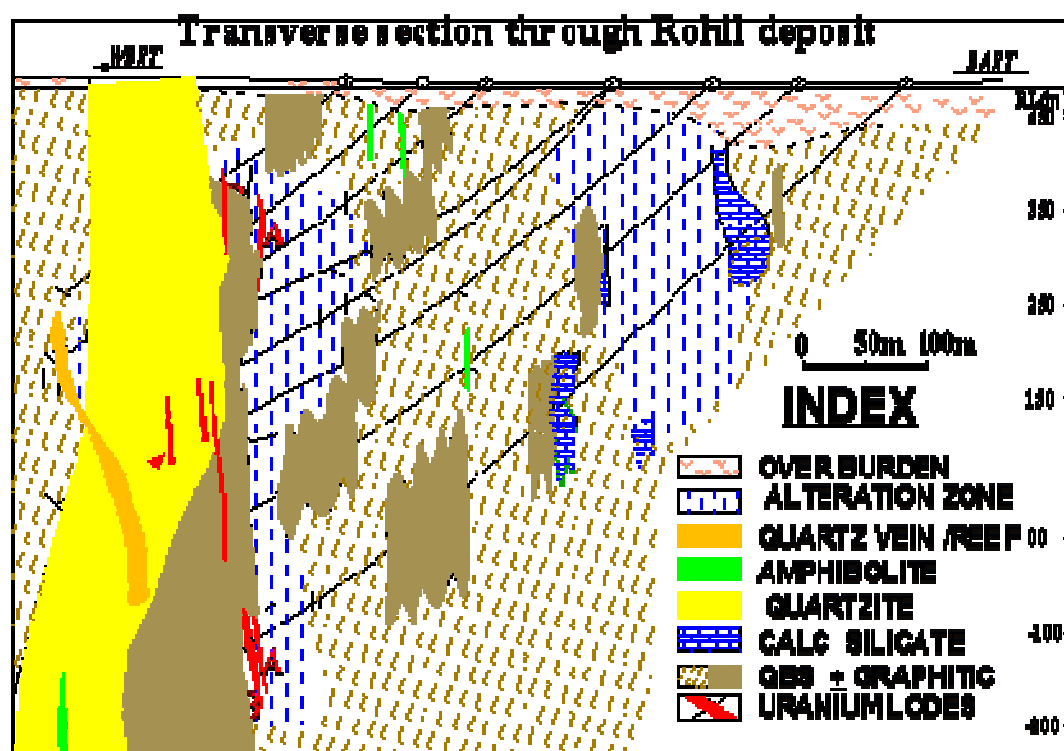


FIG. 3. Transverse section through Rohil deposit.

Ore lodes have been delineated up to a depth of 600 m from surface by core drilling and a block of 700 m × 200 m × 600 m is identified as a potential deposit for exploitation. Individual lodes with average thickness of 2.4 m to 6 m have strike extents of 350 to 700 m. Horizontal separation of adjacent lodes vary between 6 m and 50 m, and the extreme lodes have separation between 80 to 200 m. The ore body has been established between depths of 80 m and 600 m from surface, with apparent further down–depth continuity [18].

Uranium minerals are mainly uraninite with minor coffinite and brannerite. The uraninite occurs as clusters, dissemination of anhedral grains filling polymetallic veins and as minute inclusions in biotite. Common association of chlorite, fluorite, calcite and goethite can be frequently noticed. The uraninite grains are often rimmed by chlorite, pyrite or chalcopyrite. The primary fluid inclusions in quartz, occurring in uraninite veins are largely biphasic containing a H<sub>2</sub>O rich liquid and a vapor bubble and in rare cases triphasic inclusions containing a daughter crystal of NaCl. The fluid inclusions vary in size from 5 μm – 9 μm with 0.5–0.9 degree of fill. Majority of the inclusions homogenize at 200°C – 350°C. Salinity estimates obtained by heating–freezing data range between 15 – 40 wt% eNaCl. Preliminary investigation of uranium mineralized borehole core samples gave Pb–Pb isochron ages of 817±29 Ma to 839±19 Ma with μ<sub>1</sub> values of 8.96±0.9 & 7.70±0.8, respectively [13].

Different sulfide mineralization episodes in KSB resulted in richer concentrations of pyrite, chalcopyrite with minor pyrrhotite and molybdenite. The petromineralogical study indicated three phases of sulfide mineralization in Rohil area. Pyrite with minor ilmenite occurring as disseminations in Delhi metasediments is the dominant constituent in the pre–uraninite phase. The ore stage is characterized by association of uranium mineralization with polymetallic sulfides along veins. This stage shows characteristic association of uraninite with molybdenite, chalcopyrite, pyrite and pyrrhotite. The post–uraninite phase shows association of pyrite and chalcopyrite.

The metasediments, especially rich in carbonaceous matter, contain high intrinsic uranium with values up to 36 ppm U<sub>3</sub>O<sub>8</sub>. During different phases of metamorphism, deformation and igneous activities, uranium from country rocks probably got remobilized and concentrated along structurally weaker shear and fracture zones. The late–phase igneous activity in the form of albitite, pegmatite, aplite and basic intrusions (hornblendites and amphibolite) has played an important role in remobilizing uranium from the metasediments, besides acting as a possible source. Though, the uranium occurrences are confined to the albitite line in KSB, uranium mineralization is not directly attributed to the regional albitization episode [19].

#### **6.4. Associated ore mineralogy**

Uraninite, normally occurs in polymetallic veins in association with molybdenite, chalcopyrite, pyrrhotite and pyrite with gangue of chlorite, fluorite, calcite and goethite. It is often rimmed by chlorite, pyrite or chalcopyrite. The sulfide minerals occur in pre–, syn– and post–uranium ore stages. Pyrite is the main pre–ore stage mineral and has formed during syn–sedimentary volcanogenic Delhi sedimentation. The host rocks for uranium minerals, their mode of occurrence and associated mineralogy is summarized in Table 3.

#### **6.5. Ore body configuration**

Detailed systematic drilling in a block of 1 000 m × 600 m size followed by correlation of geological features and mineralized bands have been utilized in the delineation of ore body configuration and establishing a low grade (0.062%U<sub>3</sub>O<sub>8</sub>), low tonnage (3 720 tonnes U<sub>3</sub>O<sub>8</sub>) uranium deposit in Rohil. The deposit has an average thickness of 4.27 m. Five vertical to sub–vertical ore lodes have been delineated, out of which A & B are main lodes and A<sub>1</sub>, B<sub>1</sub> and B<sub>2</sub> are subsidiary lodes (Fig 4). These lodes are parallel to sub–parallel, occur in an en–echelon pattern with maximum strike extent varying from 340 m to 686 m, and have been traced up to 600 m below surface. Conformity and best disposition of ore lodes at 300 m RL is observed in level plans (Fig 4). Sheared contact of quartzite with schist is very significant for mineralization (Fig 3) and acts as an important guide in exploration

in adjoining blocks. The eastern contact is relatively richer in uranium mineralization compared to the western contact.

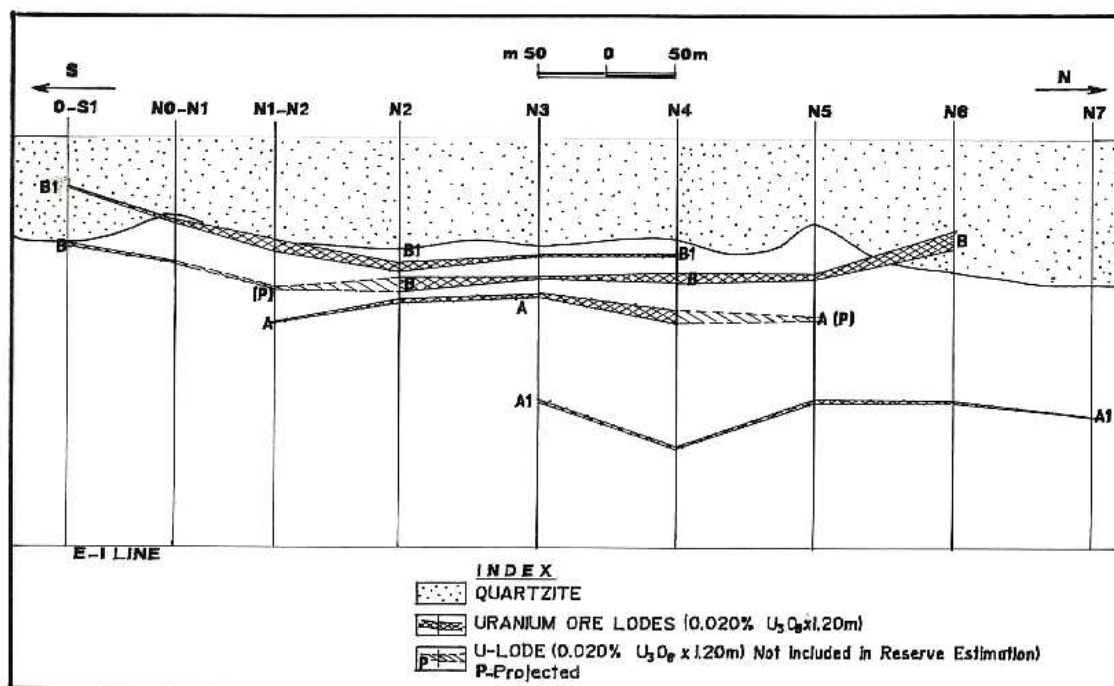


FIG. 4. Ore body plan at 300 m RL, Rohil deposit

Table 3. Host rock, uranium minerals, mode of occurrence and associated mineralogy

Host Rock	Uranium Minerals	Mode of Occurrence
Albitite & quartz-albitite	Uraninite brannerite	Polymetallic veins comprising uraninite ± pyrite ± chalcocopyrite ± pyrrhotite ± arsenopyrite ± molybdenite ± ilmenite ± fluorite. Uraninite & brannerite as cubic to anhedral disseminations.
Albitised quartz-biotite± chlorite± plagioclase± tremolite± graphite schist	Uraninite coffinite	Composite veins of uraninite ± pyrite ± chalcocopyrite ± magnetite. Uraninite as clusters and disseminations of anhedral grains.
Albitised calc – silicate rocks	Uraninite	Composite veins of subhedral – anhedral uraninite ± pyrite ± pyrrhotite ± molybdenite ± ilmenite. Cuboid uraninite rimmed either by chlorite, pyrite or chalcocopyrite.
Albitised quartz- hornblende cataclasite	Uraninite	Composite veins of uraninite ± molybdenite ± pyrite ± ilmenite.
Breccia	Adsorbed uranium	Uranium adsorbed on hydrous iron oxides.
Albitised quartzite	Uraninite	Uraninite as minute inclusions in biotite and as anhedral disseminations associated with pyrite.

## **6.6. U–Mo–Cu association**

Chemical data for core samples from ore zones of Rohil deposit indicate that besides uranium, copper and molybdenum occur in substantial concentration with an average of 1 438 ppm Cu (n=1 185) and 328 ppm Mo (n=971). In the samples analyzed, maximum values obtained are 21,119 ppm Cu and 15 390 ppm Mo. The average content of other metals are Ni (193 ppm, n=1014), Co (208 ppm, n=1 078), Pb (268 ppm, n=388), and V (293 ppm, n=1 095).

The noteworthy features observed are that with increase in the  $U_3O_8$  grade, (a)  $Fe_2O_3$  content increases which can be related to chloritic and haematitic hydrothermal alteration and explains the possibility of enhanced uranium grades with increasing proportion of alteration mineralogy or the degree of hydrothermal alteration (b) Cu content though not directly related to the  $U_3O_8$  grades, shows higher concentration with average of 1438 ppm in uranium lodes (c) Mo content shows direct relation with  $U_3O_8$ , with significantly higher concentration with average of 921ppm in samples having more than 0.10%  $U_3O_8$ . Values of Ni, Co and Pb also show increasing trend with  $U_3O_8$  grades. However, their concentrations are not very significant from economic viewpoint. Zn and V are also not significant and do not show any systematic relation with the  $U_3O_8$  grades [19].

## **6.7. Ground geophysical survey**

Initial success was met by core drilling in an otherwise thickly soil/alluvium covered area at Rohil. For further systematic planning of expensive drilling programme, ground magnetic, gravity, IP, resistivity and TURAM surveys were carried out, simultaneously with drilling. Presence of graphitic schist, sulfides in the ore zone, quartz reef/quartzite and disseminated sulfide in metasediments have produced characteristic geophysical signatures.

The regional gravity and magnetic contours follow a NNE–SSW trend parallel to strike of formations. The gravity high over Rohil has been attributed to intrusive amphibolite bodies within metasediments and possibly also to sulfides in the mineralized zones. A prominent magnetic low (–450 nT to –200 nT) characterizes the Rohil shear zone.

A prominent zone of high chargeability (30 to 80 mV/V) and low resistivity (10 ohm.m) has been delineated over a strike length of 1.3 km, coinciding with the magnetic low zone. TURAM survey has led to identification of four N–S trending conductors. One of the EM conductor axes falls in the ore zone. Other conductors either follow sulfide–rich zones or graphitic schist (Fig. 5).

Thus, the ore zone at Rohil, as established by extensive core drilling, is characterized by association of strong EM conductor, low magnetic, high chargeability, low resistivity and high gravity geophysical anomalies [20]. The integrated geophysical data has helped in delineation of favourable targets for exploratory drilling in contiguous blocks.

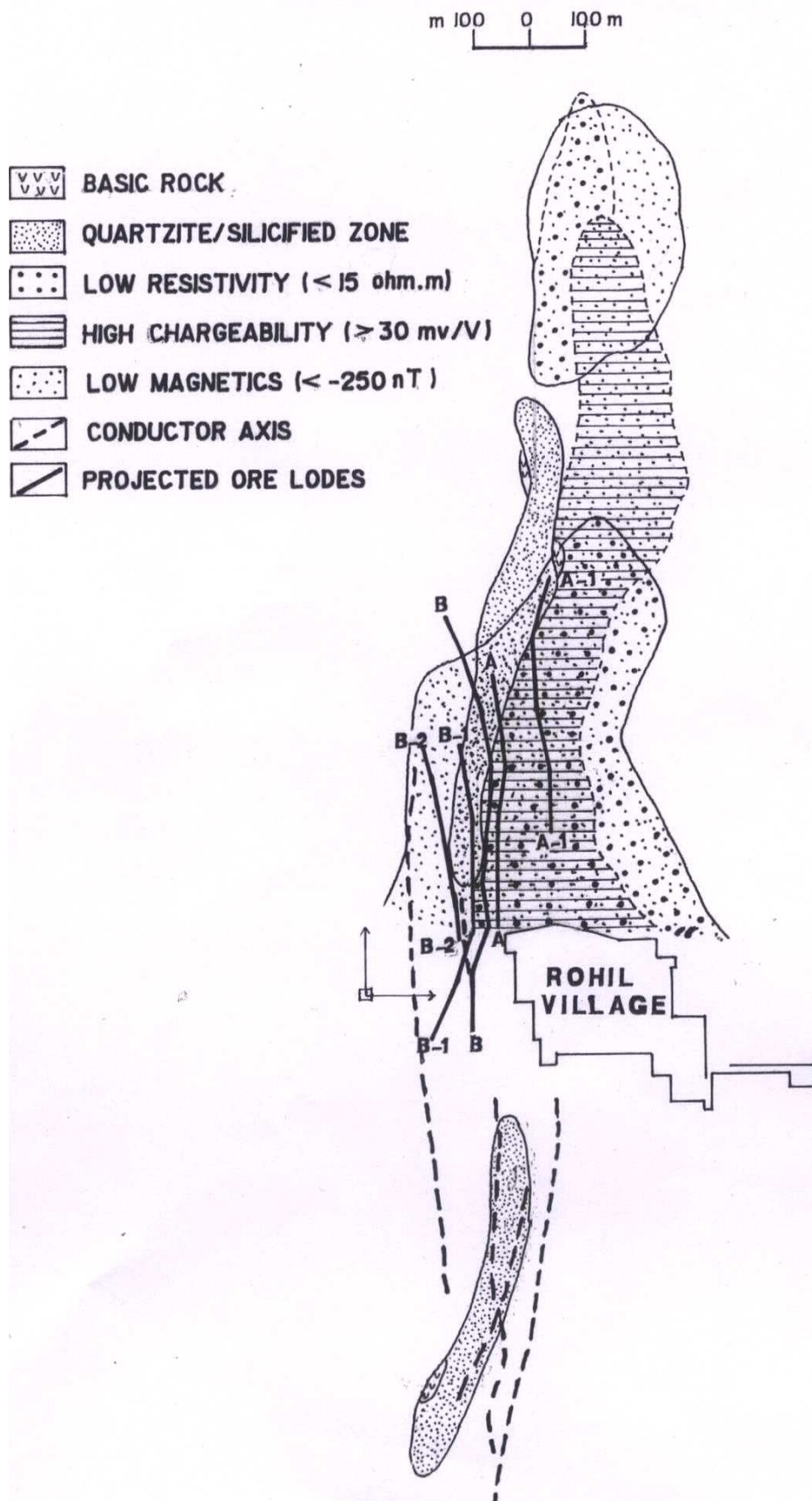


FIG. 5. Rohil block showing geophysical anomalies district Sikar, Rajasthan.

### *6.7.1. Mathematical modeling of ground geophysical and heliborne magnetic data*

The mathematical surface fitting for ground total magnetic intensity (TMI), resistivity and chargeability data has been carried out for Rohil area. The Natural Neighbour method of interpolation of data has been found to give the best statistical results on comparison with the original data.

Trend surface analysis was performed to examine the 'regional trend' of variation of the geophysical parameters. Residual plot providing 'highs' and 'lows' of the local anomalies were then estimated and plotted [21].

TMI residual plot distinctly shows Rohil ore block as a low magnetic zone. Relatively low residuals are also obtained in the North, South and NNE of Rohil area, which assume significance in uranium exploration. Heliborne TMI data for the block also gives similar features. The 2<sup>nd</sup> order polynomial produces fairly good trend surface for TMI data with a 54.10% goodness of fit.

The residual plot of ground resistivity, define shear zone as distinct low resistive zone. Ground resistivity data, however, does not produce good trend surface and is interpreted to be due to a very large contrast of resistivity between the shear zone material and the surrounding country rocks. Even with fourth order polynomial, less than 15% goodness of fit is achieved.

The chargeability residual map shows 'high' in the Rohil ore block and also in areas further to the SSW and to the NNW of Rohil, indicating presence of high chargeability material such as disseminated sulfides, graphite and finer grained hydrothermal alteration minerals of the shear zone. Cubic polynomial surface produces a reasonable goodness of fit of 36% for ground chargeability data.

It is thus apparent that the mineralized area around Rohil is characterized by the associated geophysical anomalies of high chargeability, low resistivity and low total magnetic intensity (Fig. 6).

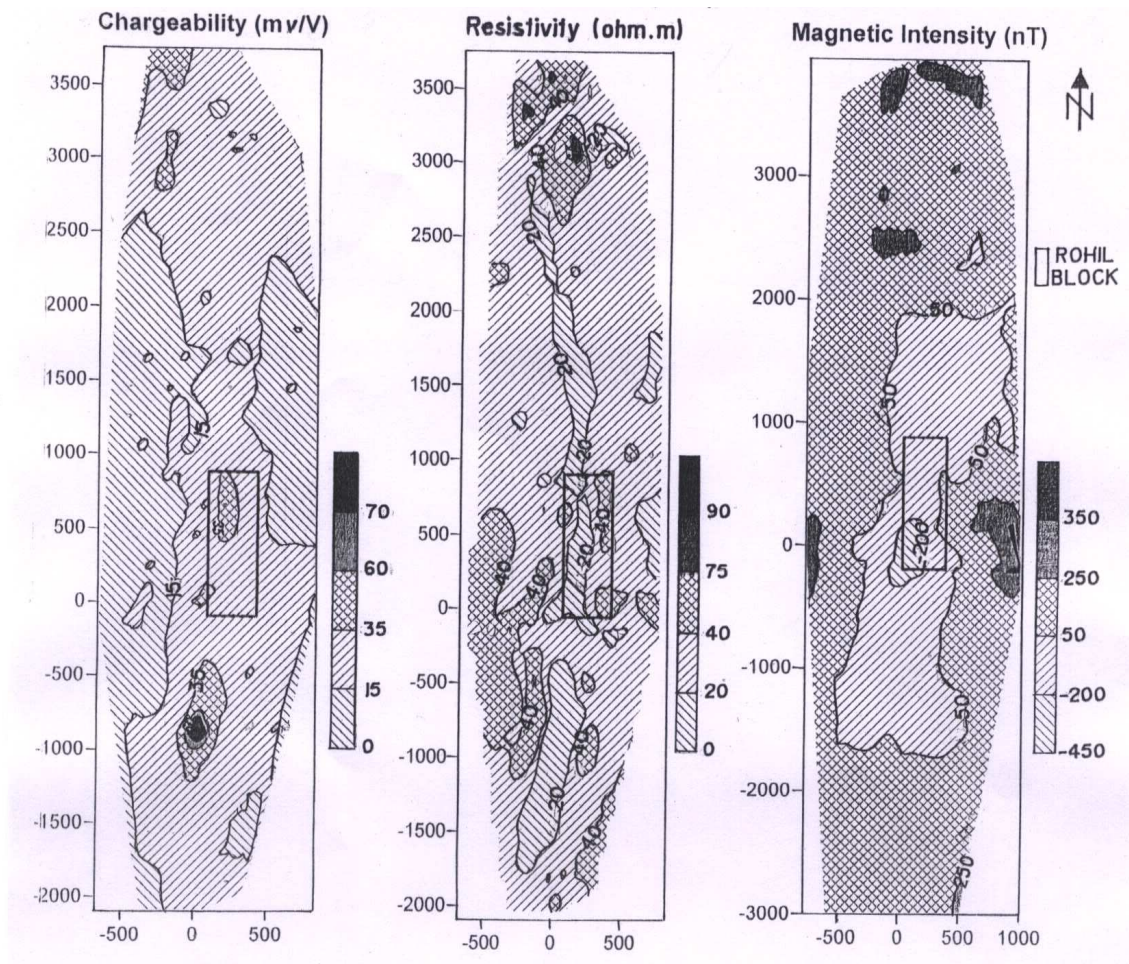


FIG. 6. Comparison of ground geophysical parameters Rohil area, district Sikar, Rajasthan.

## 7. Identification of new prospecting areas – heliborne geophysical surveys

Heliborne multisensor multiparameter geophysical surveys consisting of aero-magnetic, EM (Frequency domain) and AGRS carried out in parts of NDFB, resulted in identification of a number of favourable targets in the extension areas of Rohil uranium deposit for uranium exploration [22]. A number of concealed faults/fractures have been inferred from aeromagnetic data. Clusters of conductors roughly scatter along NW-SE direction. The area around Gauti is inferred as an interesting target based on processing and interpretation of magnetic, EM and AGRS data. The EM-conductors identified in this zone do not display characteristics of any sheet-like conducting saline/brackish ground water, rather, these are segmented in linear zones and are expressions of geological features related to bed rock conductivity [23]. Some of these inferred conductors are being tested by exploratory core drilling.

## 8. Discussions

KSB is well known for copper and uranium mineralization along NE-SW trending lineaments. The 20 km long Rohil – Kotri – Guhala sector, where many uranium occurrences were delineated, is being investigated by integrated exploration techniques and targets have been identified. Similar geological cum structural set up continues further in the NE and SW extensions. Three sub-parallel belts with known uranium anomalies within KSB are considered as prime targets for vein type deposits [24]. This includes the areas in the NE and SW extensions of the relatively well explored Rohil area, Ladi ka Bas and Arath areas to the east and west of Rohil, respectively.

Exploration data indicate high probability of existence of concealed uranium deposits akin to Rohil in Rohil North Extension, Diara–Kotri, Kerpura–Salwari, Hurra ki Dhani and Raghunathgarh–Udaipurwati sectors.

As a part of integrated exploration inputs in delineation of potential target for sub-surface investigation in parts of NDFB, heliborne geophysical surveys have been completed. Magnetic, EM and gamma–ray spectrometric data coupled with satellite imageries are being utilized in narrowing down favourable areas for ground geophysical investigations such as detailed magnetic, EM, resistivity, gravity and IP surveys with follow–up exploratory drilling. Subsurface exploration in contiguous and extension areas of Rohil deposit by exploratory core drilling is currently under progress to augment uranium resources of NDFB.

#### ACKNOWLEDGEMENTS

The Authors wish to express their sincere gratitude to Dr. Anil Kakodkar, Chairman, Atomic Energy Commission and Secretary, Department of Atomic Energy, Government of India for according permission to present this paper in URAM-2009.

The Authors are grateful to Dr. Anjan Chaki, Director, Atomic Minerals Directorate for Exploration and Research for the deep interest evinced by him in the exploration programme for uranium and providing constant guidance. The Authors are particularly indebted to all the colleagues associated with Rohil Prospect for technical discussions while finalizing this paper. The analytical support extended by various laboratories is thankfully acknowledged.

#### REFERENCES

- [1] NARAYANDAS, G.R., SHARMA, D.K., GOVIND SINGH, RAJENDRA SINGH., Uranium mineralization in Sikar District, Rajasthan, *Journal of Geological Society of India*, v. 21 (1980) 432–439
- [2] GOVIND SINGH, et al., Uranium and REE potential of the Albitite–Pyroxenite–Microcline belt of Rajasthan, India, *Exploration and Research for Atomic Minerals*, v. 11 (1998) 1–12.
- [3] JAIN, R.B., et al., Petrography and geochemistry of the radioactive albitites and their genesis. Maonda area, North Rajasthan. *J. Geol. Soc. India*, N.21 (9) (1999) 432–439.
- [4] SARASWAT, A.C., A report on radiometric survey carried out in the vicinity of Khandela, Sikar district, Rajasthan. Unpubl. AMD report, (1954)
- [5] RAY, S.K., Albitite occurrences and associated ore minerals in the Khetri copper belt, North Eastern Rajasthan, *Records, Geol. Surv. of India*, v. 113 (7) (1987) 41–49.
- [6] RAY, S.K., The albitite line of Northern Rajasthan– a fossil intra–continental rift zone, *Jour. Geol. Soc. of India*, v. 36 (1990) 413–423.
- [7] HERON, A.M.. The geology of Central Rajputana. *Mem. Geol. Surv. Ind.*, v. 79, (1953) 1–389.
- [8] BOSE, U., Correlation problems of the Proterozoic stratigraphy of Rajasthan. *Ind. Miner.*, v. 43 (3 & 4) (1989) 183–193.
- [9] SINHA–ROY, S., MALHOTRA, G. and MOHANTI, M., *Geology of Rajasthan*. Geol. Soc. Ind., First Edition, (1998) 278p.
- [10] DASGUPTA, S. P., Structural history of Khetri copper belt, Jhunjhunu and Sikar District, Rajasthan. *Mem. Geol. Sur. India*, v.98 (1968) 1–170.
- [11] GÓPALAN, K., TRIVEDI, J.R., BALASUBRAHMANYAN, M.N., RAY, S.K. and SASTRY, C.A., Rb–Sr chronology of Khetri Copper Belt, Rajasthan. *Jour. of Geol. Soc. of India*. 20 (1979) 450–456.
- [12] GUPTA, P., GUHA, D.B. AND CHATTOPADHYAY, B., Basement–cover relationships in the Khetri Copper Belt and the emplacement mechanism of the granite massifs, Rajasthan, India, *Jour. of Geol. Soc. of India* **52** (1998) 417–432.
- [13] AMD Unpublished report on Geochronological studies to determine age of Rohil Uranium

mineralization (2009).

- [14] SRINIVAS, K.N., PRASAD, R.N., PANDEY, B.K., Geochronology Report No. 2000/1 Unpublished Report AMD Hyderabad (2000)
- [15] SINHA, D.K., et al., Evidences for Soda Metasomatism in Ladera–Sakhun area, Northeastern Rajasthan, Jour. of Geol. Soc. of India **56** (2000) 573–582.
- [16] YADAV, O.P., et al., Geology and Geochemistry of uraniferous albitites of the Middle Proterozoic Delhi Supergroup, Rajasthan, India, Proceedings of National Seminar, Tectonomagmatism of Precambrian Terrains (2000) 303-320.
- [17] YADAV, O.P., SAXENA, S.K., PANDE, A.K., GUPTA, K.R., Sodic Metasomatism– a feature of tectonomagmatic activation and its implication on metallogeny in Khetri sub basin, Rajasthan, India, Geol. Sur. India., Special Publication **72** (2004) 301–312.
- [18] KHANDELWAL, M.K., et al., Status of Exploration in Rohil area, AMD, WR, Jaipur, Unpublished Report (2008).
- [19] KHANDELWAL, M.K., et al., Uranium–Copper–Molybdenum association in the Rohil Deposit, North Delhi Fold Belt, Rajasthan” Memoir Geological Society of India (Golden Jubilee Vol., Contribution to Geochemistry) **73** (2008) 117–130.
- [20] SINGH, N., et al., Role of geophysical techniques for uranium exploration over Ajabgarh Group of rocks: A case study from Ghateshwar – Rohil Sector, Sikar district, Rajasthan, Profile of Presentations, XII IGC and National Seminar on Ground Water Resources, M.L.S. University, Udaipur, Rajasthan (2000) 49.
- [21] KATTI, V.J., et al., Mathematical Modeling of Geophysical and Geochemical Data of Rohil Area, North Delhi Fold Belt, Rajasthan, AMD unpublished report (2009).
- [22] NATIONAL GEOPHYSICAL RESEARCH INSTITUTE Report on High Resolution Multi–Parameter Airborne Geophysical Surveys over Northeastern part of Albitite Line, Unpubl. Tech. Rep. (2008) 157.
- [23] BANDOPADHYAY, M., CHATURVEDI, A.K. A report on processing and interpretation of magnetic and electromagnetic data from heliborne multiparameter geophysical survey over parts of Albitite line of North Delhi Fold Belt (along Khatiwas–Palsana–Rohil–Khetri–Nim ka Thana– Narnaul tract) Rajasthan and Haryana, (2008), 28.
- [24] BISHT, B.S., et al., Report of Core Group on NDFB, Rajasthan, AMD unpublished report, (2008) 43.